

UNIVERSITAT JAUME I

# CONTINUOUS FLOW SYSTEMS FOR MULTICATALYTIC PROCESSES BASED ON SUPPORTED IONIC LIQUIDS

**PhD Thesis**

**EDGAR PERIS SALOM**



**UNIVERSITAT  
JAUME·I**

**Escuela de Doctorado Universitat Jaume I**

**Programa de Doctorado en Química Sostenible**

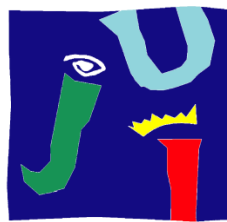
**Supervisors:**

**Dr. Santiago V. Luis Lafuente**

**Dr. Eduardo García-Verdugo Cepeda**

**November 2018**





**UNIVERSITAT  
JAUME·I**

Programa de Doctorado en

**QUÍMICA SOSTENIBLE**

**Escuela de Doctorado de la Universitat Jaume I**

Título de la Tesis

**CONTINUOUS FLOW SYSTEMS FOR MULTICATALYTIC PROCESSES  
BASED ON SUPPORTED IONIC LIQUIDS**

Memoria presentada por **EDGAR PERIS SALOM** para optar al **grado de doctor** por la Universitat Jaume I

Doctorando:

Directores de la Tesis

Edgar Peris Salom

Dr. Eduardo García-Verdugo Cepeda

Dr. Santiago V. Luis Lafuente

Castelló de la Plana, Noviembre de 2018



## **Financiación recibida**

La realización de esta Tesis Doctoral ha sido posible gracias a la concesión de una ayuda en forma de contrato predoctoral de Formación de Profesorado Universitario (**FPU13/00685**) por parte del Ministerio de Educación, Cultura y Deporte del Gobierno de España.

La financiación de la actividad investigadora ha sido posible gracias a los proyectos concedidos por el Ministerio de Economía y Competitividad del Gobierno de España (MINECO CTQ2015-68429R) y por la Generalitat Valenciana (GV-PROMETEO 2016-071)



## AGRAÏMENTS

M'agradaria escriure aquestes línies amb el meu idioma matern, per agrair a totes aquelles persones que han participat de manera directa o indirecta en la realització d'aquesta tesi.

En primer lloc agrair al grup de Química Sostenible i Supramolecular de la Universitat Jaume I i als seus membres: Santiago Luis, Maribel Burguete, Belén Altava i Eduardo García-Verdugo; per la oportunitat que em van donar d'introduir-me al món de la investigació universitària, ajudar-me a descobrir-lo i comprendre'l i guiar-me durant tot aquest procés que finalitza amb aquesta tesi. En tot moment he tingut a la meua disposició tot el que he necessitat al laboratori.

Especialment agrair als meus directors. A Santiago, per els consells, entre els que m'agradaria incloure els consells docents, de gran valor per a mi. També per transmetre la seua dedicació i passió per la química. A Eduardo, per la seua direcció dia a dia, els milers d'idees i sobretot per confiar en la meua capacitat fins i tot als mals moments.

En aquest punt, també voldria agrair a les dues persones responsables de les meues estades fora de l'UJI: el Dr. Jesús Alcázar de Janssen-Cilag S. A. i el Dr. Víctor Sans de la University of Nottingham. Tots dos em van integrar i em van fer sentir un més als respectius llocs de treball, a més de la seua dedicació al projecte que ens unia temporalment. També als companys i companyes amb qui vaig compartir aquestes dues experiències, en especial a Rocío, a qui Nottingham em va unir en una amistat que m'ha permès conèixer La Rioja.

Voldria fer extensiu el meu agraïment a la resta de companys del Departament de Química Inorgànica i Orgànica que en algun moment al llarg d'aquests anys han compartit experiències amb mi. De la mateixa manera, agrair al personal del Servei Central d'Instrumentació Científica de l'UJI, que han sigut una inestimable ajuda sempre que ho he necessitat.

El dia a dia d'aquest treball no hauria sigut possible sense els meus companys del Grup de Química Sostenible i Supramolecular. Durant cinc anys han sigut tantes les persones que he tingut la sort de conèixer i compartir amb elles vivències, que espere no oblidar-me de ningú. Per damunt de tots, agrair a Raúl Porcar, ja que sense ell segurament no hauria pogut fer tot aquest treball que ací presente. Amb el seu treball impagable ens fa molt més fàcil la vida al laboratori a tots el demés. No

existeix instrument que ell no siga capaç d'arreglar o reacció que no puga fer. Si a tot açò afegim amistat, tenim al company de laboratori perfecte. A Sergio, de qui vaig heretar aquest projecte i qui va ser un gran guia en els meus primers passos al grup. Als companys dels meus primers anys amb qui vaig descobrir Castelló i vaig iniciar aquest viatge. María M., sempre disposta a ajudar i a defensar Castelló. Silvia, exemple d'investigadora on inspirar-se i gran balladora. Daniel, un punt de vista diferent i el gust pels plaers de la vida. Raju, el nostre indi a qui hem intentat introduir a la nostra cultura i conèixer la seua, a qui a dia d'avui moltes vegades encara em costa entendre, però que per sort hi és ací per a continuar descobrint amb ell. Amb ells vaig viatjar a Bilbao al meu primer congrés que mai oblidaré. I hem compartit moltes coses més, incloent Magdalena i Falles, dues festivitats que ens han "enfrontat" i unit. A Pascual, un element necessari a qualsevol fórmula, capaç de fer riure a cada minut i a qui sempre m'agradaria tindre a prop. Als meus companys dels últims anys amb qui he compartit dies de treball, festes, mil anècdotes i més congressos increïbles. Adriana, una persona a la que aprecie moltíssim, a qui vaig conèixer com "alumna" i s'ha convertit en una gran amiga i el millor suport al laboratori. Iván, el millor fixatge. David, bona persona a qui simplement sentir parlar aporta pau i tranquil·litat i... Pura vida! Ferran, el futur del grup, per tots els partits de tennis i eixe sentit del humor que compartim. Roberta, per fer-nos sentir Erasmus a Castelló. Tots ells, a qui considere amics que he guanyat, han aconseguit que anés dia a dia al laboratori amb un somriure i espere haver sigut capaç d'aportar-los el mateix a ells. Sé que mai tindrè uns millors companys ni millor ambient de treball. Igualment, a tots els companys i companyes amb qui he coincidit al grup i dels que guarde un molt bon record: Laura G., Laura K., Vanessa, Inés, Alicia, Chen, María T., Luis i Vicent.

Vull recordar també en aquestes línies als meus companys de Llicenciatura a la Universitat de València, especialment a aquells que amb els anys s'han convertit en amics. Hem pres camins diferents a la vida, però junts començarem en aquest món de la Química i representen una de les millors aportacions que aquesta ha fet a la meua vida. Carlos, Cris, Erik, Iván, Maite, Eder, Javi, Lidia, Pedro i Joaquín; espere que mai deixem d'ajuntar-nos per recordar aquells anys i seguir mantenint la nostra amistat.

Per suposat, als meus amics de tota la vida, amb els que tan poc he parlat d'aquest treball. I, precisament, era això el que necessitava d'ells: evadir-me. Han estat sempre al meu costat recordant-me, sense saber-ho, que hi ha coses més importants i mantenint les meues arrels.



Carlos, Borja, Paco, Pep, Alberto, Ángel, Christian i Javi; espere que açò mai canvie.

A la meua xica, María. Companya, amiga, parella, amor. D'una o altra manera sempre has estat present durant tot aquest procés i amb tu he pogut compartir-ho tot. Simplement mirant els teus ulls, els mals moments deixen de ser-ho i no puc imaginar millor companya de viatge. Eres la millor aportació que la química ha fet a la meua vida.

A la meua avia, la persona que més trobe a faltar en aquest món. Ella representa eixa part de fe que tota persona, més enllà de quines siguen les seues creences, necessita.

A la meua germana Lara, l'altra científica de la família. Has sigut més intel·ligent que jo escollint el teu futur i sé que pots aconseguir el que vulgues.

Per últim i més important, als meus pares, Cristina i David. Vosaltres sou els meus ídols i referents. Tot el que tinc, tot el que sóc, us ho dec a vosaltres. I per tant, també aquest treball. Sempre he tingut el vostre suport i el senc amb 30 anys igual que el sentia amb deu. Gràcies per tot.



*“La intelectualidad se mide no por la inteligencia, sino por las dosis de humor que es capaz de utilizar”*

**Friedrich W. Nietzsche**



## ABBREVIATIONS USED

<b>AE</b>	Atom Economy
<b>AIBN</b>	2,2'-Azobis(2-methylpropionitrile)
<b>API</b>	Active Pharmaceutical Ingredient
<b>ATR-FTIR</b>	Attenuated total reflectance-Fourier transform infrared spectroscopy
<b>CAD</b>	Computer-aided design
<b>CAL-B</b>	Candida Antarctica Lipase B
<b>cEF</b>	Complete E Factor
<b>CDC</b>	Cross-dehydrogenative-coupling
<b>DCM</b>	Dichloromethane
<b>DKR</b>	Dynamic Kinetic Resolution
<b>DMF</b>	N,N-dimethylformamide
<b>DPP</b>	Diphenyl phosphine
<b>ee</b>	Enantiomeric excess
<b>EKR</b>	Enzymatic Kinetic Resolution
<b>FDM</b>	Fused Deposition Modeling
<b>Fw</b>	Formula weight
<b>GC</b>	Gas Chromatography
<b>HIPS</b>	High impact Polystyrene
<b>HNL</b>	Hydroxynitrile Lyase
<b>HPLC</b>	High performance liquid chromatography
<b>ICP-MS</b>	Inductively Coupled Plasma – Mass Spectrometry
<b>IL</b>	Ionic Liquid
<b>IPA/iPrOH</b>	Isopropyl alcohol

<b>iPr</b>	Isopropyl
<b>KR</b>	Kinetic Resolution
<b>LCA</b>	Life Cycle Assessment
<b>MBA</b>	Methylbenzylamine
<b>Me<sub>3</sub>SiNu</b>	Trimethylsilyl nucleophile
<b>mfr</b>	Mini-flow reactor
<b>MNPs</b>	Metal Nanoparticles
<b>MW</b>	Microwave
<b>NBP</b>	4-(4-nitrobenzyl)pyridine
<b>NHC</b>	N-heterocyclic carbene
<b>NMR</b>	Nuclear Magnetic Resonance
<b>OTf</b>	Triflate
<b>PBR</b>	Packed-Bed Reactor
<b>Pd-NHC</b>	Palladium N-heterocyclic carbene complex
<b>PdNPs</b>	Palladium Nanoparticles
<b>PEI</b>	Polyethyleneimine
<b>PEPPSI</b>	Pyridine-Enhanced-Precatalyst-Preparation-Stabilisation-Initiation
<b>Phos</b>	Phosphine
<b>PLP</b>	Pyridoxal Phosphate
<b>PMI</b>	Process Mass Intensity
<b>PS-DVB</b>	Polystyrene-divinylbenzene
<b>PTFE</b>	Polytetrafluoroethylene
<b>r.t.</b>	Room temperature
<b>scCO<sub>2</sub></b>	Supercritical CO <sub>2</sub>

<b>sEF</b>	Simple E Factor
<b>SIL</b>	Supported Ionic Liquid
<b>SILLP</b>	Supported Ionic Liquid-Like Phase
<b>SILP</b>	Supported Ionic Liquid Phase
<b>SLA</b>	Stereolithography
<b>SLS</b>	Selective Laser Sintering
<b>SoIFC</b>	Solventless conditions
<b>TEM</b>	Transmission Electron Microscopy
<b>TGA</b>	Thermogravimetric Analysis
<b>THF</b>	Tetrahydrofuran
<b>TMSCl</b>	Trimethylsilyl chloride
<b>TMSCN</b>	Trimethylsilyl cyanide
<b>TOF</b>	Turnover Frequency
<b>TON</b>	Turnover Number
<b>TOS</b>	Time on stream
<b>t<sub>R</sub></b>	Retention time
<b>TSIL</b>	Task Specific Ionic Liquid
<b>ω-TA</b>	ω-Transaminase
<b>2-Me-THF</b>	2-methyl tetrahydrofuran

### **SYMBOLS USED**

<b>δ</b>	Chemical shift
<b>ρ</b>	Density





## RESUMEN DE LA TESIS

La presente Tesis Doctoral se engloba dentro del área de la Química Sostenible y más concretamente en el campo de la química en flujo continuo, que podríamos considerar una herramienta de la Química Sostenible. El principal objetivo es el diseño y desarrollo de nuevos sistemas multicatalíticos en continuo basados en el uso de líquidos iónicos soportados, materiales muy interesantes por sus propiedades.

La memoria de la tesis se ha estructurado en 8 capítulos dónde los resultados y discusión de los mismos se han redactado siguiendo el formato de artículos científicos a partir del trabajo de investigación desarrollado. Los resultados obtenidos han permitido la publicación de dos artículos en la revista Green Chemistry, de la Royal Society of Chemistry, revista de alto índice de impacto y de gran consideración dentro del campo de la Química Sostenible. Además, el trabajo expuesto ha permitido la elaboración de otros tres manuscritos que serán enviados en breve esperando ser publicados también en revistas de alto impacto. En cada capítulo, junto con el artículo/manuscrito y su información adicional, se incluye un breve resumen del mismo en español. Además, las abreviaciones y símbolos empleados recurrentemente a lo largo de la descripción de este trabajo, se recogen al principio de la tesis por orden alfabético.

El primer capítulo incluye una introducción sobre los temas que se tratan en esta tesis con la finalidad de ubicar al lector y mostrarle los antecedentes, de forma que pueda seguir mejor el desarrollo de la misma y comprender la importancia de los resultados obtenidos.

A continuación, en el capítulo segundo se exponen y detallan los objetivos generales de la tesis, de forma que el lector pueda centrar su atención y comprender las motivaciones.

A partir de este punto, se detalla los resultados obtenidos y la discusión de los mismos durante cinco capítulos cuyo orden viene dado por las sucesivas reacciones de formación de enlaces C-C implementadas en los sistemas multicatalíticos de flujo continuo diseñados.

En el capítulo 3 se describe la síntesis y estudio de diversos SILLPs como catalizadores soportados para la reacción de cianosililación de aldehídos y cetonas tanto en condiciones de batch como de flujo continuo. El análisis de la influencia de los diferentes componentes estructurales modulables permitió seleccionar el SILLP ideal para esta transformación y se implementó con él un sistema en continuo de

excelente estabilidad y rendimiento. Este trabajo permitió la publicación de un artículo en la revista Green Chemistry.

En el cuarto capítulo se reportan los esfuerzos dirigidos al desarrollo de un sistema multicatalítico para la obtención de cianohidrinas quirales a través de diferentes transformaciones consecutivas en un proceso telescópico en continuo, de nuevo empleando SILLPs como catalizadores soportados. Este trabajo se puede considerar como una continuación o ampliación del tercer capítulo, pues la cianosililación corresponde a la primera etapa de esta serie de transformaciones consecutivas en continuo. Esta investigación permitió la redacción de un manuscrito listo para ser enviado a la revista especializada ChemCatChem.

El quinto capítulo recoge la investigación realizada para obtener un sistema sintético multicatalítico divergente en continuo, que permita obtener diferentes compuestos de alto valor añadido como son las cianohidrinas y los  $\alpha$ -amino nitrilos a partir de un único compuesto de partida, en este caso alcoholes alílicos. Este capítulo combina las reacciones de cianosililación y Strecker, por lo que guarda relación con los capítulos tercero y cuarto, además de introducir una nueva reacción de formación de enlaces C-C. Diferentes líquidos iónicos diseñados con funciones específicas se han utilizado como catalizadores soportados y/o como medio de reacción. Este trabajo ha llevado a la redacción de un manuscrito listo para ser enviado a la revista especializada ChemSusChem.

El sexto capítulo consiste en los estudios realizados para desarrollar sistemas catalíticos más estables y eficientes para la reacción de acoplamiento de Negishi, que permitan su realización en flujo continuo. Estos sistemas catalíticos se basan en el efecto sinérgico de los SILLPs modulables como soporte para la inmovilización de complejos de paladio con carbenos N-heterocíclicos y con ligandos fosfina formando SILLP-NHC-Pd-Phos. El uso de los SILLPs como soporte y como scavenger de especies lixiviadas de paladio se puso a prueba, resultando en una mejor comprensión del mecanismo de liberación y recaptura de catalizador que opera en este tipo de reacciones. Este estudio ha llevado a la redacción de un manuscrito listo para ser enviado a la revista ACS Catalysis.

Por último, el séptimo capítulo se desvía ligeramente de los anteriores, ya que no se emplean líquidos iónicos soportados, sino las nuevas tecnologías de impresión 3D para el desarrollo de sistemas en continuo. Este trabajo se realizó durante la estancia investigadora de tres meses en la University of Nottingham bajo la supervisión del Dr. Víctor Sans.

Mediante impresión 3D y modificación química de un reactor de Nylon, se consiguió un reactor biocatalítico estable y activo en condiciones de flujo continuo para la reacción de transaminación. Este trabajo permitió la publicación de un artículo en la revista Green Chemistry.

Finalmente, en el capítulo octavo y último, se exponen las conclusiones más relevantes derivadas del trabajo descrito en cada uno de los artículos que conforman los capítulos de desarrollo de esta tesis.



## SUMMARY OF THE THESIS

This Doctoral Thesis is framed in the area of Sustainable Chemistry and more specifically in the field of continuous flow chemistry, which can be considered a tool of Sustainable Chemistry. The main objective has been the design and development of new continuous multicatalytic systems based on the use of supported ionic liquids, materials of high interest due to their specific properties.

The thesis has been structured in 8 chapters where the results obtained and the discussion of them have been written following the format of scientific articles describing the research work developed. The results obtained have allowed the publication of two articles in the journal *Green Chemistry*, from the Royal Society of Chemistry, which has a high impact index and great consideration within the field of Sustainable Chemistry. In addition, the exposed work has allowed the elaboration of three other drafts that will be sent shortly waiting to be published also in high impact specialised journals. In each chapter, along with the article/manuscript and its additional information, a brief summary in Spanish is included. In addition, the abbreviations and symbols used recurrently throughout the description of this work are collected at the beginning of the thesis in alphabetical order.

The first chapter includes an introduction about the topics covered in this thesis in order to provide the context to the reader and highlight the background, as to facilitate the reader easily follow the development of the work and properly understand the relevance of the results obtained.

Then, in the second chapter the general objectives of the thesis have been exposed and detailed, so that the reader can focus their attention and achieve a better comprehension of the motivations for this work.

After this, the results obtained and their discussion are detailed throughout five chapters whose order is given by the successive reactions of C-C bond formation that are implemented in the multicatalytic continuous flow systems designed.

Chapter 3 describes the synthesis and study of various SILLPs as supported catalysts for the cyanosilylation reaction of aldehydes and ketones under both batch and continuous flow conditions. The analysis of the different tuneable structural parts allowed selecting the ideal SILLP for this transformation and a continuous system of excellent

stability and yield was implemented. This work allowed the publication of an article in the journal Green Chemistry.

In the fourth chapter, the efforts driven to the development of a multicatalytic system for the obtaining of chiral cyanohydrins through different consecutive transformations in a continuous telescopic process are reported, using SILLPs as supported catalysts. This work can be considered as a continuation or extension of the third chapter, since the cyanosilylation reaction represents the first step of this sequence of consecutive transformations in continuous. This investigation allowed the preparation of a manuscript ready to be sent to the specialised journal ChemCatChem.

The fifth chapter includes the research carried out to obtain a divergent multicatalytic synthetic system under continuous conditions, which allows obtaining different compounds of high added value such as cyanohydrins and  $\alpha$ -amino nitriles from a single starting product, in this case allylic alcohols. This chapter combines the reactions of cyanosilylation and Strecker, so it is related to the third and fourth chapters, but introducing a new reaction for the formation of C-C bonds. Ionic liquids designed with specific functionalities are used both as supported catalysts and as reaction media. This work resulted in the elaboration of a manuscript ready to be sent to the specialised journal ChemSusChem.

The sixth chapter consists in the studies carried out to develop more stable and efficient catalytic systems for the Negishi cross-coupling reaction, allowing it to be performed under continuous flow conditions. These catalytic systems are based on the synergistic effect of the tuneable SILLPs as supports in the immobilisation of palladium complexes involving N-heterocyclic carbenes and phosphine ligands forming SILLP-NHC-Pd-Phos. The use of the SILLPs as support and as scavenger of palladium leached species was tested, resulting in a better understanding of the release and catch mechanism that operates in this type of reactions. This study resulted in the preparation of a manuscript ready to be sent to the journal ACS Catalysis.

Finally, the seventh chapter slightly deviates from the main investigation line since supported ionic liquids were not employed. Instead, new 3D printing technologies for the development of continuous systems were implemented. This work was carried out during the three-month research stay at the University of Nottingham under the supervision of Dr. Víctor Sans. By 3D printing and chemical modification of a Nylon device, a stable and active biocatalytic reactor

was achieved for the transamination reaction under continuous flow conditions. This work allowed the publication of an article in the journal Green Chemistry.

Finally, the most relevant conclusions derived from the work described in the different chapters of this thesis have been gathered. This represents the eighth and last chapter.





## INDEX

<b>CHAPTER 1. Introduction.....</b>	<b>1</b>
<b>1.1. Green Chemistry.....</b>	<b>3</b>
<b>1.2. Catalysis.....</b>	<b>12</b>
<b>1.2.1. Supported catalysis: effects             of the immobilisation support.....</b>	<b>13</b>
<b>1.3. Solvents.....</b>	<b>19</b>
<b>1.3.1. Ionic Liquids.....</b>	<b>21</b>
<b>1.4. Supported Ionic Liquids.....</b>	<b>26</b>
<b>1.5. Continuous Flow Chemistry.....</b>	<b>37</b>
<b>1.5.1. Advanced Manufacturing: 3D printing.....</b>	<b>50</b>
<b>1.6. Synthetic approaches to C-C bond forming reactions:     cyanosilylation, Strecker and Negishi.....</b>	<b>62</b>
<b>1.6.1. Cyanosilylation of carbonyl compounds.....</b>	<b>62</b>
<b>1.6.2. Strecker reaction.....</b>	<b>70</b>
<b>1.6.3. Negishi cross-coupling reaction.....</b>	<b>79</b>
<b>CHAPTER 2. General Objectives.....</b>	<b>91</b>
<b>CHAPTER 3. Supported ionic liquid-like phases as organocatalysts for the solvent-free cyanosilylation of carbonyl compounds: from batch to continuous flow process.....</b>	<b>97</b>
<b>3.1. Manuscript resume.....</b>	<b>99</b>
<b>3.2. Supported ionic liquid-like phases as organocatalysts for the     solvent-free cyanosilylation of carbonyl compounds: from batch to     continuous flow process.....</b>	<b>107</b>
<b>3.3. Supporting information.....</b>	<b>102</b>

**CHAPTER 4. Supported Ionic Liquid-Like Phases (SILLPs) as immobilised catalysts for the multistep and multicycatalytic continuous flow synthesis of chiral cyanohydrins.....133**

**4.1. Manuscript resume.....135**

**4.2. Supported Ionic Liquid-Like Phases (SILLPs) as immobilised catalysts for the multistep and multicycatalytic continuous flow synthesis of chiral cyanohydrins.....141**

**4.3. Supporting information.....149**

**CHAPTER 5. Divergent multistep continuous synthesis enabled by immobilised catalysts on IL-phases.....175**

**5.1. Manuscript resume.....177**

**5.2. Divergent multistep continuous synthesis enabled by immobilised catalysts on IL-phases.....185**

**5.3. Supporting information.....193**

**CHAPTER 6. Synergy between Supported Ionic Liquid-Like Phase and immobilised Palladium N-Heterocyclic Carbene Phosphine complexes for the Negishi reaction under flow conditions.....205**

**6.1. Manuscript resume.....207**

**6.2. Synergy between Supported Ionic Liquid-Like Phase and immobilised Palladium N-Heterocyclic Carbene Phosphine complexes for the Negishi reaction under flow conditions.....211**

**6.3. Supporting information.....237**

**CHAPTER 7. Tuneable 3D printed bioreactors for transaminations under continuous-flow.....243**

**7.1. Manuscript resume.....245**

**7.2. Tuneable 3D printed bioreactors for transaminations under continuous-flow.....251**

**7.3. Supporting information.....257**

<b>CHAPTER 8. Final conclusions.....</b>	<b>269</b>
--	------------



*“El placer más noble es la alegría de la comprensión”*

**Leonardo da Vinci**



# **Introduction**

## **CHAPTER 1**





# Chapter 1. INTRODUCTION

## 1.1. Green Chemistry

In the past, environmental issues have been considered as part of the economic system and the rapid exploitation of natural resources. It took many years to consider the impact of the established ways that materials (feedstocks) were used. How the industrial chemical processes were designed, and what were the hazardous properties of products, the energy consumption issues and other parameters involved in the manufacture of products (life cycle, recycling, etc.) and how they affect the human health and impact the environment. Sustainable (Green) Chemistry has been for many years a relatively abstract idea with no basic principles and definitions of practical applications. Now, the term and meaning Green Chemistry is well established and recognised.<sup>1</sup> Green Chemistry is a philosophy of chemical research and engineering that encourages the design of products and processes that minimise the use and generation of hazardous substances. This philosophy, with its 12 principles would like to see changes in the conventional ways that were used for decades to make synthetic organic chemical substances and materials and the use of less toxic starting materials. By changing the methodologies of organic synthesis, health and safety will advance in the small-scale laboratory level but also will be extended to the industrial large-scale production processes through new techniques.

As Anastas<sup>2</sup> pointed out, the guided principle is the design of environmentally benign products and processes (benign by design). This concept is embodied in the 12 Principles of Green Chemistry, which can be summarised as follow:<sup>3</sup>

1. Prevention: It is better to prevent that to clean or to treat afterwards (waste or pollution). This is a fundamental principle. The developed action can change dramatically many attitudes among scientists developed in the last decades. Most of the chemical processes and synthetic routes produce waste and use toxic substances. Green

---

<sup>1</sup> P. Anastas, J. Warner, *Green Chemistry: Theory and Practice*, 1998, Oxford University Press: New York.

<sup>2</sup> P. Anastas, T. Williamsom, *Green Chemistry: Frontiers in Chemical Synthesis and Processes*, 1998, Oxford University Press, Oxford.

<sup>3</sup> P. Anastas, M. Kirchoff, *Acc. Chem. Res.*, 2002, 35, 686-693.

Chemistry can prevent the formation of waste and toxic by-products by designing the chemical processes in advance and by introducing innovative changes using alternative and non-hazardous, non-toxic reagents and feedstocks.

2. Maximise synthetic methods, Atom Economy: All synthetic methods until now were wasteful and their yields between 70-90%. Green Chemistry supports that synthetic methods can be designed in advance to maximise the incorporation of all reagents used in the chemical process into the final product, eliminating the need of recycling the by-products. The concept of Atom Economy was developed by Barry Trost of Stanford University (USA), for which he received the Presidential Green Chemistry Challenge Award in 1998.<sup>4</sup> It describes the conversion efficiency of a chemical process in terms of all atoms involved (desired products produced). In an ideal chemical process, the amount of starting materials or reactants equals the amount of all products generated and no atom is wasted.
3. Less hazardous chemical syntheses: Green Chemistry must strive, wherever practical, to design safer synthetic methods by using less toxic substances as well as less toxic byproducts of the synthesis. Less toxic materials mean lower hazards to workers in industry and research laboratories and less pollution to the environment.
4. Designing safer chemicals: Design must become a fundamental aim of Green chemists affecting the optimisation of the desired function and properties of the chemical product while minimising their toxicity to humans and the environment. At present, there are around 100.000 chemical substances and materials in the market. Most of these substances have been characterised as to their physiochemical properties and toxicities, but there is lack of ecotoxicological data for most of them. From the 1980s there is a more stringent regulation and new chemicals are monitored more effectively currently.
5. Safer solvents and auxiliary substances: Solvents, separation agents and auxiliary chemicals used in synthetic chemistry must be avoided, replaced or reduced with less toxic chemicals.
6. Design for energy efficiency: Chemists must recognise that until now there was very little thought to energy requirements in chemical synthetic processes. Designing more efficient methods is a necessity and if possible synthetic methods should be conducted at room temperature and pressure to reduce energy requirements.

---

<sup>4</sup>Trost, B. M., *Angew Chem. Int. Ed. Engl.*, 1995, 34 (3), 259-281.

7. Use of renewable raw materials and feedstocks: Starting raw materials for synthetic processes are mostly petrochemical substances and products of refining. Raw materials must have very low toxicity and if possible to be renewable, rather than depleting. We know that there are many practical problems in finding renewable raw materials. Green chemists must change the manufacturing process by discovering renewable chemicals and how to transform them.
8. Reduce intermediate derivatives: Chemists must aim for reducing unnecessary derivatisation (use of blocking groups, protection/deprotection techniques and temporary modification of physical and chemical processes) in the synthetic routes. These derivatisations use additional reagents, are wasteful and produce large amounts of by-products and waste. The principle reminds chemists to change their old ways of producing chemicals. Designing new chemical synthetic routes are desirable.
9. Catalysis: The use of catalysts is well known that can change dramatically the efficiency of chemical reactions and the yield of products. Catalytic reagents with great selectivity can be superior to stoichiometric reagents. New catalysts and more emphasis on catalytic processes is the future of green chemistry techniques.
10. Design products that degrade easily: Most chemical products and consumer items do not degrade very easily, thus causing environmental problems. Green Chemistry aims at designing products so that at the end of their useful life they break down into innocuous materials. Persistence into the environment is a negative aspect of many consumer products (e.g. plastic products) and this can be reversed by designing products that degrade in a shorter time.
11. Real-time analysis for pollution prevention: Analytical methodologies need to be further developed to allow for real time, in-process, monitoring and control prior to the formation of hazardous substances.
12. Inherently safer chemistry for accident prevention: Raw materials and chemical substances used in chemical process should be inherently safe, i.e. their properties and their degradation products to be non-toxic and not dangerous (e.g. to explode, to be flammable, allergic to humans, cause burns to skin, etc.). Green Chemistry aims to stop the use of dangerous materials for the health and safety of workers and consumers.

Implementing these Green Chemical Principles requires a certain investment, since the current, very inexpensive chemical processes

must be redesigned. However, in times when certain raw materials become more expensive and also the costs for energy increase, such an investment should be paid back as the optimised processes become less expensive than the un-optimised ones. Therefore, the development of greener procedures can be seen as an investment for the future, which also helps to ensure that the production complies with possible upcoming future legal regulations.

The key question to address is: what alternatives can be developed and used? In addition, we must ensure that future generations can also use these new alternatives. “Sustainability” is a concept that is used to distinguish methods and processes that can ensure the long-term productivity of the environment, so that even subsequent generations of humans can live on this planet. Sustainability has environmental, economic, and social dimensions. A very general definition of sustainability or sustainable development is the definition by the World Commission on Environment and Development (WCED):<sup>5</sup> “forms of progress that meet the needs of the present without compromising the ability of future generations to meet their needs”.

If we define sustainability as “meeting economic, social and environmental needs” (see Figure 1.1), and if we focus our attention on the obtaining or production of Pharmaceutical compounds, it takes a constant and constantly growing effort:<sup>6</sup>

- ❖ To render the supply processes by which the pharmaceutical industry delivers their products sustainable.
- ❖ To avoid shortages of well-known drugs.
- ❖ To allow continuing the reliable supply of much-needed medicaments to those who need them.

If we analyse that part by part, a supply process is economically sustainable if it allows the supplier to meet market requirements of the supplied product in a desirable way. Among the many factors affecting economical sustainability, such as logistics and inventory turnover ratio, we focus on the contribution of the API (Active Pharmaceutical Ingredients) and drug product (DP) manufacturing processes. The manufacturing process contributes in the following ways:<sup>5</sup>

- ❖ Ability to use economically favourable starting materials.
- ❖ Ability to use economically favourable infrastructure.

---

<sup>5</sup> World Commission on Environment and Development (WCED), *Our Common Future*, 1987, Oxford University Press, Oxford, p.43.

<sup>6</sup> P. Poehlauer, W. Skranc, *Sustainable Flow Chemistry: Methods and Applications* (Ed.: L. Vaccaro), 2017, Wiley-VCH, Weinheim (Germany), Chapter 4, 73-102.

- ❖ Efficient conversion to desired product in the required quality.
- ❖ Efficient use of energy.
- ❖ Ability to quickly respond to changing volume demand.
- ❖ Reliable process transfer between different production sites.
- ❖ Opportunity for continuous improvement.



**Figure 1.1. Sustainability and its various faces: economic, social and environmental aspects constitute sustainability as a whole.**

On the other hand, if we look at the sustainability from a social point of view, according to the Western Australia Council of Social Services (WACOSS),<sup>7</sup> “Social sustainability occurs when the formal and informal processes, systems, structures and relationships actively support the capacity of current and future generations to create healthy and liveable communities”. So in this moment one question comes to our minds: how can an efficient manufacturing of pharmaceutical products contribute here?

As Poehlauer and Skranc suggested,<sup>6</sup> future designers of APIs will consider their degradation after intended use already in the lead optimisation phase and thus offer new opportunities for product replacements. There are initial conceptual examples of “redesigns” of APIs for better biodegradability,<sup>8</sup> and this might ultimately lead to the replacement of old pharmaceuticals designed for “therapeutic effect only” by biodegradable substances with comparable, if not better, therapeutic effects. The pharmaceuticals to be replaced are widespread,

<sup>7</sup> W. M. Adams, *The Future of Sustainability: Re-thinking Environment and Development in the Twenty-first Century*. Report of the IUCN Renowned Thinkers Meeting, 2006, January 29-31.

<sup>8</sup> T. Rastogi, C. Leder, K. Kümmerer, Re-design of existing pharmaceuticals for environmental biodegradability: a tiered approach with  $\beta$ -blocker propranolol as an example, *Environ. Sci. Technol.*, 2015, 49(19), 11756-11763

have been on the market for decades, and many of them have been given in high doses. So the manufacturing processes of their replacements will have to supply large volumes of the respective medicines in an efficient and inexpensive way.

Finally we should pay attention to the environmentalist point of view. For that, some commonly accepted methods to measure sustainability exist. If we want to know how green a process is then we need metrics to measure greenness. If we focus on the Chemical Efficiency we have the Atom Economy and the E-Factor. Moreover we have mass-based metrics such as the PMI (Process Mass Intensity) or the RME (Reaction Mass Efficiency). However, mass-based metrics should be complemented by metrics that measure the environmental impact of waste, such as LCA (Life Cycle Assessment).

The first and oldest green chemistry metrics – E-factor and Atom Economy – were introduced in the early 1990s. Atom Economy (AE) has been introduced before while explaining the 12 principles of Green Chemistry.<sup>4</sup> AE is a theoretical number which assumes the use of exact stoichiometric quantities of starting materials and a chemical yield of 100%, and disregards substances, such as solvents and chemicals used in the work-up of the reaction mixture, which do not appear in the stoichiometric equation.<sup>9</sup> Atom Economy (AE) is an extremely useful tool for quickly evaluation because no experiments are needed. Moreover, AE could be used for comparing alternative routes to a particular product.

The E-Factor was proposed by Roger Sheldon<sup>10</sup> to relate the mass of a desired product to the mass of total waste generated in its synthesis. It is generally calculated as:

$$E \text{ Factor} = \frac{\text{quantity of total waste (kg)}}{\text{quantity of product obtained (kg)}}$$

A higher *E* factor means more waste and, consequently, greater negative environmental impact. The ideal *E* factor is zero, perfectly in line with the first of the twelve principles of Green Chemistry. In the table 1.1, the values for the main sectors in the chemical industry can be seen. The advantages of this metric are i) may be used to compare different processes ii) it takes into account the use of solvents and work-up agents (not considered in AE) iii) AE is applied to individual steps but

---

<sup>9</sup> R. A. Sheldon, *Green Chem.*, 2017, 19, 18-43.

<sup>10</sup> R. A. Sheldon, Catalysis and pollution prevention, *Chem. Ind. (London)*, 1997, 1, 12-15.

the *E* factor can easily be applied to a multi-step process thus facilitating a holistic assessment of a complete process. But there is also one inconvenient: it does not differentiate between different kinds of waste (aqueous, toxic, recyclable, etc.). So for a complete environmental information of a process, additional details need to be given. For this reason, new metrics were necessary and the PMI (Process Mass Intensity) was defined<sup>11</sup> by the pharmaceutical industry itself together with the American Chemical Society's Green Chemistry Institute®.

$$PMI = \frac{\text{quantity of raw materials input (kg)}}{\text{quantity of bulk API output (kg)}}$$

PMI incorporates starting materials, reagents and other reaction components. PMI allows easily comparing different routes or strategies to reach a certain API.

Industry Sector	Tonnes per annum	<b><i>E</i> factor</b> (kg waste per kg product)
Oil refining	10 <sup>6</sup> - 10 <sup>8</sup>	<0.1
Bulk chemicals	10 <sup>4</sup> - 10 <sup>6</sup>	<1-5
Fine chemicals	10 <sup>2</sup> - 10 <sup>4</sup>	5-50
Pharmaceuticals	10 - 10 <sup>3</sup>	<b>25 - &gt;100</b>

Table 1.1. *E* factors in the chemical industry

Despite the appearance of new mass-based metrics of sustainability like PMI or RME (Reaction Mass Efficiency), in opinion of R. A. Sheldon<sup>9</sup> none of these alternative metrics offer any particular advantage over the *E* factor for describing how wasteful a process is. For example the ideal PMI is 1, whereas the ideal *E* factor is 0, which more clearly reflects the ultimate goal of zero waste. The *E* factor also has the advantage that, in evaluating a multi-step process, *E* factors of individual steps are additive but PMIs are not because PMI doesn't discount step products from the mass balance.<sup>12</sup>

Anyway, the initial *E* factor concept has been further developed. More recently, the use of simple *E* factors (sEF) and complete *E* factors (cEF), depending on the stage of development of the process has been suggested.<sup>12</sup> The sEF doesn't take solvents and water into account and

<sup>11</sup> D. J. C. Constable, A. D. Curzons, V. L. Cunningham, Metrics to 'green' chemistry – which are the best?, *Green Chem.*, 2002, 4, 521-527.

<sup>12</sup> F. Roschangar, R. A. Sheldon, C. H. Senanayake, *Green Chem.*, 2015, 17, 752-768

is more appropriate for early route scouting activities, whereas the cEF accounts for all process materials including solvents and water, assuming no recycling, and is more appropriate for total waste stream analysis.<sup>13</sup> Moreover, in the original publication of the *E* factor water wasn't taken into account. The reason was that including it could mean a skewing of *E* factors and render meaningful comparison of processes difficult. However, the tendency in the pharmaceutical industry has been to include water in the *E* factor due mainly to the need of studying properly the biocatalytic processes where water has an important role.

All the metrics discussed above take only the mass of waste generated into account. One limitation is that they assign the same weighting to all types of waste. However, the environmental impact of the waste must be considered. One kg of sodium chloride doesn't have the same impact on the environment as 1 kg of a chromium salt or 1 kg of dichloromethane. This was though when the first *E* factor was introduced in 1992 and, therefore, an 'environmental quotient' (EQ) was also introduced.<sup>14</sup> This quotient is an arbitrarily multiplier "Q" assigned to the different substances depending on its toxicity, ease of recycling, etc. The problem is that arbitrariness makes this "Q" multiplier very debatable and much attention has been devoted in the last two decades to developing methodologies for quantification of "Q" values.<sup>15,16</sup> During this search appeared the option of the LCA (Life Cycle Assessment),<sup>17,18,19</sup> a methodology specifically designed to assess the environmental impact of all stages of a product's life from raw materials extraction through materials processing to distribution, use and disposal or recycling, the so called from-cradle-to-grave analysis. This metric was originally created by The Coca Cola Company in 1969 to quantify the environmental impact of the beverage cans and the term LCA was coined for the first time at the first international workshop sponsored by the Society of Environmental Technology and Chemistry (SETAC) in 1990.<sup>20</sup> Around the turn of the century, it was recognised that LCA could be used to compare the environmental footprints of conventional organic syntheses with green alternatives and the study of

---

<sup>13</sup> R. A. Sheldon, *ACS Sustainable Chem. Eng.*, 2018, 6(1), 32-48.

<sup>14</sup> R. A. Sheldon, *CHEMTECH*, 1994, 38-47.

<sup>15</sup> M. Eissen, J. O. Metzger, *Chem. Eur. J.*, 2002, 8, 3580-3585.

<sup>16</sup> K. van Aken, L. Strekowski, L. Patiny, *Beilstein J. Org. Chem.*, 2006, 2(3), 1-7.

<sup>17</sup> M. A. Curran, *Curr. Opin. Chem. Eng.*, 2013, 2, 273-277.

<sup>18</sup> J. G. Moretz-Sohn Monteiro, O. de Queiroz Fernandes Araujo, J. L. de Medeiros, *Clean. Technol. Environ. Policy*, 2009, 11, 459-472.

<sup>19</sup> G. Finnveden, M. Z. Hauschild, T. Ekvalli, T. Guinée, R. Heijungs, S. Hellweg, A. Koehler, D. Pennington, S. Suh, *J. Environ. Manage.*, 2009, 91, 1-21.

<sup>20</sup> J. A. Fava, A. Smerek, A. B. Heinrich, L. Morrison, in *Background and Future Prospects in Life Cycle Assessment* (Ed.: W. Köpffer), Springer, Dordrecht, 2014, 39-83.



the chemical processes sustainability using LCA was subsequently described by several authors.<sup>21,22,23,24,25</sup>

Full-scale cradle-to-grave LCAs are useful for comparing products and processes that have already been commercialised; nevertheless, their application to research laboratory scale is generally too difficult and time consuming.<sup>26</sup> The application of LCA to the synthesis of fine chemicals and APIs is particularly challenging owing to the acute lack of life cycle inventory data<sup>27,28</sup> and to the absence of a coherent framework for characterising the toxicological impacts of chemicals.<sup>29</sup>

After this overview, maybe the Atom Economy (AE) and the *E* factor are revealed as the most useful metrics for our interests. We shouldn't forget that the concepts of Atom Economy and *E* factor have motivated industrial and academic chemists worldwide to explicitly consider waste generation, in addition to the common criteria such as synthetic convergence or chemical yield, when designing a synthesis of a target molecule.<sup>9</sup>

So, arrived to this point and after having defined the characteristics of a sustainable process, we need to be concerned with how to achieve organic syntheses as green or sustainable as possible, especially focusing on the obtaining of APIs or compounds or intermediates of interest for pharmaceutical industries. As we have seen in the Table 1.1 the *E* factor for the pharmaceutical industry is higher, as compared with other chemical branches, and it is clearly a point for improvement. For this purpose there are some important sustainable technologies available. In the context of this work we will concentrate our efforts on the use of catalysts to develop more efficient processes, on the use of greener solvents (with less impact in the environment) or on the full elimination of solvents if possible, and on the use of continuous flow systems instead of batch reactors to develop more efficient and greener synthetic organic transformations. These sustainable technologies or

---

<sup>21</sup> T. Graedel, *Green Chem.*, 1999, 1, G126-G128

<sup>22</sup> P. T. Anastas, R. L. Lankey, *Green Chem.*, 2000, 2, 289-295

<sup>23</sup> X. Domenech, J. A. Ayllon, I. Peral, *Environ. Sci. Technol.*, 2002, 36, 5517-5520

<sup>24</sup> L. M. Gustaffson, P. Börjesson, *Int. J. Life Cycle Assess.*, 2007, 12(3), 151-159

<sup>25</sup> L. M. Gilbertson, J. B. Zimmerman, D. L. Plata, J. E. Hutchinson, P. T. Anastas, *Chem. Soc. Rev.*, 2015, 44, 5758-5777.

<sup>26</sup> L. M. Tufvesson, P. Tufvesson, J. M. Woodley, P. Börjesson, *Int. J. Life Cycle Assess.*, 2013, 18, 431-444.

<sup>27</sup> G. Köller, U. Fischer, K. Hungerbühler, *Ind. Eng. Chem. Res.*, 2000, 36, 960-972.

<sup>28</sup> G. Wernet, S. Conradt, H. P. Isenring, C. Jiménez-González, K. Hungerbühler, *Int. J. Life Cycle Assess.*, 2010, 15, 294-303.

<sup>29</sup> D. Cespi, E. S. Beach, T. E. Swarr, F. Passarinin, I. Vassura, P. J. Dunn, P. T. Anastas, *Green Chem.*, 2015, 17, 3390-3400.

strategies are closely related with the 12 principles Green Chemistry seen above.

### 1.2. Catalysis

Some of the major advances in chemistry, especially in industrial chemistry, over the past generation have been achieved in the area of catalysis.<sup>30</sup> A major cause of waste, particularly in fine chemicals and pharmaceuticals manufacture, is the use of stoichiometric, mainly inorganic, reagents in organic synthesis. The solution is evident: substitution of archaic stoichiometric methodologies for others with atom economic catalytic alternatives. Catalysis has not only advanced the level of efficiency but has also brought about concurrent environmental benefits. Through the use of new catalysts, chemist have found ways of removing the need of large quantities of reagents that would otherwise have been needed to carry out the transformations, and would ultimately have contributed to the waste stream. Catalysts also can be used to improve the selectivity of a chemical reaction. The use of catalysts appears itself as one of the essential 12 principles of the Green Chemistry. In short, one of the keys to green and sustainable chemistry is the use of catalysis in organic synthesis.<sup>30</sup>

Among the different types of catalysts we can find – heterogeneous, homogeneous, organocatalysts, organometallic catalysts, biocatalysts – for being used on organic synthesis, the ones that more advantages could present are the heterogeneous ones. Organocatalysts, organometallic catalysts and biocatalysts can be immobilised to work under heterogeneous conditions. Supported catalysts are easier to separate from the reaction crude by simple filtration and reuse. In the table 1.2 a comparison between homogeneous and heterogeneous catalysis is made.

However, some of the item values of the table 1.2 are not strictly true. The mentioned table expresses the most general ideas existent if we analyse the opinions from the literature. Many authors conform to the idea that supported catalysts are less efficient than homogeneous ones in terms of activity, stability and selectivity, in particular enantioselectivity.<sup>31</sup> Despite of that, the reality is luckily very different

---

<sup>30</sup> R. Arthur, I. Arends, U. Hanefeld, *Green Chemistry and Catalysis*, 2007, Wiley-VCH, Weinheim.

<sup>31</sup> S. Hibner, J. G. de Vries, V. Farina, *Adv. Synth. Catal.*, 2016, 358, 3-25.

and the presence of the support matrix can affect in a positive way these three parameters. The belief that the polymeric matrix has no effect, in the best case, or a negative one should be denied. Of course, the idea is to use advantageously the presence of the matrix to increase the efficiency of the supported catalytic species over that of the related homogeneous ones.

	<b>Homogeneous</b>	<b>Heterogeneous</b>
<b>Activity</b>	<b>Very good</b>	<b>Good</b>
<b>Selectivity</b>	<b>High</b>	<b>Less controllable</b>
<b>Concentration</b>	<b>Low</b>	<b>High</b>
<b>Life - Stability</b>	<b>Maybe low</b>	<b>High regeneration</b>
<b>Recovery</b>	<b>Difficult</b>	<b>Easy</b>
<b>Reproducibility</b>	<b>High</b>	<b>Poor</b>
<b>Study</b>	<b>Simple</b>	<b>Hard</b>
<b>Modification</b>	<b>Easy</b>	<b>Less affordable</b>
<b>Technology</b>	<b>Scarce</b>	<b>Elevated</b>
<b>Industrial use</b>	<b>Smaller</b>	<b>Bigger</b>

Table 1.2. Comparison between homogeneous and heterogeneous catalysts.

### **1.2.1. Supported catalysis : effects of the immobilisation support**

Another erroneous idea is that the best homogeneous catalyst will remain the best upon immobilisation, forgetting the fact that the support is not an inert matrix. The support not only determines the diffusion of the reagents to reach the catalytic active sites, also defines the new microenvironment for these catalysts. The effects of the organic polymeric matrices used as supports for catalysts has been excellently reviewed very recently by our group.<sup>32</sup>

If we talk about supported catalysts, we should start enumerating the different immobilisation strategies: ion-pair formation, encapsulation, entrapment or the most used strategy: covalent bonding, as this limits the potential leaching of the catalytically active components. Covalent bonding is the most reliable one in this regard.

Merrifield type resins (polystyrene and styrene/divinylbenzene copolymers) are the most common supports used for the preparation of

<sup>32</sup> B. Altava, M. I. Burguete, E. García-Verdugo, S. V. Luis, *Chem. Soc. Rev.*, 2018, 47, 2722-2771.

immobilised catalysts.<sup>33</sup> The wide use of these supports is due to their stability and compatibility with a broad range of reaction conditions. Moreover, these resins present reasonable high loadings of chloride groups (>1mmol/g), which allows the possibility of large number of post-functionalisation processes.<sup>34</sup>

The activity of the resulting supported catalyst is first dependent on the nature and the morphology of the polymer network, because this is going to control the diffusion of reagents and substrates into the active sites, ergo the accessibility of the active catalytic sites.<sup>35</sup> Microporous or gel-type polymeric supports do not have permanent porosity and swelling with an appropriate solvent is necessary to convert the catalytic sites inside the bead in accessible sites.<sup>36</sup> Depending on the crosslinking degree (necessary to obtain insoluble materials, usually 1-4% in Merrifield resins), some regions of the polymer will be more or less accessible. Too high crosslinking means less effective swelling and slower reaction rates due to less accessibility to the catalytic sites and this will be much dependent also on the solvent used.<sup>37</sup>

The use of alternative macroporous polymers with permanent porosity is a possibility to minimise diffusional limitations in the polymeric bead. In this case, the functional sites are distributed both at the surface, where the accessibility is improved and does not depend very much on the solvent used, and at the interior of dense polymer particles, which will not be easily accessible. With macroporous polymers, the activity of the resulting supported catalysts will depend on the balance between surface and non-surface sites.<sup>32</sup>

In the search of minimising the diffusion problems, it is worth to highlight the advantages of polymeric macroporous monoliths and porous organic polymers as supports. Macroporous monoliths present good diffusional properties due to a complex network of permanent pores in a continuous material integrated with highly crosslinked particles.<sup>38</sup> Monoliths could be moulded according to the required use but sometimes present problems in the reuse.<sup>39</sup> With porous organic polymers, enhanced accessibility of active sites and less diffusional

---

<sup>33</sup> J. Lu, P. H. Toy, *Chem. Rev.*, 2009, 109, 815-838.

<sup>34</sup> M. Benaglia, A. Puglisi, F. Cozzi, *Chem. Rev.*, 2003, 103, 3401-3430.

<sup>35</sup> B. Corain, M. Zecca, K. Jeràbek, *J. Mol. Catal. A: Chem.*, 2001, 177, 3-20.

<sup>36</sup> P. Hodge, *Chem. Soc. Rev.*, 1997, 26, 417-424.

<sup>37</sup> B. P. Santora, M. R. Gagné, K. G. Moloy, N. S. Radu, *Macromolecules*, 2001, 34, 658-661.

<sup>38</sup> M. R. Buchmeiser, *Polymer*, 2007, 48, 2187-2198.

<sup>39</sup> F. Svec, *J. Chromatogr. A*, 2010, 1217, 902-924.

limitations are found thanks to the properties of these materials: large BET surface areas and pore volumes.<sup>40</sup>

If the activity is related with the degree of diffusion, temperature will also affect the activity in supported catalysts. An important decrease of the activity is often found when lowering the temperature.<sup>32</sup>

To avoid possible polymeric negative effects (generally associated with the bulky polymeric matrix) to the catalytic properties, spacers have been used to attach the catalyst to the polymer far from the active site.<sup>41,42</sup> With that, the catalyst would be able to mimic a solution-like behaviour. Moreover, with this strategy, the accessibility to the functional sites inside the bed is also improved, promoting more active catalytic supported systems. F. Montanari and co-workers found that the use of long aliphatic spacers (up to 10 methylene units) and low crosslinking degrees (1%) increased the corresponding activities 2-4 times in polymer-supported phase transfer catalysts.<sup>43</sup> However, sometimes the spacer itself could play a non-innocent role in the catalysis by the modification of the hydrophobic/hydrophilic balance or the presence of an additional group. The election of the spacer should be carefully studied. An example of linker type broadly exploited are those with the 1,2,3-triazole moiety as the attachment point.<sup>44,45</sup>

The activity of a supported catalyst will also be affected by the presence and content of neighbouring groups in the polymeric matrix.<sup>46</sup> For example, the presence of functional groups able to favour the swelling with a given solvent can minimise the diffusional limitations in gel-type resins.<sup>32</sup>

Sometimes, the activity of polymer-bound supported catalysts is increased by low levels of functionalisation due to the so-called pseudodilution effect. Higher loadings meaning higher functionalisations could favour site to site interactions, which decrease the catalytic efficiency.<sup>47</sup>

---

<sup>40</sup> S. Das, P. Heasman, T. Ben, S. Qiu, *Chem. Rev.*, 2017, 117, 1515-1563.

<sup>41</sup> M. Watanabe, K. Soai, *J. Chem. Soc., Perkin Trans. 1*, 1994, 837-842.

<sup>42</sup> K. Soai, M. Watanabe, *Tetrahedron: Asymm.*, 1991, 2, 97-100.

<sup>43</sup> P. L. Anelli, B. Czech, F. Montanari, S. Quici, *J. Am. Chem. Soc.*, 1984, 106, 861-869.

<sup>44</sup> D. Font, S. Salayero, A. Bastero, C. Jimeno, M. A. Pericàs, *Org. Lett.*, 2008, 10, 337-340.

<sup>45</sup> C. Ayats, A. H. Henseler, M. A. Pericàs, *ChemSusChem*, 2012, 5, 320-325.

<sup>46</sup> S. D. Alexandratos, D. H. J. Miller, *Macromolecules*, 2000, 33, 2011-2015.

<sup>47</sup> L.-J. Zhao, C. K.-W. Kwong, M. Shi, P. H. Toy, *Tetrahedron*, 2005, 61, 12026-12032.

Regarding stability in supported catalysis, it exists a common confusion that should be avoided. An easier separation and reuse of the supported catalyst can contribute significantly to enhance their lifetime, but does not always mean that the catalytic species remains active in the polymeric support. Despite of that, it has been confirmed with many different experimental data that immobilisation onto a support greatly improves the stability of a catalyst, allowing several reuses.<sup>48</sup> Examples of supported catalysts reused for 15 or more runs can be found.<sup>49</sup> Moreover, in some situations the reuse is done in different processes which adds value to the immobilisation.<sup>50</sup>

One of the positive effects of the immobilisation is the improved stability for air/water sensitive catalytic species due to the formation of hydrophobic cavities around the active sites. It happens with polystyrene-divinyl benzene (PS-DVB) and related resins having hydrophobic polymeric matrix.<sup>32</sup>

It is also important to consider the chemical stability of the catalytic entities being immobilised. Sometimes a deactivation of the catalytic species occurs and regeneration is needed after a certain number of runs. This reduction in activity can also be counterbalanced by increasing the reaction time during the new runs.<sup>49</sup> For that reason, it is not only important to know the number of runs that a supported catalyst can afford, but the activity and selectivity during these successive runs should be also known. The reused catalyst must behave efficiently. Due to that, TOF (turnover frequency, related with the efficiency of the catalyst) and TON (turnover number, related with lifetime robustness) values are so important.<sup>51</sup>

In some instances, a grade of deactivation of the immobilised catalyst is observed during the first run until reaching a constant level of activity. This case normally means that the most accessible catalytic sites are easily and quickly deactivated.<sup>32</sup>

In supported organometallic catalysts the deactivation is usually related to the leaching of the metal species non-covalently bound to the support<sup>52</sup> and to the formation of deactivated metal species that remain

---

<sup>48</sup> V. A. Larionov, T. Cruchter, T. Mieke, E. Meggers, *Organometallics*, 2017, 36, 1457-1460.

<sup>49</sup> T. Nagashima, H. M. L. Davies, *Org. Lett.*, 2002, 4, 1989-1992.

<sup>50</sup> V. Sans, F. Gelat, N. Karbass, M. I. Burguete, E. García-Verdugo, S.V. Luis, *Adv. Synth. Catal.*, 2010, 352, 3013-3021.

<sup>51</sup> S. Kozuch, J. M. L. Martin, *ACS Catal.*, 2012, 2, 2787-2794.

<sup>52</sup> J. M. Fraile, J. I. Garcia, J. A. Mayoral, *Chem. Rev.*, 2009, 109, 360-417.

in the matrix.<sup>53</sup> To avoid or control leaching phenomena that occurs in supported systems based on metal nanoparticles, in particular PdNPs, catch and release strategies have been developed.<sup>50</sup> It is necessary to add some elements, like for example scavengers, to recapture the leached nanoparticles and improve the stability.

When deactivated metal species are formed, a regeneration of these supported species is needed. Sometimes the regeneration protocols for organometallic supported species require strong conditions (acids, bases, etc.) that could affect the support if are not carefully done. In other instances, the reusing is done simply by adding some extra amounts of the catalytic metal in the reaction mixture, which is not strictly a reuse of the catalytic species, but a reuse or recycle of the support.<sup>32</sup> In this regard, the use of macroporous polymers with a high and adjustable crosslinking degree and well-designed porosity could limit some of those deactivation mechanisms, increasing the turnover and the lifetime of the catalyst.<sup>54,55</sup>

The selectivity of a chemical reaction is based on very small differences in the transition state energies. Therefore, selectivity is very sensitive to any little change in the reaction conditions or in the environment. With supported catalysts, the polymeric framework is the main factor in determining the final microenvironment for the catalytic site. This explains the key role that the support has on the selectivity. However, in some instances, structural changes are needed in the catalyst to provide the required features for immobilisation. And these changes are the responsible for the selectivity variations and not the immobilisation itself.<sup>32</sup>

It is often considered that selectivity decreases with the immobilisation, especially if we talk about enantioselectivity in chiral supported catalysts. But this is not always true. Immobilisation can produce either positive or negative effects on selectivity, and positive effects can be achieved with an appropriate design.<sup>56</sup> Of course, both positive and negative effects can sometimes be minimised attaching the catalyst through a long spacer.<sup>57</sup>

---

<sup>53</sup> R. Drake, D. C. Sherrington, S. J. Thompson, *J. Chem. Soc., Perkin Trans. 1*, 2002, 1523-1534.

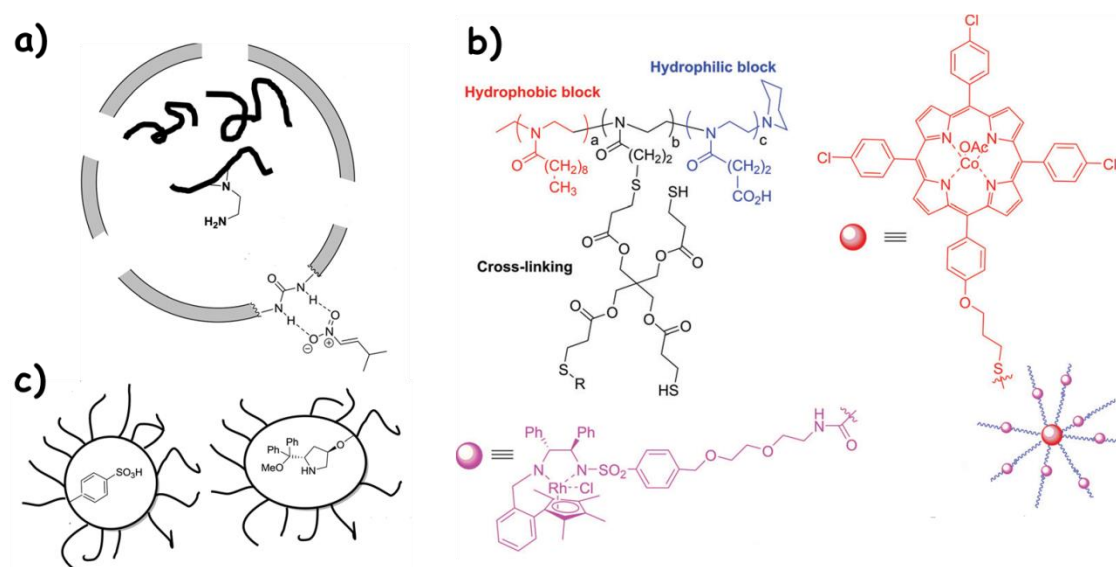
<sup>54</sup> M. Rueping, E. Sugiono, A. Steck, T. Theissmann, *Adv. Synth. Catal.*, 2010, 352, 281-287.

<sup>55</sup> T. Gokmen, F. E. Du Prez, *Prog. Polym. Sci.*, 2012, 37, 365-405.

<sup>56</sup> M. I. Burguete, A. Cornejo, E. García-Verdugo, M. J. Gil, S. V. Luis, J. A. Mayoral, V. Martínez-Merino, M. Sokolova, *J. Org. Chem.*, 2007, 72, 4344-4350.

<sup>57</sup> A. Mandoli, R. Garzelli, S. Orlandi, D. Pini, M. Lessi, P. Salvadori, *Catal. Today*, 2009, 140, 51-57.

Finally, it is worth to comment a very interesting possibility that supported catalysis allows. The preparation of active multi-catalytic systems with incompatible individual catalysts is possible.<sup>58</sup> Two non-compatible catalysts, that combined in solution would become inactive, can be immobilised on polymeric phases achieving the isolation of the different catalytic sites and giving an active multi-catalytic system.<sup>59</sup> This immobilisation strategy allows performing one-pot multistep catalytic reactions.<sup>60</sup> Novel approaches for exploiting this possibility are the use of sol-gel and star polymers,<sup>61</sup> polymeric microcapsules<sup>62</sup> and shell cross-linked micelles (SCMs).<sup>63</sup> (see Figure 1.2)



**Figure 1.2.** a) Scheme of a urea polymeric microcapsule b) scheme of Shell cross-linked micelles (SCMs) c) scheme of star polymers.<sup>32</sup>

<sup>58</sup> M. C. M. van Oers, F. P. T. Rutjes, J. C. M. Van Hest, *Curr. Opin. Biotechnol.*, 2014, 28, 10-16.

<sup>59</sup> B. Voit, *Angew. Chem. Int. Ed.*, 2006, 45, 4238-4240.

<sup>60</sup> N. T. S. Phan, C. S. Gill, J. V. Nguyen, Z. J. Zhang, C. W. Jones, *Angew. Chem. Int. Ed.*, 2006, 45, 2209-2212.

<sup>61</sup> B. Helms, S. J. Guillaudeu, Y. Xie, M. McMurdo, C. J. Hawker, J. M. J. Fréchet, *Angew. Chem. Int. Ed.*, 2005, 44, 6384-6387.

<sup>62</sup> B. P. Mason, A. R. Bogdan, A. Goswami, D. T. McQuade, *Org. Lett.*, 2007, 9, 3449-3451.

<sup>63</sup> L.-C. Lee, J. Lu, M. Weck, C. W. Jones, *ACS Catal.*, 2016, 6, 784-787.



### 1.3. Solvents

A major source of waste in chemicals manufacture, particularly in the pharmaceutical industry, is solvent losses. Moreover, so many of the favourite organic solvents of synthetic chemists, such as chlorinated hydrocarbons, have been blacklisted so the whole question of solvent use requires rethinking and has become a primary focus in the pharmaceutical industry.<sup>64</sup> In fact, the problem of solvent waste has been identified in the 12 principles of the Green Chemistry. Thus, an inventorisation of waste formed in pharmaceuticals manufacture revealed that solvents and water accounted for 58% and 28%, respectively, of the process waste compared to 8% for the raw materials.<sup>12</sup> According to another report,<sup>65</sup> solvents constitute 80-90% of the non-aqueous mass of materials used to make APIs. It has been estimated that solvents account for 50% of green-house gas emissions from pharmaceutical manufacture.<sup>66</sup>

Dipolar aprotic solvents are often deemed to be indispensable to the pharmaceutical industry where they are widely used as reaction media for nucleophilic substitutions and other reactions.<sup>9</sup> Acetonitrile, dimethylformamide (DMF) or dimethyl sulfoxide (DMSO) for example, all of them have significant toxicity or safety issues. A broader screening of other solvents was recommended but safe neoteric solvents have not been enough examined. Neoteric solvents include ionic liquids, supercritical fluids, fluorinated solvents, water and solvents from renewable raw materials, such as ethyl lactate and 2-methyl tetrahydrofuran (2-MeTHF). Only the use of 2-MeTHF grew significantly in the period 1997-2012.<sup>67</sup>

The clear need for replacement and/or reduction in the use of organic solvents in API manufacture led pharmaceutical companies to develop solvent guides to promote this process including here, for example, GSK (GlaxoSmithKline),<sup>68</sup> Pfizer<sup>69</sup> or Sanofi.<sup>70</sup> A good example of appropriate

---

<sup>64</sup> R. A. Sheldon, *Green Chem.*, 2005, 7, 267-278.

<sup>65</sup> D. J. C. Constable, C. Jiménez-González, R. K. Henderson, *Org. Process Res. Dev.*, 2007, 11, 133-137.

<sup>66</sup> C. Jiménez-González, A. D. Curzons, D. J. C. Constable, V. L. Cunningham, *Clean Technol. Environ. Policy*, 2005, 7, 42-50.

<sup>67</sup> C. W. Cho, T. P. T. Pham, Y. C. Jeon, Y. S. Yun, *Green Chem.*, 2008, 10, 67-72.

<sup>68</sup> A. D. Curzons, D. J. C. Constable, V. L. Cunningham, *Clean Technol. Environ. Policy*, 1999, 1, 82-90.

<sup>69</sup> K. Alfonsi, J. Colberg, P. J. Dunn, T. Fevig, S. Jennings, T. A. Johnson, H. P. Kleine, C. Knight, M. A. Nagy, D. A. Perry, M. Stefaniak, *Green Chem.*, 2008, 10, 31-36.

procedures is the redesign of Pfizer's sertraline manufacturing process.<sup>71</sup> Among other improvements, a three step sequence was streamlined by employing ethanol as the sole solvent, thus eliminating the need to use, distil and recover four solvents (methylene chloride, tetrahydrofuran, toluene and hexane).

There is currently a marked trend away from hydrocarbons and chlorinated hydrocarbons as solvents and towards lower alcohols, esters and, in some cases, ethers. More recently, attention has been focused on the use of solvents derived from renewable biomass (see Figure 1.3).<sup>72</sup> Inexpensive fermentation products such as ethanol have the added advantage of being readily biodegradable.

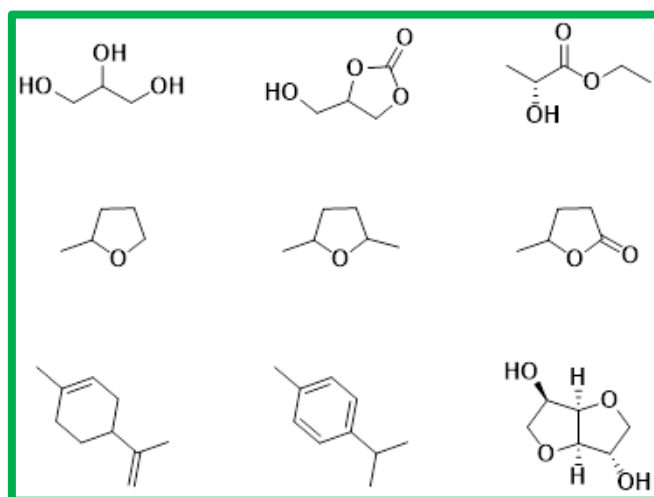


Figure 1.3. Examples of solvents derived from renewable biomass.

Despite the option of these solvents from renewable sources, the best solvent is no solvent. Organic procedures should be solventless, especially in continuous flow chemistry, as frequently as possible. But if a solvent (diluent) is needed then water has much to offer: it is non-toxic, non-inflammable, abundantly available and inexpensive. Hence, catalytic conversions in aqueous media have been extensively studied.<sup>73</sup>

Nevertheless, the use of water as solvent is not possible in most of the organic transformations. Another neoteric solvent that we want to

<sup>70</sup> D. Prat, O. Pardigon, H. W. Flemming, S. Letestu, V. Ducandas, P. Isnard, E. Guntrum, T. Senac, S. Ruisseau, P. Cruciano, P. Hosek, *Org. Process Res. Dev.*, 2013, 17, 1517-1525.

<sup>71</sup> G. P. Taber, D. M. Pfistere, J. C. Colberg, *Org. Process Res. Dev.*, 2004, 8, 385-388.

<sup>72</sup> A. G. Corrêa, M. W. Paixão, R. S. Schwab, *Curr. Org. Synth.*, 2015, 12, 675-695.

<sup>73</sup> G. Papadogianakis, R. A. Sheldon, *Catal. Today*, 2015, 247, 1-190.

highlight here is supercritical carbon dioxide,  $\text{scCO}_2$ . It is potentially attractive as a solvent. It displays properties that are a mixture of those normally related to gases or liquids: for example diffusivity approaching that of a gas combined with the solvent power of a light liquid alkane.<sup>74</sup> Such properties are especially useful in reactions involving gaseous reagents.  $\text{scCO}_2$  is easily obtained in high purity as a by-product from many processes including the fermentation of biomass, potentially a very large scale source of  $\text{CO}_2$  with the use of bioethanol increasing as a transport fuel. Furthermore,  $\text{scCO}_2$  is totally non-flammable and its properties can be manipulated by varying the applied pressure.<sup>75</sup> Although there has been a considerable volume of basic research on chemical reactions in  $\text{scCO}_2$ ,<sup>76,77</sup> the need to work with high pressures has kept the field small compared to the use of ionic liquids which can be used as “drop-in” replacements for conventional solvents in standard laboratory glassware.

### 1.3.1. Ionic Liquids

ILs are salts formed by organic cations and either inorganic or organic anions. Generally the cations are responsible for their physical properties such as melting point or viscosity, whereas the anions control chemical properties and reactivity. In Figure 1.4 the most common cations and anions can be seen. Their better charge distribution and larger ion size, as compared to classical inorganic salts, result in melting points often below 100 °C. ILs have unique and tunable properties compared with traditional molecular compounds including a wide liquid range, high ionic conductivity, negligible volatility, low flammability and high electrochemical and thermal stability, as well as good solvation ability. Such properties have led to an explosion in their use as designable solvents for a variety of processes linked to green chemistry and clean technologies (e.g. catalysis and organic synthesis). ILs can be alternatives for traditional volatile organic solvents.

The main property of the ILs is their high tunability: A wide variety of ILs can be designed, taking into account their modular character, considering structural elements such as the nature of the cation, the nature of the anion, the ion substitution patterns, the introduction of

---

<sup>74</sup> M. Skerget, Z. Knez, M. Knez-Hrncic, *J. Chem. Eng. Data*, 2011, 56, 694-719.

<sup>75</sup> M. McHugh, V. Krukonic, *Supercritical Fluid Extraction. Principle and Practice*, 1994, Butterworth-Hernemann.

<sup>76</sup> C. M. Rayner, *Org. Process Res. Dev.*, 2007, 11, 121-132.

<sup>77</sup> W. Leitner, *Acc. Chem. Res.*, 2002, 35, 746-756.

either bio-renewable or chiral moieties, etc.<sup>78</sup> Indeed, a wide range of structurally different ILs has been reported.<sup>79</sup> The unique opportunities offered by ILs have resulted in their increasing application in completely unexpected fields.<sup>80,81</sup> However, their fluidity, high viscosity, and slow gas diffusivity strongly limit their applications, recyclability and separation.<sup>78</sup> Many first generation ILs are poorly biodegradable<sup>82</sup> and exhibit aquatic ecotoxicity.<sup>83</sup> Their preparation often involves circuitous, high *E* factor processes, making them prohibitively expensive.<sup>84</sup> ILs cannot be generalised as being green or not green; their environmental impact is strongly dependent on the structure of the cation and anion.<sup>85</sup> More recently, second generation ILs containing more biocompatible cations and anions, derived from relatively inexpensive, eco-friendly natural products, such as carbohydrates and amino acids have emerged.<sup>86,87,88</sup>

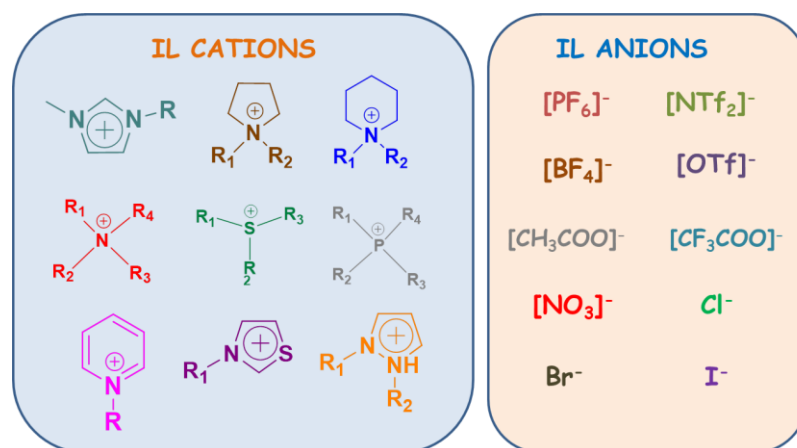


Figure 1.4. Most common cations and anions that form ionic liquids.

<sup>78</sup> E. García-Verdugo, B. Altava, M. I. Burguete, P. Lozano, S. V. Luis, *Green Chem.*, 2015, 17, 2693-2713.

<sup>79</sup> J. P. Hallet, T. Welton, *Chem. Rev.*, 2011, 111, 3508-3576

<sup>80</sup> M. Smiglak, J. M. Pringle, X. Lu, L. Han, S. Zhang, H. Gao, D. R. MacFarlane, R. D. Rogers, *Chem. Commun.*, 2014, 50, 9228-9250.

<sup>81</sup> G. Cevasco, C. Chiappe, *Green Chem.*, 2014, 16, 2375-2385.

<sup>82</sup> D. Coleman, N. Gathergood, *Chem. Soc. Rev.*, 2010, 39, 600-637.

<sup>83</sup> S. Stolte, M. Matzke, J. Arning, A. Bösch, W. R. Pitner, U. Welz-Biermann, B. Jastorff, J. Ranke, *Green Chem.*, 2007, 9, 1170-1179.

<sup>84</sup> M. Deetlefs, K. R. Seddon, *Green Chem.*, 2010, 12, 17-30.

<sup>85</sup> M. Petkovic, K. R. Seddon, L. P. N. Rebelo, C. Silva Pereira, *Chem. Soc. Rev.*, 2011, 40, 1383-1403.

<sup>86</sup> G. Imperato, B. König, C. Chiappe, *Eur. J. Org. Chem.*, 2007, 1049-1058.

<sup>87</sup> C. Chiappe, A. Marra, A. Mele, *Top. Curr. Chem.*, 2010, 295, 177-195.

<sup>88</sup> K. Fukumoto, M. Yoshizawa, H. Ohno, *J. Am. Chem. Soc.*, 2006, 127, 2398-2399.

Beyond their use as solvents, the application of ionic liquids embrace catalysis (homogeneous and heterogeneous), new magnetic and luminescent materials,<sup>89</sup> analysis (stationary phases in gas chromatography)<sup>90</sup>, energy production,<sup>91</sup> electrochemistry (ideal electrolytes)<sup>92</sup> and gas absorption (for example, the physisorption of SO<sub>2</sub> in various BF<sub>4</sub><sup>-</sup> and Tf<sub>2</sub>N<sup>-</sup> based ILs has been reported by A. Riisager and co-workers).<sup>93</sup>

Since 1914, when ionic liquids were first described by Paul Walden,<sup>94</sup> their academic research, industrial development and applications have grown in parallel.<sup>95</sup> However, the most important growth in interest in the field of ionic liquids started in 1999 with the opening of the Queen's University Ionic Liquid Laboratories (QUILL) research centre in Belfast (Northern Ireland). The number of publications on ionic liquids increased from around 1500 in 2005 to 6000 annual publications in 2013, being 46000 the total number. In the same way, the number of patents involving ionic liquids increased from around 500 in 2005 to around 12000 in 2016.<sup>96</sup>

Among other industrial giants that use ionic liquid we could find the Institut Français du Pétrole (IFP), which was the first to operate an ionic liquid plant with the Dimersol process catalysed by Nickel using chloroaluminate (III) ionic liquids as solvents.<sup>97</sup> Also Degussa company, which uses ionic liquids as additives improving final appearance and drying properties of a new range of paints.<sup>98</sup> The Central Glass Company, Ltd., Japan, was the first firm to produce pharmaceutical intermediates using ionic liquid technology. Tetraalkylphosphonium ionic liquids are used as solvents for Shonogashira couplings.<sup>95</sup>

Among other industrial giants, the BASF company is the one that has most contributed to the ionic liquid technology implement. Concisely, the BASIL™ process (Biphasic Acid Scavenging utilising Ionic Liquids) is currently the most successful example of an industrial process using

<sup>89</sup> M. Okuno, H. Hamaguchi, S. Hayashi, *Appl. Phys. Lett.*, 2006, 89, 132506.

<sup>90</sup> D. Armstrong, L. He, Y. Liu, *Anal. Chem.*, 1999, 71, 3873-3876.

<sup>91</sup> M. Smiglak, A. Metlen, R. D. Rogers, *Acc. Chem. Res.*, 2007, 40, 1182-1192.

<sup>92</sup> M. Armand, F. Endres, D. R. MacFarlane, H. Ohno, B. Scrosati, *Nat. Mater.*, 2009, 8, 621-629.

<sup>93</sup> J. Huang, A. Riisager, P. Wasserscheid, R. Fehrmann, *Chem. Commun.*, 2006, 4027-4029.

<sup>94</sup> P. Walden, *Bull. Acad. Impér. Sci. St. Pétersbourg*, 1914, 8, 405-422.

<sup>95</sup> N. V. Plechkova, K. R. Seddon, *Chem. Soc. Rev.*, 2008, 37, 123-150.

<sup>96</sup> M. Freemantle, <https://www.chemistryworld.com/features/ionic-liquids-revisited/1017383.article>, October 2016.

<sup>97</sup> IFP, *Annual Report*, 2004.

<sup>98</sup> B. Weyershausen, K. Lehmann, *Green Chem.*, 2005, 7, 15-19.

ionic liquid technology.<sup>99</sup> This process was firstly introduced to the BASF site in 2002 in Ludwingshafe, Germany. The BASIL™ process is used for the production of generic photoinitiator precursors involving alkoxyphenylphosphines (Figure 1.6). The process includes the formation of an acid that should be scavenged. However, with the original triethylamine scavenger, the resulting triethylammonium chloride formed a dense insoluble past very difficult to handle up and to separate from the final mixture. The replacement of triethylamine with 1-methylimidazole results in the *in situ* formation of the ionic liquid 1-methylimidazolium chloride, which could be easily separated from the reaction mixture. Moreover, 1-methylimidazole is recycled by a base-based decomposition of the 1-methylimidazolium chloride.<sup>100</sup> The current reaction performed at a multi-ton scale is a proof that handling large amounts of ionic liquids is possible and practical. It is worth mentioning that the IL is not used as a solvent but as the product from an acid-scavenging agent. The importance of this process was immediately highlighted by the ECN Innovation Award in 2004.

Извѣстія Императорской Академіи Наукъ. — 1914.  
(Bulletin de l'Académie Impériale des Sciences de St.-Petersbourg).

Ueber die Molekulargröße und elektrische  
Leitfähigkeit einiger geschmolzenen Salze.

(Mit 2 Figuren).

Von P. Walden.

Im Nachstehenden will ich meine Untersuchungen über die elektrische Leitfähigkeit und die aus den Kapillaritätskonstanten abgeleiteten Molekulargröße einiger organischen Ammoniumsalze mitteilen. Gewählt wurden *wasserfreie* Salze, welche bei relativ *niedrigen Temperaturen*, etwa bis zu 100° C. schmelzen. Diese niedrigen Schmelztemperaturen engten die Möglichkeit einer *Wärmespaltung* sowohl des Solvens, als auch des gelösten Salzes in der Salzschnmelze ein; sie eröffneten daher die *Reproduzierbarkeit* der bisher nur bei *hohen* Temperaturen, in den *Schnmelzen* der *wasserfreien Mineralsalze* gemachten Beobachtungen bei *niedrigen Temperaturen*; sie boten die Möglichkeit dar, mit Hilfe der für gewöhnliche Temperaturen gebräuchlichen Methoden und Apparate alle Messungen durchzuführen. Die Verhältnisse in *diesen* niedrig schmelzenden Salzen näherten sich daher den Versuchsbedingungen, wie sie für die gewöhnlichen wässrigen und nichtwässrigen Lösungsmittel eingehend erforscht worden sind und durch die osmotische Theorie van't Hoff's und die elektrolytische Dissoziationstheorie von Arrhenius beherrscht werden.

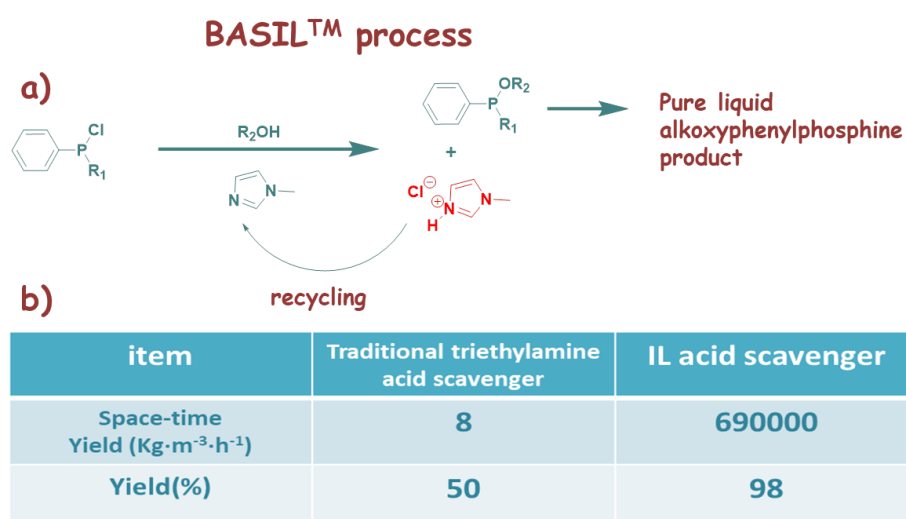


Figure 1.5. Extract of the first paper describing ionic liquids by Paul Walden in 1914 and photography of the autor.<sup>94</sup>

<sup>99</sup> R. D. Rogers, K. D. Seddon, *Science*, 2003, 302, 792-793.

<sup>100</sup> M. Maase, K. Massonne, K. Halbritter, R. Noe, M. Bartsch, W. Siegel, V. Stegmann, M. Flores, O. Huttenloch, M. Becker, *World Pat.*, WO 2003 062171, 2003.

Despite of the interesting properties as solvents, the most of modern applications of the ionic liquids, especially in industry, lie beyond their use as solvents.<sup>101</sup> Regarding synthetic applications, catalysis is the major use of ionic solvents.<sup>102</sup> However, in many examples the ionic liquid plays a dual role as catalyst and solvent in a chemical transformation. The problem arrives when the complexity of the ionic liquid difficults its use just for simple economic reasons related with the synthesis of the corresponding ionic liquid.



**Figure 1.6. a) Scheme of the BASIL™ process b) Comparison between the original triethylamine scavenger used in the process and the alternative ionic liquid.**

As a part of our concern for the use of sustainable solvents, solventless conditions have been first assayed for the systems developed in the work here presented. When that was not possible, neoteric solvents have been studied as an alternative to the traditional organic solvents. Water, ionic liquids, supercritical CO<sub>2</sub> and Me-THF have been employed as solvents in this work.

<sup>101</sup> R. Giernoth, *Angew. Chem. Int. Ed.*, 2010, 49, 2834-2839.

<sup>102</sup> P. Wasserscheid, T. Welton, *Ionic Liquids in Synthesis*, 2008, Wiley-VCH, Weinheim.

## 1.4. Supported Ionic Liquids

In the context of heterogeneous catalysts, we would like to highlight here the importance of supported ionic liquids (SILs). Due to their previously described properties, ILs have a wide number of applications in catalysis. By supporting ILs onto a solid support these interesting properties are also present on the resulting solid material. Heterogenisation of ILs offers many general advantages, some of them being typical for supported catalysts and, in general, supported systems: i) significantly reduce the amount of IL used as compared with homogeneous procedures involving ILs, ii) facilitates separation from the reaction products, iii) and accordingly reusability, iv) as well as their potential employment in continuous flow processes.

ILs can be functionalised by introducing specific functional moieties with specific catalytic functions leading to the so-called task specific ionic liquids (TSILs).<sup>103</sup> This allows to expand the range of catalytic applications of the ILs and, as a consequence, of the supported ionic liquids.

Supported ionic liquids can act as catalysts by themselves or can be used to immobilise catalytic species. These catalytic species include organocatalysts,<sup>104</sup> transition metal complexes,<sup>105</sup> metal nanoparticles (NPs)<sup>106</sup>, photocatalysts<sup>107</sup> and biocatalysts.<sup>108</sup> Moreover, the affinity of these catalysts toward the IL phase can be improved using suitable IL-like tags on the catalyst structure.<sup>109,110</sup> More detailed examples of catalysts immobilised on SILs will be discussed later.

When SILs are used themselves as catalysts without adding a co-catalyst, the catalytic role can be played either by the cation moiety (including R groups, see figure 1.4) or the anion present. M.

---

<sup>103</sup> C. Chiappe, C. S. Pomelli, *Eur. J. Org. Chem.*, 2014, 6120-6139.

<sup>104</sup> M. Gruttadauria, F. Giacalone, P. Agrigento, R. Noto in *Ionic Liquids in Biotransformations and Organocatalysis* (Ed.: P. D. De Maria), 2012, John- Wiley & Sons, Inc., 361-417.

<sup>105</sup> C. van Doorslaer, J. Wahlen, P. Mertens, K. Binnemans, V. de Vos, *Dalton Trans.*, 2010, 39, 8377-8390

<sup>106</sup> Y. L. Gu, G. X. Li, *Adv. Synth. Catal.*, 2009, 351, 817-847.

<sup>107</sup> M. I. Burguete, R. Gavara, F. Galindo, S. V. Luis, *Catalysis Communications*, 2010, 11, 1081-1084.

<sup>108</sup> E. Garcia-Verdugo, P. Lozano, S.V. Luis in *Supported Ionic Liquids – Fundamentals and Applications* (eds R. Fehrmann, A. Riisager and M. Haumann), 2014, Wiley-VCH Verlag GmbH, Weinheim, 351-368.

<sup>109</sup> R. Šebesta, I. Kmentova, Š. Toma, *Green Chem.*, 2008, 10, 484-496.

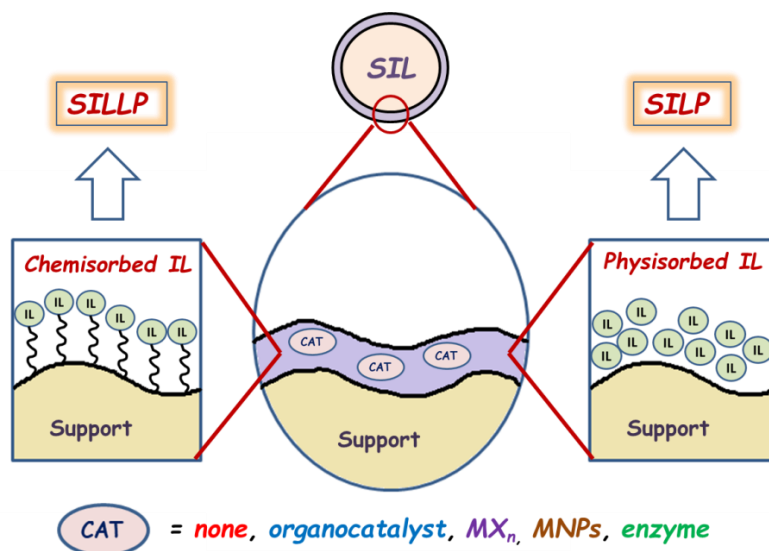
<sup>110</sup> M. Lombardo, C. Trombini, *ChemCatChem*, 2010, 2, 135-145.



Gruttadauria and co-workers reported the catalytic effect of the imidazolium counterion ( $\text{Cl}^-$ ,  $\text{Br}^-$ ,  $\text{I}^-$ ) for the cycloaddition of  $\text{CO}_2$  to epoxides catalysed by SILs.<sup>111</sup> On the other hand, G. Liu and co-workers demonstrated that the imidazolium units can enhance the asymmetric Michael addition of 1,3-dicarbonyl compounds to nitroalkenes in brine.<sup>112</sup> The imidazolium network has a phase-transfer function that provides higher catalytic activity. Moreover, as seen in section 1.2, the support can also have a catalytic effect.

SILs can be basically divided in two major categories depending on the type of interaction between the IL and the solid support:

- ❖ SILPs (Solid Ionic Liquid Phases): these are the classic SIL materials and consist on liquid IL phases adsorbed in the solid support, resulting in the presence of a physisorbed multilayer of IL in the surface (see Figure 1.7).
- ❖ SILLPs (Solid Ionic Liquid-Like Phases): in this case the IL is covalently bound to the support resulting on a IL monolayer covalently attached to the surface (see Figure 1.7). However, covalently linked multilayers can also be found (mlSILLP).<sup>113,114</sup>



**Figure 1.7. General scheme of a supported ionic liquid with schematic differences between the two major categories: SILP and SILLP.**

<sup>111</sup> P. Agrigento, S. M. Al-Amsyar, B. Soree, M. Taherimehr, M. Gruttadauria, C. Aprile, P. P. Pescarmona, *Catal. Sci. Technol.*, 2014, 4, 1598-1607.

<sup>112</sup> X. Xu, T. Cheng, X. Liu, J. Xu, R. Jin, G. Liu, *ACS Catal.*, 2014, 4, 2137-2142.

<sup>113</sup> P. Agrigento, S. M. Al-Amsyar, B. Soree, M. Taherimehr, M. Gruttadauria, C. Aprile, P. P. Pescarmona, *Catal. Sci. Tech.*, 2014, 4, 1598-1607.

<sup>114</sup> C. Aprile, F. Giacalone, P. Agrigento, L. F. Liotta, J. A. Martens, P. P. Pescarmona, M. Gruttadauria, *ChemSusChem*, 2011, 4, 1830-1837.

From these two major categories of SILs, several immobilised ionic liquid materials arise with their own acronym to create a large family of them. Some types and acronyms are quite similar and the classifying is sometimes difficult. In Figure 1.8 a kind of tree chart is presented to explain this schematically.<sup>115</sup> Among these supported ionic liquid materials widely described in the literature, altogether with their applications, we can find supported ionic liquid films,<sup>116</sup> supported ionic liquid catalysts (SILC/SILCAs),<sup>117</sup> solid catalysts with ILs (SCILs),<sup>118</sup> solid catalysts with IL layers (SCILL),<sup>119</sup> supported IL nanoparticles (SILnPs),<sup>120</sup> ionic liquid crystalline-SILP (ILC-SILP),<sup>121</sup> structured SILP (SSILP),<sup>122</sup> polymer supported ILs (PSILs)<sup>123</sup> and supported ionic liquid membranes (SILMs).<sup>124</sup>

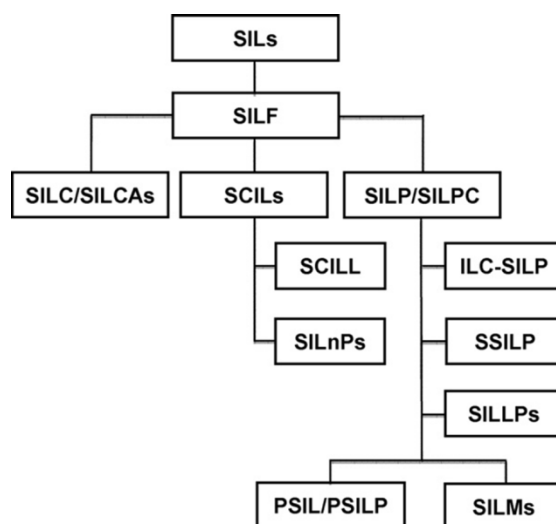


Figure 1.8. Tree chart of immobilised species derived from supported ionic liquids.<sup>115</sup>

<sup>115</sup> T. Selvam, A. Machoke, W. Schwieger, *App. Catal. A: General*, 2012, 445-446, 92-101.

<sup>116</sup> H.-P. Steinruck, J. Libuda, P. Wasserscheid, T. Cremer, C. Kolbeck, M. Laurin, F. Maier, M. Sobota, P.S. Schulz, M. Stark, *Adv. Mater.*, 2011, 23, 2571-2587.

<sup>117</sup> C. P. Mehnert, R. A. Cook, N. C. Dispenziere, M. Afeworki, *J. Am. Chem. Soc.*, 2002, 124, 12932-12933.

<sup>118</sup> Y. Gu, C. Ogawa, J. Kobayashi, Y. Mori, S. Kobayashi, *Angew. Chem. Int. Ed.*, 2006, 45, 7217-7220.

<sup>119</sup> J. Arras, M. Steffan, Y. Shayeghi, D. Ruppert, P. Claus, *Green Chem.*, 2009, 11, 716-723.

<sup>120</sup> M.E. Mahmoud, H.M. Al-Bishri, *Chem. Eng. J.*, 2011, 166, 57-167.

<sup>121</sup> M. Sobota, X. Wang, M. Fekete, M. Happel, K. Meyer, P. Wasserscheid, M. Laurin, J. Libuda, *ChemPhysChem*, 2010, 11, 1632-1636.

<sup>122</sup> M. Ruta, I. Yuranov, P.J. Dyson, G. Laurenczy, L. Kiwi-Minsker, *J. Catal.*, 2007, 247, 269-276.

<sup>123</sup> J. Wang, G. Song, Y. Peng, *Tetrahedron Lett.*, 2011, 52, 1477-1480.

<sup>124</sup> D.D. Iarikov, P. Hacırlıoğlu, S.T. Oyama, *Chem. Eng. J.*, 2011, 166, 401-406.

Regarding the type of solid materials employed as support for the SILs, a wide variety can also be found: ordered mesoporous silica,<sup>125</sup> zeolites,<sup>126</sup> spherical silica nanoparticles,<sup>127</sup> nanosilica dendrimers,<sup>128</sup> diethylaminopropylated alumina,<sup>129</sup> polystyrene,<sup>130</sup> carbon nanotubes,<sup>131</sup> halloysite<sup>132</sup> and magnetic particles<sup>133</sup> among others. The applications in catalysis of these materials have been recently reviewed by M. Gruttadauria and co-workers.<sup>134</sup> In the work here presented, Merrifield type resins (polystyrene and styrene/divinylbenzene copolymers) have been the most common supports used for the preparation of supported ionic liquids, due to their stability, compatibility with a broad range of reaction conditions and functionalisation possibilities that offer.

The two major categories of supported ionic liquids presented (SILP and SILLP), distinguished by the nature of the interaction between the IL and the support, deserve a more in depth description. The SILP concept was described for the first time in 2003 by A. Riisager and co-workers.<sup>135,136</sup> Rhodium complexes were immobilised in a IL phase for application in a continuous fixed-bed gas phase hydroformylation.

With the supported ionic liquid phase (SILP) technology, stable and easy to handle solid catalyst materials are obtained which can be used in fixed-bed reactors. Thus, the supported ionic liquid phase (SILP) technology is a fundamental, new approach to obtain liquid containing solid materials that do not evaporate, made through surface modification of a porous solid by dispersing a thin layer of ionic liquid (IL) onto it, as depicted in Figure 1.9. Owing to the extremely low vapour pressure of ILs, the surface of SILP materials is coated permanently, even under elevated reaction conditions. By variation of anions and

<sup>125</sup> B. Karimi, D. Elhamifar, J. H. Clark, A. J. Hunt, *Chem. Eur. J.*, 2010, 16, 8047-8053.

<sup>126</sup> M. J. Jin, A. Taher, H. J. Kang, M. Choi, R. Ryoo, *Green Chem.*, 2009, 11, 309-313.

<sup>127</sup> J. Y. Shin, B. S. Lee, Y. Jung, S. J. Kim, S. G. Lee, *Chem. Commun.*, 2007, 5238-5240.

<sup>128</sup> H. Hagiwara, H. Sasaki, N. Tsubokawa, T. Hoshi, T. Suzuki, T. Tsuda, S. Kubawata, *Synlett*, 2010, 1990-1996.

<sup>129</sup> H. Hagiwara, K. H. Ko, T. Hoshi, T. Suzuki, *Chem. Commun.*, 2007, 2838-2840.

<sup>130</sup> T. Kang, Q. Fen, M. Luo, *Synlett*, 2005, 2305-2308.

<sup>131</sup> M. J. Park, S. G. Lee, *Bull. Korean Chem. Soc.*, 2007, 28, 1925-1926.

<sup>132</sup> M. Massaro, S. Riela, G. Cavallaro, M. Gruttadauria, S. Milioto, R. Noto, G. Lazzara, *J. Organomet. Chem.*, 2014, 749, 410-415.

<sup>133</sup> A. Taher, J.-B. Kim, J. Y. Jung, W. S. Ahn, M. J. Jin, *Synlett*, 2009, 2477-2482.

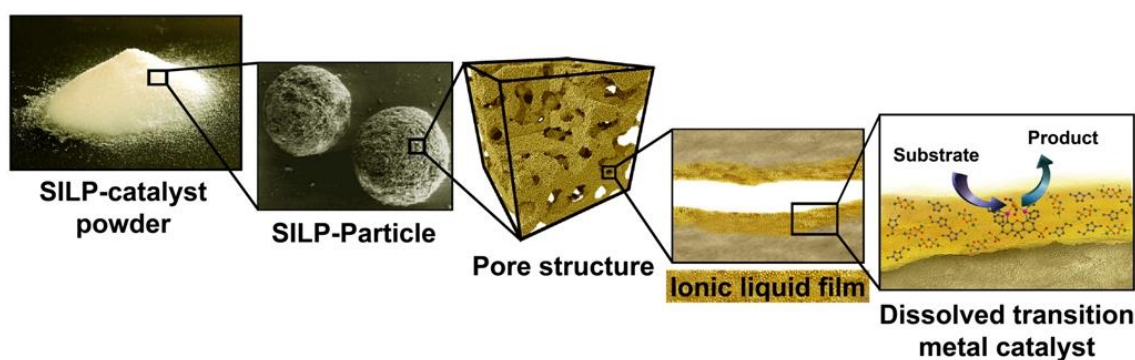
<sup>134</sup> A. M. P. Salvo, F. Giacalone, M. Gruttadauria, *Molecules*, 2016, 21, 1288-1348.

<sup>135</sup> A. Riisager, P. Wasserscheid, R. van Hal, R. Fehrmann, *J. Catal.*, 2003, 219, 452-455.

<sup>136</sup> A. Riisager, K. M. Eriksen, P. Wasserscheid, R. Fehrmann, *Catal. Lett.*, 2003, 90, 149-153.

cations, solubility, reactivity, and coordination properties of the ILs can be changed according to the special requirements of the given application.

Thus, the SILP concept allows the custom-making of solid materials, resulting in uniform and well-defined surface topologies with definite properties and constitutes an attractive methodology to circumvent the lack of uniformity of solids in traditional material science. In addition, the approach provides a great potential to create materials with new surface properties, as the transfer of specific IL properties to solid surfaces may result in “designer surfaces” with properties that are impossible to obtain with any present synthetic approach.



**Figure 1.9. Schematic representation of an ionic liquid layer supported on a porous material.**

SILPs, however, have the limitation, especially for continuous processes, of the potential lixiviation of the IL or the catalyst by abrasion and dissolution due to the non-covalent attachment. For this reason, SILP systems are preferentially used in gas phase rather than in liquid phase conditions. In recent years, A. Riisager and co-workers have reported several gas-phase applications of SILPs.<sup>137,138,139</sup> In the most recent work reported, a continuous gas-phase ethylene methoxycarbonylation has been achieved for the first time using SILP technology.<sup>140</sup>

<sup>137</sup> M. Haumann, K. Dentler, J. Joni, A. Riisager, P. Wassercheid, *Adv. Synth. Catal.*, 2007, 349, 425-431.

<sup>138</sup> H. Kolding, R. Fehrmann, A. Riisager, *Science China Chem.*, 2012, 55, 1648-1656.

<sup>139</sup> P. L. Thomassen, A. J. Kunov-Kruse, S. L. Mossin, H. Kolding, S. Kegnaes, A. Riisager, R. Fehrmann, *ES Transactions*, 2012, 50, 433-442.

<sup>140</sup> S. G. Khokarale, E. J. García-Suárez, R. Fehrmann, A. Riisager, *ChemCatChem*, 2017, 9, 1824-1829.

A worth to highlight application of SILPs, both in the laboratory and on an industrial scale, is the effective removal of mercury vapour from natural gas streams.<sup>141</sup> It has been possible using chlorocuprate (II) ionic liquids adsorbed on porous solid supports with high surface area. Considering the potential effects of the mercury, this application has a great impact and this ionic liquid based material has been commercialised within the petroleum gas production industry.

Regarding industrial SILP applications, in 2015 the German chemical company Evonik demonstrated that a SILP catalyst could reliably work for around 2000 hours in a pilot plant.<sup>142,96</sup> The IL used was based in imidazolium cations and amine-based anions and the resulting supported ionic liquid was employed to perform an industrial hydroformylation producing aldehydes from syngas or alkenes.

On the other hand, the SILLP (Supported Ionic Liquid-Like Phases) technology represents an alternative approach with the covalent functionalisation of a solid surface with IL-like moieties. With this strategy, widely developed and employed in our group with polymeric solid supports, the covalent anchoring of a monolayer of IL-like fragments onto a support occurs. Here, the IL-like fragment becomes part of the support material, thereby losing certain bulk phase properties such as solvation strength, conductivity, and viscosity. The IL can contain a certain functionality (e.g. acidity, hydrophobicity) that will be transferred to the support surface. With this, no leaching is possible, which makes SILLPs a better option for continuous flow processes compared to SILPs. Moreover, from an economical point of view, the absence or strong limitation of the IL leaching in the SILLP technique is important. SILLPs derive from insoluble 3D polymeric networks with variable crosslinking degrees. The IL-like units provide them with the main features of ILs at the molecular level (stability, tunable polarity, etc.), while the presence of the polymeric backbone offers an additional design vector to optimise their macroscopic and process properties. Thus, SILLPs can:

- i) assist the activation of the catalyst.
- ii) generate novel catalytic species.
- iii) improve catalyst stability.
- iv) optimise immobilisation and recycling.

---

<sup>141</sup> M. Abai, M. P. Atkins, A. Hassan, J. D. Holbrey, Y. Kuah, P. Nockemann, A. A. Oliferenko, N. V. Plechkova, S. Rafeen, A. A. Rahman, R. Ramli, S. M. Shariff, K. R. Seddon, G. Srinivasan, Y. Zou, *Dalton Trans.*, 2015, 44, 8617-8624.

<sup>142</sup> <https://corporate.evonik.com/en/media/search/pages/news-details.aspx?newsId=52454>

- v) facilitate product isolation.
- vi) influence the selectivity of the reaction.
- vii) be employed in continuous flow processes.

SILLPs have been applied in catalysis as organocatalytic species by themselves or immobilising and stabilising a wide range of catalysts ranging from organocatalysts,<sup>143,144</sup> metal NPs,<sup>145</sup> organometallic catalysts, biocatalysts<sup>146</sup> and photocatalysts.<sup>107</sup> Their potential includes preparing multifunctional SILLPs<sup>147</sup> and SILLP-cocktails<sup>148</sup> with each of the different SILLPs playing a complementary role. Despite of the fact that SILLPs are heterogeneous catalysts, the catalyst immobilised in the IL of the surface experiences a homogeneous-like environment and acts like in homogeneous phase, which improves the catalytic activity. As we can see in Figure 1.10, SILLPs present a high degree of tunability. Depending on the counterion and the substitution/functionalisation of the imidazole we can achieve some catalytic properties on the resulting SILLP, exactly in the same way described for ILs.

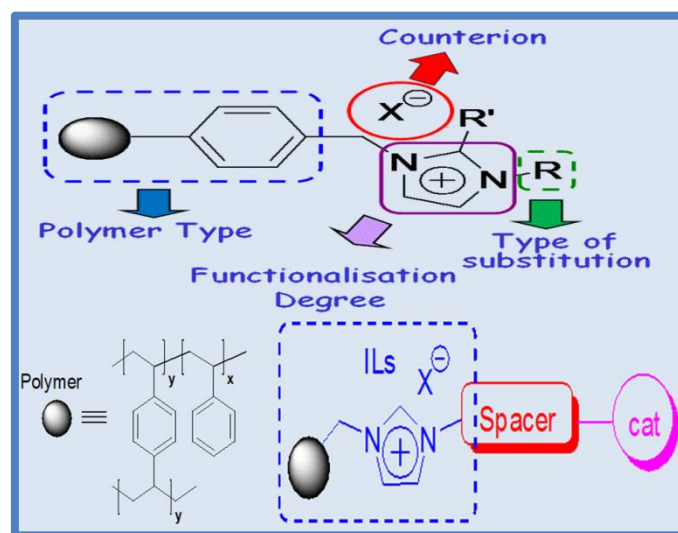


Figure 1.10. Parts and tunability of a SILLP.

<sup>143</sup> M. Gruttadauria, S. Riela, C. Aprile, P. L. Meo, F. D'Anna, R. Noto, *Adv. Synth. Catal.*, 2006, 348, 82-92.

<sup>144</sup> C. Aprile, F. Giacalone, M. Gruttadauria, A. M. Marculescu, R. Noto, J. D. Revell, H. Wennemers, *Green Chem.*, 2007, 9, 1328-1334.

<sup>145</sup> J. Restrepo, P. Lozano, M. I. Burguete, E. García-Verdugo, S. V. Luis, *Catal. Today*, 2015, 255, 97-101.

<sup>146</sup> E. Karjalainen, D. F. Izquierdo, V. Martí-Centelles, S. V. Luis, H. Tenhu, E. García-Verdugo, *Polym. Chem.*, 2014, 5, 1437-1446.

<sup>147</sup> S. Montolio, C. Vicent, V. Aseyev, I. Alfonso, M. I. Burguete, H. Tenhu, E. García-Verdugo, S. V. Luis, *ACS Catal.*, 2016, 6, 7230-7237.

<sup>148</sup> V. Sans, F. Gelat, N. Karbass, M. I. Burguete, E. García-Verdugo, S. V. Luis, *Adv. Synth. Catal.*, 2010, 352, 3013-3021.

SILLPs can act as organocatalysts by themselves depending on the cation and counterion moieties. The possibility to modify the type of cation and anion gives SILLPs a great adaptability as potential catalysts. A tailor-made design to meet the requested needs can be done in the SILLPs structure. SILLPs have been used as organocatalysts in numerous applications.<sup>149</sup> In 2012, the transesterification reaction of tripalmitin with methanol to give methylpalmitate was achieved using a poly(ionic liquid) SILLP material with  $\text{CF}_3\text{SO}_3^-$  as counterion. Yields close to 100%, higher than those achieved with the analogous homogeneous ionic liquid, were reached and the catalyst was reused for five times.<sup>150</sup> In 2014, the Biginelli condensation reaction was successfully catalysed, for a wide range of aldehydes, using a IL-based periodic mesoporous organosilica (PMO) material with sulfonic acid functionalisation on the IL units.<sup>151</sup> In 2015, a SILLP based on a Brønsted acid ionic liquid covalently supported on a magnetic mesoporous material,  $\text{Fe}_3\text{O}_4@\text{SiO}_2$ , was used successfully as a catalyst for biodiesel production from oleic acid giving yields > 90% and good reusability.<sup>152</sup>

As we have seen, SILLPs offer great possibilities in catalysis. Moreover, if a different catalytic activity is needed, a large variety of catalysts can be immobilised in SILLPs. In these cases, where the whole SILLP acts as the support for another catalyst, the SILLP support may play an additional role complementing the introduced catalyst functionality. By designing the anion, cation or support of the SILLP, the affinity of the supported catalyst can be increased. Moreover, with these catalytic systems, the presence of “release and catch” mechanisms is usual.<sup>153</sup> The catalyst, non-covalently attached to the SILLP, is released to the solution where the reaction takes place, being the catalyst ideally recaptured by the SILLP at the end of the reaction. These mechanisms allows to combine the benefits of both homogeneous and heterogeneous catalysis. If the desired recapture of the catalyst after the reaction does not happen, leaching phenomena occur decreasing the catalytic activity of the SILLP-catalyst system.

A great example of the use of SILLPs as supports for organocatalysts can be found in the use of L-proline or the tripeptide H-Pro-Pro-Asp-NH<sub>2</sub>

---

<sup>149</sup> B. Xin, J. Hao, *Chem. Soc. Rev.*, 2014, 43, 7171-7187.

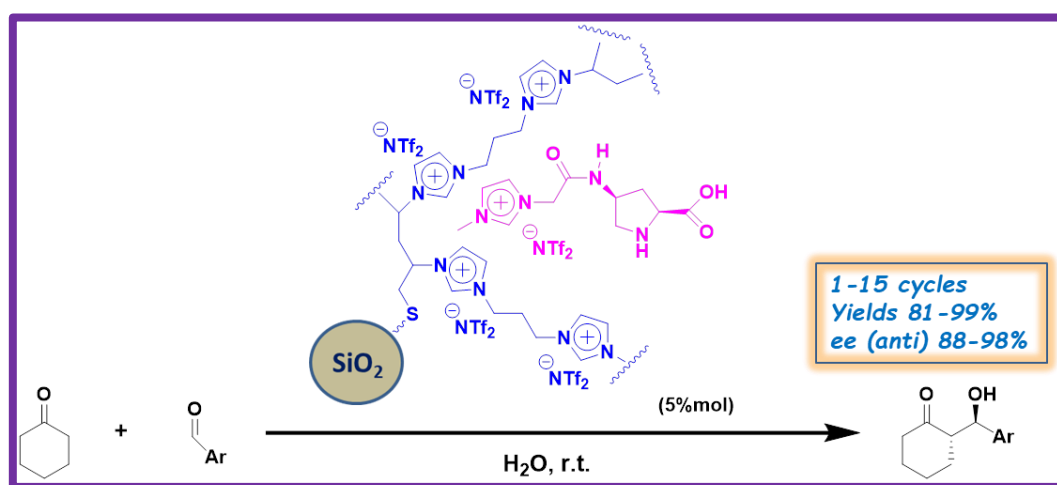
<sup>150</sup> F. Liu, L. Wang, Q. Sun, L. Zhu, X. Meng, F.-S. Xiao, *J. Am. Chem. Soc.*, 2012, 134, 16948-16950.

<sup>151</sup> D. Elhamifar, M. Nasr-Esfahani, B. Karimi, R. Moshkelgosha, A. Shábani, *ChemCatChem*, 2014, 6, 2593-2599.

<sup>152</sup> H. Wan, Z. Wu, W. Cheng, G. Guan, Y. Cai, C. Chen, Z. Li, X. Liu, *J. Mol. Catal. A*, 2015, 398, 127-132.

<sup>153</sup> M. Gruttadauria, F. Giacalone, R. Noto, *Green Chem.*, 2013, 15, 2608-2618.

supported on SILLP-based materials as catalysts for the asymmetric intermolecular aldol reaction reported by M. Gruttadauria and co-workers.<sup>154</sup> In further improvements, the affinity of the proline organocatalyst towards the IL was increased by an ionic tag strategy, which results in increased reaction rates for an excellent “release and catch” catalytic system (see Figure 1.11).<sup>155</sup> The same approach was also described for the SILLP immobilisation of TEMPO-based catalysts (TEMPO = 2,2,6,6-tetramethylpiperidine-1-oxyl) for the oxidation of alcohols.<sup>156</sup>



**Figure 1.11. Asymmetric aldol reaction catalysed by a *L*-proline organocatalyst supported in a SILLP.<sup>155</sup> The *L*-proline has been modified with an imidazolium tag to increase the affinity toward the SILLP and favor the catalyst recapturing. The presence of the same counterion in the catalytic species and the SILLP increases the affinity. This is an example of an ideal “release and catch” catalytic system based on SILLPs.**

In some instances, the catalytic activity of metals is needed. In our group, imidazolium based ionic liquids supported on gel-type Merrifield resins have been used to prepare palladium N-heterocyclic carbene (Pd-NHC) complexes.<sup>157</sup> Merrifield resins with different chlorine loading were used as starting polymeric materials giving SILLP-Pd-NHC complexes with Pd loadings between 0.17 and 0.34 mmol/g. These resulting Pd catalysts were employed in the Shonogashira reaction between phenylacetylene and phenyl iodide (employing 0.1 mol% of Pd) showing

<sup>154</sup> M. Gruttadauria, S. Riela, P. Lo Meo, F. D’Anna, R. Noto, *Tetrahedron Lett.*, 2004, 45, 6113-6116.

<sup>155</sup> M. Montroni, M. Lombardo, A. Quintavalla, C. Trombini, M. Gruttadauria, F. Giacalone, *ChemCatChem*, 2012, 4, 1000-1006.

<sup>156</sup> H. A. Beejapur, F. Giacalone, R. Noto, P. Franchi, M. Lucarini, M. Gruttadauria, *ChemCatChem*, 2013, 5, 2991-2999.

<sup>157</sup> V. Sans, F. Gelat, M. I. Burguete, E. García-Verdugo, S. V. Luis, *Macromol. Symp.*, 2012, 317-318, 259-266.



that changes on the loading and the counterion produced TOF values to change in the 450-25000 h<sup>-1</sup> range. It was demonstrated that the catalytic active species were soluble species released from the SILLP support with stronger coordination anions hampering the release of the soluble catalytic Pd species. Moreover, low Pd loadings provided higher catalytic activities.

The catalytic importance of metal nanoparticles (MNPs) due to their great activity (high surface/volume ratio) and selectivity is widely known.<sup>158,159</sup> On the other hand, the thermodynamically favoured tendency of these MNPs to form larger aggregates represents a problem and there is a need to find strategies to stabilise these nanoparticles. The preparation of NP catalysts requires a stabilising ligand that provides a balance between NP stability and catalytic activity. The pioneering work of Dupont of co-workers revealed that ionic liquids could be a great answer.<sup>160,161,162</sup> The immobilisation of MNPs in SILLPs forming NP@SILLPs provides a fine balance between NP stability and catalytic activity. In our group, gold nanoparticles have been immobilised in Merrifield resin-based SILLPs and successfully employed to perform the oxidation of 1-phenylethanol to acetophenone.<sup>145</sup>

Choosing the right combination of IL cation and anion allows for a tuning of the interactions between the IL and the NP surface, and therefore the resulting catalytic properties of the NPs. In recent times, particular interest has been paid in our group to the preparation of multifunctional NP@SILLP catalysts,<sup>147</sup> in which an organic moiety incorporated into the IL structure plays an active role in the catalytic transformation in cooperation with MNPs. The preparation of multifunctional MNP@SILLP catalysts emphasises how the SILLP concept provides a molecular approach to assemble supported catalysts in a flexible and controlled manner to provide innovative catalytic materials.<sup>163</sup> These MNP@SILLP catalysts present several advantages: i) reduced quantities of ILs required, ii) improved mass transport into and from the catalytic site through the IL phase, iii) enhanced MNP stability and activity, iv) implementation in continuous flow processes.

---

<sup>158</sup> D. Astruc, F. Lu, J. R. Aranzaes, *Angew. Chem. Int. Ed.*, 2005, 44, 7852-7872.

<sup>159</sup> J. M. Campelo, D. Luna, R. Luque, J. M. Marinas, A. A. Romero, *ChemSusChem*, 2009, 2, 18-45.

<sup>160</sup> J. Dupont, G. S. Fonseca, A. P. Umpierre, P. F. P. Fichtner, S. R. Teixeira, *J. Am. Chem. Soc.*, 2002, 124, 4228-4229.

<sup>161</sup> J. Dupont, J. D. Scholten, *Chem. Soc. Rev.*, 2010, 39, 1780-1804.

<sup>162</sup> J. D. Scholten, B. C. Leal, J. Dupont, *ACS Catal.*, 2012, 2, 184-200.

<sup>163</sup> P. Migowski, K. L. Luska, W. Leitner in *Nanocatalysis in Ionic Liquids* (ed. M. H. G. Precht), 2017, Wiley-VCH Verlag GmbH & Co. KGaA., Weinheim, 249-273.

Among the MNPs, Pd nanoparticles have a great interest due to their catalytic activity in C-C coupling reactions, which are probably the most important reactions in the synthesis of pharmaceuticals and fine chemicals.<sup>164</sup> Several catalytic applications of these PdNP@SILLPs have been reported in last years by M. Gruttadauria and co-workers,<sup>165,166,167</sup> including continuous flow Suzuki and Heck cross-coupling reactions.<sup>168,169</sup> In our group, multitask PdNP@SILLP species able to perform multiple and consecutive Heck, Shonogashira and Suzuki cross-coupling reactions were developed.<sup>148</sup> Moreover, with these PdNP@SILLP, a continuous flow Heck coupling reaction using scCO<sub>2</sub> as solvent was achieved for more than 3 hours with yields of *ca.* 80%.

Enzymes can also be immobilised on SILLPs. Adsorption of biocatalysts onto solid supports relies on hydrophobic, salt bridge, van der Waals, and hydrogen bonding interactions between the protein or cell, and the support used for immobilisation.<sup>170</sup> Adsorption is easier to perform, and can avoid enzyme denaturalisation because of the minimal distortion of the protein required for the immobilisation. Nevertheless, immobilisation lifetimes and efficiencies can be lower than for comparable covalent immobilisation.<sup>171</sup> Despite of that, it should be noted that not all the proteins are suitable for covalent immobilisation,<sup>172</sup> and, as we will see, immobilisation by adsorption over SILLPs can be an interesting alternative.

In our group, the enzyme CAL-B has been successfully immobilised in different SILLPs and successfully used for several transformations including the enzymatic resolution of *rac*-1-phenylethanol,<sup>173,174</sup> and the synthesis of methyl oleate (biodiesel),<sup>175</sup> with excellent results. This

---

<sup>164</sup> C. Torborg, M. Beller, *Adv. Synth. Catal.*, 2009, 351, 3027-3043.

<sup>165</sup> M. Gruttadauria, L. F. Liotta, A. M. P. Salvo, F. Giacalone, V. La Parola, C. Aprile, R. Noto, *Adv. Synth. Catal.*, 2011, 353, 2119-2130.

<sup>166</sup> C. Pavia, F. Giacalone, L. A. Bivona, A. M. P. Salvo, C. Petrucci, G. Strappaveccia, L. Vaccaro, C. Aprile, M. Gruttadauria, *J. Mol. Catal. A: Chem.*, 2014, 387, 57-62.

<sup>167</sup> R. Buscemi, F. Giacalone, S. Orecchio, M. Gruttadauria, *ChemPlusChem*, 2014, 79, 421-426.

<sup>168</sup> C. Pavia, E. Ballerini, L. A. Bivona, F. Giacalone, C. Aprile, L. Vaccaro, M. Gruttadauria, *Adv. Synth. Catal.*, 2013, 355, 2007-2018.

<sup>169</sup> C. Petrucci, G. Strappaveccia, F. Giacalone, M. Gruttadauria, F. Pizzo, L. Vaccaro, *ACS Sustainable Chem. Eng.*, 2014, 2, 2813-2819.

<sup>170</sup> T. Jesionowski, J. Zdarta, B. Krajewska, *Adsorption*, 2014, 20, 801-821.

<sup>171</sup> J. Britton, C. L. Raston, G. A. Weiss, *Chem. Commun.*, 2016, 52, 10159-10162.

<sup>172</sup> J. Britton, S. Majumdar, G. A. Weiss, *Chem. Soc. Rev.*, 2018, 47(15), 5891-5918.

<sup>173</sup> D. F. Izquierdo, J. M. Bernal, M. I. Burguete, E. García-Verdugo, P. Lozano, S. V. Luis, *RSC Adv.*, 2013, 3, 13123-13126.

<sup>174</sup> D. F. Izquierdo, M. Yates, P. Lozano, M. I. Burguete, E. García-Verdugo, S. V. Luis, *React. Funct. Polym.*, 2014, 85, 20-27.

<sup>175</sup> P. Lozano, E. García-Verdugo, J. M. Bernal, D. F. Izquierdo, M. I. Burguete, G. Sánchez-Gómez, S. V. Luis, *ChemSusChem*, 2012, 5, 790-798.

enzymatic resolution of *rac*-1-phenylethanol by CAL-B-SILLP was also achieved under continuous flow continuous in scCO<sub>2</sub> with excellent yields and enantioselectivities.<sup>176</sup> The continuous resolution was performed for four hours-cycles and the setup assembled worked for more than three weeks without a reduction in performance.

As demonstrated by the former examples, supported ionic liquids have shown a great potential in heterogeneous catalysis. More extensive compilations of the catalytic applications of both SILPs and SILLPs have been reported in recent years by M. Gruttadauria and co-workers.<sup>177,178</sup> In connection with our interest in continuous flow chemistry, SILLPs present very interesting properties and much work has been carried out in this area in recent years. Moreover, as mentioned above, the use of SILLPs allows applications in organocatalysis, organometallic catalysis and biocatalysis. For all these reasons, we consider SILLPs as a key tool for developing new multicatalytic continuous flow synthetic systems.

## 1.5. Continuous Flow Chemistry

Continuous Flow processing was recommended as number one key green research area to promote green and sustainable manufacturing by global pharmaceutical companies and the pharmaceutical roundtable founded by the ACS Green Chemistry Institute (GCI) in 2007.<sup>179</sup> The main advantages of the use of Continuous Flow Chemistry include:

- i) Enhanced heat and mass transfer.
- ii) Efficient mixing even with immiscible phases.
- iii) Precise control over the residence time and local stoichiometry.
- iv) Shorter process times.
- v) Increased safety.
- vi) Reproducibility.
- vii) Better product quality.
- viii) Easy scalability.

<sup>176</sup> P. Lozano, E. García-Verdugo, N. Karbass, K. Montague, T. de Diego, M. I. Burguete, S. V. Luis, *Green Chem.*, 2010, 12, 1803-1810.

<sup>177</sup> F. Giacalone, M. Gruttadauria, *ChemCatChem*, 2016, 8, 664-684.

<sup>178</sup> V. Campisciano, F. Giacalone, M. Gruttadauria, *Chem. Rec.*, 2017, 17, 918-938.

<sup>179</sup> C. Jiménez-González, P. Poehlauer, Q. B. Broxterman, B. S. Yang, D. am Ende, J. Baird, C. Bertsch, R. E. Hannah, P. Dell'Orco, H. Noorman, S. Yee, R. Reintjens, A. Wells, V. Massonneau, J. Manley, *Org. Process Res. Dev.*, 2011, 15, 900-911

In flow chemistry, a chemical reaction is run in a continuously flowing stream rather than in batch production. In other words, pumps move fluids into a tube, and where tubes join one another, the fluids contact one another. If these fluids are reactive, a reaction takes place. Flow chemistry is a well-established technique for being used at a large scale when manufacturing of large quantities of a given material is required. It gathers a range of process technologies, tools and strategies now routinely used for explorative or preparative chemistry in many research groups.<sup>180,181</sup> Continuous flow synthetic methodologies can also be easily combined with other enabling technologies,<sup>182</sup> such as microwave irradiation, supported reagents or catalysts, photochemistry, inductive heating, electrochemistry, new solvent systems, 3D printing or microreactor technologies.

As O. Kappe and D. Dallinger rightly pointed out,<sup>183</sup> a green process needs to be scalable to have the greatest environmental impact, and ideally a direct translation from lab-to industrial scale would be desirable. Consequently, it is essential that a safe, robust and cost effective process is developed already in the earliest design stages by merging ideas stemming from both green chemistry and green engineering. We can say that continuous flow chemistry is located in the convergence of the green chemistry and green engineering principles (see Figure 1.12). Continuous flow processing specifically address these needs and for a large number of processes a distinct advantage over batch processing can be achieved in terms of cost, equipment size, energy consumption, waste generation, safety, efficiency and product quality. These benefits correspond exactly to the drivers highlighted by the pharmaceutical industry in API manufacturing.

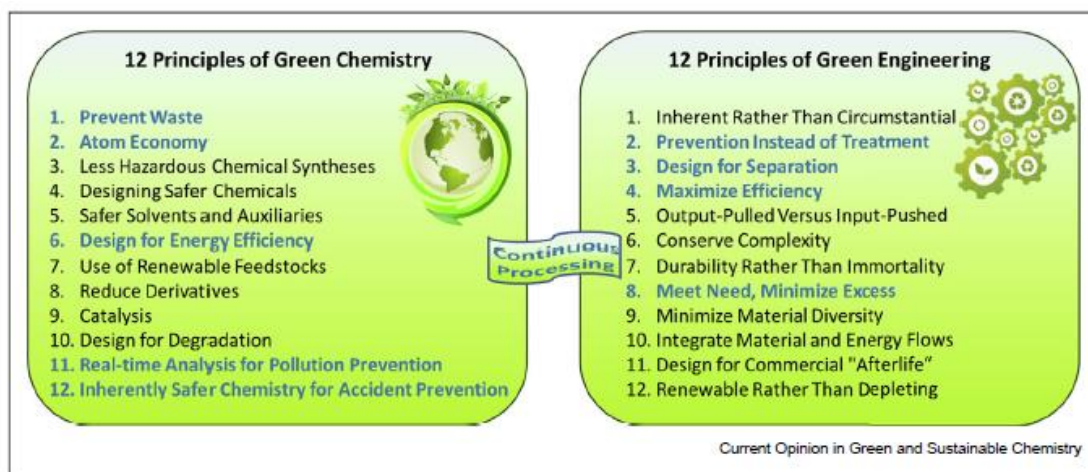
---

<sup>180</sup> M. B. Plutschack, B. Pieber, K. Gilmore, P. H. Seeberger, *Chem. Rev.*, 2017, 117, 11796-11893

<sup>181</sup> K. F. Jensen, *AIChE J.*, 2017, 63, 858-869.

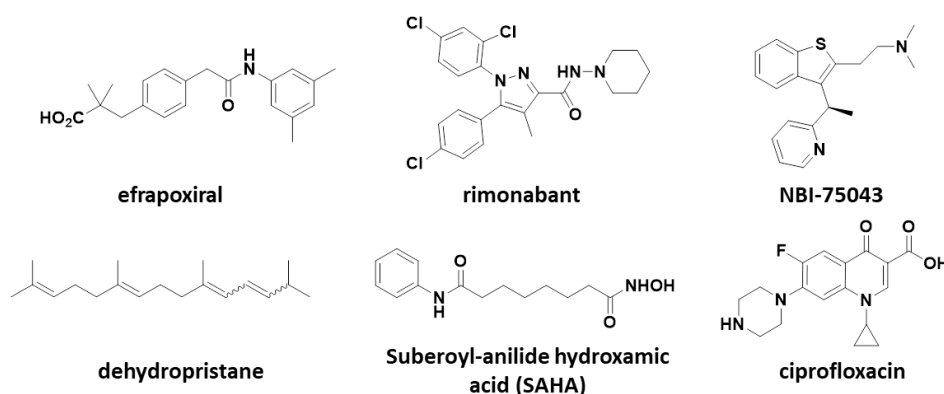
<sup>182</sup> J. Wegner, S. Ceylan, A. Kirschning, *Adv. Synth. Catal.*, 2012, 354, 17.

<sup>183</sup> D. Dallinger, C. O. Kappe, *Current Opinion in Green and Sustainable Chemistry*, 2017, 7, 6-12.



**Figure 1.12. Twelve principles of Green Chemistry and Green Engineering and the impact of continuous processing highlighted in blue (taken from ref. 183).**

The first published examples of flow chemistry applied to the synthesis of pharmaceutically active molecules emerged in the early 2000s when several research groups reported on specific flow transformations that enabled a new synthesis of some known pharmaceuticals.<sup>184</sup> Examples of these early endeavours include the syntheses of efraproxiral and rimonabant using a  $\text{AlMe}_3$ -mediated direct amidation in flow (see Figure 1.13).<sup>185</sup> In further years more complex APIs and syntheses were achieved.<sup>186,187</sup>



**Figure 1.13. Pharmaceutical structures targeted in early flow syntheses.**

<sup>184</sup> M. Baumann, I. R. Baxendale, *Beilstein J. Org. Chem.*, 2015, 11, 1194-1219.

<sup>185</sup> L. A. Radesca, Y. S. Lo, J. R. Moore, M. E. Pierce, *Synth. Commun.*, 1997, 27, 4373-4384.

<sup>186</sup> C. Battilocchio, I. R. Baxendale, M. Biava, M. O. Kitching, S. V. Ley, *Org. Process Res. Dev.*, 2012, 16, 798-810.

<sup>187</sup> J. Hartwig, S. Ceylan, L. Kupracz, L. Coutable, A. Kirschning, *Angew. Chem. Int. Ed.*, 2013, 52, 9813-9817.

From the different features that can be associated to Flow processes, as mentioned above, the following aspects can be highlighted:

- ❖ Safety has a key importance in any chemical procedure and it can be notably increased by flow processing. For example, in flow, gases like CO, H<sub>2</sub> or O<sub>2</sub> can be accurately dosed and mixed efficiently with the liquid stream allowing a safe and reliable performance of multiphase reactions.<sup>188,189</sup> Moreover, the fraction of gas volume in a pressurised liquid-filled system is significantly reduced. This is crucial to avoid evaporation of low-boiling reagents or formation of explosive gas mixtures. Something similar occurs with the use of unstable or hazardous intermediates. These intermediates are generated *in situ* and directly transformed inside the flow line or the flow reactor. These unstable or hazardous compounds never go out of the system. So it is not necessary to employ cryogenic conditions, with the energy save that it means. The reactions could be performed at room temperature without compromising the product quality.<sup>190</sup>
- ❖ High T/p are against the traditional green chemistry recommendations. Due to the excellent heat-exchange commented above and the small reactor volumes (as compared with batch processes) such harsh conditions can be avoided in flow. Flow processes not only need less energy, flow reactions also use smaller equipments than a comparable batch reaction. This can be illustrated by the following example: in a real case LCA study, the overall resource consumption for the production of galantamine HBr (anti-Alzheimer medication from Janssen Pharmaceutica) was evaluated and by changing only just one step to a flow process a 24% decrease in the overall resource requirements for the final API could be reached.<sup>191</sup> Importantly, the exceptional heat-exchange efficiency of microreactors suppresses the formation of hot spots, temperature gradients, or the accumulation of heat, elements that usually lead to a concomitant decrease in reaction selectivity, even for fast and highly exothermic reactions.<sup>192,193</sup> The miniaturisation, furthermore, has an immediate effect on radical chain reactions and the propagation of explosions is suppressed.<sup>194</sup>

---

<sup>188</sup> C. J. Malilla, I. R. Baxendale, *Org. Process Res. Dev.*, 2016, 20, 327-360.

<sup>189</sup> C. Hone, D. Roberge, C. O. Kappe, *ChemSusChem*, 2017, 10, 32-41.

<sup>190</sup> J. I. Yoshida, H. Kim, A. Nagaki, *ChemSusChem*, 2011, 4, 331-340.

<sup>191</sup> G. Van der Vorst, W. Aelterman, B. De Witte, B. Heirman, H. Van Langenhove, J. Dewulf, *Green Chem.*, 2013, 15, 744-748.

<sup>192</sup> B. Gutmann, D. Cantillo, C. O. Kappe, *Angew. Chem. Int. Ed.*, 2015, 54, 6688-6728.

<sup>193</sup> K. F. Jensen, B. J. Reizmana, S. G. Newman, *Lab Chip*, 2014, 14, 3206-3612.

<sup>194</sup> K. Jähnisch, V. Hessel, H. Löwe, M. Baerns, *Angew. Chem. Int. Ed.*, 2004, 116, 410-451.

- ❖ Due to the small volume required, flow processes can be used to perform a fast screening of the reaction conditions, and then, with the optimised conditions in hand, the reaction can be scaled up. This reaction scale up in flow reactors is easier than in batch and three different strategies can be used to prepare large amounts of compounds: i) scaling out: the easiest one, to run the process longer; ii) numbering up: multireactors in parallel; iii) scaling up: the process can be performed on larger continuous reactors.<sup>195</sup>
- ❖ Yield and product quality improvement, which means less need of purification procedures. Thanks to the enhanced mixing and exceptional heat-exchange efficiency, accurate control of the reaction temperature and residence time are possible, what enables reaction performance at conditions that minimise impurity formation, enhance selectivity and maximise yield. Not only is the purification of final products significantly reduced with flow strategies, also the one for the intermediates. The reaction intermediates can be generated and further *in situ* processed in telescoped multi-step sequences.
- ❖ Telescoping of multistep syntheses, which accompanied by in-line separations reduces solvent and energy waste and makes the process safer. Telescoped reactions consist in the implementation of multiple chemical steps within the same continuous flow network. This revolutionary approach avoids the handling of unstable intermediate molecules and their risks. Safety of the processes at industrial scale is drastically improved with telescoped synthesis. Examples of continuous flow telescoped processes have been reported especially for pharmaceutical products, including flucytosin,<sup>196</sup> diazepam and atropine among others.<sup>197</sup> J.-C. Monbaliu and co-workers have reported the implementation of the multi-step synthesis of four well-known pharmaceutical drugs (diphenhydramine hydrochloride, lidocaine hydrochloride, diazepam and fluoxetine hydrochloride) in a modular continuous flow telescoped process.<sup>198</sup> Processes with a really high complexity have been described through an uninterrupted continuous flow network. S. Kobayashi and co-workers reported the eight-step continuous flow

<sup>195</sup> N. G. Anderson, *Org. Process Res. Dev.*, 2012, 16, 852-869.

<sup>196</sup> A. Harsanyi, A. Conte, L. Pichon, A. Rabion, S. Grenier, G. Sandford, *Org. Process Res. Dev.*, 2017, 21, 273-276.

<sup>197</sup> A. C. Bédard, A. R. Longstreet, J. Britton, Y. Wang, H. Moriguchi, R. W. Hicklin, W. H. Green, T. F. Jamison, *Bioorg. Med. Chem.*, 2017, 25, 6233-6241.

<sup>198</sup> A. Adamo, R. L. Beingsner, M. Behnam, J. Chen, T. F. Jamison, K. F. Jensen, J.-C. M. Monbaliu, A. S. Myerson, E. Revalor, D. R. Snead, T. Stelzer, N. Weeranoppanant, S. Y. Wong, P. Zhang, *Science*, 2016, 352, 61-67.

telescoped synthesis of (*R*)- and (*S*)-rolipram.<sup>199</sup> The whole transformation of the commercial available aldehyde 3-(cyclopentyloxy)-4-methoxybenzaldehyde into chiral rolipram was achieved smoothly under continuous flow conditions employing a compendium of heterogeneous catalysts, without the isolation of any intermediates, catalysts, co-products, by-products or excess reagents. Moreover, this system demonstrated to be stable for at least one week and could also be applicable to the synthesis of other GABA (gamma-aminobutyric acid) derivatives.

Some significant advances of preparative continuous flow organic chemistry overlap with important societal challenges. The implications solely in the pharmaceutical industry are immense, and can contribute and even solve current and very sensitive societal concerns such as drug shortages, poor investment in orphan drugs, availability of medicines in remote areas, prohibitive production costs for developing countries, and overall slow development of new drugs.<sup>200,201</sup> The various aspects of flow chemistry also contribute to the design of new synthetic strategies helping in the transition from an exclusively petrobased to biobased industry, with applications ranging from commodity to specialty chemicals.<sup>202,203,204,205</sup>

Due to all these properties and the green advantages of continuous flow chemistry mentioned, the investment in the continuous flow chemistry field and in his application on drug synthesis research have been increasing constantly (see Figure 1.14). Consequently, numerous studies have been published in recent years detailing the beneficial outcome of flow chemistry applied to single or indeed multistep syntheses of target compounds on various reaction scales.

As suggested by S. Kobayashi and co-workers, continuous flow systems can be generally divided into four categories (Figure 1.15).<sup>199</sup> In type I, all of the reagents are flowed through the reactor, and at the end, the product is collected. In type II, one of the reactants is supported onto a solid and confined into the reactor; the substrate is passed through the reactor, and if the reaction goes to completion, the exiting reaction mixture will contain the desired product only. Both types I and II do not

---

<sup>199</sup> T. Tsubogo, H. Oyamada, S. Kobayashi, *Nature*, 2015, 520, 329-332.

<sup>200</sup> S. A. May, *J. Flow Chem.*, 2017, 7, 137-145.

<sup>201</sup> L. Malet-Sanz, F. Susanne, *J. Med. Chem.*, 2012, 55, 4062-4098.

<sup>202</sup> B. Gutmann, C. O. Kappe, *J. Flow Chem.*, 2017, 7, 65-71.

<sup>203</sup> J. Yue, *Catal. Today*, 2018, 308, 3-19.

<sup>204</sup> C. A. Hone, D. M. Roberge, C. O. Kappe, *ChemSusChem*, 2017, 10, 32-41.

<sup>205</sup> L. Vaccaro, D. Lanari, A. Marrocchi, G. Strappaveccia, *Green Chem.*, 2014, 16, 3680-3704.



require the use of any catalyst during the reaction. In type III, a homogeneous catalyst is employed; the catalyst flows through the reactor together with the reactants; so, at the end, a separation step of the product from the catalyst and possible byproducts is required. In type IV, the catalyst resides into the reactor, while the reagents passed. The catalyst should be immobilised before and, in principle, no separation of the product from the catalyst is needed. In addition, with this strategy the catalyst can be easily recycled.

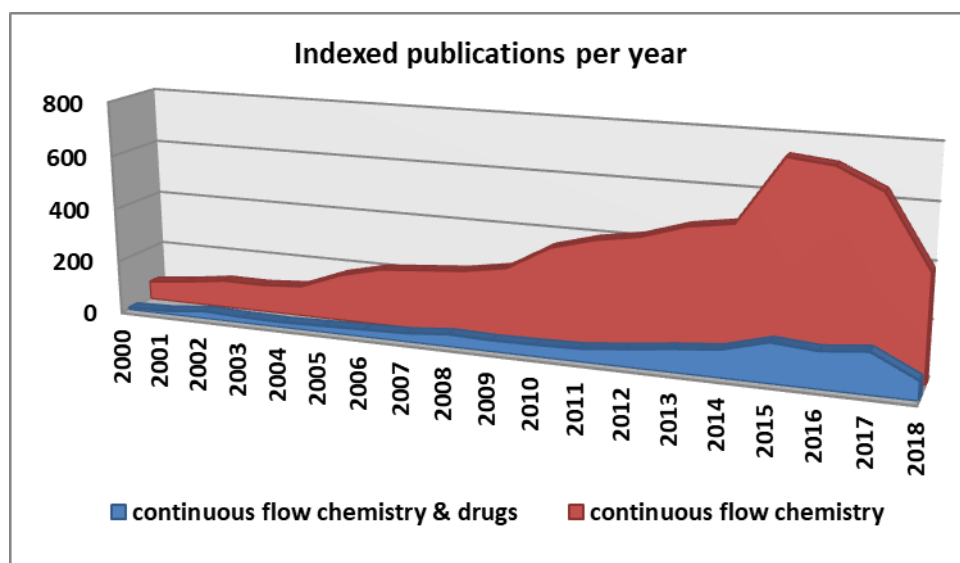


Figure 1.14. Indexed publications that appear with the searches “continuous flow chemistry” and “continuous flow chemistry” + “drugs” in the Scopus database.

The latter type is generally considered the most convenient method to perform a reaction under continuous flow conditions. But not only for simple continuous flow reactions, type IV systems also are the best candidates for performing multistep synthesis in flow.<sup>206</sup> As mentioned they provide the possibility of avoiding catalyst separation and facilitate its recycling. Additionally, the reaction product can be further functionalised by using other catalytic reactors, without any additional operation. In this way a telescoped synthesis of complex organic molecules starting from simple substrates can be accomplished under continuous conditions.<sup>199</sup>

Moreover, type IV reactors can be classified into three main classes depending on the method used to incorporate an immobilised catalyst into the device:<sup>199</sup> i) packed-bed: the catalyst is immobilised onto an

<sup>206</sup> R. Porta, M. Benaglia, A. Puglisi, *Org. Process. Res. Dev.*, 2016, 20, 2-25.

insoluble support and is randomly charged into the reactor; ii) monolithic: the catalyst is prepared in the form of a structured material, consisting on a regular or irregular network of channels. In general the monolith is built up by the copolymerisation of different monomers (one of them containing the catalytic or precatalytic unit) in the presence of a porogen inside the reactor. The main advantage of a monolithic reactor with respect to a packed-bed is that the packing is more homogeneous and a more controlled fluidodynamics is generally achieved; iii) inner wall-functionalised: the catalyst is covalently attached onto the interior wall of the reactor. The use of this last type is still limited due to the complexity of the corresponding preparation.

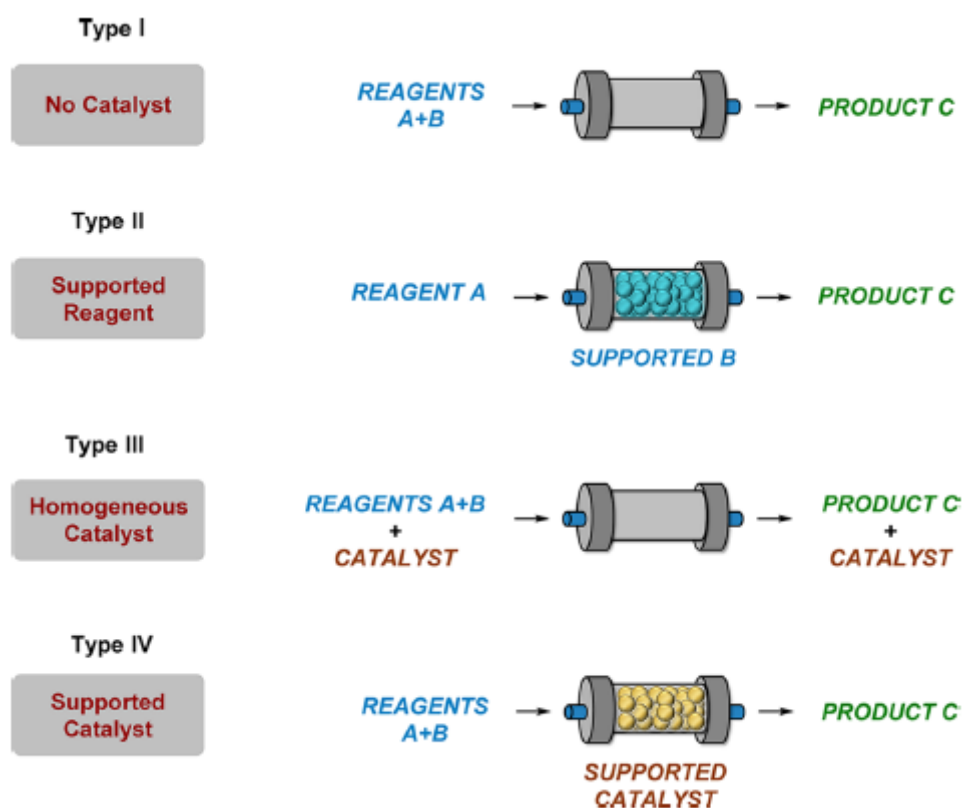


Figure 1.15. Types of continuous flow systems described by S. Kobayashi and co-workers<sup>199</sup> (taken from ref. 206).

There are important differences between batch and flow processes with respect to production time and yield.<sup>207</sup> In batch, production reaction time is determined by how long a vessel is held at a given temperature, while in the flow regime the reactor volume and the bulk flow rate determine the production rate. Stoichiometry in flow reactors is defined

<sup>207</sup> A. Kirschning, *Beilstein J. Org. Chem.*, 2009, 5, No. 15.

by the concentration of reagents and the ratio of their flow rate. In batch processes, this is defined by the concentration of chemical reagents and their volumetric ratio. A given reaction can be accelerated and the production rate of a flow device can be increased by increasing flow rates. Multistep reaction sequences can be conducted in a completely different fashion in flow as compared to batch processes. With miniaturised bench-sized flow systems being commercially available, continuous-flow processes can be operated in a common laboratory with important pros such as facile automation, reproducibility, safety and process reliability due to constant reaction parameters.

A great deal of research efforts have been directed in last years to achieve autoregulated continuous flow processes by creating an intelligent and responsive system.<sup>208,209</sup> S. V. Ley and co-workers described the three layers that must be considered when creating a telescoped flow synthesis process:<sup>210</sup> i) chemical transformations involved (chemical layer); ii) how to transfer the synthetic materials between the stages in an uninterrupted way (engineering); and iii) the transmission and monitoring of data to achieve total control of the system (information) (Figure 1.16). The engineering part does not represent a problem due to the number of low cost continuous flow tools available. Packed-tube heterogeneous catalysts and reagents,<sup>211</sup> liquid-liquid separators,<sup>212</sup> continuous filtration devices,<sup>213</sup> continuous chromatography,<sup>214</sup> continuous solvent evaporators and distillation devices among others can be found.<sup>215</sup> Computer control can be used for the third part (information).

S. V. Ley and co-workers introduced an algorithm based computer control to achieve the autoregulated continuous three-step telescoped synthesis of 2-aminoadamantane-2-carboxylic acid.<sup>210</sup> The three steps

<sup>208</sup> H. Lange, C. F. Carter, M. D. Hopkin, A. Burke, J. G. Goode, I. R. Baxendale, S. V. Ley, *Chem. Sci.*, 2011, 2, 765-769.

<sup>209</sup> J. S. Moore, K. F. Jensen, *Org. Process Res. Dev.*, 2012, 16, 1409-1415.

<sup>210</sup> R. J. Ingham, C. Battilocchio, D. E. Fitzpatrick, E. Sliwinski, J. M. Hawkins, S. V. Ley, *Angew. Chem. Int. Ed.*, 2015, 54, 144-148.

<sup>211</sup> L. J. Martin, A. L. Marzinzik, S. V. Ley, I. R. Baxendale, *Org. Lett.*, 2011, 13, 320-323.

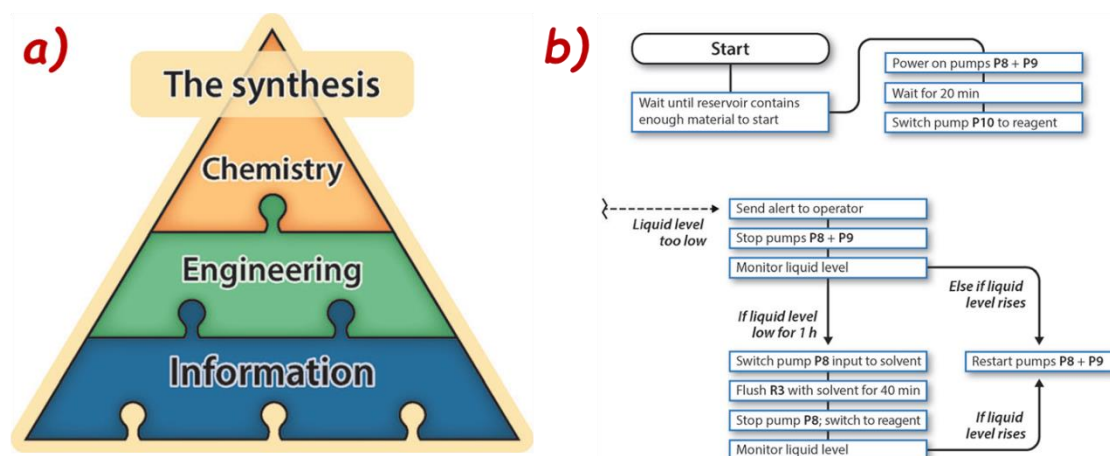
<sup>212</sup> M. O'Brien, P. Koos, D. L. Browne, S. V. Ley, *Org. Biomol. Chem.*, 2012, 10, 7031-7036.

<sup>213</sup> S. Mascia, P. L. Heider, H. Zhang, R. Lakerveld, B. Benyahia, P. I. Barton, R. D. Braatz, C. L. Cooney, J. M. B. Evans, T. F. Jamison, K. F. Jensen, A. S. Myerson, B. L. Trouost, *Angew. Chem. Int. Ed.*, 2013, 52, 12359-12363.

<sup>214</sup> A. G. O'Brien, Z. Horváth, F. Lévesque, J. W. Lee, A. Seidel-Morgenstern, P. H. Seeberger, *Angew. Chem. Int. Ed.*, 2012, 51, 7028-7030.

<sup>215</sup> B. J. Deadman, C. Battilocchio, E. Sliwinski, S. V. Ley, *Green Chem.*, 2013, 15, 2050-2055.

involve seven operating reactors but enough autonomy and self-regulation were achieved to be managed by a single operator. For example, the second step does not start until an in-line IR spectrometer detects the product of the first step and this data is coupled with a switching valve and the downstream pumps. Moreover, computer control enables stable and autonomous operation of some devices. The result was a total control of the complex system configurations where small changes could be implemented very quickly. An example of algorithm employed can be seen in Figure 1.16.



**Figure 1.16. a) Three layer chart where S. V. Ley and co-workers represented the three aspects that should be considered when creating a telescoped flow process; b) Example of algorithm programmed by S. V. Ley and co-workers to achieve an autoregulated multi-step telescoped continuous flow procedure (both taken from ref. 210).**

Regarding the most common components of a continuous flow setup, reactors are typically tube like and manufactured from non-reactive materials such as stainless steel, glass and polymers. Mixing methods include none (if the diameter of the reactor is small e.g. <1 mm, such as in microreactors) and static mixers.<sup>216</sup> Continuous flow reactors are typically characterised by narrow and well-defined channels with internal dimensions in the  $10^2$ - $10^3$   $\mu\text{m}$  range, and by internal volumes ranging from a few microliters to several millilitres, and are named either micro- or mesofluidic reactors based upon their respective internal diameters and volumes. Continuous flow reactors allow good control over reaction conditions including heat transfer, time and mixing. The residence time of the reagents in the reactor (i.e. the

<sup>216</sup> A. Pashkova, L. Greiner, *Chemie-Ingenieur-Technik*, 2011, 83, 1337-1342.

amount of time that the reaction is heated or cooled) is calculated from the volume of the reactor and the flow rate through it:<sup>217</sup>

$$\text{Residence time} = \text{Reactor Volume} / \text{Flow Rate}$$

In order to achieve a longer residence time, and therefore longer reaction time, reagents can be pumped at slower flow rates and/or a larger volume reactor be used. Production rates may vary from nanoliters to liters of product per minute. There are different types of flow reactors attending to the conditions of the reaction to perform. Some examples of flow reactor are spinning disk reactors, spinning tube reactors, multi-cell flow reactors, microreactors, hex reactors, continuous-stirred tank reactors (CSTR), Plug Flow reactors (PFR), and the ones that we have most employed in the work described in the following chapters: packed-bed reactors (PBR).<sup>4</sup>

A packed-bed reactor is a tubular reactor that is packed with solid catalyst particles. The reaction takes place on the surface of the catalyst. Consequently, the reaction rate is based on the mass of solid catalyst rather than on the reactor volume.

Multiple integrated continuous flow setups are commercially available for applications on various scales ranging from micrograms to hundreds of kilograms of processed material per day. Additionally, continuous flow setups can be conveniently constructed with low tech, widely available parts such as PFA capillaries and HPLC connectors,<sup>218</sup> thus greatly facilitating technology adoption in conventional laboratory environments. Materials usually used for the tubes and connexions to build continuous flow systems generally include: FEP (fluorinated ethylene propylene), PEEK (polyether ether ketone), PFA (perfluoroalkoxy alkanes) and PTFE (polytetrafluoroethylene) besides standard stainless steel.

One aspect of continuous flow synthesis that delayed its progress for a long time involved the way in which reagents streams were delivered into the reactors. In much of the early flow chemistry work delivery of liquid streams was achieved using simple syringe pumps. Unfortunately syringe pump applications are significantly limited by relatively low working pressures and often needed manual intervention when recharging the syringe, which precluded a fully continuous and automated process.<sup>184</sup>

---

<sup>217</sup> V. Sans, N. Karbass, M. I. Burguete, E. García-Verdugo, S. V. Luis, *RSC Advances*, 2012, 2, 8721-8728.

<sup>218</sup> J. Britton, T. F. Jamison, *Nat. Protoc.*, 2017, 12, 2423-2446.

Alternatively the use of piston or rotatory pumps (HPLC pumps for example) can be employed, but these also have drawbacks being often characterised by inaccurate flow rates or fouling over prolonged periods of use due to their direct interactions with the chemicals being pumped (for example, organozinc reagents damage internal parts of HPLC pumps). In addition both of these pumping mechanisms require homogeneous solutions where particulates or precipitates are extremely detrimental. These shortcomings obviously impact the performance of flow reactors when attempting reaction scale-up, especially when precise and consistent reagent delivery is crucial. In order to address these issues flow equipments utilising adapted peristaltic pumps have been developed and applied to several mesoscale syntheses. The pump design uses specific fluorinated polymers for the feed tubing that is placed on the rotor of a modified peristaltic pump resulting in a smooth and consistent delivery of a solution that can be drawn directly out of the supplier's reagent bottle. A first application of a commercial system like this was reported by the S. V. Ley group with their continuous synthesis of the important anti-cancer agent tamoxifen in 2013.<sup>219</sup>

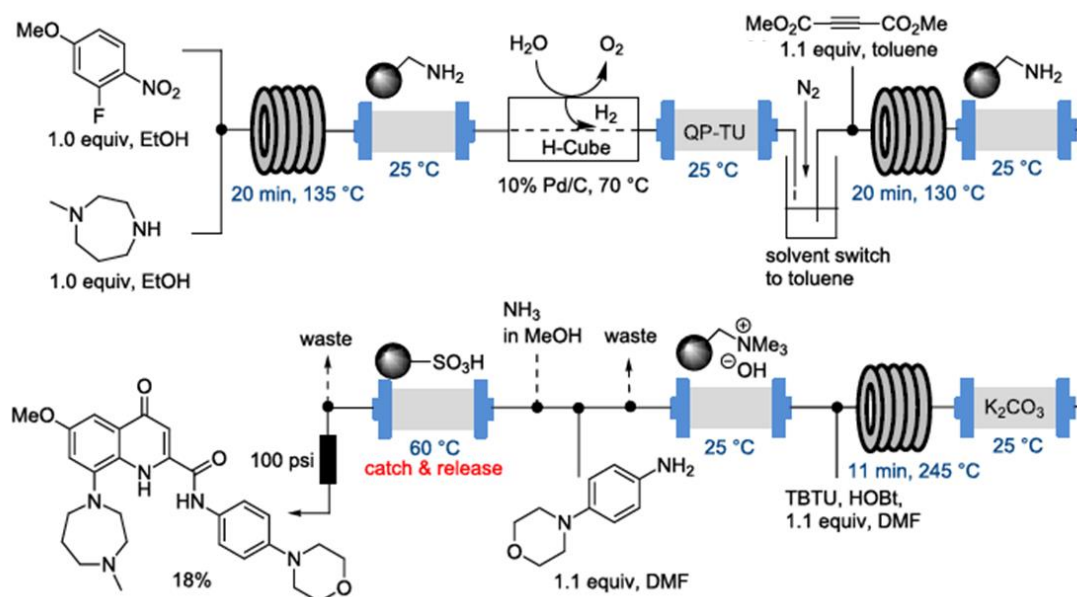
In last years a considerable increase in complexity in continuous flow processes has been observed, especially for applications toward active pharmaceuticals. Flow chemistry has rapidly evolved from single step reactions to fully integrated telescoped multistep processes. Figure 1.17 shows an example of a complete telescoped multistep flow synthesis for the potent 5HT1B antagonist reported by the Innovative Technology Centre (ITC) in 2010.<sup>220</sup>

The coupling of several reactions in a telescopic procedure is one of the main objectives of this work and will be developed in further chapters to synthesise key molecules of synthetic interest. With the use of a sequential set of mini-reactors under flow conditions the potential for practical use and their "green character" is implemented. This allows the simple compartmentalisation of the different catalytic systems and enables to operate at different P and T conditions, according to the needs of each individual step. This facilitates the work-up, particularly recycling and reuse, decreases the toxicity of catalytic materials and can significantly reduce the final amount of waste. The performing of organocatalytic, biocatalytic and organometallic catalysed reactions in the same whole procedure is allowed by connecting several reactors under continuous flow conditions.

---

<sup>219</sup> P. R. D. Murray, D. L. Browne, J. C. Pastre, C. Butters, D. Guthrie, S. V. Ley, *Org. Process Res. Dev.*, 2013, 17, 1192-1208.

<sup>220</sup> Z. Qian, I. R. Baxendale, S. V. Ley, *Synlett*, 2010, 505-508.



**Figure 1.17. Flow synthesis of a potent 5HT<sub>1B</sub> antagonist.<sup>220</sup> The API is assembled through a five step continuous synthesis including a S<sub>N</sub>Ar reaction, heterogeneous hydrogenation, Michael addition-cyclisation and final amide formation. This sequence makes use of in-line scavenging resins for purification purposes and demonstrates the utility of in-line solvent switching protocols and high temperature reactor coils operating at 130-245°C, well above the boiling points of the solvents employed (taken from ref. 184).**

All these continuous flow chemistry assets, appropriately combined, can help drastically reduce time and space footprints for chemical processes.<sup>221</sup> However, as R. Gérardy *et al.* properly remarked,<sup>222</sup> some conditions remain challenging for flow conditions, such as the handling of highly viscous materials or the handling of slurries and solids. Not all reactions are to be performed in flow, and a careful analysis must be carried out for balancing the investment in time and equipment and the return in terms of concrete chemical/process efficiency.<sup>223</sup>

Another possible concern associated with the use of continuous flow reactors is the clogging of the reactor, that is, the blockage of the channels mainly due to precipitation of solids.<sup>206</sup> This is a very common situation for a synthetic organic chemist, who constantly deals with precipitation of inorganic salts or insoluble materials during a reaction. In some cases, this can represent an amenable situation. An example is the process for which the reaction product precipitates from the reaction mixture, thus facilitating the purification process. However, it

<sup>221</sup> V. Hessel, D. Kralisch, N. Kockmann, T. Noël, Q. Wang, *ChemSusChem*, 2013, 6, 746-789.

<sup>222</sup> R. Gérardy, N. Emmanuel, T. Toupy, V.-E. Kassim, N. N. Tshibalonza, M. Schmitz, J.-C. M. Monbaliu, *Eur. J. Org. Chem.*, 2018, 2301-2351.

<sup>223</sup> R. L. Hartman, J. P. McMullen, K. F. Jensen, *Angew. Chem. Int. Ed.*, 2011, 50, 7502-7519.

is easy to understand that this represents a problem in the case of a flow system. This is the reason why more sophisticated technologies for the handling of solids in continuous flow processes have been recently developed, although technical advances are still needed.

Further improvement is also possible in the application of stereoselective catalysis under flow conditions. The synthesis in continuo of chiral APIs through stereoselective catalysis is still not explored enough or not developed enough.<sup>224</sup> Stereoselective biocatalysis,<sup>225</sup> or organometallic catalysis<sup>226</sup> in continuous flow are more extended, but the use of potentially toxic metal species has to be avoided.<sup>227</sup> Thus stereoselective organocatalysis in flow is a very innovative and rapidly expanding methodology to prepare enantioenriched (complex) molecules and would be ideal for pharmaceutical applications.<sup>228</sup>

Recognition of the problematic aspects of flow chemistry is essential to allow a unified effort from the chemistry and chemical engineering communities in order to surmount these obstacles and for us to achieve the vision of true continuous manufacture of pharmaceuticals.<sup>184</sup>

### 1.5.1. Advanced Manufacturing : 3D printing

Regarding materials for continuous flow reactors and systems, new 3D printing technologies represent an important element of progress. 3D printing is also termed under the general denomination of additive manufacturing technologies, as it works by depositing multiple layers, one by one, to finally achieve the final design from a previous made CAD (computer-aided design). In 1986, the first stereolithographic 3D printer was invented by C. Hull,<sup>229</sup> and several 3D printing processes or strategies have been developed since this moment. From the initial discovery, 3D printing has been extensively applied in different unrelated fields like education,<sup>230</sup> food industry,<sup>231</sup> or with biomedical

---

<sup>224</sup> D. Zhao, K. Ding, *ACS Catal.*, 2013, 3, 928-944

<sup>225</sup> L. H. Andrade, W. Kroutil, T. F. Jamison, *Org. Lett.*, 2014, 16, 6092-6095.

<sup>226</sup> B. Castano, E. Gallo, D. J. Cole-Hamilton, V. Dal Santo, R. Psaro, A. Caselli, *Green Chem.*, 2014, 16, 3202-3209.

<sup>227</sup> I. V. Gursel, T. Noel, Q. Wang, V. Hessel, *Green Chem.*, 2015, 17, 2012-2026.

<sup>228</sup> I. Atodiressei, C. Vila, M. Rueping, *ACS Catal.*, 2015, 17, 1972-1985.

<sup>229</sup> C. W. Hull, U.S. Patent 4575330, March 11, 1986.

<sup>230</sup> S. Rossi, M. Benaglia, D. Brenna, R. Porta, M. Orlandi, *J. Chem. Educ.*, 2015, 92, 1398-1401.

<sup>231</sup> J. Sun, W. Zhou, D. Huang, J. Y. H. Fuh, G. S. Hong, *Food Bioproc. Tech.*, 2015, 8, 1605-1615.



purposes.<sup>232</sup> Of course, this new technology has also aroused interest in the universe of chemistry. However, the first applications in chemistry were mainly related with analytical areas.<sup>233,234</sup> It has been in recent years when applications related to catalysis or the possibility to create chemical labware, reactionware and research equipment have grown up.<sup>235</sup>

The combination of additive manufacturing technologies with catalysis offers unprecedented opportunities, and challenges, to the modern chemist.<sup>236,237</sup> One of the fields where additive manufacturing is really making the difference is flow chemistry.<sup>238</sup> Thanks to this, many different materials can replace glass, steel and silicon, allowing the production of devices with an easier protocol, inexpensive manner and short times.<sup>239</sup> Microfluidic devices and, in general, tailored reactors have been designed.<sup>240,241</sup> A large variety of materials can be used for 3D printing like polylactic acid (PLA), high impact polystyrene (HIPS), polyvinyl alcohol (PVA), polyethylene terephthalate (PET), polycarbonate (PC) or polyamides (Nylon). This wide choice of printable materials is one of the most significant advantages of 3D printing. But, at the same time, one of the most important limitations of 3D printing applications in organic synthesis is represented by the nature of the material used in the printing process. From a chemical point of view, the choice of the best material for a given application is extremely important, since its inertness is a mandatory requisite for any application, in order to maintain the integrity of the device.<sup>239</sup>

As mentioned, different 3D printing processes or techniques have been developed since the invention of the first 3D printer. The most common are fused deposition modelling (FDM), stereolithography (SLA), selective laser sintering (SLS), selective laser melting (SLM), electronic beam melting (EBM), digital light processing (DLP), binder jetting (BJ) and laminated object manufacturing (LOM). From this compilation of

<sup>232</sup> F. P. Melchels, J. Feijen, D. W. Grijpma, *Biomaterials*, 2010, 31, 6121-6130.

<sup>233</sup> M. Pohanka, *Anal. Lett.*, 2016, 49, 2865-2882.

<sup>234</sup> G. Scotti, S. M. E. Nilsson, M. Haapala, P. Poho, G. B. af Gennas, J. Yli-Kauhahuoma, T. Kotiaho, *React. Chem. Eng.*, 2017, 2, 299-303.

<sup>235</sup> J. M. Pearce, *Science*, 2012, 337, 1303-1304.

<sup>236</sup> X. Zhou, C.-j. Liu, *Adv. Funct. Mater.*, 2017, 27, 1701134.

<sup>237</sup> C. Hurt, M. Brandt, S. S. Priya, T. Bhatelia, J. Patel, P. R. Selvakannan, S. Bhargava, *Catal. Sci. Technol.*, 2017, 7, 3421-3439.

<sup>238</sup> A. J. Capel, S. Edmondson, S. D. Christie, R. D. Goodridge, R. J. Bibb, M. Thurstans, *Lab Chip*, 2013, 13, 4583-4590.

<sup>239</sup> S. Rossi, A. Puglisi, M. Benaglia, *ChemCatChem*, 2018, 10, 1-15.

<sup>240</sup> A. K. Au, W. Huynh, L. F. Horowitz, A. Folch, *Angew. Chem. Int. Ed.*, 2016, 55, 3862-3881.

<sup>241</sup> T. Monaghan, M. J. Harding, R. A. Harris, R. J. Friel, S. D. Christie, *Lab Chip*, 2016, 16, 3362-3373.

techniques, we want to highlight two: Stereolithography (SLA) and fused deposition modelling (FDM).

- i) Fused deposition modelling (FDM) is also called fused filament fabrication (FFF). S. S. Crump was the first who patented this technique in the late 1980s and in 1990 the first 3D printer based on it was commercialised by Stratasys.<sup>242</sup> As S. Rossi *et al.* perfectly explain, “*with this technology, a thermoplastic filament (1.75 or 3.00 mm diameter) is unwound from a coil, fed into a hot nozzle (regulated by a temperature control unit) and passed in a viscous-flow state and extruded through an extruder that can be moved in both X and Y direction while the build plate lowers the object layer by layer in the Z direction according to the virtual design. In this way, the molten material is deposited one layer on top of the other to which it will bond once gently solidified in a heated enclosure. Generally, the desired object is built from the bottom to the top; sometime, when the object present overhanging parts, the presence of (removable) supports is required*” (see Figure 1.18).<sup>239</sup> Some advantages of this method are the wide choice of printable materials relatively inexpensive and easy-to-handle and the fact that today FDM 3D printers are accessible at low cost and are commonly available in many stores. Moreover, despite the fact that not all the materials are appropriate for applications in organic synthesis due to the effects that the organic solvents can cause in the material (including health concerns involving the hazardous fumes that can be generated), polymers with increased resistance to organic solvents are under development.<sup>243</sup> For all these reasons FDM is the most largely used additive manufacturing process for applications related with chemical transformations as will be seen in recent examples described. For example, in 2014 L. Cronin reported the preparation by FDM 3D printing of monolithic sealed hydrothermal reactors made of polypropylene. These sealed reactors had reactants added directly during the 3D printing process and were successfully employed to perform organic reactions under high temperature and pressure.<sup>244</sup> Another representative example was the FDM 3D printing of standard

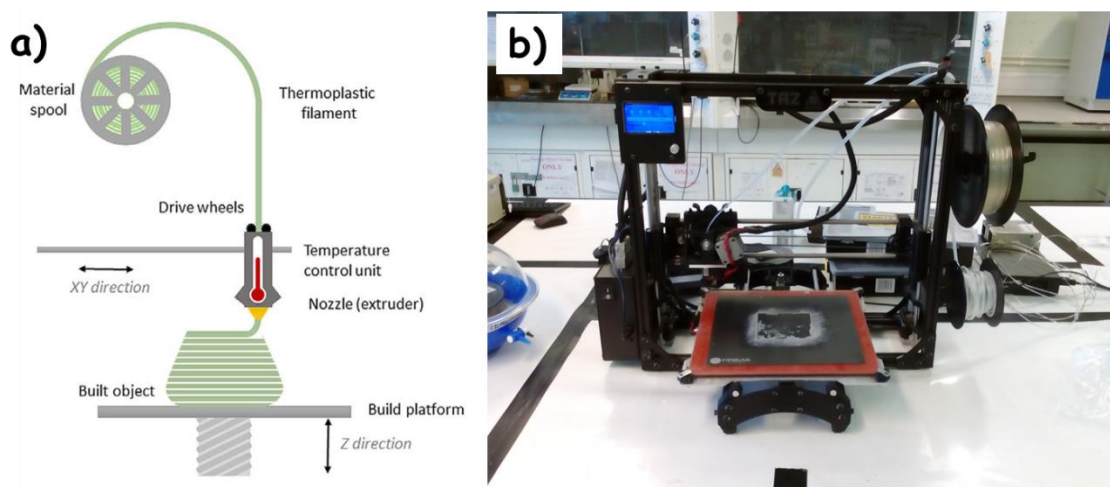
---

<sup>242</sup> S. S. Crump, U.S. Patent 5121329, June 9, 1992.

<sup>243</sup> F. A. Kucherov, E. G. Gordeev, A. S. Kashin, V. P. Ananikov, *Angew. Chem. Int. Ed.*, 2017, 56, 15931-15935.

<sup>244</sup> P. J. Kitson, R. J. Marshall, D. Long, R. S. Forgan, L. Cronin, *Angew. Chem. Int. Ed.*, 2014, 53, 12723-12728.

labware reported by V. P. Ananikov in 2017.<sup>243</sup> This method will be used in chapter 7.



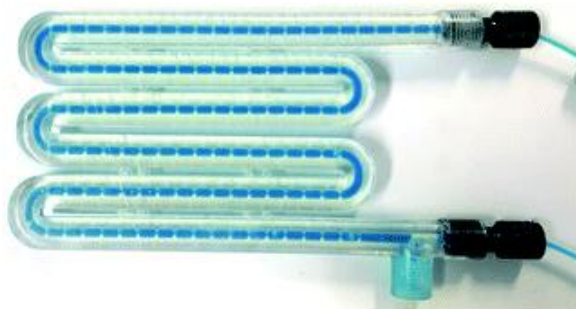
**Figure 1.18. a) Schematic representation of FDM model by S. Rossi *et al.* (taken from ref. 239) b) FDM 3D printer from the group of Dr. Víctor Sans in the University of Nottingham**

- ii) Stereolithography (SLA): its importance lies in the fact it was the first technique used. It involves the use of an ultraviolet laser that is focused onto a vat containing a photopolymerable resin. The advantages of this technique compared with FDM are higher resolutions and higher building speeds.<sup>245</sup> More detail level can be reached employing this method. However, the variety of materials (resins) that can be used is quite limited, due to the fact that they are all based on epoxy, urethanes or acrylic derivatives. Moreover, the high viscosity of the resins makes difficult a proper printing of small channels, which is a crucial point for 3D printed reactors. Despite of the differences, SLA and FDM have aspects in common like the creation of the final structure in a layer-by-layer mode where each layer is built on top of the preceding one. A very interesting example of continuous flow reactor printed by SLA was reported by V. Sans and co-workers in 2017.<sup>246</sup> The higher level of detail achievable with the SLA method allowed to obtain continuous oscillatory baffled reactors (COBR) (Figure 1.19). Those reactors, compared with the tubular ones, allow more optimised mixing due to the fact that baffled cells can be

<sup>245</sup> B. C. Gross, J. L. Erkal, S. Y. Lockwood, C. Chen, D. M. Spence, *Anal. Chem.*, 2014, 86, 3240-3253.

<sup>246</sup> O. Okafor, A. Weilhard, J. A. Fernandes, E. Karjalainen, R. Goodridge, V. Sans, *React. Chem. Eng.*, 2017, 2, 129-136.

envisioned as a number of continuous stirred tank reactors. Those reactors were successfully employed to obtain silver nanoparticles under continuous flow conditions.



**Figure 1.19. Continuous oscillatory baffled reactor 3D printed with the SLA method by V. Sans and co-workers (taken from ref. 246).**

There are several general steps to be carried out before the physical 3D printing process: i) creation of a virtual design file with CAD (computer aided-design) software; ii) conversion of the CAD file to STL format (standard tessellation language); iii) to fix the technical parameters and instrumental setup. They are independent from the type of 3D printing approach used. However, due to the different technologies to process the materials in each 3D printing method, the same virtual file design could derivate in final objects with different physical looks.

The rest of technologies present some interesting characteristics like the possibility to work with almost any material available in powder form even adding additives in the binder jetting (BJ) method or the reduced positioning errors in the XY plane in the digital light processing (DLP). However, all of them are expensive and unaffordable compared to FDM, the most used additive manufacturing process for rapid prototyping.

These 3D printing techniques offer numerous possibilities for chemists. For example, catalysts can be directly printed in the desired form, which can be of importance for heterogeneous catalytic systems. Thus, in 2016 E. Sotelo and A. Gil reported for the first time the fabrication of a copper heterogeneous catalytic system to promote Ullmann reactions.<sup>247</sup> This system was 3D printed using a Cu/Al<sub>2</sub>O<sub>3</sub> mixture and the final catalyst consisted on Cu(NO<sub>3</sub>)<sub>2</sub>·2.5H<sub>2</sub>O supported on a Al<sub>2</sub>O<sub>3</sub> support; demonstrating to be a robust, efficient and reusable catalytic system (see Figure 1.20.a). The synthesis of N-aryl substituted imidazoles, benzimidazoles and N-aryl amides was achieved with

<sup>247</sup> C. R. Tubío, J. Azuaje, L. Escalante, A. Coelho, F. Guitian, E. Sotelo, A. Gil, *J. Catal.* 2016, 334, 110-115.

excellent yields and short reaction times, and reusing the catalyst during 10 cycles without activity loss. One year later, a similar Al<sub>2</sub>O<sub>3</sub> recyclable 3D printed catalyst able to catalyse multicomponent Biginelli and Hantzsch reactions was reported by the same group.<sup>248</sup>

Another application is the above mentioned 3D printing creation of chemical labware, reactionware and research equipment (see Figure 1.20.b). In this case, the choice of the correct material is strictly connected to the chemical transformation that has to be performed or investigated with this labware. 3D printed reactors could be considered here. Actually, a glass vessel or a round bottom flask can be considered as reactors due to the fact that chemical reactions happen inside them. As mentioned, 3D printing offers the possibility to replace glass for other polymeric materials like polylactic acid (PLA), polyethylene terephthalate (PET), polycarbonate (PC), polypropylene (PP), polystyrene (PS) or Nylon. Moreover, new designs can be created providing the specifically designed reactor structure for the specific chemical transformation desired. The first reusable 3D printed reactionware was fabricated and reported by L. Cronin and co-workers in 2012.<sup>249</sup> This reactionware, printed with acetoxysilicon, included printed-in catalysts and other components and was designed in order to perform the synthesis of phenanthridine-based heterocycles (see Figure 1.20.d). Yields higher than 90% were observed for the desired product after 21 h. One year later the same group reported an evolution of this reactor consisting in a sealed reactionware where reagents, catalysts and purification apparatus were integrated into a single monolithic device (see Figure 1.20.e).<sup>250</sup> In 2016, an automated robot for the synthesis of racemic ibuprofen was also built by L. Cronin and co-workers using a FDM 3D printing platform with the incorporation of liquid handling components (see Figure 1.20.c).<sup>251</sup>

The recent developments in additive manufacturing technologies has led to an expansion of the possibilities in the field of continuous flow chemical devices, more concisely in the field of micro- and *meso* fluidic devices. Advanced manufacturing allows to replace traditional materials by new ones and create new designs according to the needs of mixing, injection or pathway of the continuous flow transformations to be performed. Thanks to 3D printing, improved devices can be produced

---

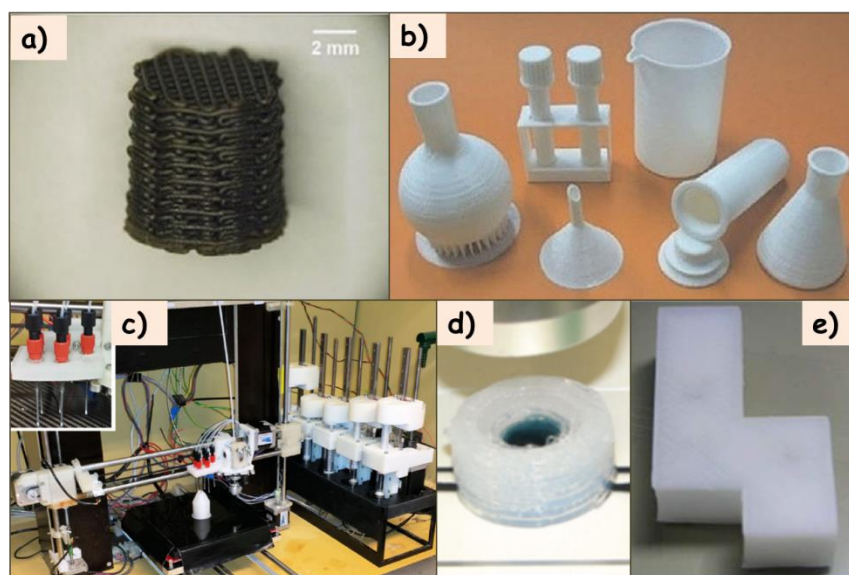
<sup>248</sup> J. Azuaje, C. R. Tubío, L. Escalante, M. Gomez, F. Guitian, A. Coelho, O. Caamano, A. Gil, E. Sotelo, *Appl. Catal. A*, 2017, 530, 203-210.

<sup>249</sup> M. D. Symes, P. J. Kitson, J. Yan, C. J. Richmond, G. J. Cooper, R. W. Bowman, T. Vilbrandt, L. Cronin, *Nat. Chem.*, 2012, 4, 349-354.

<sup>250</sup> P. J. Kitson, M. D. Symes, V. Dragone, L. Cronin, *Chem. Sci.*, 2013, 4, 3099.

<sup>251</sup> P. J. Kitson, S. Glatzel, L. Cronin, *Beilstein J. Org. Chem.*, 2016, 12, 2776-2783.

with an easier protocol, inexpensive manner and short times. Unfortunately, not all the 3D printing methods mentioned above can be used for obtaining continuous flow fluidic devices. Only stereolithography (SLA), selective laser sintering (SLS), laminated object manufacturing (LOM), binder jetting (BJ) and fused deposition modelling (FDM) have found application in this field,<sup>238</sup> being our intention to highlight the use of SLA and FDM.



**Figure 1.20.** a) Copper heterogeneous 3D printed catalyst developed by E. Sotelo and A. Gil to perform Ullman reactions<sup>247</sup> b) Examples of typical labware made by FDM 3D printing<sup>243</sup> c) Automated robot with an adapted 3D printer developed by L. Cronin and co-workers for the synthesis of racemic ibuprofen<sup>251</sup> d) Reusable 3D printed reactionware with printed-in catalysts and other components developed by L. Cronin and co-workers to perform the synthesis of phenanthridine-based heterocycles<sup>249</sup> e) Sealed reactionware for the same purpose as “d” where reagents, catalysts and purification were integrated in a single monolithic device.<sup>250</sup>

Despite of the increase of the use of 3D printed flow devices, most of those fluidic devices have been employed for analytical applications<sup>233</sup> and only a few examples illustrate their potential for organic synthesis. In 2012, L. Cronin and co-workers reported the first 3D printed “milli fluidic reactor” for organic synthesis.<sup>252</sup> This reactor was made with polypropylene (PP) by the FDM method and was employed in the synthesis of dibenzylamine and also to perform alkylation reactions to obtain tertiary amines. Polypropylene was chosen due to its thermostability up to 150°C, high chemical inertia and low cost. The device was a three-inlet reactor with an approximate reactor volume of

<sup>252</sup> P. J. Kitson, M. H. Rosnes, V. Sans, V. Dragone, L. Cronin, *Lab Chip*, 2012, 12, 3267-3271.

270  $\mu\text{L}$ , a circular channel shape and 0.8 mm of internal diameter. This protocol was improved and reported by the same group one year later.<sup>253</sup> In this case, two 3D printed polypropylene fluidic devices were connected in continuous flow to achieve first the formation of imines and then their reduction to obtain secondary amines (Figure 1.21). It deserves to be mentioned that the connections between reactors were made with common polytetrafluoroethylene (PTFE) tubing and standard HPLC connectors, the same used with traditional glass or silicon flow reactors. This highlights how 3D printing technology can be easily interfaced with common laboratory equipment. One of our targets is to perform consecutive coupled reactions in continuous flow and these examples demonstrate that additive manufacturing is a very interesting tool to be integrated in our work.

More examples of continuous flow 3D printed devices were reported in the following years, including the porous structured reactor designed by R. von Rohr and co-workers in 2015 using a SLS method.<sup>254</sup> This reactor was made with an aluminium oxide-zinc oxide base layer coated with palladium and was used successfully for the continuous flow reduction of 2-methyl-3-butyn-2-ol to the corresponding alkane under solvent-free conditions. Another example can be found in the early 2017 when S. D. Christie and co-workers reported the creation of different multifunctional fluidic devices with embedded reaction monitoring capability for the synthesis of heterocycles.<sup>255</sup>

Within the field of multicyclic continuous flow systems, it is important to focus on the synthesis of Active Pharmaceutical Ingredients (APIs). In this regard, in 2015 M. Benaglia and co-workers reported the first example of a stereoselective, catalytic synthesis of different chiral products of pharmaceutical interest performed under continuous flow conditions using 3D printed mesoreactors.<sup>256</sup> Different 3D printed reactors were prepared by the FDM method using HIPS, PLA and nylon as materials. APIs like (1*R*,2*S*)-norephedrine, (1*R*,2*S*)-metaraminol and (1*R*,2*S*)-methoxamine, all of them vasoconstrictor compounds, were prepared with these 3D printed mesoreactors.

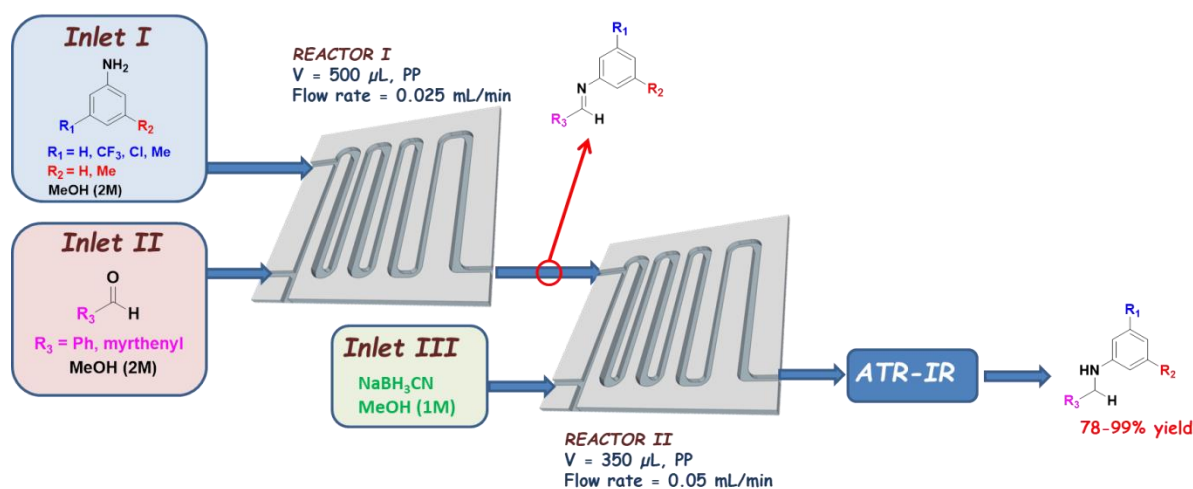
---

<sup>253</sup> V. Dragone, V. Sans, M. H. Rosnes, P. J. Kitson, L. Cronin, *Beilstein J. Org. Chem.*, 2013, 9, 951-959.

<sup>254</sup> Y. Elias, P. R. von Rohr, W. Bonrath, J. Medlock, A. Buss, *Chem. Eng. Process*, 2015, 95, 175-185.

<sup>255</sup> A. J. Capel, A. Wright, M. J. Harding, G. W. Weaver, Y. Li, R. A. Harris, S. Edmondson, R. D. Goodridge, S. D. Christie, *Beilstein J. Org. Chem.*, 2017, 13, 111-119.

<sup>256</sup> S. Rossi, R. Porta, D. Brenna, A. Puglisi, M. Benaglia, *Angew. Chem. Int. Ed.*, 2017, 56, 4290-4294.



**Figure 1.21. Two 3D printed PP fluidic devices connected in series for the synthesis and reduction of secondary amines under continuous flow conditions.<sup>253</sup>**

The synthesis of those APIs was made in two steps. The first one consists in the Henry reaction of aromatic aldehydes with nitroethane catalysed by  $\text{Cu}(\text{OAc})_2 \cdot \text{H}_2\text{O}$  in the presence of an aminopyridine derived chiral ligand. With a 3D printed PLA mesoreactor (1 mL volume) at  $-20^\circ\text{C}$  during 30 minutes of residence time and with 5% of the chiral catalyst, the expected 1,2-nitroalcohols were obtained in high yield (72-96%) and high enantioselectivity (80-87% ee *anti*).

The second step was the hydrogenation of the nitroalcohol derivatives using a commercially available H-Cube apparatus, able to generate hydrogen *in situ* from the electrolysis of water under very safe conditions. The hydrogenation took place with 10% Pd as the catalyst at  $30^\circ\text{C}$  under  $\text{H}_2$  pressure (15 bar) in approximately 2 hours (98-99% yield). No erosion of the stereochemical integrity occurs in this step.

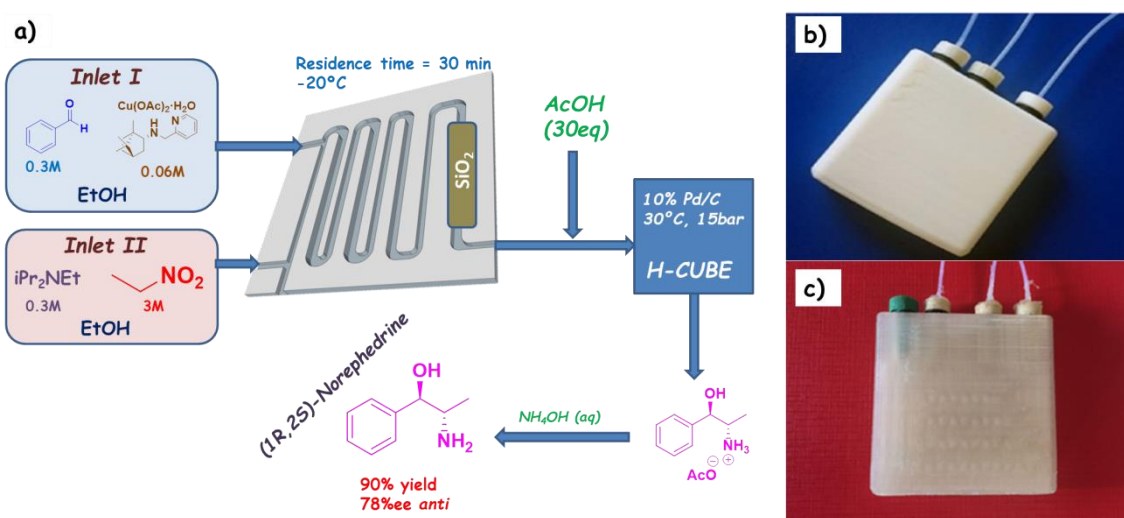
Then, M. Benaglia and co-workers developed a continuous flow synthesis of norephedrine combining both steps together in flow. It is important to remind at this point that the Cu catalyst and the chiral ligand were injected in the 3D printed reactor together with the reagents and should be removed before the hydrogenation. With this purpose, the nitroalcohol solution was just filtered through a short pad of silica and washed with ethanol. Acetic acid was then added to the nitroalcohol solution and the hydrogenation in-flow performed to obtain the desired 1,2-aminoalcohols after treatment with a base (90% yield, 78% ee *anti*).

The large design possibilities offered by additive manufacturing allowed preparing a new reactor containing the flow channels and the short



column of silica in a single device, achieving a more automated continuous flow process (Figure 1.22). With this new system, the (1*R*,2*S*)-Norephedrine was obtained in 96% yield and 83% ee (*anti*).

The former example shows some important characteristics and possibilities of the use of advanced manufacturing in continuous flow chemistry for APIs preparation. Despite of the important examples seen in recent years, it is worth to comment that none of the flow devices contain an incorporated catalyst. Some of the mentioned reactions do not need a catalyst and in others the catalyst is injected together with the reagent(s) with the posterior need of separation. The use of immobilised catalysts in flow chemistry using advanced manufacturing devices represents, thus, an important approach to be developed.



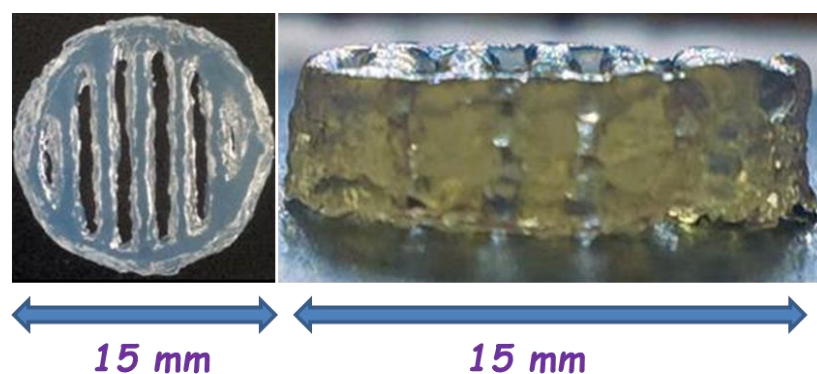
**Figure 1.22. Norephedrine continuous flow synthesis employing a PLA 3D printed fluidic mesoreactor with an in-line silica column b) 3D printed reactor without the in-line silica column. Two inlets and one outlet can be observed c) 3D printed reactor combined with a silica column.<sup>256</sup>**

This idea was achieved by K. S. Rabe and co-workers in 2018 with the 3D printing of flow reactor cartridges with biocatalytic agarose-based inks containing thermostable enzymes (Figure 1.23).<sup>257</sup> For this purpose, temperature-controlled 3D printing processes and thermostable enzymes were needed. Several strategies have been used before for the mild encapsulation of enzymes in natural and synthetic polymers.<sup>258,259</sup> However, these materials do not usually meet the

<sup>257</sup> M. Maier, C. P. Radtke, J. Hubbuch, C. M. Niemeyer, K. S. Rabe, *Angew. Chem. Int. Ed.*, 2018, 57, 5539-5543.

<sup>258</sup> R. Fan, M. Piou, E. Darling, D. Cormier, J. Sun, J. Wan, *J. Biomater. Appl.*, 2016, 31, 684-692.

requirements for advanced manufacturing processes like 3D printing. Agarose was chosen as the 3D printing material because it is inexpensive, non-toxic, easy to handle, prepare and store and the bioink resulting of the combination with enzymes is totally biodegradable. The prepared agarose-based hydrogels have the property of being thermoreversible and also stabilise the biocatalyst,<sup>260</sup> being the resulting bioink able to work under flow conditions even in buffer/THF mixtures. It is essential to have a complete knowledge of the thermostability of the target enzyme to set the elevated temperatures required for the processing of the biocatalytic ink during the whole 3D printing process. Biocatalytic 3D printed fluidic reactors were prepared with decarboxylase and alcohol dehydrogenase enzymes. With those 3D printed catalytic bioreactors, the decarboxylation reaction of ketoisovalerate into isobutiraldehyde was carried out under continuous flow conditions with good results.



**Figure 1.23.** 3D printed cartridge of an enzyme containing agarose-based hydrogel.<sup>257</sup>

This last example is a representative proof of concept demonstrating the possibility offered by additive manufacturing technologies to directly print biocatalytic flow reactors using enzyme containing bioinks. However, in the case of simple syringe based extrusion printing processes (like FDM, the most common), elevated temperatures are necessary and these are not compatible with all enzymes. Enzymes with an experimental thermostability of  $>60^{\circ}\text{C}$  are needed.<sup>261</sup> Despite of the fact that the number of available thermostable enzymes is steadily

<sup>259</sup> H. W. Kang, S. J. Lee, I. K. Ko, C. Kengla, J. J. Yoo, A. Atala, *Nat. Biotechnol.*, 2016, 34, 312-319.

<sup>260</sup> S. R. Caliari, J. A. Burdick, *Nat. Methods*, 2016, 13, 405-414.

<sup>261</sup> I. Schomburg, A. Chang, C. Ebeling, M. Gremse, C. Heldt, G. Huhn, D. Schomburg, *Nucleic Acid Res.*, 2004, 32, D431-D433.

increasing,<sup>262</sup> and also regular enzymes could be adapted to higher temperatures by protein engineering,<sup>263,264</sup> this 3D printing strategy is not affordable with all the enzymes and to catalyse a broad spectre of biocatalytic process as would be desirable.

The alternative approach that we have followed in this area involves the printing of the fluidic reactor and then the immobilisation of the enzyme in the printed device. The surface of the polymeric materials employed in additive manufacturing like nylon can be chemically modified in order to have a surface capable to covalently immobilise enzymes. Some protocols for chemically modify the surface of nylon and attach enzymes have been reported in recent years.<sup>265,266,267</sup>

With this strategy, a broader number of enzymes and biocatalytic processes become suitable to be used under continuous flow employing advanced manufacturing technologies. The challenge consists in being able to immobilise the enzyme without affecting its catalytic activity and without suffering from enzyme leaching. To develop stable biocatalytic 3D printed reactors has been one of the objectives of this work.

Moreover, not only enzymes would be suitable to be immobilised into the modified surfaces of the 3D printed materials. After obtaining the appropriate functional groups in the surface, most likely other attractive molecules such as ionic liquid-like fragments or catalysts could be supported.

As we have seen, several applications of advanced manufacturing in flow chemistry have been developed in recent years and new applications continue to appear. In chapter 7 we have taken advantage of this growing and developing technology to create new catalytic systems for flow chemistry.

---

<sup>262</sup> M. E. DeCastro, E. Rodríguez-Belmonte, M. I. González-Siso, *Front. Microbiol.*, 2016, 7, 1521-1526.

<sup>263</sup> K. Solanki, W. Abdallah, S. Banta, *Biotechnol. J.*, 2016, 11, 1483-1497.

<sup>264</sup> H. P. Modarres, M. R. Mofrad, A. Sanati-Nezhad, *RSC Adv.*, 2016, 6, 115252-115270.

<sup>265</sup> F. H. Isgrove, R. J. H. Williams, G. W. Niven, A. T. Andrews, *Enzyme and Microbial Technology*, 2001, 28, 225-232.

<sup>266</sup> E. Fatarella, D. Spinelli, M. Ruzzante, R. Pogni, *Journal of Molecular Catalysis B: Enzymatic*, 2014, 102, 41-47.

<sup>267</sup> W. Neto, M. Schürmann, L. Panella, A. Vogel, J. M. Woodley, *Journal of Molecular Catalysis B: Enzymatic*, 2015, 117, 54-61.

## 1.6. Synthetic approaches to C-C bond forming reactions: cyanosilylation, Strecker and Negishi

Carbon-carbon (C-C) bonds form the “backbone” of nearly every organic molecule and its formation is regarded as the key transformation in organic synthesis.<sup>268</sup> Their importance still increase if we talk about molecules of pharmaceutical interest. In the development of organic chemistry, carbon-carbon bond formation has always been one of the most studied, useful and fundamental reactions, and as a result, there is an ever-growing number of methods for carbon-carbon bond formation.<sup>269,270</sup>

Those C-C bond forming reactions have been profusely studied and are well known. However, nowadays there is an increasing focus on transforming those processes in more sustainable ones. The last decade has seen a tremendous effort towards savings in energy consumption, use of eco-friendly catalysts and solvents, proficiency in atom economy, and minimisation of wastes from reactions in order to design novel green synthetic protocols for organic compounds of interest.<sup>271,272,273</sup> By applying continuous flow conditions, our target is to develop more green and efficient methods for some of the well-known C-C bond forming reactions. But the use of continuous flow conditions is not the only sustainable chemistry tool that we are going to study and discuss. Also the use of efficient catalysts, green solvents or mild reaction conditions is going to be discussed.

### 1.6.1. Cyanosilylation of carbonyl compounds

The cyanosilylation of carbonyl compounds is one important strategy for the formation of new C-C bonds nowadays. In this process, protected silyl ethers of cyanohydrins are created with the concomitant formation of a new C-C bond between the original carbonyl carbon atom and the cyanide group. Cyanohydrins are highly valued compounds because of

<sup>268</sup> G. Brahmachari, *RSC Adv.*, 2016, 6, 64676-64725.

<sup>269</sup> A. Bhunia, R. S. Yetra, A. T. Biju, *Chem. Soc. Rev.*, 2012, 41, 3140-3152.

<sup>270</sup> G. Brahmachari, *Chem. Rec.*, 2016, 16, 98-123.

<sup>271</sup> K. Kaneda, T. Mizugaki, *Energy Environ. Sci.*, 2009, 2, 655-673.

<sup>272</sup> G. Brahmachari, B. Banerjee, *Curr. Green Chem.*, 2015, 2, 274-305.

<sup>273</sup> A. Farrán, C. Cai, M. Sandoval, Y. Xu, J. Liu, M. J. Hernáiz, R. J. Linhardt, *Chem. Rev.*, 2015, 115, 6811-6853.

their considerable potential as synthetic chiral building blocks due to the existence of a hydroxyl group and a cyano group on the same chiral carbon. Cyanohydrins can experiment a wide range of further different transformations providing access to a large number of chiral molecules, and to a variety of different functionalities, especially interesting in the fields of pharmaceuticals and agrochemicals:  $\beta$ -amino alcohols,  $\alpha$ -hydroxyacids,  $\alpha$ -hydroxyaldehydes and  $\alpha$ -hydroxyketones among others.<sup>274</sup> Cyanohydrins have already been used as precursors of different drugs, such as fluoxetine, duloxetine and its derivatives,<sup>275</sup> capuramycin,<sup>276</sup> bufuralol,<sup>277</sup> denopamine and salbutamol.<sup>278</sup> Cyanohydrins are present in over 3000 plants, bacteria, fungi and many insects forming part of the selfdefense system,<sup>279,280</sup> which highlights their natural importance. Cyanohydrins also serve as source of nitrogen for the biosynthesis of amino acids. For those reasons, much effort and consideration have been devoted in the last two decades to the synthesis of cyanohydrins.<sup>281,282,283</sup>

The synthesis of cyanohydrins by the addition of hydrogen cyanide (HCN) to carbonyl compounds was first reported at the beginning of the XX century by Arthur Lawport.<sup>284</sup> Those initial cyanohydrins syntheses employed HCN as a cyanide source. However, due to the toxicity, harmful character and difficulties in handling HCN, a number of alternative different cyanide sources with less harmful properties and easier to handle have been subsequently introduced. Among other cyanide agents like the cyanide salts KCN or NaCN, trimethyl silyl cyanide (TMSCN) was revealed as an interesting alternative due to its safer and easier handling and the option to obtain silyl protected cyanohydrin ethers. For those reasons, cyanosilylation reactions employing TMSCN started to grow in importance during the second half of the XX century.<sup>285,286</sup>

<sup>274</sup> J.-M. Brunel, I. P. Holmes, *Angew. Chem. Int. Ed.*, 2004, 43, 2752-2778.

<sup>275</sup> R. K. Rej, T. Das, S. Hazra, S. Nanda, *Tetrahedron: Asymmetry*, 2013, 24, 913-918.

<sup>276</sup> M. Kurosu, K. Li, D. C. Crick, *Org. Lett.*, 2009, 11, 2393-2396.

<sup>277</sup> K. Mo, Y. Yang, Y. Cui, *J. Am. Chem. Soc.*, 2014, 136, 1746-1749.

<sup>278</sup> R. F. C. Brown, A. C. Donohue, W. R. Jackson, T. D. McCarthy, *Tetrahedron*, 1994, 50, 13739-13752.

<sup>279</sup> F. F. Fleming, *Nat. Prod. Rep.*, 1999, 16, 597-606.

<sup>280</sup> D. -S. Park, J. R. Coats, *J. Pest. Sci.*, 2005, 30, 99-102.

<sup>281</sup> R. J. Gregory, *Chem. Rev.*, 1999, 99, 3649-3682.

<sup>282</sup> M. North, D. L. Usanov, C. Young, *Chem. Rev.*, 2008, 108, 5146-5226.

<sup>283</sup> H. Pellissier, *Adv. Synth. Catal.*, 2015, 357, 857-882.

<sup>284</sup> A. Lawport, *J. Chem. Soc. Trans.*, 1903, 83, 995-1005.

<sup>285</sup> D. Evans, L. Truesdale, G. Carroll, *J. Chem. Soc. Chem. Comm.*, 1973, 1, 55-56.

<sup>286</sup> M. Golinski, C. P. Brock, D. S. Watt, *J. Org. Chem.*, 1993, 58, 159-164.

Traditionally, chiral cyanohydrins are obtained by two enzymatic procedures: i) hydrocyanation of aldehydes or ketones catalysed by hydroxynitrile lyases (HNL) and ii) enantioselective acylation or hydrolytic deacylation of racemic cyanohydrin esters catalysed by esterases or lipases. Strictly speaking, this last process represents an specific example of enzymatic kinetic resolution (KR) or, when combined with a catalyst for the epimerisation of the unreacted substrate, dynamic kinetic resolution (DKR) and should convert racemic cyanohydrins (or cyanohydrine derivatives) in their enantiopure derivatives. From all the different enzymatic catalytic systems, the (*R*) and (*S*) selective HNLs (hydroxynitrile lyases) are the biocatalysts most often selected for the synthesis of cyanohydrins according to the industrial applications reported.<sup>287,288</sup> HNLs are C-C lyases and can be typically found in plants, bacteria and arthropods.<sup>289,290</sup> The main shortcoming for those biocatalytic processes is the need of HCN, a more hazardous chemical reagent than TMSCN. Moreover, in this enzymatic process, the reversibility of the reaction may cause deterioration of the enantiomeric excess.<sup>291</sup> Biocatalytic syntheses of chiral cyanohydrins by HNLs have been reported even under continuous flow conditions. In 2015, F. P. J. T. Rutjes and co-workers described a chemoenzymatic two-step cascade process successfully performed in continuous flow for the synthesis of enantiopure cyanohydrins.<sup>292</sup> The chemoenzymatic aqueous formation of cyanohydrins was integrated with a subsequent organic phase protection step. The protected cyanohydrin derivatives were obtained in good yields and high to excellent enantioselectivity. However, 15 equivalents of the cyanide source KCN were used in the chemoenzymatic first step, plus 13 equivalents of acetic anhydride and DIPEA in the subsequent protection step. Moreover, dichloromethane was used as the solvent in this second step and the catalysts had to be injected together with the reagents in the reaction stream. Decreasing the number of equivalents of reagents used, a safer cyanide source and supported catalysts appeared clearly as points to improve.

---

<sup>287</sup> U. Hanefeld, *Chem. Soc. Rev.*, 2013, 42, 6308-6568.

<sup>288</sup> E. Lanfranchi, K. Steiner, A. Glieder, I. Hajnal, R. A. Sheldon, S. van Pelt, M. Winkler, *Recent Pat. Biotechnol.*, 2013, 7, 197-206.

<sup>289</sup> M. Dadashipour, M. Yamazaki, K. Monomoi, K. Tamura, K. Fuhshuku, Y. Kanase, E. Uchimura, G. Kaiyun, Y. Asano, *J. Biotechnol.*, 2011, 153, 100-110.

<sup>290</sup> M. A. Kassim, K. Rumbold, *Biotechnol. Lett.*, 2014, 36, 223-228.

<sup>291</sup> A. Brahma, B. Musio, U. Ismayilova, N. Nikbin, S. B. Kamptmann, P. Siegert, G. E. Jeronim, S. V. Ley, M. Pohl, *Synlett*, 2016, 27, 262-266.

<sup>292</sup> M. M. E. Delville, K. Koch, J. C. M. van Hest, F. P. J. T. Rutjes, *Org. Biomol. Chem.*, 2015, 13, 1634-1638.

S. V. Ley and co-workers developed a continuous telescopic process including two sequential biotransformations, initially obtaining the cyanohydrin that was further acylated with Ac<sub>2</sub>O its rasemisation.<sup>291</sup>

On the other hand, kinetic resolutions of racemic cyanohydrins catalysed by lipases are well-known procedures to obtain enantiopure cyanohydrins. This process is a well established reaction under batch conditions.<sup>293</sup> Several examples of KR or EKR (enzymatic kinetic resolution) reactions of cyanohydrins have already been described including acylation by *Candida Antarctica* lipase B,<sup>294</sup> hydrolysis by *Bacillus coagulans*,<sup>295</sup> *Candida rugosa*,<sup>296</sup> metagenome-derived esterases,<sup>297</sup> and several other proteases,<sup>298</sup> and alcoholysis by *Candida Antarctica* lipase A<sup>299</sup> and B<sup>300</sup>, *Candida rugosa*,<sup>301</sup> and *Pseudomonas fluorescens*.<sup>302</sup> These reported results showed that, depending on the substrate structure, although good enantioselectivities could be reached, long reactions times were often required.

Although EKR reactions have been increasingly carried out in continuous flow mode,<sup>303</sup> cyanohydrins have so far been unexplored as continuous flow resolutions substrates.<sup>304</sup> In 2016, L. Piovan and co-workers reported the continuous flow preparation of optically active cyanohydrins catalysed by CAL-B.<sup>305</sup> The lipase *Candida Antarctica B* (CAL-B) is commercially available in supported form as Novozym®-435 (acrylic resin hydrophobic support), which is a great opportunity for performing continuous enzymatic resolutions of cyanohydrins. This supported enzyme could act in a wide range of pH values and

<sup>293</sup> L. Veum, M. Kuster, S. Telalovic, U. Hanefeld, T. Maschmeyer, *Eur. J. Org. Chem.*, 2002, 1516-1522.

<sup>294</sup> S. S. Ribeiro, I. M. Ferreira, J. P. F. Lima, B. A. Sousa, R. C. Carmona, A. A. Santos, A. L. M. Porto, *J. Braz. Chem. Soc.*, 2015, 26, 1344-1350.

<sup>295</sup> H. Ota, Y. Miyamae, G. Tsuchihashi, *Agric. Biol. Chem.*, 1989, 53, 281-283.

<sup>296</sup> N. M. Maguire, A. Ford, S. L. Clarke, K. S. Eccles, S. E. Lawrence, M. Brossat, T. S. Moody, A. R. Maguire, *Tetrahedron: Asymmetry*, 2011, 22, 2144-2150.

<sup>297</sup> G. S. Nguyen, R. Kourist, M. Paravidino, A. Hummel, J. Rehdorf, R. V. A. Orru, U. Hanefeld, U. T. Bornscheuer, *Eur. J. Org. Chem.*, 2010, 2753-2758.

<sup>298</sup> K. Konigsberger, K. Prasad, O. Repic, *Tetrahedron: Asymmetry*, 1999, 10, 679-687.

<sup>299</sup> L. C. Bencze, C. Paizs, M. I. Toşa, E. Vass, F. Irimie, *Tetrahedron: Asymmetry*, 2010, 21, 443-450.

<sup>300</sup> Y. N. Belokon, A. J. Blacker, L. A. Clutterbuck, D. Hogg, M. North, C. Reeve, *Eur. J. Org. Chem.*, 2006, 4609-4617.

<sup>301</sup> K. Lundell, T. Rajjola, L. T. Kanerva, *Enzyme Microb. Technol.*, 1998, 22, 86-93.

<sup>302</sup> R. Zhou, J. H. Xu, *Biochem. Eng. J.*, 2005, 23, 11-15.

<sup>303</sup> I. I. Junior, L. S. M. Miranda, R. O. M. A. Souza, *J. Mol. Catal. B*, 2013, 85-86, 1-9.

<sup>304</sup> A. Hamberg, S. Lundgren, E. Wingstrand, C. Moberg, K. Hult, *Chem. Eur. J.*, 2007, 13, 4334-4341.

<sup>305</sup> J. C. Thomas, B. B. Aggio, A. R. Marques de Oliveira, L. Piovan, *Eur. J. Org. Chem.*, 2016, 5964-5970.

temperatures (20-110°C) and in anhydrous conditions. Its supported form in beads allows easily packing a fixed-bed flow reactor with it.

The continuous procedure that L. Piovan and co-workers described employed *n*-butanol (0.4 equivalents) and toluene as the solvents with 0.1 M concentrations of cyanohydrin esters and with a fixed-bed flow reactor filled with 200 mg of Novozym®-435. With this protocol good conversions, close to 50%, and ee values in the 97-99% range were obtained with some of the cyanohydrins studied. However, with some substrates, conversions higher than 50% produced lower ee% of the enantiopure cyanohydrin. Perhaps, one of the most relevant data provided by this work relates with the comparison between batch and continuous flow resolution processes. With the same reagents, catalyst and conditions, productivity values under continuous flow mode were from 2.4 to 8.7 times higher than in batch mode (Figure 1.24). Moreover, the reaction times were reduced from hours in batch mode to minutes in continuous flow mode.

Despite of the clear advantages of the continuous flow EKR of cyanohydrins, an important limitation must be taken into account. Due to the intrinsic nature of the process, only 50% of conversion could be achieved as a maximum, remaining the other 50% of the substrate as cyanohydrin ester (non-transformer epimer). In a successful resolution, the remaining cyanohydrin ester should be also enantiopure and could have interest as a key pharmaceutical or fine chemistry intermediate. When a 100% of the enantiopure cyanohydrin is the target, the alternative approach is the dynamic kinetic resolution (DKR). In DKR, the remaining enantiopure or enantioenriched cyanohydrin ester is involved on several consecutive cycles of racemisation and kinetic resolution until achieving yields of the desired chiral cyanohydrin near to 100%. Promising DKR reactions of cyanohydrins have also been reported involving different racemisation agents.<sup>306,307,308</sup> However, reaction times are longer than those needed for EKR reactions, and the achievement of high enantiomeric excesses is strongly dependent on the racemisation agent and the substrate structure.

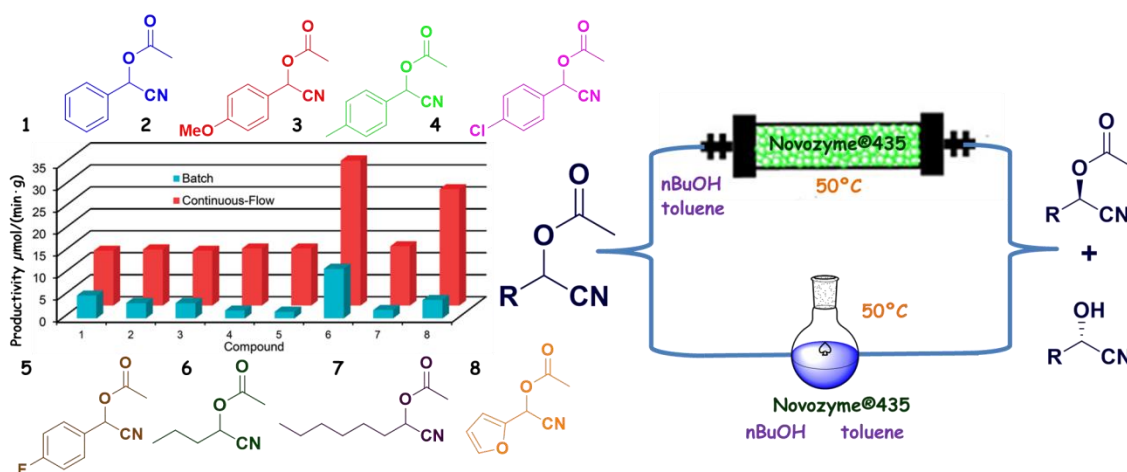
---

<sup>306</sup> A. Laurell, C. Moberg, *Eur. J. Org. Chem.*, 2011, 3980–3984.

<sup>307</sup> M. Sakulsombat, P. Vongvilai, O. Ramström, *Org. Biomol. Chem.*, 2012, 9, 1112–1117.

<sup>308</sup> Y. Q. Wen, R. Hertzberg, I. Gonzalez, C. Moberg, *Chem. Eur. J.*, 2014, 20, 3806–3812.





**Figure 1.24.** Comparison between batch and continuous flow EKR for cyanohydrins as reported by L. Piovan and co-workers.<sup>305</sup>

It is clear that before performing a EKR or DKR, either in batch or flow, the corresponding cyanohydrin needs to be obtained first. For this purpose, the development of efficient catalysts for the addition of TMS-CN to carbonyl compounds has been the focal research point. As a consequence, various Lewis acids, Lewis bases, metal alkoxides, as well as inorganic salts have been successfully employed in order to improve this transformation.<sup>309,310,311,312,313</sup> Chemically, trimethylsilyl nucleophiles ( $\text{Me}_3\text{SiNu}$ ) featuring silicon atoms bound to carbon, nitrogen, oxygen or sulphur, are effective and valid alternatives to protonated nucleophiles ( $\text{HNu}$ ) for addition reactions of nucleophiles to aldehydes and ketones. This is due to the properties of the silicon atom, which allows the formation of active nucleophilic species in different conditions, which is not the case with the use of  $\text{HNu}$  type sources for the nucleophile. The activation of the nucleophiles requires the presence of Lewis bases or acids, but while  $\text{HNu}$  species may require the presence of a strong base (if it is a weak acid), which might be incompatible with the reaction conditions or some functional group present, this is not needed for  $\text{Me}_3\text{SiNu}$  species. Desilylation and activation of the nucleophile in the  $\text{Me}_3\text{SiNu}$  case occurs under mild conditions due to the affinity of silicon for oxygen or fluorine atoms.<sup>314</sup>

<sup>309</sup> Y. Hamashima, D. Sawada, H. Nogami, M. Kanai, M. Shibasaki, *Tetrahedron*, 2001, 57, 805-814.

<sup>310</sup> B. Karimi, L. Ma'Mani, *Org. Lett.*, 2004, 6, 4816-4815.

<sup>311</sup> N. Kuroono, M. Yamaguchi, K. Suzuki, T. Ohkuma, *J. Org. Chem.*, 2005, 70, 6530-6532.

<sup>312</sup> S. Matsukawa, I. Sekine, A. Iitsuka, *Molecules*, 2009, 14, 3353-3359.

<sup>313</sup> X. Cui, M. C. Xu, L. J. Zhang, R. X. Yao, X. M. Zhang, *Dalton Trans.*, 2015, 44, 12711-12716.

<sup>314</sup> J. Gawronski, N. Wascinska, J. Gajewy, *Chem. Rev.*, 2008, 108, 5227-5252.

The activation of silyl cyanide can be carried out using an organocatalytic or an organometallic system. Traditionally, Lewis-type organometallic systems have been used. They carry out the activation through complexation with the carbonyl groups of the substrate and with the cyano group of the TMSCN.<sup>315,316</sup> However, an organocatalytic Lewis base reacts with the Si atom of TMSCN producing a more reactive silicon hypercoordinated intermediate. For this reason, in the last two decades organocatalysis has received much attention.<sup>317,318</sup> Organic species like amines,<sup>319</sup> phosphines,<sup>319</sup> phosphazanes<sup>320</sup> and N-heterocyclic carbenes<sup>321,322</sup> have been employed as catalysts for the cyanosilylation of carbonyl compounds. However, most of them present some drawbacks, especially the need for high catalyst loadings and long reaction times. Therefore, developing still more efficient organocatalysts is desirable.

With this scenario, ionic liquids appeared as a promising alternative. ILs have wide applications in chemistry, as has been discussed above, due to some of their inherent properties. In the case of the transformation here studied, ionic networks (organic cations and anions) in ILs may replace the role of the Lewis acid/base in the activation of the TMSCN and act as a stable and robust catalytic species for cyanosilylations (Figure 1.25).<sup>323,324</sup> One of the first examples was reported in 2005 by T. P. Loh and co-workers who successfully employed [OMIM][PF<sub>6</sub>] as an efficient and recyclable reaction media for the cyanosilylation of aldehydes.<sup>323</sup> Years later, in 2009, S. Lee and co-workers showed that the catalytic activity of lanthanide triflates, particularly scandium triflate, increased dramatically in the ionic liquid [BMIM][SbF<sub>6</sub>], allowing the cyanosilylation of a variety of aldehydes and ketones with a turnover frequency up to 48000 mol/h and a total turnover number of 100000.<sup>325</sup> Despite of the good results showed using scandium triflate, the idea for a more sustainable process is to avoid the use of metals.

---

<sup>315</sup> M. North, *Angew. Chem. Int. Ed.*, 2010, 49, 8079-8081.

<sup>316</sup> Z. Zhang, J. Chen, Z. Bao, G. Chang, H. Xing, Q. Ren, *RSC Adv.*, 2015, 5, 79355-79360.

<sup>317</sup> M. A. Lacour, N. J. Rahier, M. Taillefer, *Chem. Eur. J.*, 2011, 17, 12276-12279.

<sup>318</sup> M. North, M. Omedes-Pujol, C. Young, *Org. Biomol. Chem.*, 2012, 10, 4289-4298.

<sup>319</sup> S. E. Denmark, W. Chung, *J. Org. Chem.*, 2006, 71, 4002-4005.

<sup>320</sup> Z. Wang, B. Fetterly, J. G. Verkade, *J. Organomet. Chem.*, 2002, 646, 161-166.

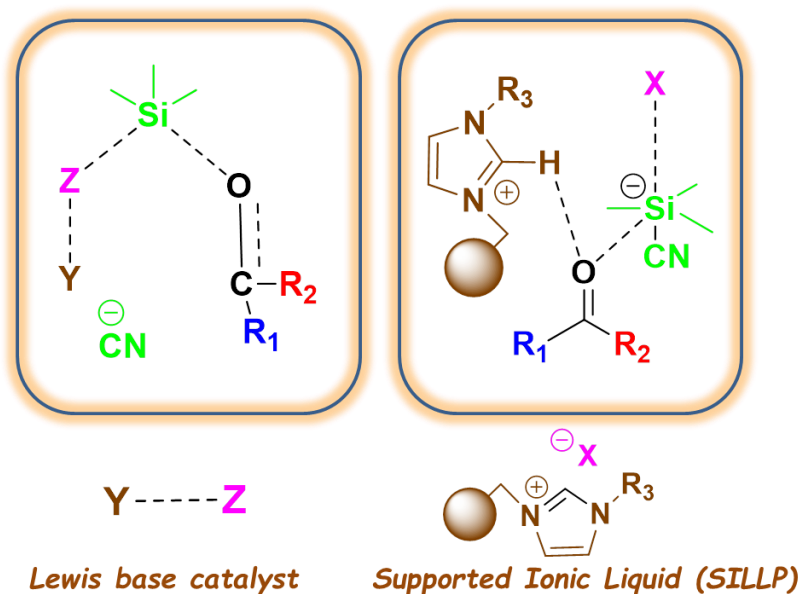
<sup>321</sup> Y. Suzuki, M. D. A. Bakar, K. Muramatsu, M. Sato, *Tetrahedron*, 2006, 62, 4227-4231.

<sup>322</sup> D. Enders, O. Niemeier, A. Henseler, *Chem. Rev.*, 2007, 107, 5606-5655.

<sup>323</sup> Z. L. Shen, S. J. Ji, T. P. Loh, *Tetrahedron Lett.*, 2005, 46, 3137-3139.

<sup>324</sup> H. Olivier-Bourbigou, L. Magna, D. Morvan, *Appl. Catal. A*, 2010, 373, 1-56.

<sup>325</sup> B. Y. Park, K. Y. Ryu, J. H. Park, S. Lee, *Green Chem.*, 2009, 11, 946-948.



**Figure 1.25. Activation of TMSCN during the cyanosilylation reaction catalysed by a Lewis base or a SILLP.**

In 2017, Q. Ren and co-workers reported the use of the commercially and readily available IL [EMIM][OAc] as a highly efficient catalyst for the cyanosilylation of aldehydes and ketones.<sup>326</sup> With only amounts of the range 0.0001-0.1 mol % of this IL, various aldehydes and ketones were converted into their corresponding protected cyanohydrins in excellent yields (92-95% for ketones and 56-100% for aldehydes) in 5 minutes under solvent-free and r.t. conditions. High TOF values, from 10843 h<sup>-1</sup> to 10602410 h<sup>-1</sup>, were reported, revealing this IL as the most efficient organocatalyst and highlighting, once more, the potential of ILs as catalysts. Mechanistic investigations done by Q. Ren and co-workers based on their experimental results showed that the reaction operates via a synergistic activation mode in which the imidazolium cation interacts with the carbonyl compounds facilitating the attack of the acetate activated anion of TMSCN. The same synergistic mechanism would be extrapolable to different ILs with different organic anions.

These results confirmed our observations (chapters 3 and 4) where we developed a strategy to improve the cyanosilylation under continuous flow conditions. We have described before the benefits of the continuous flow chemistry in chemical transformations. Moreover, IL species can be supported in polymeric materials producing supported ionic liquid-like phases (SILLPs) that can be used in continuous flow processes and the

<sup>326</sup> B. Ullah, J. Chen, Z. Zhang, H. Xing, Q. Yang, Z. Bao, Q. Ren, *Scientific Reports*, 2017, 7, Article number 42699.

catalytic properties of the ILs can be transferred to the solid phase.<sup>327</sup> Thus, combining the benefits of ILs as catalysts and continuous flow processes is possible.

An example of continuous flow cyanosilylation using supported catalysts was reported in 2013. L. Vaccaro and co-workers reported a protocol for the cyanosilylation of carbonyl compounds using TMSCN and triphenylphosphine supported on polystyrene as a catalyst under solvent-free conditions.<sup>328</sup> A mixture of acetophenone and TMSCN (1.1 equivalents) was pumped through a fixed-bed reactor (0.04 mL/min) packed with PS-TPP dispersed in borosilicate micro spheres, at 60°C with a flow rate of 0.04 mL/min during 20 hours under solvent-free conditions, obtaining the protected cyanohydrin ether in 99% yield and with a low  $E_{\text{factor}}$  (0.16).

In this context, the results presented in chapters 3 and 4 summarise our efforts to achieve the synthesis of enantiopure cyanohydrins from carbonyl compounds. They combine a continuous flow cyanosilylation with TMSCN catalysed by SILLPs and a continuous flow EKR catalysed by Novozyme®-435 in a muticatalytic continuous flow system. The underlying hypothesis was that employing supported ILs (SILLPs), the reactivity of a continuous flow cyanosilylation system could be enhanced, increasing the flow rate and achieving more efficient and productive systems even at room temperature. The benefits of the continuous flow chemistry and those of ILs as supported catalysts could be exploited with this strategy reaching a greener and more efficient process.

### 1.6.2. Strecker reaction

The three component Strecker reaction involves the transformation of a carbonyl compound (aldehyde or ketone) into a  $\alpha$ -amino nitrile by reacting with an amine and TMSCN as a cyanide source. Again, a new C-C bond is being formed between the original carbonyl carbon atom and the cyanide group. In this case, however, an amino group is present in the final product instead of the derivatised alcohol group of the cyanosilylation.

---

<sup>327</sup> V. Sans, N. Karbass, M. I. Burguete, V. Compañ, E. García-Verdugo, S. V. Luis, M. Pawlak, *Chem. Eur. J.*, 2011, 17, 1894-1906.

<sup>328</sup> G. Strappaveccia, D. Lanari, D. Gelman, F. Pizzo, O. Rosati, M. Curini, L. Vaccaro, *Green Chem.*, 2013, 15, 199-204.

$\alpha$ -Amino nitriles are key and versatile building blocks for pharmaceuticals, agrochemicals and heterocyclic chemistry, and suitable prototypes for modern drug design and development.<sup>329,330</sup> The versatility of  $\alpha$ -amino nitriles is due to the presence of the amino and nitrile functional groups that can be further transformed into pharmaceutically important compounds such as  $\alpha$ -amino acids,  $\alpha$ -amino aldehydes,  $\alpha$ -amino alcohols or 1,2-diamines. Their value for drug design is high because of the capacity of the amino function to act as hydrogen bond donor and acceptor (due to the inductive effect of the nitrile group) or to be involved into electrostatic interactions, while the nitrile group can be involved into hydrogen-bonding or  $\pi$ - $\pi$  interactions.

In 1850, Adolph Strecker documented the reaction between acetaldehyde and hydrogen cyanide, in an aqueous ammonia solution, producing 2-aminopropane nitrile in good yield (Figure 1.26).<sup>331</sup> This three component reaction has become one of the oldest known multi-component condensation reactions and the most used route for the synthesis of  $\alpha$ -amino acids on both laboratory and industrial scale till nowadays.<sup>332</sup> Moreover, the direct hydrocyanation of imines appeared as a modified version of the Strecker reaction (Figure 1.26). As C. E. Puerto Galvis rightly remarks,<sup>333</sup> more than 160 years after the Strecker reaction still remains as a very popular and significant tool in the synthesis of diverse synthetic drugs such as anti-platelet agent clopidogrel (Plavix),<sup>334</sup> opioid analgesic 4-anilidopiperidine-based drugs (carfentanil, remifentanil and alfentanil)<sup>335,336</sup> or the anti-HIV agent DPC 083 (see Figure 1.27).<sup>337</sup> Strecker intermediates are also successfully used in the synthesis of numerous pharmaceutically important indole alkaloids like reserpine,<sup>338</sup> hirsutine<sup>339</sup> or eburnamonine,<sup>340</sup> which can act as potent antihypertensive agents.

---

<sup>329</sup> H. Gröger, *Chem. Rev.*, 2003, 103, 2795-2828.

<sup>330</sup> J. Martens, *ChemCatChem*, 2010, 2, 379-381.

<sup>331</sup> A. Strecker, *Justus Liebigs Ann Chem.*, 1850, 75, 27-45.

<sup>332</sup> E. Marqués-López, R. P. Herrera (eds.) in *Bucherer-bergs and Strecker multicomponent reactions in multicomponent reactions: concepts and applications for design and synthesis*, 2015, John Wiley & Sons, Inc, Hoboken, NJ.

<sup>333</sup> V. V. Kouznetsov, C. E. P. Galvis, *Tetrahedron*, 2018, 74, 773-810.

<sup>334</sup> L. Wang, J. Shen, Y. Tang, Y. Chen, W. Wang, Z. Cai, Z. Du, *Org. Process Res. Dev.*, 2007, 11, 487-489.

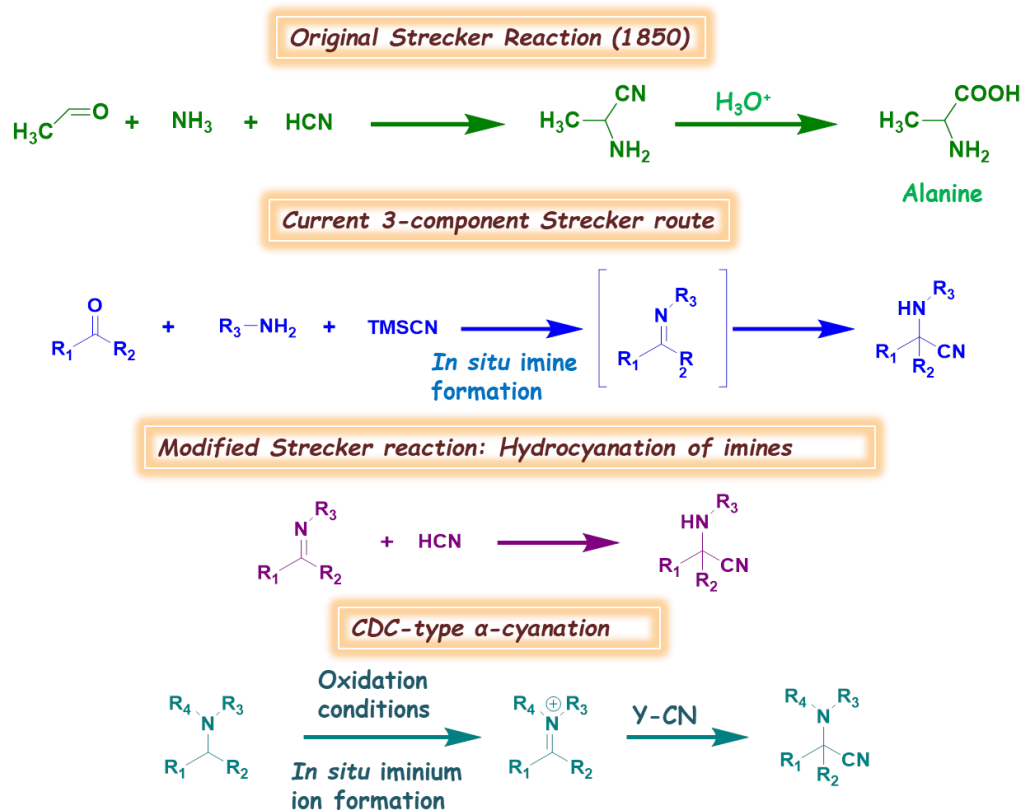
<sup>335</sup> P. L. Feldman, M. F. Brackeen, *J. Org. Chem.*, 1990, 55, 4207-4209.

<sup>336</sup> A. J. Walz, F. L. Hsu, *Tetrahedron Lett.*, 2014, 55, 501-502.

<sup>337</sup> F. G. Zhang, X.-Y. Zhu, S. Li, J. Niea, J.-A. Ma, *Chem Commun.*, 2012, 48, 11552-11554.

<sup>338</sup> G. Stork, *Pure Appl. Chem.*, 1989, 61, 439-442.

<sup>339</sup> M. Lounasma, J. Miettinen, P. Hanhinen, R. Jokela, *Tetrahedron Lett.*, 1997, 38, 1455-1458.



**Figure 1.26. Different types of Strecker-type reactions for the synthesis of  $\alpha$ -amino nitriles.**

As happens with the cyanosilylation reaction previously described, gaseous hydrogen cyanide or its alkaline metal cyanides were used at the beginning as the cyanide sources. Due to the hazardous and difficult handling of the HCN and the highly alkaline reaction conditions produced by KCN and NaCN, diverse alternative cyanide sources have been proposed and tested for use in this process: diethyl phosphorocyanidate ((EtO)<sub>2</sub>P(O)CN),<sup>341</sup> tributyltin cyanide (Bu<sub>3</sub>SnCN),<sup>342</sup> diethylaluminum cyanide (Et<sub>2</sub>AlCN),<sup>343</sup> trimethylsilyl cyanide (TMSCN),<sup>344,345</sup> acetyl cyanide (MeCOCN),<sup>346</sup> and ethyl cyanofornate

<sup>340</sup> A. Da Silva Goes, C. Ferroud, J. Santamaria, *Tetrahedron Lett.*, 1995, 36, 2235-2238.

<sup>341</sup> S. Harusawa, Y. Hamada, T. Shioiri, *Tetrahedron Lett.*, 1979, 20, 4663-4666.

<sup>342</sup> Z. F. Xie, G. L. Li, G. Zhao, J. D. Wang, *Synthesis*, 2009, 2035-2039.

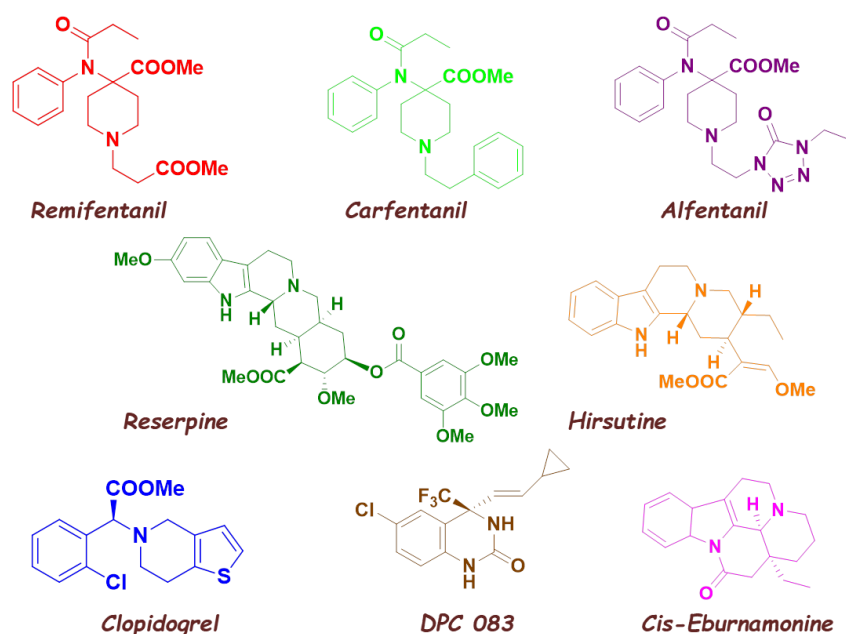
<sup>343</sup> S. Nakamura, N. Sato, M. Sugimoto, T. Toru, *Tetrahedron Asymm.*, 2004, 15, 1513-1517.

<sup>344</sup> J. Mulzer, A. Meier, J. Buschmann, P. Luger, *Synthesis*, 1996, 123-132.

<sup>345</sup> K. Shen, X. H. Liu, Y. F. Cai, L. L. Lin, X. M. Feng, *Chem. Eur. J.*, 2009, 15, 6008-6014.

<sup>346</sup> F. Cruz-Acosta, A. Santos-Exposito, P. Armas, F. García-Tellado, *Chem. Commun.*, 2009, 6839-6841.

(CNCOOEt)<sup>347</sup> among others. Each of these reagents has its limitations: ones require the intervention of metal species or strong reaction conditions, others are unstable or corrosive liquids and most of them are expensive and sensitive to moisture. Finally, due to its less hazardous nature, easier handling and the properties of the silicon atom, TMSCN has become; without any doubt, the more used cyanating agent also for the Strecker reaction, although it should be always carefully handled.



**Figure 1.27. Selected drugs and natural products prepared by using Strecker-type reactions or Strecker intermediates.<sup>333</sup>**

The three component Strecker reactions occurs through the formation of an imine intermediate, which sometimes can be the limiting step of the reaction (see Figure 1.26). Depending on the structure of the carbonylic substrate, especially in ketones, imine formation can be difficult. Then, the cyanide ion attacks the imine or iminium ions generated. There is also a competitive possible transformation in the three component Strecker reaction: the cyanosilylation of the carbonyl compound by the TMSCN. This is especially important in those cases in which the formation of the imine is not favoured.

The three component Strecker reactions involve mostly aldehydes, while the same reactions using ketones as the substrate remain a more

<sup>347</sup> J. P. Abell, H. Yamamoto, *J. Am. Chem. Soc.*, 2009, *131*,15118-15119.

difficult process and are usually substituted by the less desirable hydrocyanation reactions of the previously prepared ketimines.

Without chiral control, both Strecker and hydrocyanation reactions afford only racemic  $\alpha$ -amino nitriles. During the last decade, a wide compend of reaction conditions has been proposed for racemic  $\alpha$ -amino nitriles obtaining, mostly describing the synthesis of *tertiary*  $\alpha$ -amino nitriles starting from aromatic amines and aldehydes, while the use of ketones as substrates to give *quaternary*  $\alpha$ -amino nitriles is still nowadays limited. When chiral control is desired, the hydrocyanation of preformed ketimines represents the most efficient strategy developed up to now.

Recently, a very attractive alternative to the Strecker reaction has emerged as the cross-dehydrogenative-coupling(CDC)-type  $\alpha$ -cyanation of secondary or tertiary amines in the presence of an oxidant and a cyanide source (see Figure 1.26).<sup>348,349</sup> This transformation represents a particular example of oxidative CDC methods, which is a very important emerging area thanks to a wide range of applications for the formation of new C-C bonds.<sup>350</sup>

In this work we were interested on the three-component Strecker reaction using carbonyl compounds as starting materials. And once more, a catalytic flow system is intended to be created for this purpose. A catalyst achieving the efficient transformation of both aldehydes and ketones and which could be used under continuous flow conditions was the target. A extremely wide number of catalyst of different types have been tested and reported for the three-component Strecker reaction. It should be mentioned that catalyst-free multicomponent Strecker reactions with TMSCN have been reported.<sup>351,352</sup> However, non-catalytic strategies require large times, considerable amounts of toxic solvents, high temperatures or excess of TMSCN. Moreover, the absence of catalyst can favour the undesired cyanosilylation depending on the chemical nature of the reactants and their order of addition.<sup>353</sup> From the large number of literature examples it can be seen that the addition of acid catalysts results not only in significant increases in reaction rates, especially in the case of ketones, but also extends the

---

<sup>348</sup> Y. Ping, Q. Ding, Y. Peng, *ACS Catal.*, 2016, 6, 5989-6005.

<sup>349</sup> M. North, *Angew. Chem. Int. Ed.*, 2004, 43, 4126-4128.

<sup>350</sup> B. V. Varun, J. Dhineshkumar, K. R. Bettadapur, Y. Siddaraju, K. Alagiri, K. R. Prabhu, *Tetrahedron Lett.*, 2017, 58, 803-824.

<sup>351</sup> R. Martínez, D. Ramón, M. Yus, *Tetrahedron Lett.*, 2005, 46, 8471-8474.

<sup>352</sup> B. Nammalwar, C. Fortenberry, R. A. Bunce, *Tetrahedron Lett.*, 2014, 55, 379-381.

<sup>353</sup> J. Wang, Y. Masui, M. Onaka, *Eur. J. Org. Chem.*, 2010, 1763-1771.



applicability of the reaction to a wider range of substrates, including several sterically hindered aldehydes and ketones.

In recent years, a broad spectrum of different types of homogeneous Lewis acids ( $\text{RhI}_3$ ,<sup>354</sup>  $\text{CoCl}_2$ ,<sup>355</sup>  $\text{H}_3\text{BO}_3$ <sup>356</sup>), heterogeneous Lewis acids ( $\text{Fe}_3\text{O}_4@Zr\text{O}_2/\text{SO}_4^{2-}$ ,<sup>357</sup> SnHBeta zeolite,<sup>358</sup> Silica-based scandium(III)<sup>359</sup>), heterogeneous Brønsted acids ( $\text{Fe}_3\text{O}_4@cellulose\text{-OSO}_3\text{H}$ ,<sup>360</sup> Cellulose sulphuric acid,<sup>361</sup> MCM-41- $\text{SO}_3\text{H}$ <sup>362</sup>), bases, metal complexes ( $\text{K}_2\text{PdCl}_4$ ,<sup>363</sup> NHC-Pd complexes<sup>364</sup>), organo-catalysts (L-proline,<sup>365</sup>  $\text{HCOOH}$ ,<sup>366</sup> glycerol<sup>367</sup>), polymeric materials and resins (Nafion-Fe,<sup>368</sup> Nafion®SAC-13<sup>369</sup>) and ionic liquids ([BMIM][ $\text{BF}_4$ ] and [BMIM][ $\text{PF}_6$ ]<sup>370</sup>) have been tested for the three-component Strecker reaction. From all of them, the successful use of ionic liquids must be highlighted once more. Again, this opens the possibility to support these ionic liquids synthesising SILLPs capable to be used under continuous flow conditions. Moreover, the tunability of SILLPs allows to easily include in their final structure, if needed, Lewis acid species such as lanthanide triflates, which have shown a great catalytic activity for this transformation.<sup>371</sup>

Regarding the three-component continuous flow Strecker reaction, it must be noted that in 2008 C. Wiles and P. Watts reported a 50-membered library of  $\alpha$ -amino nitriles obtained under continuous flow conditions by using two supported catalysts: i) Polymer-supported

<sup>354</sup> A. Majhi, S. S. Kim, S. T. Kadam, *Tetrahedron*, 2008, 64, 5509-5514.

<sup>355</sup> S. K. De, *Beilstein J. Org. Chem.*, 2005, 8.

<sup>356</sup> Z. Karimi-Jaberi, A. Bahrani, *J. Chem. Res.*, 2012, 36, 326-327.

<sup>357</sup> H. Ghafuri, A. Rashidzadeh, B. Ghorbani, M. Talebi, *New. J. Chem.*, 2015, 39, 4821-4829.

<sup>358</sup> K. Iwanami, H. Seo, J. Choi, T. Sakakura, H. Yasuda, *Tetrahedron*, 2010, 66, 1898-1901.

<sup>359</sup> B. Karimi, A. A. Safari, *J. Organomet. Chem.*, 2008, 693, 2967-2970.

<sup>360</sup> A. Maleki, E. Akhlaghi, R. Paydar, *Appl. Organomet. Chem.*, 2016, 30, 382-386.

<sup>361</sup> A. Shaabani, A. Maleki, *Appl. Catal. A Gen.*, 2007, 331, 149-151.

<sup>362</sup> M. G. Dekamin, Z. Mokhtari, *Tetrahedron*, 2012, 68, 922-930.

<sup>363</sup> B. Karmakar, J. Banerji, *Tetrahedron Lett.*, 2010, 51, 2748-2750.

<sup>364</sup> J. Jarusiewicz, Y. Choe, K. S. Yoo, C. P. Park, K. W. Jung, *J. Org. Chem.*, 2009, 74, 2873-2876.

<sup>365</sup> A. Nasreen, *Tetrahedron Lett.*, 2013, 54, 3797-3800.

<sup>366</sup> H. Ghafuri, M. Roshani, *RSC Adv*, 2014, 4, 58280-58286.

<sup>367</sup> S. R. Ghogare, K. Rajeshwari, A. V. Narsaiah, *Lett. Org. Chem.*, 2014, 11, 688-692.

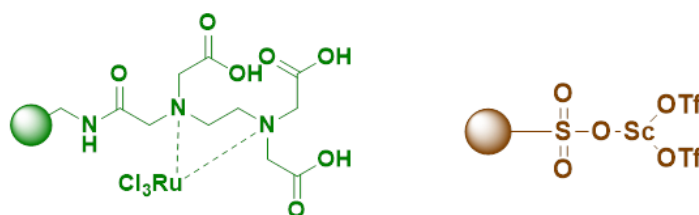
<sup>368</sup> G. K. S. Ghafuri, I. Bychinskaya, E. R. Marinez, T. Mathew, G. A. Olah, *Catal. Lett.*, 2013, 143, 303-312.

<sup>369</sup> G. K. S. Prakash, T. E. Thomas, I. Bychinskaya, A. G. Prakash, C. Panja, H. Vaghoo, G. A. Olah, *Green Chem.*, 2008, 10, 1105-1110.

<sup>370</sup> J. S. Yadav, B. V. S. Reddy, B. Eshwaraiah, M. P. Srinivas, P. Vishnumurthy, *New J. Chem.*, 2003, 27, 463-465.

<sup>371</sup> S. Kobayashi, T. Busujima, *Chem. Commun.*, 1998, 981-982.

(ethylenediaminetetraacetic acid) ruthenium (III) chloride (PS-RuCl<sub>3</sub>)<sup>372</sup> and ii) Polymer-bound scandium (III) bis-(trifluoromethanesulfonate) [Ps-Sc(OTf)<sub>2</sub>]<sup>373</sup> (Figure 1.28). In the continuous flow catalytic system designed by C. Wiles and P. Watts, these supported catalysts were packed in a borosilicate glass micro reactor with three inlets for each one of the Strecker reaction components organised in such a way the inlet for TMSCN appears after a mixing channel where the imine should be previously formed (see Figure 1.29.a). Although a large diversity of  $\alpha$ -amino nitriles was prepared, all of them derived from aldehydes and reactions for less reactive ketones were not reported. Yields up to 99% were reported with residence times between 0.5 and 1 hour at room temperatures with flows ranging between 0.02 and 0.04 mL/min and 1:1:1 stoichiometries, using acetonitrile as the solvent (0.2 M concentration of the reagents). Improvement for this interesting approach can be considered if higher flows, to obtain better productivities, and a greener solvent or even solvent-free conditions could be applied to this process.



**Figure 1.28. Supported catalysts reported by C. Wiles and P. Watts to perform continuous flow Strecker reactions. Left: Polymer-supported (ethylenediaminetetraacetic acid) ruthenium(III) chloride (PS-RuCl<sub>3</sub>);<sup>372</sup> right: Polymer-bound scandium (III) bis-(trifluoromethanesulfonate).<sup>373</sup>**

Four years later, the same authors encouraged by the homogeneous investigations of G. A. Olah and co-workers,<sup>374</sup> reported a gallium triflate supported catalyst [PS-Ga(OTf)<sub>2</sub>], directly related to the previous scandium catalyst, for the three-component continuous flow Strecker (see Figure 1.29.b,c).<sup>375</sup> With this supported catalyst, five ketonic Strecker reactions could be finally achieved. With four acetophenone derivatives and cyclohexanone, yields up to 99% were reached for the corresponding  $\alpha$ -amino nitriles at 40°C with a flow rate of 0.02 mL/min

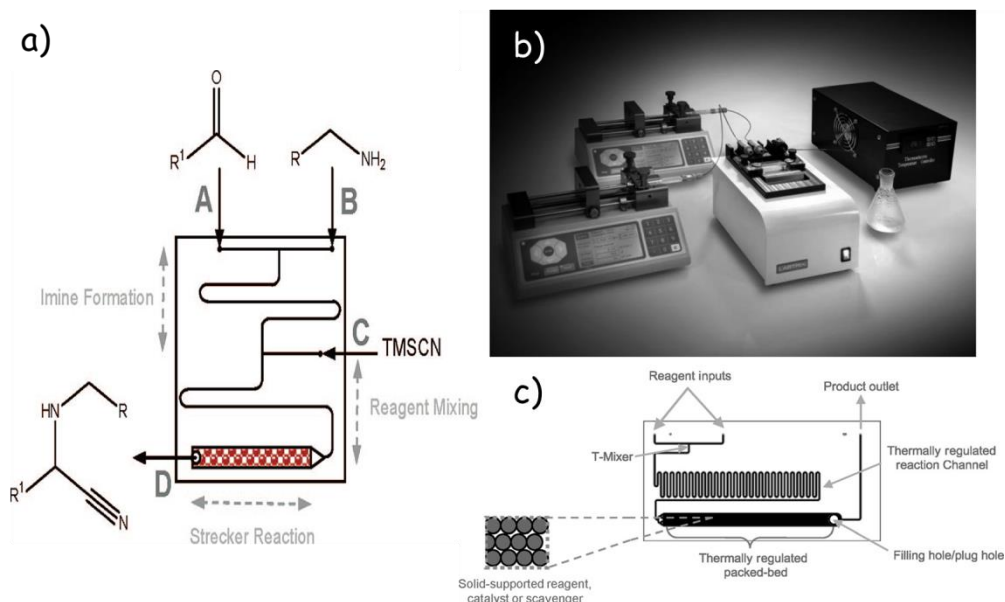
<sup>372</sup> C. Wiles, P. Watts, *Org. Proc. Res. Dev.*, 2008, 12, 1001-1006.

<sup>373</sup> C. Wiles, P. Watts, *Eur. J. Org. Chem.*, 2008, 5597-5613.

<sup>374</sup> G. K. S. Prakash, T. Mathew, C. Panja, S. Alconcel, H. Vaghoo, C. Do, G. A. Olah, *Proc. Natl. Acad. Sci. USA*, 2007, 104, 3703 – 3706.

<sup>375</sup> C. Wiles, P. Watts, *ChemSusChem*, 2012, 5, 332-338.

and 1:1:1 stoichiometries under continuous flow conditions, using in this case dichloromethane as the solvent (0.2 M concentration of the reagents). Again the reactions needed to use of a non-green solvent and low flow rates. The comparison between the results obtained in batch reactions with homogeneous  $\text{Ga}(\text{OTf})_3$  by G. A. Olah and co-workers and the ones obtained under continuous flow conditions with the same supported triflate are of clear interest. Higher yields were obtained under flow conditions, reducing the equivalents of  $\text{TMSCN}$  from 3 to 1 and reducing the reaction times from 4-6 hours to minutes. Moreover, the supported catalyst showed to be quite stable and no quantitative leaching of Ga was reported.

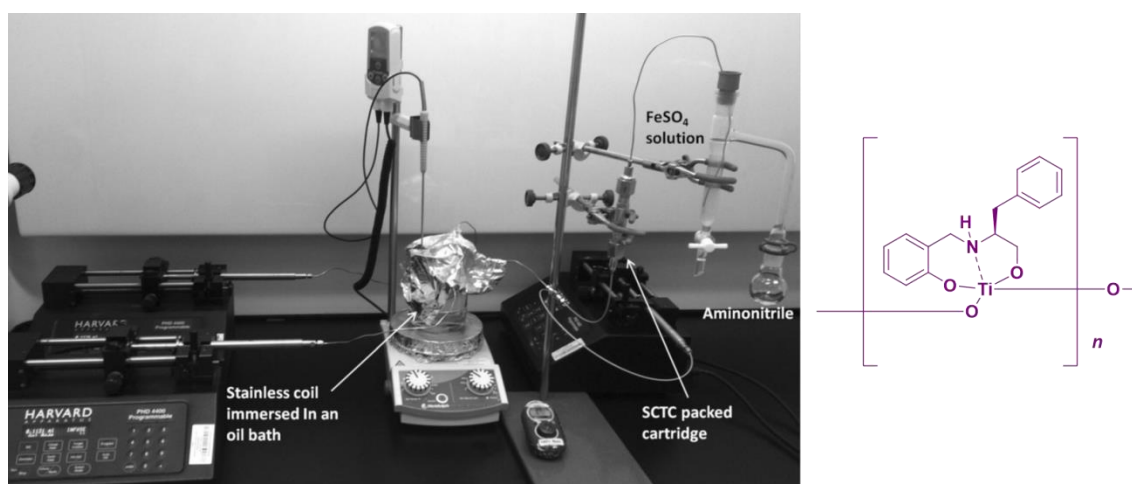


**Figure 1.29. a) Scheme of the flow microreactor designed by C. Wiles and P. Watts in 2008 for the three-component Strecker reaction.<sup>373</sup> The flow microreactor has three inlets and a mixing channel after the first two inlets for imine formation. b) Setup used by C. Wiles and P. Watts in 2012 for the Strecker reaction of ketones with  $\text{PS-Ga}(\text{OTf})_3$  as the supported catalyst.<sup>375</sup> Two syringe pumps and a microreactor with two inlets can be observed. c) Scheme of the flow microreactor of the setup shown in b.**

In the same 2012, the first continuous asymmetric three-component Strecker reaction was reported.<sup>376</sup> By using a self-supported chiral titanium cluster (SCTC) as a supported catalyst (see Figure 1.30), K. Yoshinaga and co-workers achieved yields of up to 90% and 47-98 % ee for nine different  $\alpha$ -amino nitriles. It is worth mentioning that the nine substrates were aromatic aldehydes, the most favoured ones for this transformation. A stainless coil reactor at 60-70°C was used to favour

<sup>376</sup> A. M. Seayad, B. Ramalingam, C. L. L. Chai, C. Li, M. V. Garland, K. Yoshinaga, *Chem. Eur. J.*, 2012, 18, 5693-5700.

imine formation before of the TMSCN inlet (see Figure 1.30). 1:1:1.3 (aldehyde:amine:TMSCN) stoichiometries, 0.01-0.02 mL/min flow rates and toluene as the solvent (0.5 M concentrations of aldehyde and amine, and 0.33 M for the TMSCN were injected) were used. Once more, a non-green solvent and low flow rates needed to be used. Moreover, the supported catalyst (titanium cluster) was hard and laborious to obtain.



**Figure 1.30.** Setup and catalyst designed by K. Yoshinaga and co-workers in 2012 for the asymmetric 3-component continuous flow Strecker reaction of aldehydes.<sup>376</sup> Three syringe pumps (each one for each reagent) can be seen. A stainless steel coil was set before of the TMSCN incorporation to favour the previous formation of imine. The cartridge was packed with the titanium cluster shown at right and finally a  $\text{FeSO}_4$  solution was used at the end for cyanide quenching.

Here again, an underlying hypothesis for our work was that the catalytic properties of SILLPs could help to develop a more efficient Strecker reaction specially under continuous flow conditions. Moreover, SILLPs are easier to synthesise, as compared with the titanium cluster discussed above, and could integrate in their structure Ga or Sc triflates, which have been shown as the most efficient Lewis acid catalysts for these processes, even for some aromatic ketones.

A new efficient and green catalytic continuous flow system for the three-component Strecker reaction is reported in the chapter 5. Our system allows the transformation of less reactive aliphatic ketones under flow conditions using functionalised supported ionic liquids as a key player.

### 1.6.3. Negishi cross-coupling reaction

The Negishi reaction is one of the cross-coupling reactions and owes its name to the Japanese chemist Eiichi Negishi, who won the Nobel Prize in Chemistry in 2010. The term “cross-coupling reactions” broadly refers to the substitution of alkyl, aryl, and vinyl halides or pseudo halides by nucleophiles, catalysed by a transition-metal complex, leading to the formation of C-C and C-heteroatom bonds, and following a relatively common mechanistic pathway involving oxidative addition, transmetalation and reductive elimination steps.<sup>377</sup> In these cross-coupling reactions nucleophilic and electrophilic partners are both involved. The nucleophilic partners are commonly organometallic reagents,<sup>378,379</sup> but they can also be carboxylic acids,<sup>380</sup> or even C-H bonds under certain reaction conditions.<sup>381</sup> The electrophilic cross-coupling partners are not only halides or pseudo halides<sup>382,383</sup> but also diazonium salts<sup>384</sup> and inert ethers or alcohols.<sup>385</sup>

The field of cross-coupling was initially developed by F. Ullman in 1901 with his copper-catalysed biaryl synthesis from aryl halides.<sup>386</sup> Then, the discovery of modern transition-metal catalysed cross-coupling reactions started in the decade of 1970s with the discovery of the Kumada coupling,<sup>387</sup> followed by the Heck,<sup>388</sup> Sonogashira,<sup>389</sup> Negishi,<sup>390,391</sup> Suzuki,<sup>392</sup> and other cross-coupling reactions.

Concisely, the Negishi cross coupling is the organic reaction between an organic halide or triflate and an organozinc compound using a palladium or nickel catalyst to achieve the coupled product displaying a new C-C bond formed. This transformation has been widely applied in modern organic synthesis and its applications in the synthesis of organic molecules of chemical, biological or pharmaceutical importance

<sup>377</sup> S. L. Buchwald, *Acc. Chem. Res.*, 2008, 41, 1439.

<sup>378</sup> C. E. I. Knappke, A. von Wangelin, *Chem. Soc. Rev.*, 2011, 40, 4948-4962.

<sup>379</sup> Y. Xia, D. Qiu, J. Wang, *Chem. Rev.*, 2017, 117, 13810-13889.

<sup>380</sup> Y. Wei, P. Hu, M. Zhang, W. Su, *Chem. Rev.*, 2017, 117, 8864-8907.

<sup>381</sup> C. S. Yeung, V. M. Dong, *Chem. Rev.*, 2011, 111, 1215-1292.

<sup>382</sup> A. Rudolph, M. Lautens, *Angew. Chem. Int. Ed.*, 2009, 48, 2656-2670.

<sup>383</sup> C. C. C. Johansson Seechum, M. O. Kitching, T. J. Colacot, V. Sniekus, *Angew. Chem. Int. Ed.*, 2012, 51, 5062-5085.

<sup>384</sup> N. Oger, M. D'Halluin, E. Le Grogneq, F.-X. Felpin, *Org. Process. Res. Dev.*, 2014, 18, 1786-1801.

<sup>385</sup> D.-G. Yu, B.-J. Li, Z.-J. Shi, *Acc. Chem. Res.*, 2010, 43, 1486-1495.

<sup>386</sup> F. Ullmann, J. Bielecki, *Ber. Dtsch. Chem. Ges.*, 1901, 34, 2174-2185.

<sup>387</sup> K. Tamao, K. Sumitani, M. Kumada, *J. Am. Chem. Soc.*, 1972, 94, 4374-4376.

<sup>388</sup> R. F. Heck, J. P. Nolley, *J. Org. Chem.*, 1972, 37, 2320-2322.

<sup>389</sup> K. Sonogashira, Y. Tohda, N. Hagihara, *Tetrahedron Lett.*, 1975, 16, 4467-4470.

<sup>390</sup> S. Baba, E. Negishi, *J. Am. Chem. Soc.*, 1976, 98, 6729-6731.

<sup>391</sup> E. Negishi, *Acc. Chem. Res.*, 1982, 15, 340-348.

<sup>392</sup> N. Miyaoura, K. Yamada, A. Suzuki, *Tetrahedron Lett.*, 1979, 20, 3437-3440.

have been reported.<sup>393,394</sup> The Negishi cross-coupling is less commonly used for industrial applications than other cross-coupling reactions, like Suzuki and Heck couplings, due mainly to the air and water sensitivity of the organozinc reagents involved. On the other hand, the higher reactivity of these alkyl Zn compounds means faster reactions.<sup>395</sup> One recently reported interesting application of the Negishi cross-coupling is the synthesis of unnatural amino acids.<sup>396</sup>

Compared with Grignard reagents, unique functional group tolerance and good reactivity are offered by organozinc reagents. This, together with the property of the C-Zn bond of readily undergoing transmetalation with transition metals, makes organozinc compounds very valuable reagents for cross-coupling reactions.<sup>397</sup> It must be noted that, in contraposition to the highly pyrophoric conventional dialkylzinc reagents, alkyl or aryl zinc halides can be easily handled and stored using some precautions. Sometimes LiCl is added to stabilise the organozinc reagent due to its capacity to accelerate Csp<sup>3</sup>-halide insertions and solubilise the formed zinc reagent by forming RZnX·LiCl species.<sup>398</sup> A considerable number of strategies for preparing organozinc reagents is known, the simplest and most typical being probably the reaction of organic halides with elemental zinc.<sup>399,400</sup> However, for some substrates this reaction is difficult and the corresponding preparation must be done *via* a Grignard reagent with an immediate magnesium/zinc exchange.<sup>401</sup>

One strategy for the preparation of organozinc reagents recently developed that is of high relevance for our work allows a continuous flow preparation. This protocol has been reported by J. Alcázar and co-workers in 2018.<sup>402</sup> A glass column reactor (with a glass heat exchanger) is filled with granular Zn and then this Zn is activated with a solution (10 mL, 0.6 M TMSCl and 0.24 M 1-bromo-2-chloroethane in dry THF) pumped through the column at 40°C (possible variation to 25, 60 or even 100°C depending on the desired organozinc) with a flow rate

---

<sup>393</sup> V. B. Phapale, D. J. Cárdenas, *Chem. Soc. Rev.*, 2009, 38, 1598-1607.

<sup>394</sup> M. M. Heravi, E. Hashemi, N. Nazari, *Mol. Diversity*, 2014, 18, 441-472.

<sup>395</sup> P. Devendar, R.-Y. Qu, W.-M. Kang, B. He, G.-F. Yang, *J. Agric. Food. Chem.*, 2018, 66, 8914-8934.

<sup>396</sup> W. D. G. Brittain, S. L. Cobb, *Org. Biomol. Chem.*, 2018, 16, 10-20.

<sup>397</sup> A. D. Dilman, V. V. Levin, *Tetrahedron Lett.*, 2016, 57, 3986-3992.

<sup>398</sup> A. Krasovkiy, V. Malakhov, A. Gavryushin, P. Knochel, *Angew. Chem. Int. Ed.*, 2006, 45, 6040-6044.

<sup>399</sup> G. Dagousset, C. Francois, T. Leon, R. Blanc, E. Sansiaume-Dagousset, P. Knochel, *Synthesis*, 2014, 46, 3133-3171.

<sup>400</sup> J. H. Kim, Y. O. Ko, J. Bouffard, S. Lee, *Chem. Soc. Rev.*, 2015, 44, 2489-2507.

<sup>401</sup> Z.-L. Shen, P. Knochel, *ACS Catal.*, 2015, 5, 2324-2328.

<sup>402</sup> M. Berton, L. Huck, J. Alcázar, *Nature Protocols*, 2018, 13, 324-334.

of 1 mL/min. After zinc activation, a solution of the correspondent alkyl or allyl halide (0.5 M in THF) is pumped at 0.5 mL/min through the activated Zn column maintaining the temperature at 40°C (or the appropriate temperature). The organozinc halide compound resulting (obtained as a THF solution) is collected in a sealed flask of vial under N<sub>2</sub> atmosphere. In fact, both activating and alkyl (or allyl) halide solutions should be prepared also under a N<sub>2</sub> atmosphere. Finally, titration with I<sub>2</sub> of the resultant organozinc solution was performed to know the approximate organozinc halide concentration in THF (*ca.* 0.5 M desired).

With this strategy, the on-demand synthesis of 18 different organozinc halides under continuous flow was achieved with the remarkable advantage of using the same Zn column for the different organozinc prepared till the consumption of approximately the 75% of the zinc. There are some practical problems that can occur, like the high temperatures that should be used for some organozinc halides or the blockage or overpressure of the system due to the precipitation of organozinc halides or to a overpackaged Zn column. Despite that, this is a very relevant method because continuous flow techniques can be considered as a step forward for the safe generation of organozinc reagents,<sup>403</sup> in particular in comparison with the traditional methods.<sup>404,405</sup> In our group, this protocol has been successfully reproduced (Figure 1.31).

Regarding the catalysts for these cross coupling transformations, the reactivities and limitations of several transition metals like palladium,<sup>406,407</sup> nickel,<sup>408</sup> ruthenium,<sup>409</sup> rhodium,<sup>410</sup> etc. have been studied and reported. Specially, palladium catalysed cross coupling reactions represent one of the most versatile, interesting and powerful tools used by organic chemists to produce fine chemicals at the ton-scale.<sup>411,412</sup> A large number of advances in Pd-catalysed C-C bond formation, including decarboxylative couplings, continue being widely

<sup>403</sup> R. D. Rieke, P. M. Hudnall, S. J. Uhm, *J. Chem. Soc. Chem. Commun.*, 1973, 269-270.

<sup>404</sup> D. Soorukram, N. Boudet, V. Malakov, P. Knochel, *Synthesis*, 2007, 3915-3922.

<sup>405</sup> L. Malet-Sanz, S. Flavien, *J. Med. Chem.*, 2012, 55, 4062-4098.

<sup>406</sup> X. Chen, K. M. Engle, D.-H. Wang, J.-Q. Yu, *Angew. Chem. Int. Ed.*, 2009, 48, 5094-5115.

<sup>407</sup> P. Ruiz-Castillo, S. L. Buchwald, *Chem. Rev.*, 2016, 116, 12564-12649.

<sup>408</sup> M. Tobisu, N. Chatani, *Acc. Chem. Res.*, 2015, 48, 1717-1726.

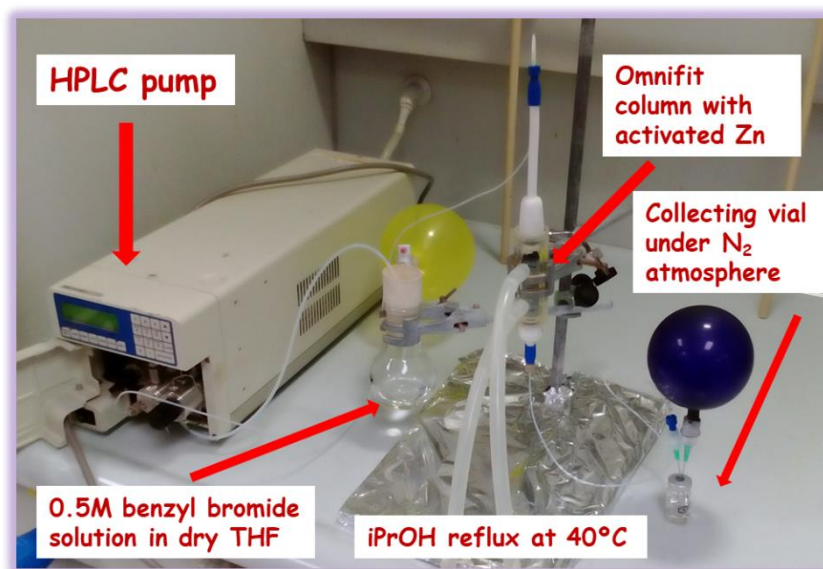
<sup>409</sup> L. Ackermann, *Acc. Chem. Res.*, 2014, 47, 281-295.

<sup>410</sup> N. Kuhl, N. Schöder, F. Glorius, *Adv. Synth. Catal.*, 2014, 356, 1443-1460.

<sup>411</sup> C. Torborg, M. Beller, *Adv. Synth. Catal.*, 2009, 351, 3027-3043.

<sup>412</sup> J. Magano, J. R. Dunetz, *Chem. Rev.*, 2011, 111, 2177-2250.

reported.<sup>413,414</sup> A convincing proof of the growing importance of Pd-catalysed cross-coupling reactions can be found in the Nobel Prize in chemistry of the year 2010, which was awarded to R. F. Heck, E. Negishi and A. Suzuki for their investigations on such transformations. When considering palladium catalysts for the Negishi reaction, this normally refers to palladium (II) precatalyst species. These Pd(II) complexes or compounds then are *in situ* converted in the Pd(0) catalytically active species. The best precatalysts are those who are capable of rapidly generating the Pd(0) species under mild conditions.<sup>415</sup>



**Figure 1.31.** Setup used in our group for reproducing the protocol developed by J. Alcázar and co-workers<sup>402</sup> for preparing organozinc reagents in continuous flow.

In addition to the catalytic metals, some specific ligands are broadly used for the Negishi cross-coupling reactions. Probably, the most important and used are phosphines and N-heterocyclic carbene ligands (NHCs). Regarding NHCs, they present some beneficial properties, increasing the reactivity and making them an essential tool for those transformations.<sup>395</sup> The oxidative addition and reductive elimination steps involved can be both accelerated by the steric and electronic properties of the NHC ligands. Moreover, a broader scope of products and milder reaction conditions can be achieved. For all these reasons,

<sup>413</sup> C. C. C. Johansson, T. J. Colacot, *Angew. Chem. Int. Ed.*, 2010, 49, 676-707.

<sup>414</sup> A. M. R. Smith, K. K. Hii, *Chem. Rev.*, 2011, 111, 1637-1656.

<sup>415</sup> D. Haas, J. M. Hammann, R. Greiner, P. Knochel, *ACS Catal.*, 2016, 6, 1540-1552.



the application of a large variety of these NHCs has been reported.<sup>416,417,418</sup>

On the other hand, different types of phosphines such as trialkyl or triaryl phosphines,<sup>419</sup> dialkylbiaryl phosphines<sup>420</sup> (e.g. Hartwig's QPhos<sup>421</sup> and Buchwald's XPhos<sup>422</sup>) and secondary phosphine oxides<sup>423</sup> have been broadly used as ligands in cross-coupling reactions. The dialkylbiaryl phosphines first described in 1998 by S. L. Buchwald deserve to be highlighted.<sup>424</sup> They are sterically-hindered and electron-rich phosphines with the capacity to modulate the chemical reactivity of palladium, allowing the increase of the scope of products potentially achievable in the Negishi transformation, as well as in other cross coupling reactions (see Figure 1.32). Larger dialkylbiaryl phosphine ligands favour the formation of catalytic active species  $LPd^0$ , which have been demonstrated to accelerate oxidative addition.<sup>425</sup> Electron-donating alkyl groups on the phosphorous atom accelerate the oxidative addition, while larger alkyl groups on the phosphorous and ortho-substitution of the non-phosphine-containing aryl ring promote the reductive elimination. Monoligated palladium catalysts are the more appropriate due to the minimised steric hindrance that facilitates the transmetalation stage.

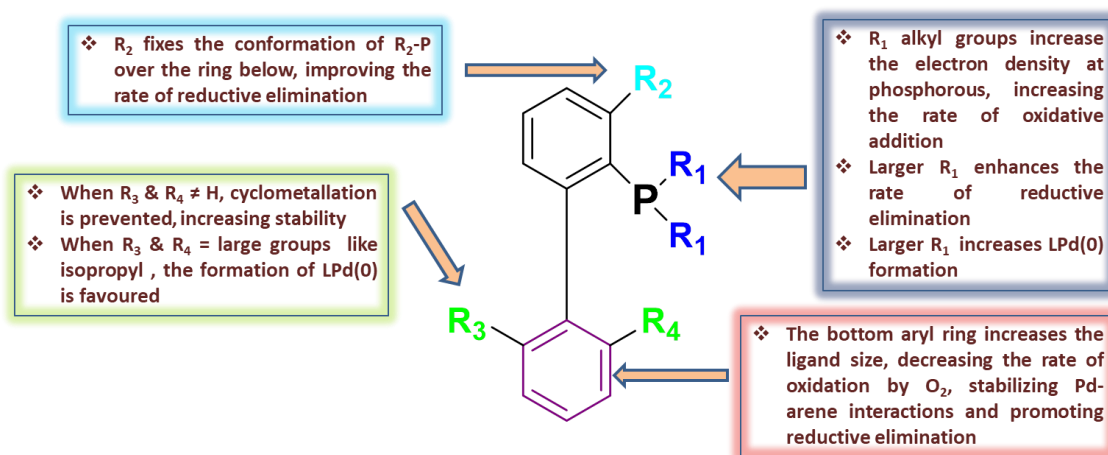


Figure 1.32. Structural effects in dialkyl biaryl phosphines.

<sup>416</sup> O. Kühn, *Chem. Soc. Rev.*, 2007, 36, 592-607.

<sup>417</sup> S. Díez-González, N. Marion, S. P. Nolan, *Chem. Rev.*, 2009, 109, 3612-3676.

<sup>418</sup> N. Marion, S. P. Nolan, *Acc. Chem. Res.*, 2008, 41, 1440-1449.

<sup>419</sup> J. L. Methot, W. R. Roush, *Adv. Synth. Catal.*, 2004, 346, 1035-1050.

<sup>420</sup> J. P. Wolfe, S. L. Buchwald, *J. Org. Chem.*, 2000, 65, 1144-1157.

<sup>421</sup> G. D. Vo, J. F. Hartwig, *Angew. Chem.*, 2008, 120, 2157-2160.

<sup>422</sup> D. S. Surry, S. L. Buchwald, *Angew. Chem. Int. Ed.*, 2008, 47, 6338-6361.

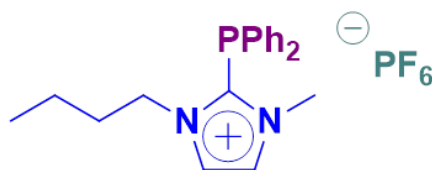
<sup>423</sup> T. M. Shaikh, C.-M. Weng, F.-E. Hong, *Coord. Chem. Rev.*, 2012, 256, 771-803.

<sup>424</sup> D. W. Old, J. P. Wolfe, S. L. Buchwald, *J. Am. Chem. Soc.*, 1998, 120, 9722-9723.

<sup>425</sup> P. G. Gildner, T. J. Colacot, *Organometallics*, 2015, 34, 5497-5508.

The development of these phosphine ligands was important due to the fact that the triphenylphosphines previously used needed harsh conditions and provided access to a really limited scope of products (aryl bromides and iodides at elevated temperatures). Since their discovery, extensive work has been done in this field by the Buchwald's group, among others, to develop new dialkylbiaryl phosphines, which are informally known as "Buchwald ligands".<sup>426</sup>

Ionic Liquids have been used as reaction media or catalysts/ligands, either in IL form, functionalised IL form or supported IL-phase for these cross-couplings. A large number of examples can be found for the cross-coupling Stille, Sonogashira, Ullmann, Heck or Suzuki reactions. Most of them were widely reviewed by G.-H. Gao and co-workers in 2009.<sup>427</sup> However, almost no Negishi cross-coupling reaction involving ILs has been reported up to now. The first case was reported by J. Sirieix and co-workers in 2000.<sup>428</sup> The IL [BMIM][PF<sub>6</sub>] was employed both as a reaction media and as a ligand after functionalisation with a phosphine. The presence of the phosphine functionalised IL ligand (see Figure 1.33) in a biphasic [BMIM][PF<sub>6</sub>]/toluene medium facilitated the Pd-catalysed Negishi coupling between aryl or benzyl zinc halides and various aryl iodides. Yields between 70 and 92% in times ranging from 20 minutes to 5 hours were reached. Moreover, a rapid cross-coupling was achieved at room temperature and a facile work-up was allowed due to easy phases separation by decantation of the IL phase which contained the Pd catalyst and the IL-Phos ligand. However, the recycling of the IL phase led to a significant decrease in yield. Thus, although ionic liquids are an almost unexplored field for Negishi cross-coupling reactions, the study of their application in this reaction could afford new advances.



**Figure 1.33. Phosphine functionalised IL ligand used in Negishi cross-couplings by J. Sirieix and co-workers.**<sup>428</sup>

Some efforts have been done in the last five years to develop Negishi cross-coupling transformations under continuous flow conditions and

<sup>426</sup> D. S. Surry, S. L. Buchwald, *Angew. Chem. Int. Ed.*, 2011, 47, 6338-6361.

<sup>427</sup> Y. Liu, S.-S. Wang, W. Liu, Q.-X. Wan, H.-H. Wu, G.-H. Gao, *Curr. Org. Chem.*, 2009, 13, 1322-1346.

<sup>428</sup> J. Sirieix, M. Ossberger, B. Betzemeier, P. Knochel, *Synlett*, 2000, 1613-1615.

most of these efforts have been led by J. Alcázar and co-workers from Janssen-Cilag S. A. The first continuous Negishi cross-coupling was reported by them in 2014.<sup>429</sup> With the strategy above described to prepare alkyl and benzylzinc halides, a telescoped continuous synthesis of organozinc halides coupled to Negishi reactions was successfully achieved. Organozinc reagents have an unstable and highly reactive nature and telescoped continuous flow is an ideal tool for handling such intermediates.<sup>430,431</sup> By preparing and coupling a second reactor column packed with a transition metal catalyst, the freshly prepared organozinc passes directly to it. Different supported palladium complexes were tested for continuous cross-coupling reactions by J. Alcázar and co-workers in previous reports,<sup>432</sup> and SiliaCat DPP-Pd was found to effectively catalyse a wide range of Negishi reactions.<sup>433</sup> In this commercially available catalyst, the palladium is supported on silica and has diphenylphosphine as ligand. It must be noted that the theoretically more efficient dialkylbiaryl phosphine ligands (Buchwald's ligands) are not being used. However, SiliaCat DPP-Pd had shown to be an efficient supported catalyst for other previous continuous flow cross-coupling reactions and no leaching of Pd was detected.<sup>432,433</sup> Thus, a solution of alkyl or benzyl halide (0.3 M in dry THF, with 1 eq of LiCl when appropriate) was passed through a first reactor filled with Zn (previously activated as described above, Omnifit column with 12 g of Zn) using a Vapourtec R2+R4 system at the desired temperature (r.t., 60 or 110°C depending on the organozinc) and a flow rate of 0.2 mL/min (10 minutes residence time). The resulting organozinc solution was mixed in a T piece with a solution of aryl halide (0.2 M in dry THF) pumped at 0.2 mL/min and the mixture passed through a second reactor filled with SiliaCat DPP-Pd (Omnifit glass column, 1 g of SiliaCat DPP-Pd) at the required temperature (60 or 80°C) and a total flow rate of 0.4 mL/min (residence time of 2.5 minutes) (see Figure 1.34). Eighteen different Negishi cross-coupling products with yields between 71 and 93% were achieved. Moreover, a stability of 13 hours was assessed for the process reaching a productivity of 3.3 mmol/h and a turnover number of 175 for the catalyst, for the overall process.

---

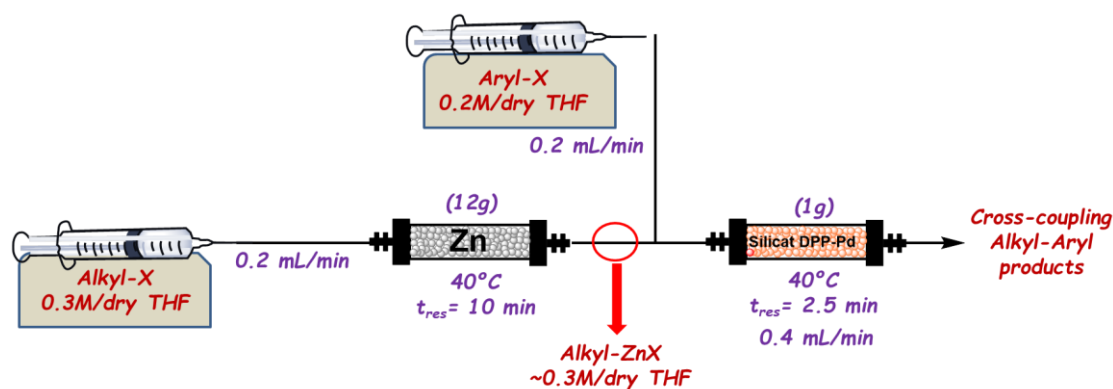
<sup>429</sup> N. Alonso, L. Z. Miller, J. de M. Muñoz, J. Alcázar, D. T. McQuade, *Adv. Synth. Catal.*, 2014, 356, 3737-3741.

<sup>430</sup> T. Illg, P. Löb, V. Hessel, *Bioorg. Med. Chem.*, 2010, 18, 3707-3719.

<sup>431</sup> R. L. Hartman, J. P. McMullen, K. F. Jensen, *Angew. Chem. Int. Ed.*, 2011, 50, 7502-7519.

<sup>432</sup> J. de M. Muñoz, J. Alcázar, A. de la Hoz, A. Díaz-Ortiz, *Adv. Synth. Catal.*, 2012, 354, 3456-3460.

<sup>433</sup> B. Egle, J. de M. Muñoz, N. Alonso, W. M. deBorggraeve, A. de la Hoz, A. Díaz-Ortiz, J. Alcázar, *J. Flow. Chem.*, 2014, 4, 22-25.



**Figure 1.34. Scheme of the telescopic continuous Negishi cross-coupling process developed by J. Alcázar and co-workers.<sup>429</sup> Both reagent solutions were pumped by syringe pumps.**

In the present work, in collaboration with Dr. J. Alcázar, the aim was to introduce SILLP-Pd as catalyst. Palladium can be immobilised using the imidazolium units of a SILLP as NHC-Pd carbene species or as a counterion involving PdX or anionic Pd-complex forms.

In 2018, a new telescoped Negishi continuous process catalysed by Nickel and induced by visible light has been reported by J. Alcázar and co-workers.<sup>434</sup> Compared with traditional dual photocatalysis, where non sustainable rare metals photocatalysts are used,<sup>435,436</sup> an exogenous photosensitizer is not needed. This example represents the first work reported using organozinc reagents in a photochemical reaction. Moreover, Ni neither has been reported before for visible-light-induced transition-metal-catalysed transformations, unlike cobalt, iron, copper or palladium.<sup>437</sup> Irradiation at 450nm in a Vapourtec UV-150 photoreactor (coil volume = 10 mL, flow rate = 0.5 mL/min, 20 minutes of residence time) at 60°C took place after the alkyl or benzylzinc halide coupled preparation. NiCl<sub>2</sub>·glyme (2-5 mol%) and dtbbpy (7.5 mol%) were pumped together with the aryl halide in a THF/DMF solution. Twenty-three different Negishi cross-coupling isolated products with yields between 44 and 96% were achieved. When no light induction participates, yields decrease significantly and even some products were not formed at all. For one of the Negishi products, the stability of the process was assessed for 8 hours with a productivity of 800 mg/h.

<sup>434</sup> I. Abdiaj, A. Fontana, M. V. Gómez, A. de la Hoz, J. Alcázar, *Angew. Chem. Int. Ed.*, 2018, 57, 8473–8477.

<sup>435</sup> U. K. Sharma, H. P. G. L. Gemoets, F. Schröder, T. Noël, E. V. Van der Eycken, *ACS Catal.*, 2017, 7, 3818–3823.

<sup>436</sup> J. C. Tellis, C. B. Kelly, D. N. Primer, M. Jouffroy, N. R. Patel, G. A. Molander, *Acc. Chem. Res.*, 2016, 49, 1429–1439.

<sup>437</sup> M. Parasram, V. Gevorgyan, *Chem. Soc. Rev.*, 2017, 46, 6227–6240.

Moreover, 93% yield of the isolated product was obtained as compared with the 39% obtained in batch. It is worth to highlight that chloroarenes have been successfully used in this coupling process while had only rarely been described before in literature in this context.<sup>438</sup>

This last example demonstrates that Ni, with light induction, represents an interesting alternative to Pd for performing continuous flow Negishi coupling processes. However, Ni is pumped during the whole process together with the reagents and no recycling or reusing of the catalyst occurs. Ni also could be immobilised in supported ionic liquids, which could represent a simple solution for this shortcoming if the immobilisation does not introduce any limitation for the light induction.

In the last two years, M. G. Organ and co-workers have developed two Pd-PEPPSI catalysts supported in silica for continuous flow Negishi couplings. Pd-PEPPSI-IPr-SiO<sub>2</sub><sup>439</sup> and Pd-PEPPSI-IPent-SiO<sub>2</sub><sup>440</sup> have been synthesised and tested (see Figure 1.35). PEPPSI refers to a group of palladium catalysts developed also by M. G. Organ and co-workers in 2005,<sup>441</sup> and the meaning is Pyridine-Enhanced-Precatalyst-Preparation-Stabilisation-Initiation. These Pd-NHC carbene based catalysts have a great stability compared with other Pd complexes and have demonstrated their suitability to catalyse various cross-coupling reactions like Suzuki, Heck or Negishi.<sup>442,443,444</sup> These PEPPSI catalysts are usually employed in homogeneous catalysis and their immobilisation has been barely reported.<sup>445</sup> For their covalently immobilisation on silica, a triethoxysilyl functionalisation *via* azidealkyne cycloaddition chemistry has been necessary.<sup>446</sup>

Both flow processes described by M. G. Organ and co-workers are not telescopic. The organozinc reagents used were previously obtained in batch on a previous laborious reaction or were commercially available.

<sup>438</sup> V. B. Phapale, D. J. Cárdenas, *Chem. Soc. Rev.*, 2009, 38, 1598–1607.

<sup>439</sup> G. A. Price, A. R. Bogdan, A. L. Aguirre, T. Iwai, S. W. Djuric, M. G. Organ, *Catal. Sci. Technol.*, 2016, 6, 4733–4742.

<sup>440</sup> G. A. Price, A. Hassan, A. R. Bogdan, S. W. Djuric, M. G. Organ, *Angew. Chem. Int. Ed.*, 2017, 56, 13347–13350.

<sup>441</sup> N. Hadei, E. A. B. Kantchev, C. J. O'Brien, M. G. Organ, *Org. Lett.*, 2005, 7, 3805–3807.

<sup>442</sup> C. Valente, M. E. Belowich, N. Hadei, M. G. Organ, *Eur. J. Org. Chem.*, 2010, 4343–4354.

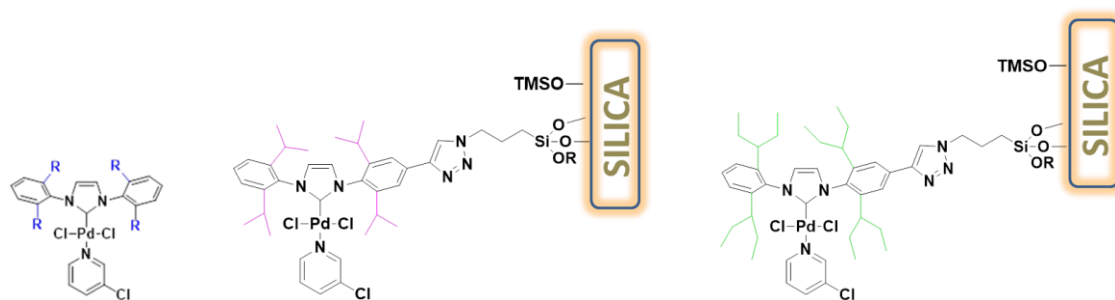
<sup>443</sup> J. L. Farmer, M. Pompeo, A. J. Lough, M. G. Organ, *Chem. – Eur. J.*, 2014, 20, 15790–15798.

<sup>444</sup> S. Sharif, R. P. Rucker, N. Chandrasoma, D. Mitchell, M. J. Rodriguez, R. D. J. Froese, M. G. Organ, *Angew. Chem. Int. Ed.*, 2015, 54, 9507–9511.

<sup>445</sup> K. Mennecke, A. Kirschning, *Synthesis*, 2008, 3267–3272.

<sup>446</sup> V. V. Rostovtsev, L. G. Green, V. V. Fokin, K. B. Sharpless, *Angew. Chem. Int. Ed.*, 2002, 41, 2596–2599.

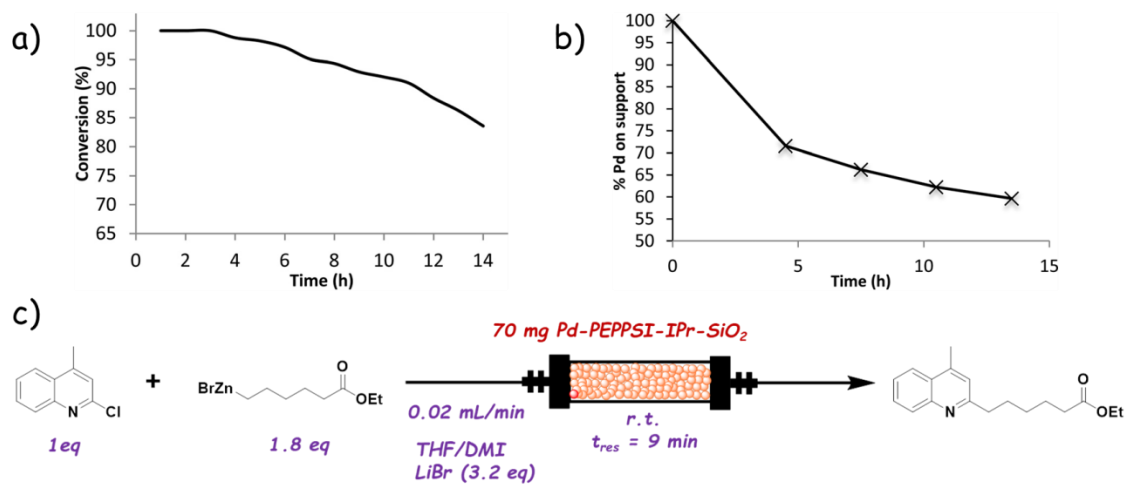
In the case of non-commercially-available organozinc compounds, the telescopic flow process with the in-line preparation clearly shows to be more advantageous. With the Pd-PEPPSI-IPr-SiO<sub>2</sub> (70-350 mg) catalyst in a packed bed reactor, sixteen different Negishi products were obtained with yields from 23 to 95% at room temperature and flow rates from 0.02 to 0.05 mL/min (residence times from 35 to 10 minutes). However, stability studies showed that quantitative palladium leaching occurs and conversion starts to decrease in a couple of hours when the process is maintained in time (see Figure 1.36). Moreover, when secondary alkyl organozinc reagents were used, a preference for the non-desired rearranged product was observed. The heterobiaryl cross-coupling Negishi reaction was also pursued and problems appeared again with the Pd-PEPPSI-IPr-SiO<sub>2</sub> giving the undesired homocoupled product.



**Figure 1.35.** Left: general structure of PEPPSI catalysts. Center: supported Pd-PEPPSI-IPr-SiO<sub>2</sub> developed by M. G. Organ and co-workers.<sup>439</sup> Right: supported Pd-PEPPSI-IPent-SiO<sub>2</sub> developed by M. G. Organ and co-workers.<sup>440</sup>

In the light of these results, Pd-PEPPSI-IPent-SiO<sub>2</sub> was developed and better results achieved. Four heterobiaryl Negishi cross-couplings products were obtained with yields between 60 and 99%. Moreover, with this catalyst the system remained stable for 12 hours (with flow rates of 0.06 mL/min or lower) and no important leaching is observed.

These favourable Pd-PEPPSI catalysts may also be immobilised in SILLPs with the intention to develop catalytic flow systems more stable and able to transform a wider scope of substrates.



**Figure 1.36.** a) Long-term stability study b) Leaching study c) Scheme of the continuous flow Negishi setup employed to study the stability and leaching of the catalyst Pd-PEPPSI-IPr-SiO<sub>2</sub> by M. G. Organ and co-workers.<sup>439</sup>





# **General Objectives**

## **CHAPTER 2**



## Chapter 2. GENERAL OBJECTIVES

The aim of the thesis here presented is the design and development of new continuous flow systems for multicatalytic processes with potential applications in the synthesis of key building blocks such as cyanohydrins or  $\alpha$ -aminonitriles, especially for pharmaceuticals and fine chemicals. Among the heterogeneous catalysts studied, supported ionic liquids have played a key role due to their physico-chemical and catalytic properties and the wide range of possibilities they offer due to their tunability.

Designing and developing the corresponding flow processes as close as possible to the Green Chemistry principles has been a key element in this regard.

In this context, the general objectives considered for the current PhD work were as follows:

- A. Optimise the green parameters in each continuous flow process implemented. Design and develop processes with lower E factors compared with the existent ones based on:
  - i. High atom economy chemical transformations.
  - ii. Efficient immobilised catalysts based on SILLPs tunability and catalytic properties. Long-term stability and reusability of the catalysts as a key factor.
  - iii. Implementation of solventless processes. If not possible (for example with solid products in continuous flow), neoteric solvents will be studied.
- B. Designing, synthesising and characterising a variety of SILLPs and SILLP-based immobilised catalysts and evaluate their properties as catalysts for three important C-C bond forming reactions such as cyanosilylation, Strecker and Negishi cross coupling.
- C. Implement the use of different continuous flow equipments, techniques and strategies. For example including stop-flow stages or supercritical CO<sub>2</sub> continuous flow extractions.

- D. Development of efficient and long-time stable individual and telescoped multistep continuous flow syntheses. In some instances, attention was to be paid to the scope of products achievable.
- E. Assembly different individual continuous flow procedures to implement a divergent telescopic multistep complex system able to produce molecules with wide structural diversity (see Figure 2.1).

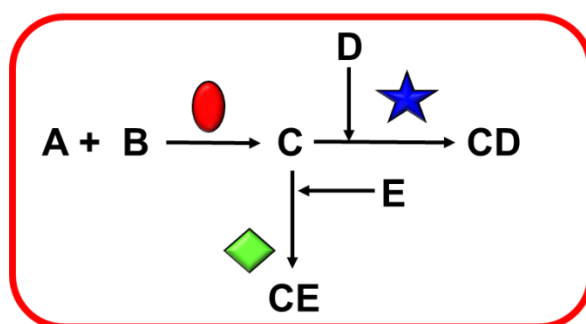


Figure 2.1. Scheme of a catalytic divergent synthesis

- F. Combine organocatalysts, organometallic catalysts and biocatalysts in a multistep catalytic continuous flow process assisted by the compartmentalisation of catalysts in sequential flow stages.
- G. Contribute to the understanding and solving of unresolved problems of continuous flow chemistry, including leaching of immobilised catalysts or the blockage of the flow systems.
- H. Study the possibilities of new additive manufacturing technologies for the development of new continuous flow catalytic reactors.

More concise objectives can be defined as follows:

- 1) Design and development of an efficient and stable continuous flow process for the cyanosilylation of carbonyl compounds based on SILLPs.
- 2) Development of a sustainable, efficient and long-term stable telescoped multi-step continuous flow procedure for the obtaining of valuable chiral cyanohydrins.

- 3) Design and development of an efficient and stable continuous flow process for the three-component Strecker reaction of carbonyl compounds, especially being of application for less reactive aliphatic ketones, which had not been described in the literature until now.
- 4) Combine cyanosilylation and Strecker flow procedures to achieve a unique complex divergent telescoped continuous process able to synthesise both valuable cyanohydrins and  $\alpha$ -aminonitriles. A previous isomerisation of allylic alcohols to ketones coupled in flow could provide a broader range of substrates.
- 5) Study and understand the effects of SILLPs over Pd immobilised catalysts for Negishi cross coupling reactions. SILLPs properties as support, NHC-carbene ligands or scavengers will be evaluated and long-term stable continuous flow procedures are aimed.
- 6) Development of 3D printing continuous flow bioreactors with proved catalytic activity.

Different chapters summarise the efforts done for the implementation of continuous flow multicatalytic processes for the reactions studied. The following points resume the general methodology employed:

- i) Design and synthesis of immobilised catalysts.
- ii) Test the different catalysts in a batch model reaction and conditions optimisation.
- iii) Choose and design the most appropriate continuous flow system.
- iv) Test the catalyst in continuous flow conditions.



**Supported ionic liquid-like  
phases as organocatalysts for the  
solvent-free cyanosilylation of  
carbonyl compounds: from batch  
to continuous flow process**

**CHAPTER 3**



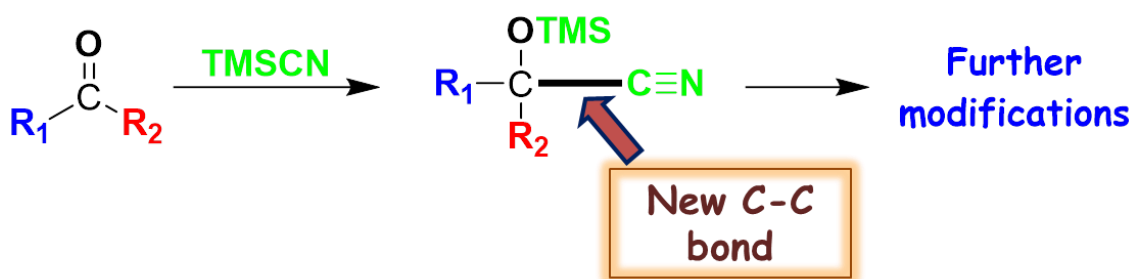


## Chapter 3. Supported ionic liquid-like phases as organocatalysts for the solvent-free cyanosilylation of carbonyl compounds: from batch to continuous flow process.

### 3.1 RESUMEN DEL MANUSCRITO

En este capítulo se estudia el desarrollo de sistemas órgano-catalíticos basados en SILLPs (Supported Ionic Liquid-like Phases) para llevar a cabo reacciones de cianosililación de compuestos carbonílicos empleando condiciones de flujo continuo.

La reacción de cianosililación se encuentra entre las estrategias más importantes para la formación de enlaces C-C en síntesis orgánica, ya que nos permite crear un nuevo enlace C-C entre el carbono carbonílico y el grupo nitrilo (Figura 3.1). Además, el nitrilo puede ser modificado posteriormente para dar lugar a otras funcionalidades de interés.



**Figura 3.1. Formación del nuevo enlace C-C en la reacción de cianosililación de compuestos carbonílicos**

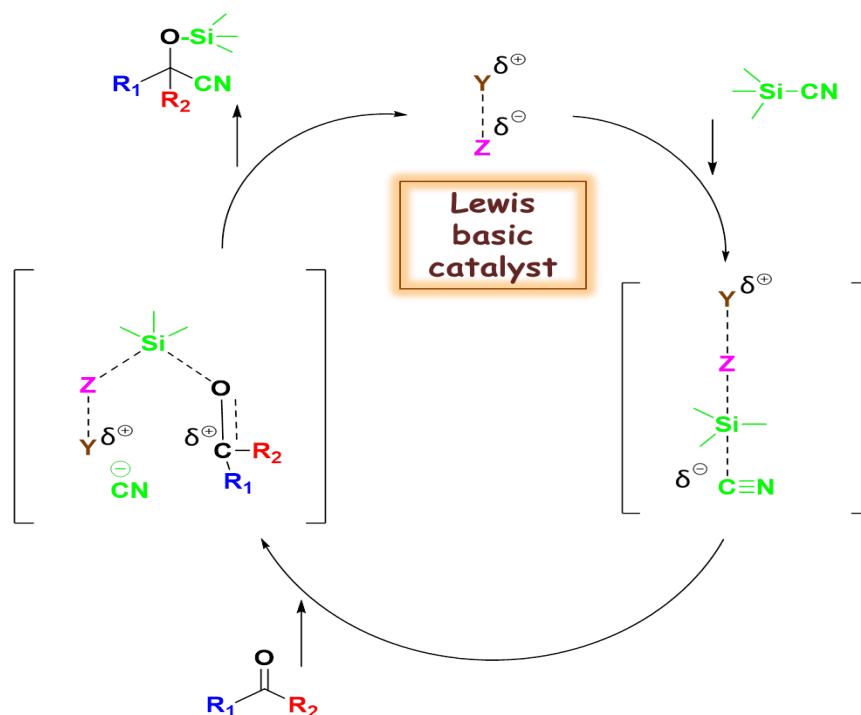
Las cianohidrinás presentan un gran interés industrial ya que son intermedios clave en la síntesis de moléculas de alto valor añadido como pueden ser los  $\alpha$ -hidroxiácidos,  $\alpha$ -hidroxialdehidos,  $\beta$ -aminoalcoholes,  $\alpha$ -hidroxicetonas,  $\beta$ -hidroxiaminas primarias y secundarias,  $\alpha$ -aminonitrilos, 2-hidroxiésteres,  $\alpha$ -sulfoniloxinitrilos,  $\alpha$ -fluoronitrilos, 3-amino-2-trimetilsililoxi-2-alquenoatos, piperidinas 2,3-disustituidas o azacicloalcan-3-oles, así como  $\alpha$ -cetoésteres y acil nitrilos, además de otros compuestos biológicamente activos. Por tanto, podemos decir que

la cianosililación de compuestos carbonílicos es una transformación sintética altamente versátil, lo que le confiere un gran interés.

Entre los diferentes reactivos comúnmente utilizados en las reacciones de cianosililación, como fuente de  $-CN$ , podemos destacar el empleo de  $HCN$ ,  $NaCN$  o  $KCN$  entre otros. Estos presentan una serie de desventajas importantes en comparación con el empleo de trimetilsilil cianuro (TMSCN). En primer lugar, considerando el riesgo inherente a cualquier fuente de cianuro, el trimetilsilil cianuro es más seguro y fácil de manejar que otras alternativas, sin que deba desdeñarse, por ello, la precaución que hay que tener en su manejo. Químicamente, los nucleófilos de trimetilsililo ( $Me_3SiNu$ ), con átomos de silicio unidos a carbono, nitrógeno, oxígeno o azufre, son alternativas eficientes a los nucleófilos protonados ( $HNu$ ) para las reacciones de adición nucleofila a aldehídos y cetonas. Esto se debe a las propiedades del átomo de silicio, que permiten la formación de especies nucleofílicas activas en condiciones más suaves que las empleadas para las fuentes de tipo  $HNu$ . La activación de ambos tipos de nucleófilos requiere de la presencia de bases de Lewis. Así, las especies  $HNu$  requieren, en general, de la presencia de una base fuerte, cosa que puede resultar incompatible con las condiciones de reacción o con algún grupo funcional presente en la molécula. En cambio, la desililación y activación del nucleófilo, en el caso  $Me_3SiNu$ , ocurre en condiciones suaves debido a la afinidad del silicio por átomos de oxígeno o flúor.

Además, el uso de TMSCN nos proporciona una reacción con un 100% de economía atómica siendo una transformación sintética altamente eficiente, donde todos los átomos de los reactivos forman parte del producto final. La elevada economía atómica viene enunciada en el segundo principio de la Química Verde; principios que van a estar presentes durante el completo desarrollo de esta tesis. El cumplimiento, aplicación y desarrollo de estrategias que observen los principios de la Química Sostenible es el principal objetivo transversal de este compendio de trabajos.

Como ya hemos apuntado, el uso de TMSCN en reacciones de cianosililación requiere de una activación catalítica. Tradicionalmente se han empleado sistemas organometálicos con propiedades como ácidos de Lewis que realizan la activación mediante complejación con los grupos carbonilo del sustrato y el grupo nitrilo del TMSCN. Sin embargo, también los sistemas organocatalíticos con propiedades de ácidos o bases de Lewis proporcionan la activación del TMSCN, lo que permite evitar el uso de especies metálicas (Figura 3.2).



**Figura 3.2. Mecanismo de activación del TMSCN mediante una base de Lewis en la reacción de cianosililación de aldehídos y cetonas.**

Entre los diferentes organocatalizadores que permiten una activación suave del TMSCN se encuentran los Líquidos Iónicos (ILs). Esto se debe a la naturaleza del líquido iónico, donde el anión y el catión poseen propiedades de base y de ácido de Lewis, respectivamente, que pueden inducir mecanismos de doble activación. Así, se ha descrito el empleo de ILs como medio de reacción y catalizador para llevar a cabo la adición de TMSCN a compuestos carbonílicos en condiciones suaves de reacción.

Las propiedades de los ILs pueden ser transferidas a un soporte sólido mediante la síntesis de materiales tipo SILLP (Supported Ionic Liquid-Like Phases), en cuyo desarrollo y aplicaciones se ha trabajado recientemente en nuestro grupo. Esta estrategia permite combinar las ventajas de los ILs con las del soporte polimérico: i) reduciendo la cantidad de IL empleada, ii) facilitando la separación y reciclado del catalizador, iii) aumentando la estabilidad del catalizador, iv) mejorando la actividad y selectividad del catalizador, v) facilitando el desarrollo de procesos en condiciones de flujo continuo.

Otra propiedad que dota de gran interés catalítico a los SILLPs es su gran modularidad, que permite adaptarse a las necesidades de diferentes reacciones. Los SILLPs pueden ser modificados mediante diferentes elementos estructurales (Figura 3.3) como son: i) naturaleza

del anión y el catión, ii) la sustitución del catión y iii) la naturaleza del soporte polimérico.

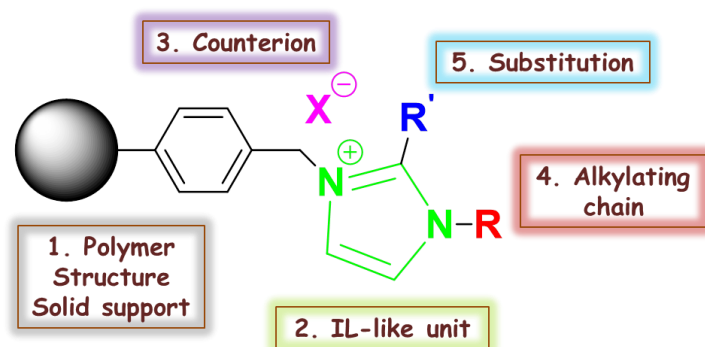


Figura 3.3. Partes que conforman el SILLP y que pueden ser modificadas

La hipótesis de trabajo fue que si las características ácido-base de Lewis de los ILs siguen presentes en los SILLPs, éstos podrán actuar como catalizadores activando el TMS-CN para su reacción con aldehídos y cetonas. La figura 3.4 presenta el posible mecanismo de la reacción de cianosililación catalizada por SILLPs.

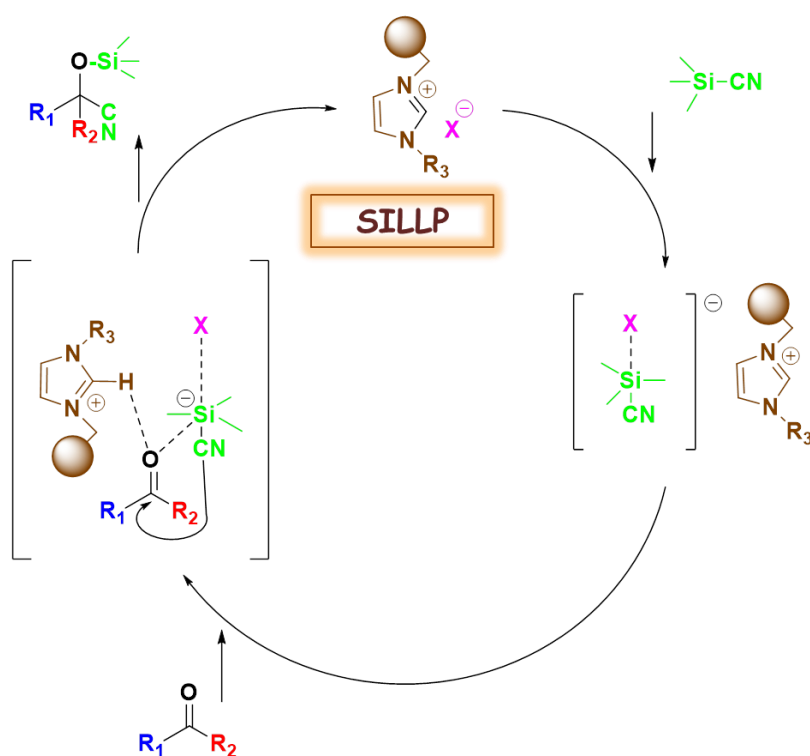


Figura 3.4. Mecanismo propuesto de activación del TMS-CN mediante un catalizador tipo SILLP en la reacción de cianosililación de aldehídos y cetonas.

La reacción de cianosililación entre acetofenona (**14**) y TMSCN (**15**) es la reacción modelo elegida para este estudio (Figura 3.5).

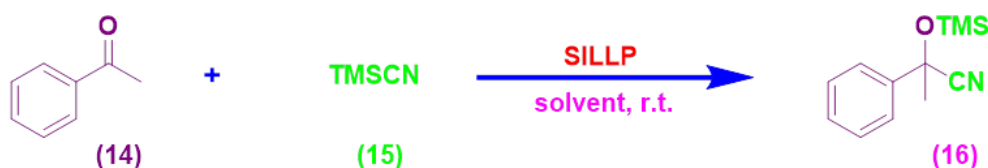


Figura 3.5. Reacción de cianosililación modelo estudiada

Los SILLPs evaluados como catalizadores se obtuvieron por modificación química de diferentes resinas de estireno-divinilbenceno (PS-DVB) de tipo Merrifield con diferentes alquil-imidazoles como agentes alquilantes mediante métodos previamente implementados y descritos en nuestro grupo. Las resinas empleadas presentan diferentes grados de entrecruzamiento, lo que las diferencia entre microporosas (o tipo gel, bajo entrecruzamiento, 2% DVB) y macroporosas (alto entrecruzamiento), así como diferentes cargas de cloruro (1.2 mmol Cl/g, 2.1 mmol Cl/g ó 4.3 mmol Cl/g) lo que permitió obtener una familia de SILLPs con una apreciable variabilidad estructural (Figura 3.6).

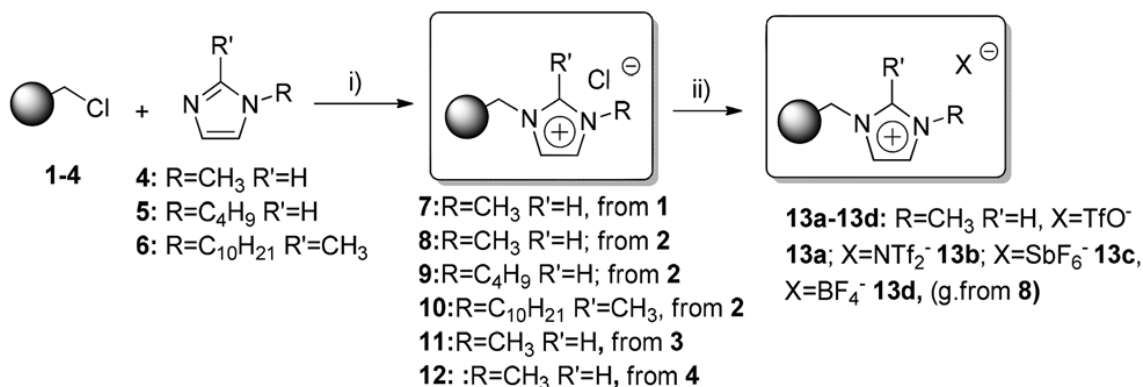


Figura 3.6. Diferentes SILLPs sintetizados. **1:** resina microporosa, 1.2 mmol Cl/g; **2:** resina microporosa, 2.1 mmol Cl/g; **3:** resina microporosa, 4.3 mmol Cl/g y **4:** resina macroporosa, 1.2 mmol Cl/g.

En primer lugar se evaluó la reacción en discontinuo (batch), a temperatura ambiente, sin disolvente y con diferentes disolventes, empleando como catalizador el SILLP-**7**. El mejor resultado se obtuvo en ausencia de disolvente con un 92% de rendimiento en 24 horas

comparado con el 81% obtenido con el mejor disolvente (acetonitrilo). Además, el SILLP-7 es capaz de catalizar también la cianosililación, a temperatura ambiente y sin disolvente, de diferentes benzaldehídos sustituidos así como un aldehído alifático y una cetona cíclica. Estos resultados iniciales demuestran la idoneidad de los SILLPs para catalizar la cianosililación de diferentes compuestos carbonílicos a temperatura ambiente y en ausencia de disolvente, dos aspectos de gran relevancia para obtener un proceso sostenible desde el punto de vista químico. A continuación, se estudió el efecto de las posibles variaciones estructurales de los SILLPs sobre su eficiencia catalítica en la reacción de cianosililación estudiada:

- ❖ Carga de unidades tipo IL: Los SILLPs con cargas intermedias de grupos imidazolio en el polímero (2.1 mmol Cl/g) mostraron mayor eficiencia a tiempos cortos (2h) mientras que a tiempos largos no se observa diferencia.
- ❖ Sustitución del catión imidazolio: La mayor actividad catalítica se obtuvo con el grupo metilo (-CH<sub>3</sub>) (**8**) como N-sustituyente, frente a los resultados obtenidos cuando se usaban los grupos butilo (- (CH<sub>2</sub>)<sub>3</sub>-CH<sub>3</sub>) (**9**) o decilo (- (CH<sub>2</sub>)<sub>9</sub>-CH<sub>3</sub>) (**10**), para resinas de tipo gel y carga intermedia (2.1 mmol Cl/g).
- ❖ Contraión: Los aniones que son bases de Lewis fuertes (Cl<sup>-</sup> y TfO<sup>-</sup>) mostraron una mayor actividad catalítica que aquellos que son bases de Lewis más débiles (NTf<sub>2</sub><sup>-</sup>, BF<sub>4</sub><sup>-</sup> y SbF<sub>6</sub><sup>-</sup>) siguiendo la tendencia Cl<sup>-</sup> >> TfO<sup>-</sup> > NTf<sub>2</sub><sup>-</sup> >> BF<sub>4</sub><sup>-</sup> > SbF<sub>6</sub><sup>-</sup>. Estos datos concuerdan con el mecanismo propuesto en la Figura 3.4 donde el anión se coordina con el átomo de silicio, formando una especie más reactiva que al mismo tiempo es estabilizada por el catión imidazolio mediante interacciones débiles como puentes de hidrógeno o fuerzas de Van der Waals.

También se evaluó el posible reciclado del catalizador viendo que el SILLP-7 es capaz de catalizar diversos ciclos consecutivos de la reacción sin perder actividad. Por tanto, es un catalizador suficientemente estable para ser llevado a condiciones de flujo continuo. Además, los problemas derivados de la falta de estabilidad mecánica del catalizador tipo SILLP al agitarlo en batch, desaparecen con su uso en continuo. Para ello se desarrolló un sistema simple formado por una bomba de HPLC, un mini reactor de lecho fijo lleno con el SILLP y un equipo de ATR-FTIR acoplado en continuo para monitorizar la reacción.

La reacción modelo en flujo continuo proporcionó excelentes rendimientos (>90%), una vez se alcanzó un régimen estacionario tras un periodo de inducción inicial, aparentemente debido al llenado del sistema (bomba, conducto de entrada y volumen muerto del reactor). Estos rendimientos se mantuvieron al incrementar el flujo de 0.1 a 0.5 mL/min.

Además, se evaluó el efecto de la morfología del catalizador (microporoso, macroporoso o monolítico) en la eficiencia del proceso en condiciones de flujo. La difusión de los reactivos y productos es altamente dependiente de la morfología del catalizador soportado. Así, la difusión de los reactivos y productos en los catalizadores soportados basados en resinas microporosas es altamente dependiente del hinchamiento (“swelling”) en el disolvente correspondiente. Para que se produzca un hinchado adecuado, que influirá en la accesibilidad de los sitios catalíticos, es necesario que el disolvente o la combinación de reactivos sea compatible con la naturaleza del soporte polimérico del catalizador. En cambio, los polímeros macroporosos presentan una porosidad fija que no depende de los disolventes ni los reactivos, por lo que la difusión dependerá del poro que presenta el polímero. Por último, se preparó también un minireactor monolítico polimerizando en un reactor tubular una mezcla de 4-clorovinilbenceno y divinilbenceno en presencia de un porógeno, modificando posteriormente los grupos clorometilo con metilimidazol y obteniendo una estructura análoga a los SILLPs micro (**7**) y macroporoso (**12**), ambos con metilo como sustituyente en el imidazol, y con una baja carga de grupos clorometilo en la resina inicial (1.2 mmol Cl/g).

Los resultados obtenidos en flujo fueron excelentes y similares con los SILLPs micro y macroporoso, con la única diferencia de un mayor tiempo de inducción inicial necesario para el SILLP macroporoso (**12**) debido a un mayor volumen muerto del reactor. En cambio, los peores resultados se obtuvieron con el mini reactor monolítico, necesitando flujos más bajos para obtener rendimientos aceptables.

Por lo que respecta a la estabilidad del sistema a largo plazo, con el SILLP-**7** tipo gel se consiguió un sistema en continuo, activo y estable durante al menos 48 horas a 0.01 mL/min sin pérdida de actividad.

Finalmente, el sistema desarrollado se comparó, en términos de productividad y factor E, con otras cianosililaciones recientes descritas en la literatura y que presentaran alguno de los elementos utilizados en nuestro sistema: líquidos iónicos, (organo)catalisis, ausencia de disolventes y química en flujo. Ninguno de los procesos estudiados

presenta un factor E inferior al aquí desarrollado y sólo alcanza una productividad mayor el que emplea  $\text{Sc}(\text{OTf})_3$  como catalizador en  $[\text{BMIM}][\text{SbF}_6]$ .

Podemos decir que el proceso desarrollado enriquece la metodología existente para reacciones de cianosililación y se ajusta perfectamente a los preceptos de la Química Verde: 100% de economía atómica, no se producen residuos, no se emplea disolvente, la actividad y la estabilidad catalítica son excelentes y el empleo de sistemas de flujo continuo permite una fácil separación del catalizador y del producto. Esto se consigue gracias al empleo de SILLPs y al adecuado diseño de un proceso en continuo.



## Supported ionic liquid-like phases as organocatalysts for the solvent-free cyanosilylation of carbonyl compounds: from batch to continuous flow process†

Cite this: *Green Chem.*, 2014, **16**, 1639

Sergio Martín, Raúl Porcar, Edgar Peris, María Isabel Burguete, Eduardo García-Verdugo\* and Santiago V. Luis\*

Received 30th October 2013,  
Accepted 20th December 2013

DOI: 10.1039/c3gc42238k

www.rsc.org/greenchem

Supported ionic liquid-like phases (SILLPs) are able to efficiently catalyse the cyanosilylation of carbonyl compounds using trimethylsilyl cyanide under solvent-free conditions. These organic catalysts were efficient for various carbonyl compounds including aromatic, aliphatic and  $\alpha,\beta$ -unsaturated. This process perfectly conforms to the features of green chemistry: no waste regarding side-products and unconverted reactants, solvent-free, excellent catalytic activity, and no requirement for separation. Furthermore the supported nature of the SILLPs allows for the development of continuous flow synthesis of cyanohydrin trimethylsilyl ethers. The effect of the morphology of the polymer (gel-type or macroporous bead resins or, alternatively, a monolithic polymer) has also been studied, which has allowed selecting suitable materials for the efficient continuous flow single pass synthesis of cyanohydrin trimethylsilyl ethers.

### Introduction

Hydrocyanation and cyanosilylation of carbonyl compounds are among the most important strategies for C–C bond-forming reactions in organic synthesis as, for instance, cyanohydrin trimethylsilyl ethers are industrially valuable and important intermediates for the synthesis of many valuable molecules such as  $\alpha$ -hydroxy acids,  $\alpha$ -hydroxy aldehydes and  $\beta$ -amino alcohols and other biologically active compounds.<sup>1,2</sup>

Although there are different methods for the preparation of trialkylsilyl cyanides, the addition to carbonyl compounds of trimethylsilyl cyanide (TMSCN), which is a safe and easily handled reagent compared to HCN, NaCN or KCN,<sup>3</sup> allows obtaining silyl protected products in high yields and readily accessible for further manipulations.<sup>4</sup> However, the use of silyl cyanides requires catalytic activation by an organometallic or organocatalytic system. Thus, the traditional organometallic systems (Lewis acid catalysts) are based on the complexation of a metal to both the carbonyl group and the cyano group of TMSCN.<sup>5,6</sup> However, the organocatalytic systems (Lewis basic catalysts) often react with the silicon atom of TMSCN to produce more reactive hypercoordinated silicon intermediates.

The use of ionic liquids (ILs) has been demonstrated to be an efficient and environmentally friendly reaction media as well as a promoter for the cyanosilylation of aldehydes under mild conditions without the need for a Lewis acid (or base) or any other special activation.<sup>7</sup> The presence of catalytic amounts of lanthanide triflates, particularly scandium triflate, in the ILs increased largely their catalytic efficiency in terms of the resulting turnover frequency and total turnover number.<sup>8</sup>

In the last few years, we have focused our efforts on the development of the so-called supported ionic liquid-like phases (SILLPs) prepared by the immobilization of molecules with IL-like structures onto solid supports (Fig. 1). These advanced materials allow to transfer the IL properties to the solid phase leading to either monolithic or gel supported ionic liquid-like phases (m- or g-SILLPs) sharing, therefore, the properties of true ILs and the advantages of a solid support.<sup>9</sup> Catalytic processes based on the use of SILLPs allow (i) to

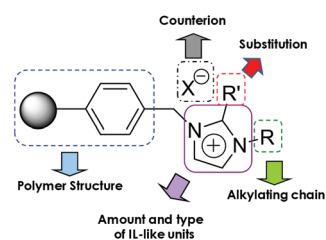


Fig. 1 Design vectors used to fine-tune the organocatalytic properties of supported ionic liquid-like phases (SILLPs).

Departamento de Química Inorgánica y Orgánica, Universidad Jaume I, Av. Sos Baynat s/n, 12071 Castellón, Spain. E-mail: luiss@uji.es, cepeda@uji.es

†Electronic supplementary information (ESI) available: GC methods and <sup>1</sup>H NMR spectra of the products Table 2 and calculation Table 4. See DOI: 10.1039/c3gc42238k

minimize the amount of ILs used, (ii) easy separation and recyclability and (iii) to develop mini-flow reactors for continuous processes using either conventional solvents or supercritical fluids (scFs).<sup>10</sup> Thus, a wide range of polymer-supported ionic liquid-like phases (SILLPs) or “solid ionic solvents” with tunable properties can be easily prepared in order to (1) generate novel (bio)catalytic species, (2) improve the stability of the (bio)catalyst, (3) optimize immobilization and recyclability, (4) assist in the activation of the (bio)catalyst, (5) facilitate product isolation, and (6) influence the selectivity of the reaction, which are some of the essential roles of conventional solvents.

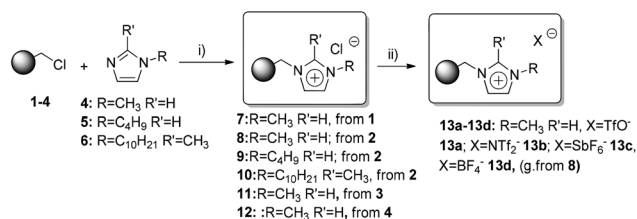
Taking this into account, supported ionic liquid-like materials (SILLPs) offer good potential as substitutes of bulk ILs for the cyanosilylation reaction, and here we report our efforts towards this goal. The process has been carried out by the smooth addition of TMSCN to carbonyl compounds using polymeric SILLPs as new bifunctional organocatalysts, under different batch conditions and, preferentially, under continuous flow solvent-free conditions.

## Results and discussion

Different PS-DVB polymers containing alkylimidazolium chloride subunits (7–12) were prepared from commercially available Merrifield resins having different chloride loadings and crosslinking degrees as previously reported by us.<sup>11</sup> Initially, gel-type microporous chloromethylated resins (1–3) in the form of beads, bearing a low crosslinking degree (2% DVB) and with chloride loadings ranging from 1.2 to 4.3 mmol Cl g<sup>-1</sup> were used. The synthetic protocol for the preparation of the SILLPs has been previously optimized by our group and has been described in detail, allowing a quantitative transformation of the chloromethylated fragments into alkyl benzyl imidazolium groups as is shown in Scheme 1.<sup>12</sup>

The cyanosilylation reaction between acetophenone (13) and TMSCN (14) was selected as the benchmark reaction, as, in general, most of the reported methods for the cyanosilylation of carbonyl compounds are largely limited to aldehydes as well as to the more reactive aliphatic ketones.

First, the role of the solvent was studied by carrying out the reaction either under solvent-free conditions or in a range of solvents from a non-polar one, such as CH<sub>2</sub>Cl<sub>2</sub>, to polar ones



**Scheme 1** Synthesis of SILLPs: (i) alkylimidazole, 90 °C; (ii) NaX or HX, H<sub>2</sub>O. **1–3** resins are microporous beads with 2% crosslinking, **1** (1.2 mmol Cl g<sup>-1</sup>), **2** (2.1 mmol Cl g<sup>-1</sup>) and **3** (4.3 mmol Cl g<sup>-1</sup>); **4** macroporous resin (1.2 mmol Cl g<sup>-1</sup>).

**Table 1** Effect of the solvent in the cyanosilylation reaction between (14) and (15) catalysed by SILLP-7 at r.t. and 24 hours of reaction time<sup>a</sup>

Entry	Solvent	Yield <sup>b</sup> (%)	TON
1	CH <sub>2</sub> Cl <sub>2</sub>	64	29
2	Acetonitrile	81	37
3	2-MeTHF	29	13
4	H <sub>2</sub> O	0	0
5	MeOH	0	0
6	—	92	41
7 <sup>c</sup>	—	20	—

<sup>a</sup> 75 mg of SILLP 7, 3 mmol of acetophenone, 3.6 mmol of TMSCN and 5 mL of solvent, stirring at room temperature during 24 hours.

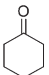
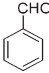
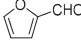
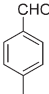
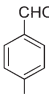
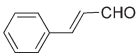
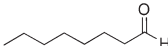
<sup>b</sup> Calculated by GC. <sup>c</sup> Reaction in the absence of catalyst.

like MeOH or water. The SILLP-7 (R = CH<sub>3</sub>, R' = H, X = Cl, low loading) was used as the initial catalyst. As shown in Table 1, the cyanosilylation reaction was more efficient under solvent-free conditions than using organic solvents or water. The reaction proceeded smoothly at room temperature to afford the corresponding cyanohydrin in 92% yield under solvent-free conditions (Table 1, entry 6). It should be noted that the reaction only led to low yields (20% yield) in the absence of the SILLP-7. Regarding the use of solvents, both MeOH and water led to non-conversion of the carbonyl compound. Low to modest yields were obtained when either CH<sub>2</sub>Cl<sub>2</sub> or 2-MeTHF was used (Table 1, entries 1 and 3). The best solvent was clearly acetonitrile, leading to 81% yield (Table 1, entry 2). In view of these results, various aldehydes and ketones were tested under solvent-free conditions at room temperature using SILLP-7 as the catalyst to evaluate the general applicability of this protocol. All the results are summarized in Table 2.

The SILLP-7 was able to catalyse the solvent-free cyanosilylation for substituted and unsubstituted benzaldehydes (Table 2, entries 2–5) with similar results to those found for acetophenone. Excellent yields of the corresponding products were obtained, almost in pure form, without any additional purification step except the catalyst filtering. In addition, a cyclic ketone and an open chain aliphatic aldehyde (Table 2, entries 1 and 7) were also converted into the corresponding TMS-cyanohydrins in good yields. It should also be noted that an aromatic α,β-unsaturated aldehyde also underwent the cyanosilylation reaction efficiently (Table 2, entry 6). These preliminary results suggest that these supported ionic liquid-like phases are quite a promising system to develop simple, efficient, room temperature and solvent free cyanosilylation reactions for different classes of carbonyl compounds.

One of the potential advantages of the use of SILLPs is that, like in the bulk ILs, it is easy to vary several of their structural features (loading of IL-like units, substitution pattern, the nature of the counterion, the type of polymeric backbone, *etc.*) to fine-tune their physical and chemical properties. These changes may have a big impact on the catalytic properties of the SILLPs as organocatalysts for the cyanosilylation reaction as we have already demonstrated to apply for other (bio)catalytic systems.<sup>9,10,13</sup> Hence, we studied the effects of some of

**Table 2** Cyanosilylation of various carbonyl compounds under solvent-free conditions catalysed by SILLP-7 at r.t. and 24 hours<sup>a</sup>

Entry	Reagent	Conv. <sup>b,c</sup> (%)
1		>99
2		>99
3		>99
4		99
5		>99
6		99
7		>99

<sup>a</sup> 75 mg of SILLP 7, 3 mmol of carbonyl compound and 3.6 mmol of TMSCN, stirring at room temperature during 24 hours. <sup>b</sup> Calculated by GC. <sup>c</sup> A single product corresponding to the one expected for the cyanosilylation reaction was detected by <sup>1</sup>H NMR of the crude of the reaction.

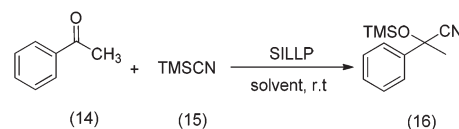
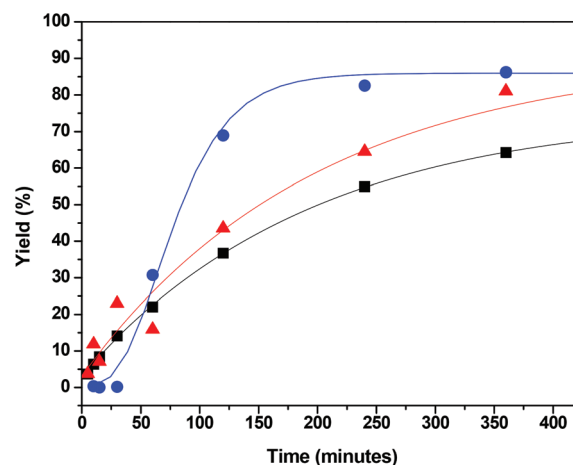
these structural variables on the catalytic efficiency for the solvent free reaction between acetophenone and TMSCN.

First, the effect of the loading of the IL-like moieties in the polymeric backbone was tested. At long reaction times (24 hours) all the catalysts showed very good yields (*ca.* 90%) independent of the SILLP-loading. However, the catalytic efficiency of the SILLP measured in moles of products converted per unit of time and mole of catalyst, before completion of the reaction, was quite loading dependent. Indeed, when the same amount of solid catalysts was used, the most efficient SILLP was the one having a medium loading of imidazolium groups (SILLP-11, 40% IL-like units by weight) showing a TOF = 7.7 (mol 15 per mol cat h) calculated at two hours of reaction time, while the SILLP with higher (SILLP-8, 63% IL-like units by weight) and lower (SILLP-7, 18% IL-like units by weight) amounts of functionality only presented a catalytic efficiency (TOF) of 4.6 and 2.3 respectively. Most likely, this effect of the loading can be associated with the accessibility to the catalytic sites inside the polymeric beads. This can be difficult for low loadings, because of the formation of polar/apolar domains in the resin, but also in the resins containing a high degree of IL-like functionalization, where the IL-fragments can be strongly associated through the formation of anion-cation supramolecular structures.

Another factor that can be used to tune the catalytic activity of the SILLPs is the substitution pattern of the imidazole

moiety that can be achieved through the use of different alkyl residues (R and R'). Thus, three different SILLPs (SILLP-8, SILLP-9 and SILLP-10) were synthesized from the same starting Merrifield resin. Therefore, three different resins having the same loading (high loading) but a different substitution pattern (R = CH<sub>3</sub>- and R' = H- (SILLP-8); R = CH<sub>3</sub>-(CH<sub>2</sub>)<sub>3</sub>- and R' = H (SILLP-9) and R = CH<sub>3</sub>-(CH<sub>2</sub>)<sub>9</sub>- and R' = CH<sub>3</sub>- (SILLP-10)) were evaluated as catalysts for the benchmark cyanosilylation reaction (Scheme 2). In all the cases, the SILLPs were active to catalyze the reaction. However, the time-course profiles of the product yield (see Fig. 2) present significant differences for each of the SILLPs. Thus, the SILLP-8 was the more active one, reaching an 85% yield in *ca.* six hours, while the presence of a longer alkyl chain at the imidazolium ring led to a reduction of the catalytic efficiency.

It is noteworthy that the SILLP-8 containing the smaller substituents showed some induction time, which is not noticeable for the other SILLPs. Most likely, this observation must be related to the highly hydrophilic character of SILLP-8 that makes this resin rather hygroscopic. The observed induction time should be related to the larger amount of residual water present in this case in the polymer and that can interfere with the reaction of interest, by reacting with TMSCN instead of the chloride anion (the first step of the catalytic cycle). Indeed, the water content for these SILLPs varied from *ca.* 11% for the SILLP-8 to a maximum of 6–7% for the more hydrophobic ones SILLP-9 and SILLP-10. As can be observed in Fig. 2, after this induction period the SILLP-8 displayed the best catalytic

**Scheme 2** Cyanosilylation between (14) and (15) organocatalyzed by SILLPs.**Fig. 2** Effect of the substitution pattern of the SILLPs as catalysts for the cyanosilylation reaction between (14) and (15) at r.t. and 24 hours of reaction time. ● R = CH<sub>3</sub> and R' = H (SILLP-8); ▲ R = CH<sub>3</sub>(CH<sub>2</sub>)<sub>3</sub> and R' = H (SILLP-9) and ■ R = CH<sub>3</sub>(CH<sub>2</sub>)<sub>9</sub> and R' = CH<sub>3</sub> (SILLP-10).

behavior. Thus, the exact microenvironment at the imidazolium moiety can have a key influence on the overall catalytic cycle.

Once established that the best results in terms of yield and catalytic efficiency were obtained for the SILLP based on methyl-imidazolium, we decided to study the effect of the counterion. Our previous results have proved that very significant variations in the physico-chemical properties of the SILLPs can be obtained by varying the anion of the ionic-liquid-like moieties grafted onto a polymeric matrix. Therefore, SILLPs bearing five different anions and the same loading of the methyl-imidazolium cation were tested as catalysts for the cyanosilylation reaction. The nature of the anion has a significant effect on the catalytic efficiency as can be appreciated in the time-course profiles of the product yield (Fig. 3). Hence, reactions performed with catalysts based on SILLPs containing the harder Lewis bases as the anions ( $\text{Cl}^-$  and  $\text{TfO}^-$ ) showed a better activity than those with catalysts bearing softer Lewis base anions such as  $\text{NTf}_2^-$ ,  $\text{BF}_4^-$  or  $\text{SbF}_6^-$ . Indeed, the calculated reaction rates change followed the sequence  $\text{Cl}^-$  ( $r = 0.5848 \text{ h}^{-1}$ )  $\gg$   $\text{TfO}^-$  ( $r = 0.0224 \text{ h}^{-1}$ )  $>$   $\text{NTf}_2^-$  ( $r = 0.0417 \text{ h}^{-1}$ )  $\gg$   $\text{BF}_4^-$  ( $r = 0.0065 \text{ h}^{-1}$ )  $>$   $\text{SbF}_6^-$  ( $r = 0.0050 \text{ h}^{-1}$ ) being the enhancement in the reaction rate up to *ca.* 117 folds going from  $\text{SbF}_6^-$  to  $\text{Cl}^-$  (see Fig. 3). According to known mechanistic data, the anion must coordinate to the Si atom to form a more reactive pentacoordinated silicate for the reaction to occur. This binding leads to a polarization of the adjacent bonds, thereby increasing the electron density at the peripheral atoms, activating the  $\text{CN}^-$  to attack the carbonyl group.<sup>14,15</sup> Thus, the presence of a hard Lewis base, for instance the chloride in the SILLP, should facilitate this mechanism of action. On the other hand, in the catalytic cycle, the imidazolium cation may contribute to stabilize the more reactive pentacoordinated silicate through additional weak interactions such as hydrogen bonding, hydrophobic and van der Waals attraction together with ionic interactions with the anion.

The possible recycling of the catalyst was also evaluated. The nature of the support, being a gel type resin, makes it very sensitive to mechanical damage by the abrasion produced by

the magnetic stirring bar. This often hampers an efficient filtration to separate the catalyst from the reagents and products, precluding the practical recycling of the supported catalyst. Therefore, we designed a simple device allowing for a reactive filtration process. The supported-catalyst was maintained in a syringe body with an adequate filter at the top and the bottom of the material, and then the solvent free mixture of the reagents (*ca.* 3 mL) was eluted through the catalytic bed and separated from the solid by simple gravimetric flow (Fig. 4). The contact time of the reagents with the SILLP-7 was long enough to achieve an average product yield of 85% for three consecutive batches of *ca.* 3 mL each. In summary, the SILLP-7 was stable enough to produce *ca.* 15 g of cyanosilylether per gram of catalyst used during three consecutive recycles, without showing any significant decrease in its activity.

The former results also suggest that these catalytic SILLPs can be stable enough as to develop a continuous flow system.<sup>16–18</sup> For this purpose, a simple set-up allowing a forced continuous flow-through process was evaluated.<sup>19</sup> The system was based on a HPLC pump, a fix-bed catalytic reactor and a continuous flow ATR-FTIR cell to facilitate the monitoring and optimisation of the process (see Fig. 5).<sup>20</sup>

A careful analysis of the nature and shape of the catalyst under consideration is always needed for a proper design of the corresponding mini-flow reactors (*mfr*). Indeed, the morphology and shape of the catalyst can lead, in some cases, to significant differences in catalytic performance.<sup>16,21–23</sup> Therefore, for the preparation of mini-flow fix-bed catalytic reactors, we decided to study polymers with different morphologies. First, the use of gel-type lightly crosslinked resins was evaluated for the preparation of the reactor (*mfr*-SILLP-7-gel).<sup>24</sup> This was the type of polymer successfully used for batch experiments. Indeed, both reagents and catalysts based on gel-type resin have been successfully used for different C–C bond formation reactions.<sup>25,26</sup> However, it should be taken into account that these polymers only swell in certain solvents. In the absence of a good swelling, intraparticle diffusion of the

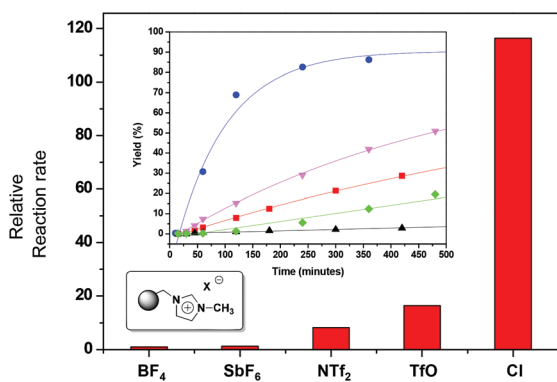


Fig. 3 Effect of the SILLP counterion on the cyanosilylation reaction between (13) and (14) catalysed by SILLP-8 and SILLP-13a–d at r.t. and 24 hours. ● (X = Cl), ▼ (X = TfO), ■ (X = NTf<sub>2</sub>), ◆ (X = SbF<sub>6</sub>), ▲ (X = BF<sub>4</sub>).

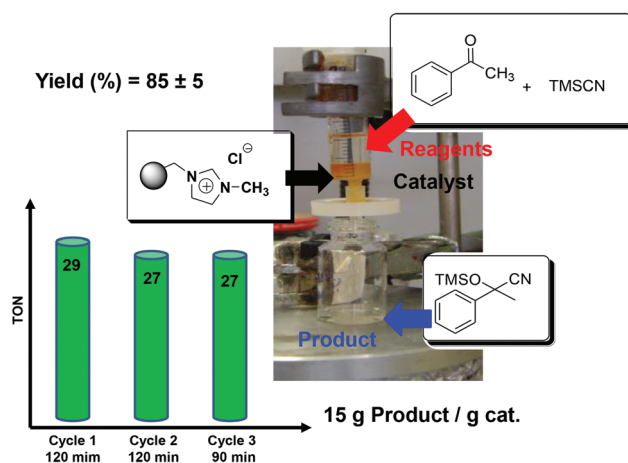
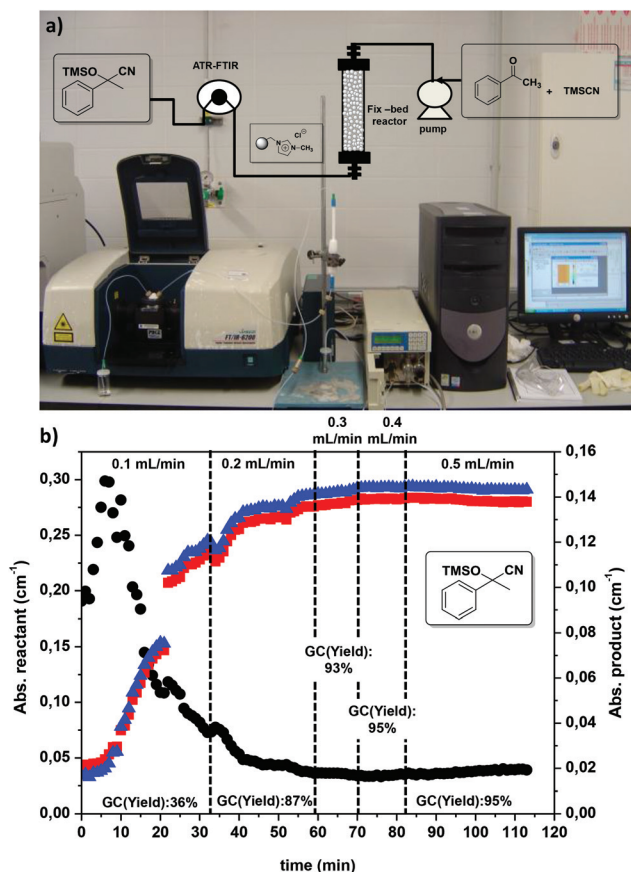


Fig. 4 Recycling of the SILLP-7 for the cyanosilylation reaction between (14) and (15) at r.t. during 24 hours.



**Fig. 5** Continuous flow reactor, including continuous monitoring, for the cyanosilylation reaction between (14) and (15) catalysed by SILLP-7 at r.t. (a) Photo and scheme of the set-up. (b) Evolution with time of the characteristic peaks of both reactant (14) and product (16) for the model cyanosilylation in the mini-flow reactor *mfr*-SILLP-7-g at r.t. and under different flow conditions. ● (C=O at 1768 cm<sup>-1</sup>), ■ (C-OTMS at 1115 cm<sup>-1</sup>), ▲ (Si-O at 995 cm<sup>-1</sup>).

reagents and substrates can be the limiting rate factor. Therefore, suitable swelling conditions are required to allow the flow through the generated internal microchannels of the resin (usually beads).<sup>21,26</sup> Furthermore, the swelling is accompanied by a change in volume that can be very important, thus affecting the packing.<sup>21</sup> In this regard, a regulating device was used to properly adjust the volume of the reactor to that of the swollen resin. In this way, it is feasible to achieve a reproducible flow through systems based on gel-type polymers.<sup>27</sup>

The initial results for the fix-bed reactor (*mfr*-SILLP-7-gel) prepared with the gel-type resin SILLP-7 are depicted in Fig. 5. The continuous monitoring of the effluent by FT-IR allowed a direct analysis of the results for this continuous flow process. The graph in Fig. 5 displays the evolution with time of the characteristic peaks for both the reactant (14) and the product (16). The data show the presence of an important induction time before the stationary regime is reached. Once this is achieved, the flow system can be maintained with the same productivity and high yields without observing any decrease in the activity of the catalyst with time. As a matter of fact, at this

**Table 3** Continuous flow solventless cyanosilylation reaction between 14 and 15 at r.t. using different polymeric materials<sup>a</sup>

Entry	Reactor	Flow mL min <sup>-1</sup>	Yield <sup>b</sup> (%)	Productivity (g 16 per g cat) h <sup>-1 c</sup>
1	<i>mfr</i> -SILLP-7-gel	0.1	99	9.0
2	<i>mfr</i> -SILLP-7-gel	0.3	99	27.1
3	<i>mfr</i> -SILLP-7-gel	0.5	99	45.1
4	<i>mfr</i> -SILLP-12-macro	0.1	99	9.0
5	<i>mfr</i> -SILLP-12-macro	0.3	98	26.8
6	<i>mfr</i> -SILLP-12-macro	0.5	96	43.7
7	<i>mfr</i> -SILLP-17-molth	0.01	95	0.2
8	<i>mfr</i> -SILLP-17-molth	0.03	85	0.3
9	<i>mfr</i> -SILLP-17-molth	0.05	75	0.6

<sup>a</sup> *mfr*-SILLP-7-gel: 600 mg of SILLP-7, 1.01 meq g<sup>-1</sup>; *mfr*-SILLP-12-macro: 600 mg of SILLP-12 1.09 meq g<sup>-1</sup>, *mfr*-SILLP-17-molth: 3.38 g, 3.03 meq g<sup>-1</sup>; 3.67 M of 14 in a mixture of acetophenone-TMSCN 1 : 1 molar. <sup>b</sup> Calculated by GC. <sup>c</sup> Calculated as [flow rate (mL min<sup>-1</sup>) × concentration (mmol mL<sup>-1</sup>) × (yield%/100) × Fw(16) (mg mmol<sup>-1</sup>) × (1/1000)]/[cat. (g) × loading cat. (mmol g<sup>-1</sup>)].

point the flow can be significantly increased (from 0.1 to 0.5 mL min<sup>-1</sup>) maintaining the same outcome for the reaction. The results obtained show a productivity for the reactor with this particular configuration of 45.1 g of 16 per g SILLP-7 h<sup>-1</sup> for a flow of 0.5 mL min<sup>-1</sup> (Table 3, entry 3).

As mentioned above, proper swelling of resin is essential to provide accessibility to the catalytic sites that are embedded in the interior of the polymeric beads. The swelling of this gel-type polymeric catalyst (SILLP-7, 600 mg used) is significant, with ca. 100% swelling in the presence of an equimolar mixture of 14 and 15 for 24 hours ( $v_i = 1$  mL,  $v_f = 2$  mL).<sup>28</sup>

Alternatively, a mini-flow reactor (*mfr*-SILLP-12-macro) reactor was packed with an analogous supported catalyst prepared from a macroporous resin. In contrast to gel-type or microporous resins, the beads from macroporous polymers display a permanent porosity regardless of the solvents or reagents, which usually makes them more suitable for flow processes. The reactor showed a similar behaviour as the first one, leading to yields of 99–95% of the desired product at flow rates ranging from 0.1 to 0.5 mL min<sup>-1</sup> (Table 3, entries 4–6). The slight difference observed for both reactors can be assigned to the different void volume observed for each reactor. Although the total volume occupied by the wet and swollen polymer is not very different (2 mL for *mfr*-SILLP-7-gel and 1.8 mL for *mfr*-SILLP-12-macro), there is a significant difference in the void volume due to the different swelling observed. Thus, in the case of the gel-type resin (*mfr*-SILLP-7-gel), the void volume can be estimated to be ca. 0.4 mL, while for the reactor packed with the macroporous catalyst (*mfr*-SILLP-12-macro) it is ca. 1.2 mL. These differences provide slightly different residence times for each reactor. Thus, the residence time for a flow rate of 0.1 mL min<sup>-1</sup> is 4 min for *mfr*-SILLP-7-gel and 12 min for *mfr*-SILLP-12-macro.

Fig. 6 depicts the yield vs. time course for the cyanosilylation reaction between 14 and 15 using either *mfr*-SILLP-7-g or *mfr*-SILLP-12-macro at 0.1 mL min<sup>-1</sup>. In both cases the induction time observed was ca. 3–2.5 fold the residence time

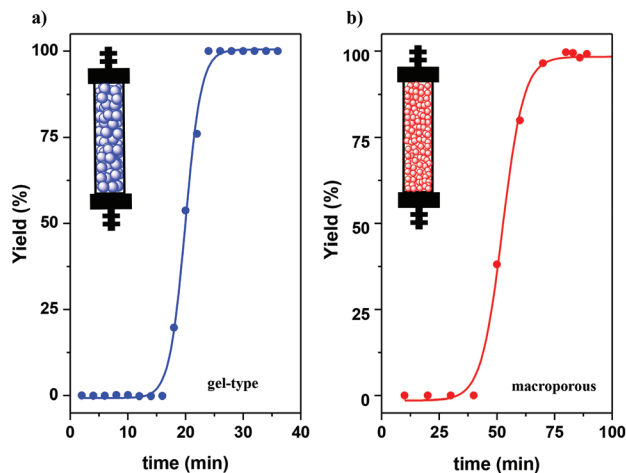


Fig. 6 Evolution with time of the yield of the product (16) for the model cyanosilylation between (14) and (15) obtained by the min-flow reactors (a) *mfr-SILLP-7-gel* and (b) *mfr-SILLP-12-macro* at  $0.1 \text{ mL min}^{-1}$ .

required to fill the reactor void volume. It must be noted that the induction time observed is much higher than that detected in the previous batch experiments. In this regard, several factors need to be taken into consideration to understand the process of catalyst conditioning before reaching the optimal operational behaviour. The first factor to be taken into consideration is the process of filling the void spaces of the system (tubing and interparticle void-spaces in the reactor) and this can be associated with the initial period for which an increase in the amount of starting material in the effluent is observed.

Volumetric calculations based on the volume spent during this period of time afforded a total volume for the system which is in good agreement with the one estimated according to the length and diameter of the tubing and to the volume of the reactor and the density (in the dry state) of the polymeric beads (ca.  $0.4 \text{ mL}$  and  $1.2 \text{ mL}$  overall void volume). On the other hand, as has been mentioned above, reaction of the chloride with TMSCN represents the first step of the catalytic cycle, but water can efficiently compete with chloride for the reaction with TMSCN when present at the polymeric beads, significantly reducing the efficiency of the process. Thus, the induction period can be associated with two main factors: (a) the wetting and swelling of the polymeric beads by the fluid containing the substrate and the reagent;<sup>21</sup> (b) the reaction of the TMSCN with any residual water. Indeed, if the columns are preheated in an oven at  $100 \text{ }^\circ\text{C}$  overnight, the induction time observed is significantly reduced to 1–1.5 fold the residence time required to fill the reactor void volume.

Furthermore, the systems showed a good stability after 48 hours of continuous use without any significant catalytic deactivation, allowing the synthesis during this time of 23.8 g of the corresponding cyanosilylated compound (see Fig. 7).

Finally, the use of a mini-flow reactor prepared from a monolithic polymeric rod was also studied. The monolithic reactor was prepared as reported by us and others by polymerisation of a mixture of 4-chlorovinylbenzene and

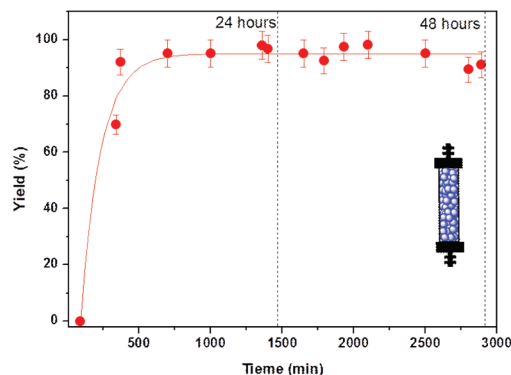


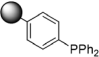
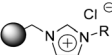
Fig. 7 Stability study: evolution with time of the yield of the product for the cyanosilylation between benzaldehyde and (15) obtained by the min-flow reactor (a) *mfr-SILLP-7-gel* at  $0.01 \text{ mL min}^{-1}$ .

divinylbenzene in the presence of the right porogenic agent.<sup>12,29</sup> Further modification of the chloromethyl groups of the monolith with methylimidazole led to a monolithic reactor with an analogous chemical structure as SILLP-7 and SILLP-12.<sup>29</sup> This mini-flow reactor (*mfr-SILLP-17-molth*) was then evaluated using the same experimental continuous flow set-up and different flow rates ranging from  $0.5$  to  $0.01 \text{ mL min}^{-1}$ . In this case, only moderate yields (30%) were detected for  $0.5 \text{ mL min}^{-1}$  flow rate and smaller flow rates (longer residence time) were needed to achieve satisfactory yields (Table 3, entries 7–9).

Table 3 summarises the results obtained for the three mini-flow reactors prepared with SILLPs presenting similar functional loadings but different polymer morphologies. Although previous studies from different groups, including our own results, have revealed that monolithic flow-through reactors can provide, in some instances, significantly better performances;<sup>13,21,25</sup> in this case, the fix-bed reactors prepared from polymeric beads delivered the most efficient system. No significant differences were observed between the gel-type and macroporous catalysts with a maximum productivity of  $43\text{--}45 \text{ g of } 16 \text{ per g cat h}^{-1}$ . This must be associated with the very low flow rates required to achieve reasonable conversions, which suggest a reduced accessibility of the catalytic sites in the monolith. The presence of the functional groups on the surface of the porous structure of the monolith can provide a high local concentration of IL-like moieties strongly associated and ordered, substantially hampering the participation of the chloride anions in the first step of the catalytic cycle. Thus, this effect should be reminiscent of the one found for high loading resins. The use of a porogenic solvent like dodecanol is known to provide monoliths with large macropores, which is accompanied by a reduction in the total surface. Besides, polar fragments tend to be located at the interface with the porogenic agent becoming the accessible surface of the final polymer.

Table 4 shows a comparison of some of the more efficient methodologies reported up to now for the cyanosilylation reaction here considered. All these previous methods combine at

**Table 4** Comparison between the different catalytic processes developed for the cyanosilylation reaction of carbonyl compounds

Ref	Solvent	Cat.	Conditions	Prod. <sup>a</sup>	E factor
7 <sup>b</sup>	[OMIM][PF <sub>6</sub> ]	[OMIM][PF <sub>6</sub> ]	r.t., batch, 24 h	0.55	156
8 <sup>b</sup>	[BMIM][SbF <sub>6</sub> ]	Sc(OTf) <sub>3</sub>	r.t., batch, 30 min	20 000	96
30 <sup>c</sup>	SolFC		60 °C, flow, 0.04 mL min <sup>-1</sup>	25	0.16
— <sup>c</sup>	SolFC		r.t. flow, 0.5 mL min <sup>-1</sup>	42	0.05

<sup>a</sup> Productivity as (mol 16 per mol cat) h<sup>-1</sup>. <sup>b</sup> Made with benzaldehyde. <sup>c</sup> Made with acetophenone.

least two of the elements applied in our system, namely: ionic liquids, (organo)catalysis, solventless conditions (SolFC) and flow chemistry. Two main parameters have been selected for comparison: productivity and E factor. The first one is related with the chemical efficiency of the process, while the E factor highlights its greenness. Entries 1 and 2 summarise the results obtained using ILs as the solvent. Even when the ILs could be recycled, the use of an additional organic solvent was required to isolate the product, which is reflected in the significant increase of the E factor, in spite of the really high productivity obtained when Sc(OTf)<sub>3</sub> is present. The use of solid/supported catalysts (entries 3 and 4, Table 4) facilitates the isolation of the product and the reuse of the catalyst by simple filtration, which is reflected by a large reduction in the E factor (>100 fold reduction). In the case of the SILLP-7, besides, the productivity observed is twofold that of the recently reported supported phosphine.<sup>30</sup> No additional solvent is required neither for the reaction nor for the isolation step leading to a further E factor reduction.

The two polymer-supported systems do not provide the impressive productivity of the reaction catalysed by Sc(OTf)<sub>3</sub> in ILs; however both are organocatalytic solvent-free and metal free reactions with very low E factors. Although a comparison of this type can be excessively simplistic, at the level considered, it allows illustrating how the combination of different tools from the Green Chemistry “tool box” can lead to synergies helping us to move forward towards more sustainable processes.

## Conclusions

The results here presented highlight the advantages of the use of supported ionic liquid-like phases (SILLPs) to develop greener and more efficient catalytic processes. Indeed such SILLPs allowed us to design organocatalytic species for the solvent free cyanosilylation reaction of carbonyl compounds. The modular structural features of the SILLPs allow to fine-tune the catalytic efficiency by varying parameters such as the SILLP loading, the substitution pattern of the imidazolium units and the nature of the anion. The optimization of these parameters led to stable organocatalytic supported systems that facilitate the development of a continuous flow system

implementing the productivity of the system, the product isolation and a simple catalyst recycling. The use of a flow system has also been shown to minimize the negative effects associated with the low mechanical stability of the polymeric materials employed in this work, which precludes proper recovery of the catalyst under pure batch processes. The connection of the effluent tubing to a flow-cell in a FT-IR has allowed continuous monitoring of the reaction, assisting in its optimization. This process perfectly conforms to the features of green chemistry: 100% atom economy, no waste regarding side-products and unconverted reactants, solvent-free, excellent catalytic activity, and no requirement for separation, along with continuous monitoring.

## Experimental

### Synthesis and characterization of SILLPs

Polymers modified with ionic-liquid-like moieties were synthesized by chemical modification of polymer-bound chloromethyl groups with the corresponding substituted imidazole (4, 5 or 6) following the experimental procedures previously described.<sup>12</sup> Commercially available Merrifield-gel polymers with different loadings (1.2, 2.1, 4.3 mmol Cl<sup>-</sup> g<sup>-1</sup>, 1–3) were used to afford the SILLPs 7–12 (Scheme 1). The metathesis of chloride by different anions (BF<sub>4</sub><sup>-</sup>, TfO<sup>-</sup>, NTF<sub>2</sub><sup>-</sup>, and SbF<sub>6</sub><sup>-</sup>) yielded a new series of SILLPs with an exchanged anion (13a–d).

### Synthesis and characterization of SILLP-17-monolith

A solution of divinylbenzene (2.4 mL; 80% technical grade), 4-vinylbenzene chloride (1.6 mL; 90% purity grade), 1-dodecanol (4.0 mL) and AIBN (42 mg) was prepared. A 15 mm × 100 mm Omnifit® column was filled with this stock solution, both ends of the column were sealed and the system was introduced into a bath at 70 °C for 24 h. A white polymeric monolith was obtained. This monolithic column was connected to a HPLC pump and washed with THF at 1 mL min<sup>-1</sup> for 2 h at r.t. Then, methylimidazole (25 mL) was pumped at a flow rate of 0.2 mL min<sup>-1</sup> for 24 h, the column being maintained at 60 °C. The column was then washed with THF at 1 mL min<sup>-1</sup> for 2 h at r.t.

All of the polymeric materials were characterized by FT-IR spectroscopy, Raman microspectroscopy, and elemental

analysis, which confirmed the expected structures. The details of the synthesis and characterization of these compounds can be found in our previous publications.<sup>9,11,12,29</sup>

### Batch cyanosilylation reaction

3 mmol of the corresponding carbonyl compound were added over 75 mg of the catalyst followed by the addition of 3.1 mmol of TMSCN. The mixture was gently stirred during 24 hours at 25 °C. To determine the kinetic profiles an aliquot of 20 µL was regularly taken (30 min, 1 hour, 2 hours, 4 hours, 6 hours, 8 hours and 24 hours) and diluted in 1 mL of CH<sub>2</sub>Cl<sub>2</sub>. Samples were then analysed by G.C. and <sup>1</sup>H-NMR (see ESI†).

### Reactive filtration cyanosilylation reaction

A regular 5 mL syringe equipped with a nylon filter was filled with 0.4764 mg of the catalyst SILLP-7. The mixture of the reagents (1 : 1 mol acetophenone–TMSCN) was added to the top of the syringe and was eluted through the catalytic bed and separated from the solid by simple gravimetric flow. Aliquots were taken at constant time intervals (15 min) and analysed by G.C.

### Continuous flow cyanosilylation reaction

The reactor was set up by introducing the SILLP-7 (ca. 600 mg) in a glass Omnifit® column (5 mm × 10 cm), which was connected at the head to a Jasco HPLC pump (PU2080 plus) and at the bottom to a continuous flow cell for a Pike-ATR MIRacle™ single reflection ATR (diamond/ZnSe) adapted to a Jasco-6300 FT-IR spectrometer by standard tubing connectors. A solution of the reagents (1 : 1.1 mol acetophenone–TMSCN) was pumped through the catalytic bed at different flow rates. The IR spectra were recorded at continuous intervals of time (2–4 min) during the run. In all the cases, aliquots were collected at the outlet of the reactor and were analysed by GC.

## Acknowledgements

This work was partially supported by MINECO, Spain (Ref: CTQ2011-28903) and Generalitat Valenciana (PROMETEO 2012/020 and ACOMP GV-2013/207). Cooperation of the SCIC of the UJI for instrumental analyses is also acknowledged.

## Notes and references

- J. M. Brunel and I. P. Holmes, *Angew. Chem., Int. Ed.*, 2004, **43**, 2752–2778.
- R. J. H. Gregory, *Chem. Rev.*, 1999, **99**, 3649–3682.
- R. I. Kureshy, S. H. R. Abdi, S. Agrawal and R. V. Jasra, *Chem. Rev.*, 2008, **252**, 593–623.
- J. Gawronski, N. Wascinska and J. Gajewy, *Chem. Rev.*, 2008, **108**, 5227–5252.
- A. D. Dilman and S. L. Loffe, *Chem. Rev.*, 2003, **103**, 733–772.
- (a) C. Wiles and P. Watts, *ChemSusChem*, 2012, **5**, 332–338; (b) C. Wiles and P. Watts, *Org. Process Res. Dev.*, 2008, **12**, 1001–1100.
- Z. L. Shen, S. J. Jib and T. P. Loh, *Tetrahedron Lett.*, 2005, **46**, 3137–3139.
- Y. P. Boyoung, Y. R. Ka, H. P. Jung and L. Sang-gi, *Green Chem.*, 2009, **11**, 946–948.
- V. Sans, N. Karbass, M. I. Burguete, V. Compañ, E. García-Verdugo, S. V. Luis and M. Pawlak, *Chem.–Eur. J.*, 2011, **17**, 1894–1906.
- M. I. Burguete, E. García-Verdugo, I. Garcia-Villar, F. Gelat, P. Licence, S. V. Luis and V. Sans, *J. Catal.*, 2010, **269**, 150–160.
- M. I. Burguete, E. García-Verdugo, S. V. Luis and J. A. Restrepo, *Phys. Chem. Chem. Phys.*, 2011, **13**, 14831–14838.
- M. I. Burguete, H. Erythropel, E. García-Verdugo, S. V. Luis and V. Sans, *Green Chem.*, 2008, **10**, 401–407.
- P. Lozano, E. García-Verdugo, N. Karbass, K. Montague, T. De Diego, M. I. Burguete and S. V. Luis, *Green Chem.*, 2010, **12**, 1803–1810.
- M. Kira, K. Sato and H. Sakurai, *J. Am. Chem. Soc.*, 1988, **110**, 4599–4602.
- S. Rendler and M. Oestreich, *Synthesis*, 2005, 1727–1747.
- S. V. Luis and E. García-Verdugo, *Chemical Reactions and Processes under Flow Conditions*, RSC Green Chemistry Series, The Royal Society of Chemistry, Cambridge, 2010.
- For examples of continuous flow systems see: *Beilstein J. Org. Chem., Chemistry in flow systems I and II*, ed. A. Kirschning, 2011.
- (a) B. P. Mason, K. E. Price, J. L. Steinbacher, A. R. Bogdan and D. T. McQuade, *Chem. Rev.*, 2007, **107**, 2300–2318; (b) B. Ahmed-Omer, J. C. Brandtand and T. Wirth, *Org. Biomol. Chem.*, 2007, **5**, 733–740; (c) P. Watts and C. Wiles, *Chem. Commun.*, 2007, 443–467; (d) T. Fukuyama, M. T. Rahman, M. Sato and I. Ryu, *Synlett*, 2008, 151–163; (e) K. Geyer, T. Gustafsson and P. H. Seeberger, *Synlett*, 2009, 2382–2391; (f) S. Marrea and K. F. Jensen, *Chem. Soc. Rev.*, 2010, **39**, 1183–1202; (g) D. Webb and T. F. Jamison, *Chem. Sci.*, 2010, **1**, 675–680; (h) J. Yoshida, H. Kim and A. Nagaki, *ChemSusChem*, 2011, **4**, 331–340.
- J. Wegner, S. Ceylan and A. Kirschning, *Chem. Commun.*, 2011, **47**, 4583–4592.
- (a) S. Suga, M. Okajima, K. Fujiwara and J. Yoshida, *J. Am. Chem. Soc.*, 2001, **123**, 7941–7942; (b) M. Rueping, T. Bootwicha and E. Sugiono, *Beilstein J. Org. Chem.*, 2012, **8**, 300–307.
- V. Sans, N. Karbass, M. I. Burguete, E. García-Verdugo and S. V. Luis, *RSC Adv.*, 2012, **2**, 8721–8728.
- A. R. Bogdan, B. P. Mason, K. T. Sylvester and D. T. McQuade, *Angew. Chem., Int. Ed.*, 2007, **46**, 1698–1701.
- A. El Kadib, R. Chimenton, A. Sachse, F. Fajula, A. Galarneau and B. Coq, *Angew. Chem., Int. Ed.*, 2009, **48**, 4969–4972.



- 24 The reactors are named as *mfr*-SILLP-N-type, where *mfr* indicates a mini-flow reactor, SILLP-N refers to the number assigned to the catalyst (N); and type defines the morphology of the polymer: *gel* for microporous beads (gel type), *macro* for macroporous beads, and *molth* for the macroporous monolith.
- 25 S. V. Luis and E. García-Verdugo, Continuous Flow Systems Using Polymer-Supported Chiral Catalysts, in *Polymeric Chiral Catalyst Design and Chiral Polymer Synthesis*, ed. S. Itsuno, John Wiley & Sons, Inc., DOI: 10.1002/9781118063965.ch5, 2012.
- 26 (a) P. Kasaplar, C. Rodríguez-Esrich and M. A. Pericàs, *Org. Lett.*, 2013, **15**, 3498–3501; (b) E. Alza, C. Rodríguez-Esrich, S. Sayalero, A. Bastero and M. A. Pericàs, *Chem.–Eur. J.*, 2009, **15**, 10167–10172.
- 27 Commercially available Omnifit(R) glass chromatography columns with adjustable height end pieces (lunger) were used.
- 28 Swelling  $(v_f - v_i/v_i \times 100)$ .
- 29 (a) N. Karbass, V. Sans, E. García-Verdugo, M. I. Burguete and S. V. Luis, *Chem. Commun.*, 2006, 3095–3097; (b) P. Lozano, E. García-Verdugo, R. Piamtongkam, N. Karbass, T. de Diego, M. I. Burguete, S. V. Luis and J. L. Iborra, *Adv. Synth. Catal.*, 2007, **7**, 1077–1084.
- 30 G. Strappaveccia, D. Lanari, D. Gelman, F. Pizzo, O. Rosati, M. Curini and L. Vaccaro, *Green Chem.*, 2013, **15**, 199–204.



# **Supported Ionic Liquid-Like Phases as Organocatalysts for the Solvent-Free Cyanosilylation of Carbonyl Compounds: From Batch to Continuous Flow Process.**

Sergio Martín, Raúl Porcar, Edgar Peris, María Isabel Burguete, Eduardo García-Verdugo\* and Santiago V. Luis\*

Departamento de Química Inorgánica y Orgánica, Universitat Jaume I, Av. Sos Baynat s/n 12071 Castellón

Email: [luiss@uji.es](mailto:luiss@uji.es), [cepeda@uji.es](mailto:cepeda@uji.es)

## **Supporting information index**

- 1. General procedures**
- 2. Characterization**
- 3. NMR Spectra.**
- 4. Calculations of E-factor and Productivity.**
- 5. Swelling of the supported catalysts.**

## 1. General procedures

Reagents were supplied by Aldrich and were used without further purification (octanal was distilled before being used).  $^1\text{H}$  NMR experiments were obtained using a Varian INOVA 500 ( $^1\text{H}$ , 500 MHz) spectrometer. The chemical shifts are given in delta ( $\delta$ ) values (ppm). Samples were analyzed by GC VARIAN 3900.

## 2. Characterization.

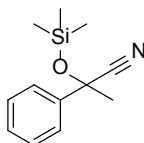
All the products here synthesized were previously reported and purified by medium pressure column chromatography (Combi-Flash Teledyne ISCO) with n-Hexane-Ethylacetate. According to bibliography data the compounds were characterized as following:

Compound (**13**) and compounds entries 1, 3 and 5, Table 2, were analyzed by the following GC method (VARIAN 3900). Analysis time: 60 min., Column Cyclodex B Pressure: 15.00 Psi Oven Temperature:  $T_0=60^\circ\text{C}$ ,  $T_f=130^\circ\text{C}$ . Rate:  $1.2^\circ\text{C}/\text{min}$  Detector: T:  $300^\circ\text{C}$ , Injector: T:  $230^\circ\text{C}$ , Helium flow:  $25\text{mL}/\text{min}$ , Nitrogen flow:  $30\text{mL}/\text{min}$ , Air flow:  $300\text{mL}/\text{min}$ .

Compound entry 2, Table 2 was analyzed by GC VARIAN 3900. Analysis time: 30 min., Column CyclodexB Pressure: 15.00 Psi Oven Temperature:  $T_0=60^\circ\text{C}$ ,  $T_f=130^\circ\text{C}$ . Rate:  $10^\circ\text{C}/\text{min}$  Detector: T:  $300^\circ\text{C}$ , Injector: T:  $230^\circ\text{C}$ , Helium flow:  $25\text{mL}/\text{min}$ , Nitrogen flow:  $30\text{mL}/\text{min}$ , Air flow:  $300\text{mL}/\text{min}$ .

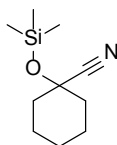
Compounds entry 4, 6 and 7, Table 2 were analyzed by using a Varian INOVA 500 ( $^1\text{H}$ , 500 MHz) spectrometer.

### 2-phenyl-2-((trimethylsilyl)oxy)propanenitrile (**13**)



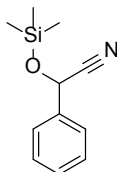
$^1\text{H-RMN}$  ( $\text{CDCl}_3$ , 500 MHz):  $\delta$  0.181 (s, 9H,  $3\times\text{CH}_3$ ), 1.868 (s, 3H,  $\text{CH}_3$ ), 7.515-7.403 (m, 5H, Ph).

**1-((trimethylsilyl)oxy)cyclohexanecarbonitrile** (Table 2 entry 1).



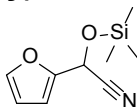
<sup>1</sup>H-RMN (CDCl<sub>3</sub>, 500 MHz): δ 0.230 (s, 9H, 3xCH<sub>3</sub>), 1.519-2.027 (m, 10H, cyclohexyl).

**2-phenyl-2-((trimethylsilyl)oxy)acetonitrile** (Table 2 entry 2).



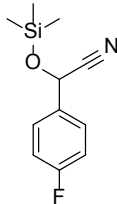
<sup>1</sup>H-RMN (CDCl<sub>3</sub>, 500 MHz): δ 0.181 (s, 9H, 3xCH<sub>3</sub>), 5.503 (s, 1H, CH), 7.400-7.499 (m, 5H, Ph).

**2-(furan-2-yl)-2-((trimethylsilyl)oxy)acetonitrile** (Table 2 entry 3).



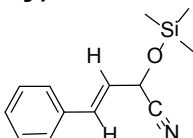
<sup>1</sup>H-RMN (CDCl<sub>3</sub>, 500 MHz): δ 0.226 (s, 9H, 3xCH<sub>3</sub>), 5.559 (s, 1H, CH), 6.427-6.539 (m, 1H, 2xfuran), 7.445-7.454 (m, 1H, furan).

**2-(4-fluorophenyl)-2-((trimethylsilyl)oxy)acetonitrile** (Table 2 entry 4).



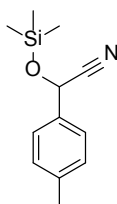
<sup>1</sup>H-RMN (CDCl<sub>3</sub>, 500 MHz): δ 0.246 (s, 9H, 3xCH<sub>3</sub>), 5.478 (s, 1H, CH), 7.056-7.126 (m, 2H, Ph), 7.433-7.480 (m, 2H, Ph).

**(E)-4-phenyl-2-((trimethylsilyl)oxy)but-3-enitrile** (Table 2 entry 5).



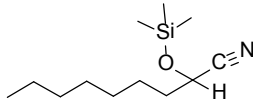
<sup>1</sup>H-RMN (CDCl<sub>3</sub>, 500 MHz): δ 0.275 (s, 9H, 3xCH<sub>3</sub>), 5.117-5.132 (m, 1H, CH), 6.172-6.216 (m, 1H, CH), 6.800-6.834 (m, 1H, CH), 7.239-7.419 (m, 5H, Ph).

**2-(p-tolyl)-2-((trimethylsilyl)oxy)acetonitrile (Table 2 entry 6).**



**<sup>1</sup>H-RMN** (CDCl<sub>3</sub>, 500 MHz): δ 0.221 (s, 9H, 3xCH<sub>3</sub>), 2.372 (s, 3H, CH<sub>3</sub>), 5.458 (s, 1H, CH), 7.226-7.380 (m, 4H, Ph).

**2-((trimethylsilyl)oxy)nonanenitrile (Table 2 entry 7).**



**<sup>1</sup>H-RMN** (CDCl<sub>3</sub>, 500 MHz): δ 0.180 (s, 9H, 3xCH<sub>3</sub>), 0.892 (s, 3H, CH<sub>3</sub>), 1.270-1.538 (m, 10H, CH<sub>2</sub>), 1.756-1.801 (m, 2H, CH<sub>2</sub>), 4.369-4.395 (m, 1H, CH).

#### 4. Productivity calculation

Productivity= (mol product/mol cat.) x (1/time(h))

##### REF. 6:

Mol product= mol benzaldehyde x Yield= 0,001mol x 99%= 0,00099 mol

Mol cat. = V x ρ/Fw = (0,5mL x 1,231g/mL) / (340,29g/mol)= 0,0018087 mol

Time= 24h

**Productivity= (0,00099mol/0,0018087mol) x (1/24h) = 0,023**

##### REF. 7:

Mol product= mol benzaldehyde x Yield= 0,005mol x >99% = 0,005 mol

Mol cat.= 0,01% Mol product= 0,005mol x(0,01/100)=0,0000005 mol

Time= 30min= 0,5h

**Productivity= (0,005mol/0,0000005mol) x (1/0,5h) = 20000**

##### REF. 26:

Mol product= mol acetophenone x Yield= 0,200mol x 99%= 0,198 mol

Mol cat. = 0,125g x 3,2mmol/g = 0,4mmol = 0,0004mol

Time= 20h

**Productivity= (0,198mol/0,0004mol) x (1/20h) = 25**

#### E factor calculation

E factor= kg waste/kg product

E factor=[ (mol benzaldehyde x Fw benzaldehyde) + (mol TMSCN x Fw TMSCN )+( mL solvent x ρ solvent) – (mol benzaldehyde x Yield x Fw product) ]/ [mol benzaldehyde x Yield x Fw product]

##### REF. 6:

Solvent= 3x15mL diethyl ether

ρ diethyl ether= 0,7134 g/mL

$$\text{E factor} = [(0,001\text{mol} \times 106\text{g/mol}) + (0,002\text{mol} \times 99,21\text{g/mol}) + (3 \times 15\text{mL} \times 0,7134\text{g/mL}) - (0,001\text{mol} \times (99/100) \times 205,09\text{g/mol})] / [0,001\text{mol} \times (99/100) \times 205,09\text{g/mol}] = \mathbf{158,6}$$

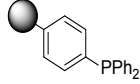
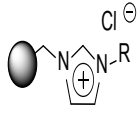
**REF. 7:**

Solvent= 3x50mL hexane

$\rho$  hexane= 0,6548 g/mL

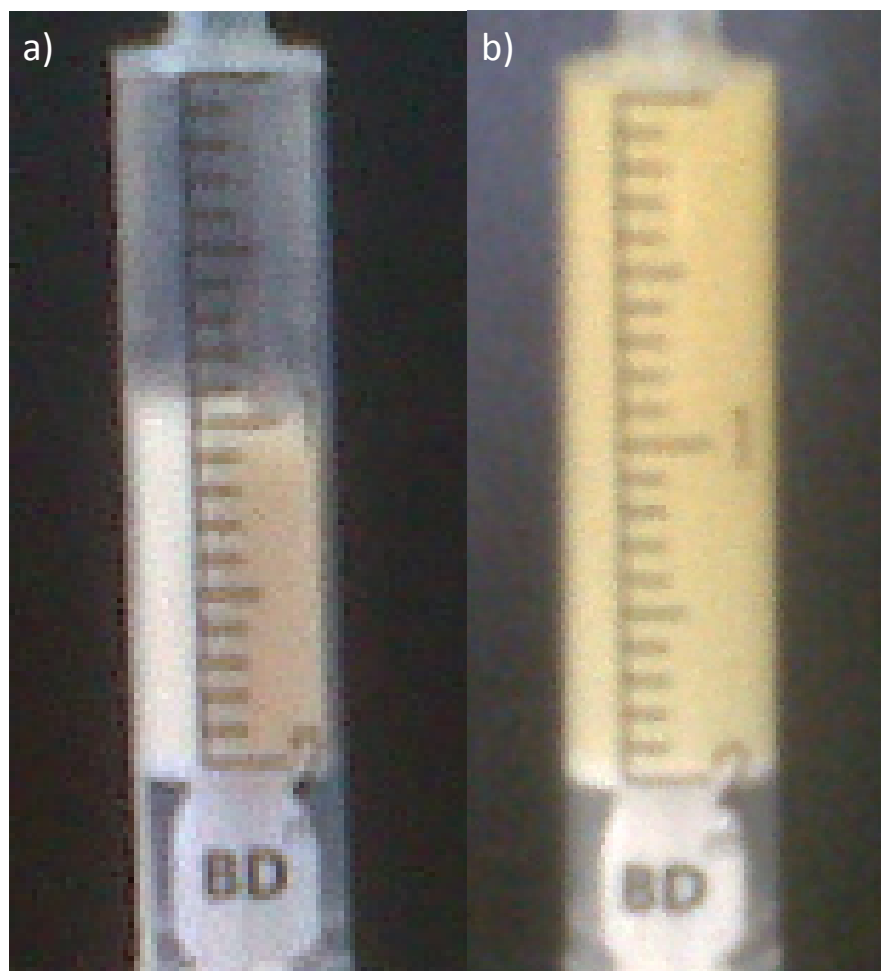
$$\text{E factor} = [(0,005\text{mol} \times 106\text{g/mol}) + (0,006\text{mol} \times 99,21\text{g/mol}) + (3 \times 50\text{mL} \times 0,6548\text{g/mL}) - (0,005\text{mol} \times >99\% \times 205,09\text{g/mol})] / [0,005\text{mol} \times >99\% \times 205,09\text{g/mol}] = \mathbf{95,8 \approx 96}$$



	SOLVENT	CAT.	CONDITIONS	YIELD	TIME	TEMP.	TYPE OF REACTOR
REF. 6	[OMIM]PF <sub>6</sub>	[OMIM]PF <sub>6</sub> 0,5 mL	1mmol benzaldehyde/ 2 mmol TMSCN	99%	24 h	r.t.	batch
REF. 7	[BMIM]SBF <sub>6</sub>	Sc(OTf) <sub>3</sub> 0,01%	5 mmol benzaldehyde/ 6 mmol TMSCN	>99%	30 min	r.t.	batch
REF. 26	SoIFC	 0,125g	200 mmol acetophenone/ 220 mmol TMSCN	99%	20 h	60°C	flow
OUR	SoIFC	 600 mg	114 mmol acetophenone/ 125 mmol TMSCN	99%	4 min <sup>a</sup>	r.t.	flow

a) Residence time for a flow rate of 0.1 mL/min

## 5. Swelling of the supported catalyst.

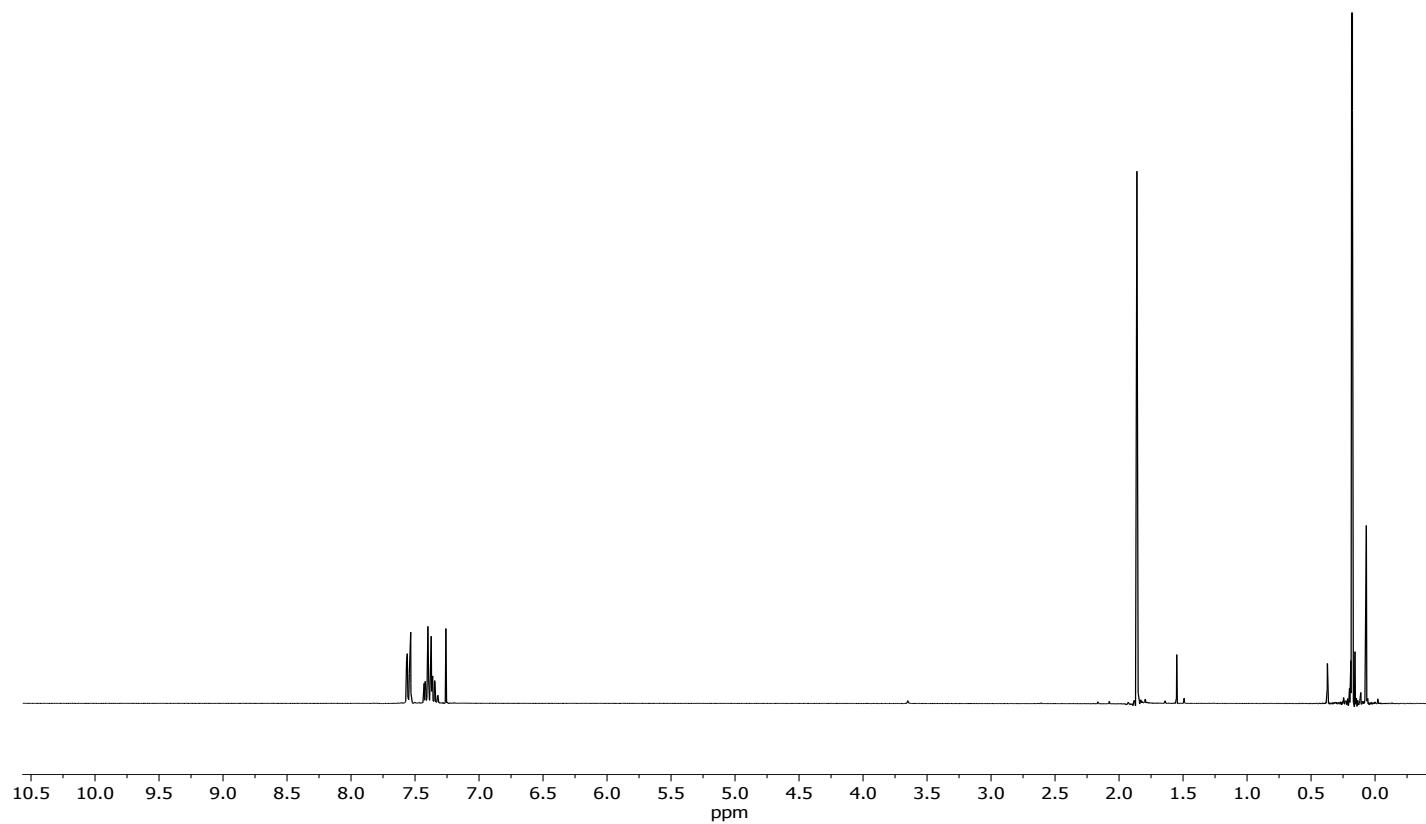
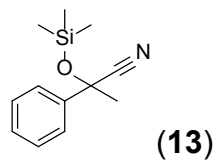


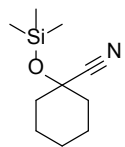
a) Dry volume = 1 ml

b) Wet volume at 25,5h = 2mL

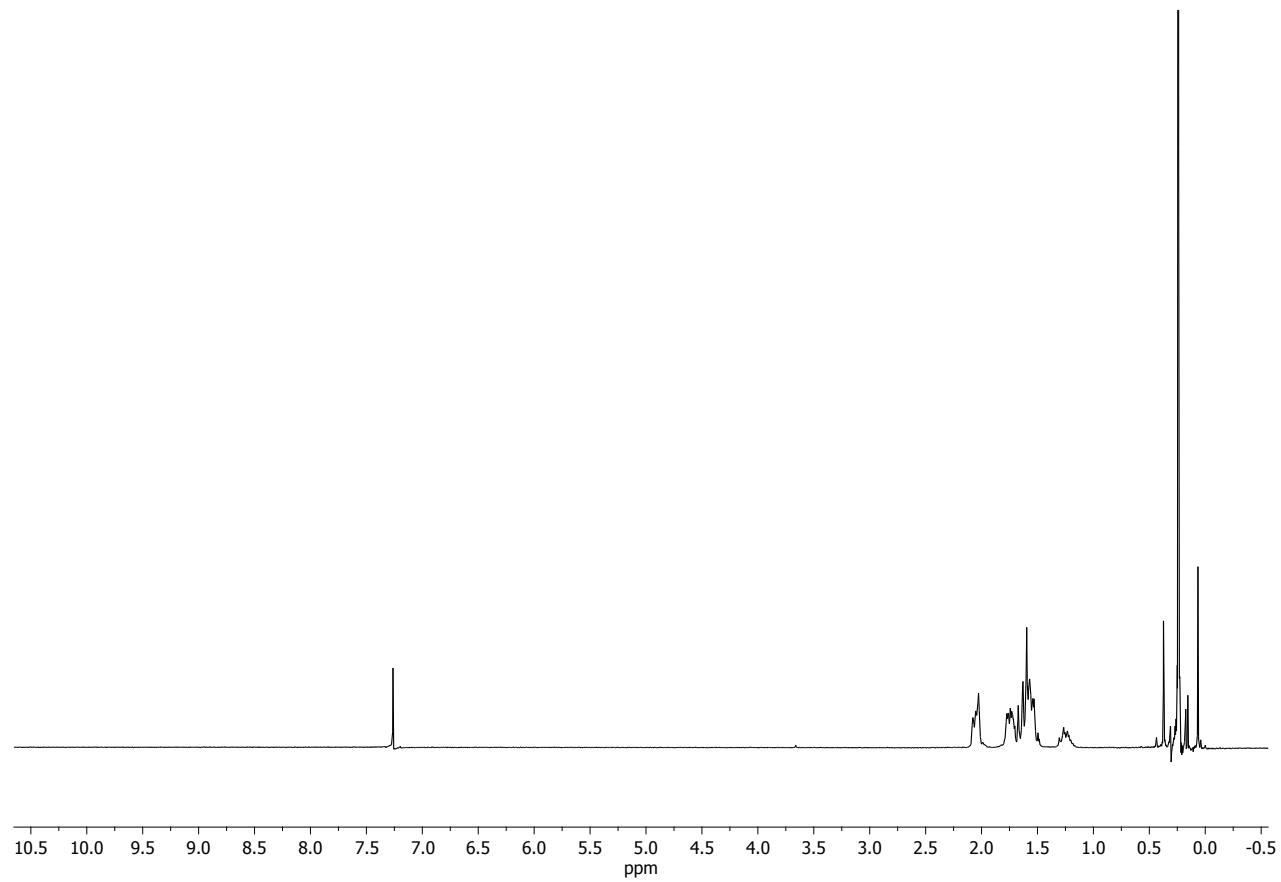
Swelling ( $(v_f - v_i) / v_i \times 100$ ).

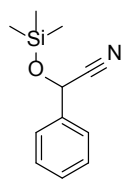
### 3. NMR Spectra (corresponding with the reaction crude).



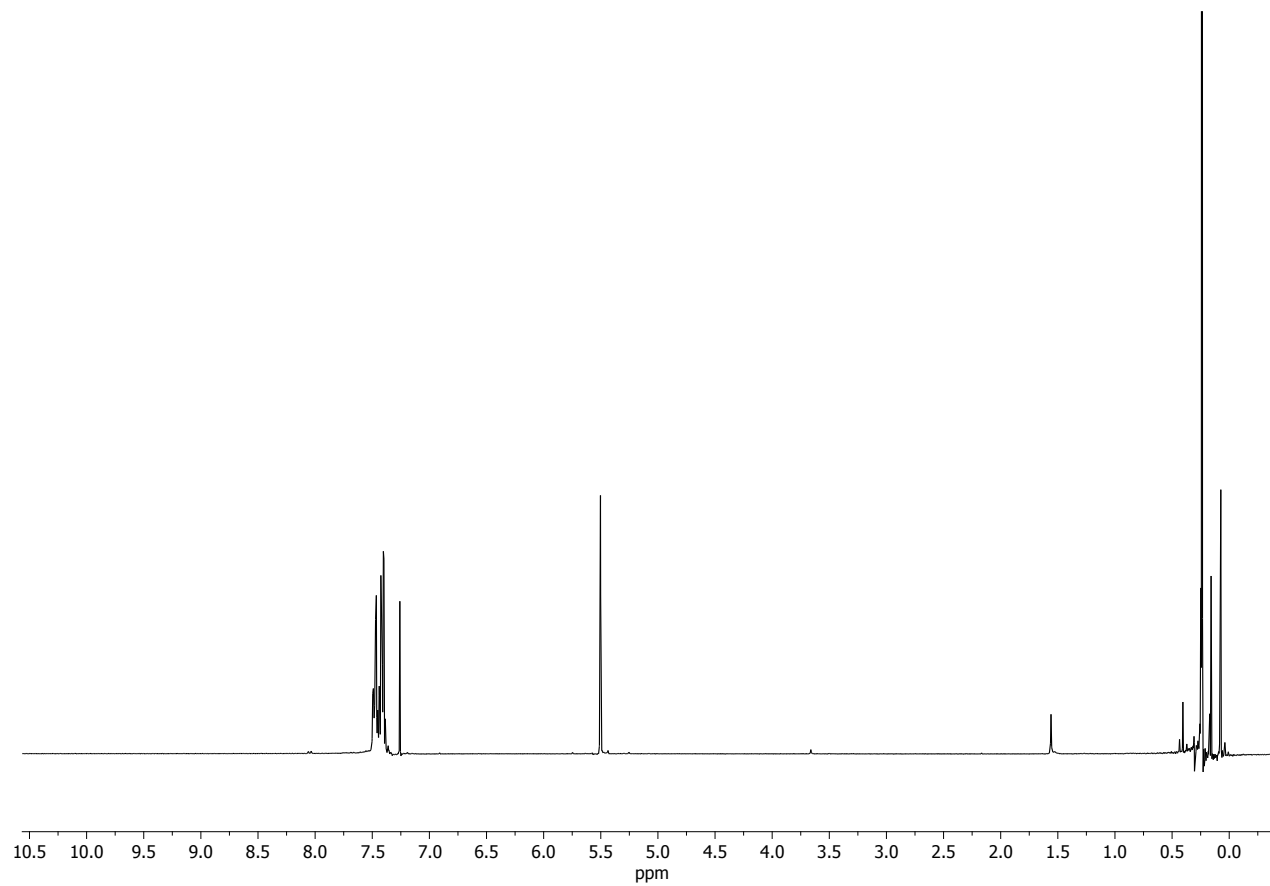


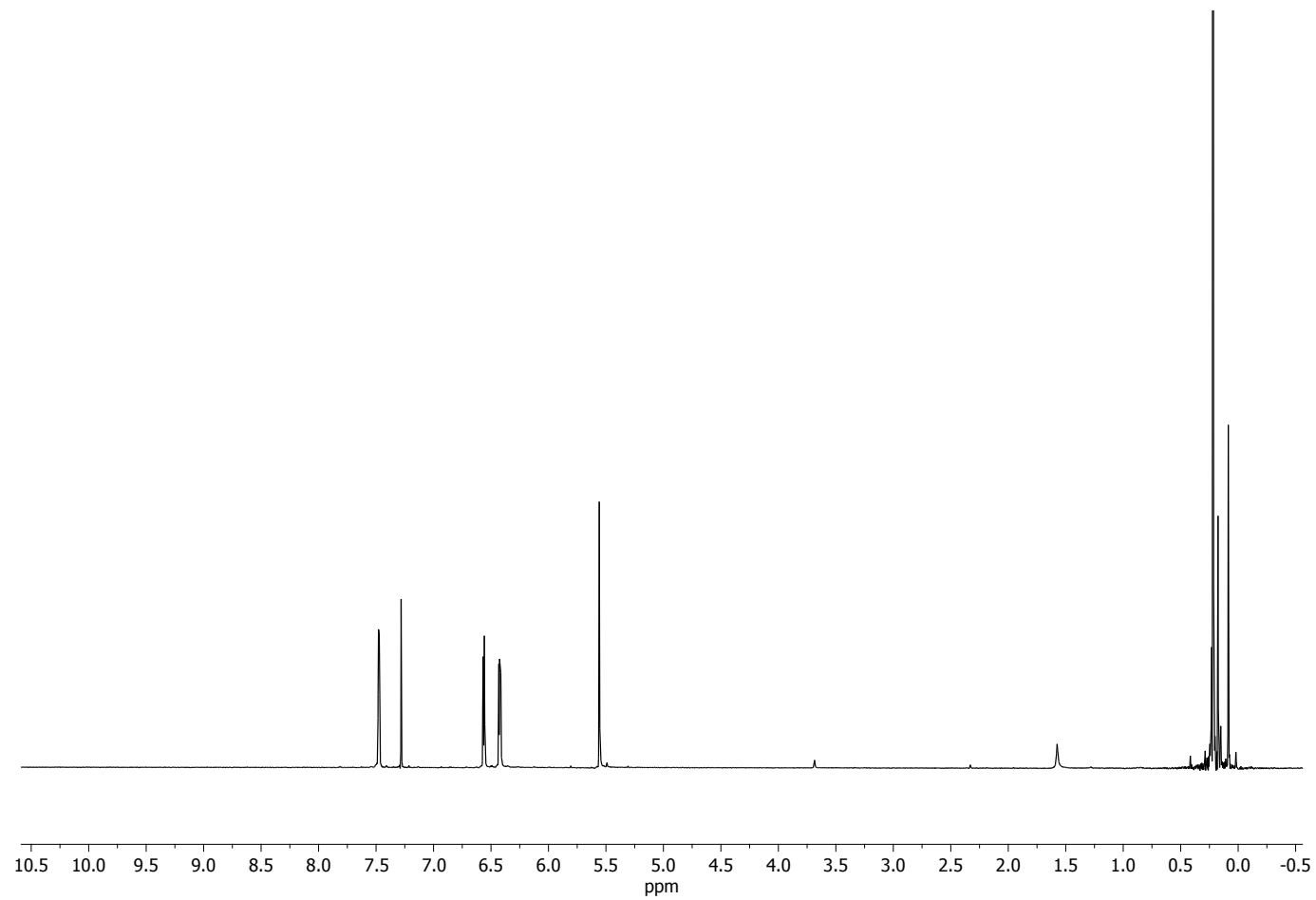
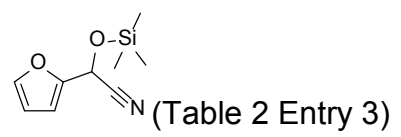
(Table 2 Entry 1)

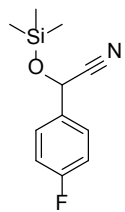




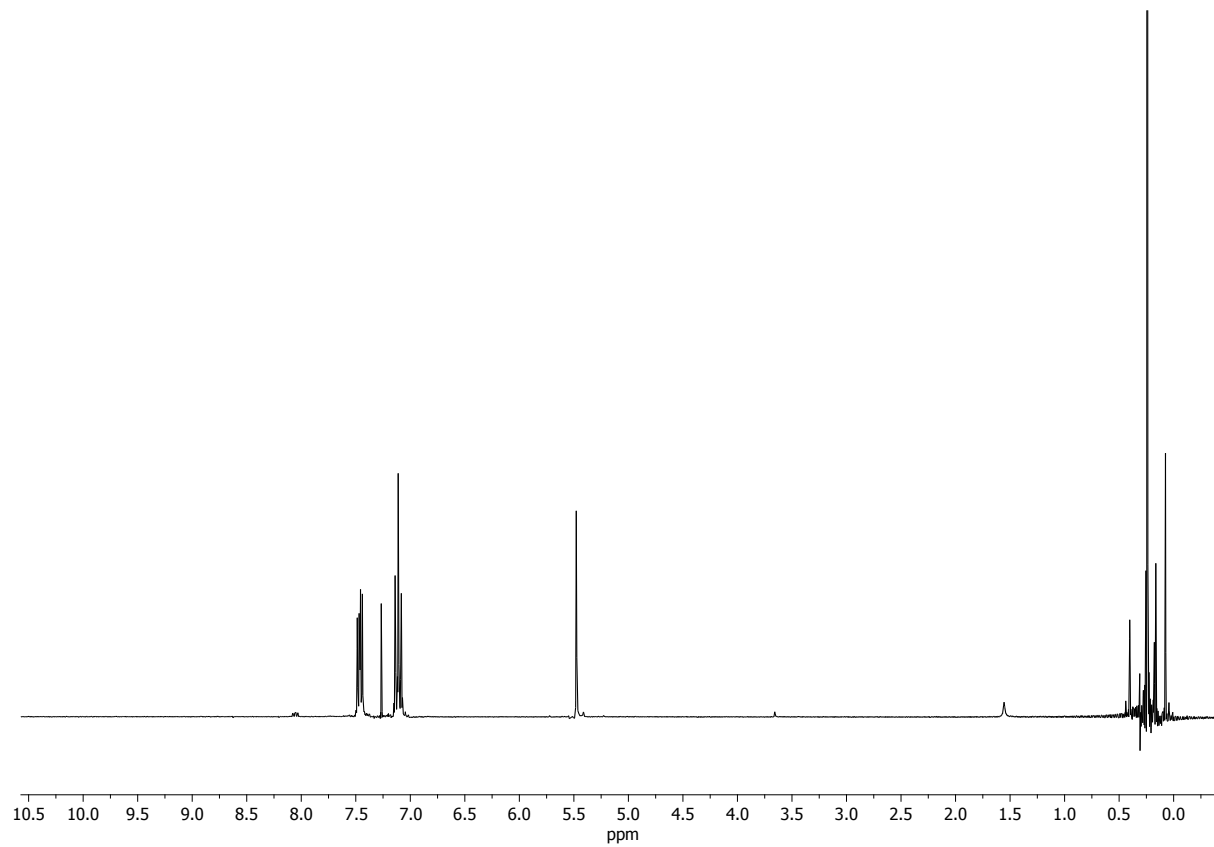
(Table 2 Entry 2)

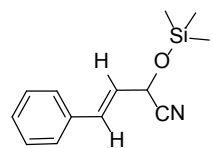




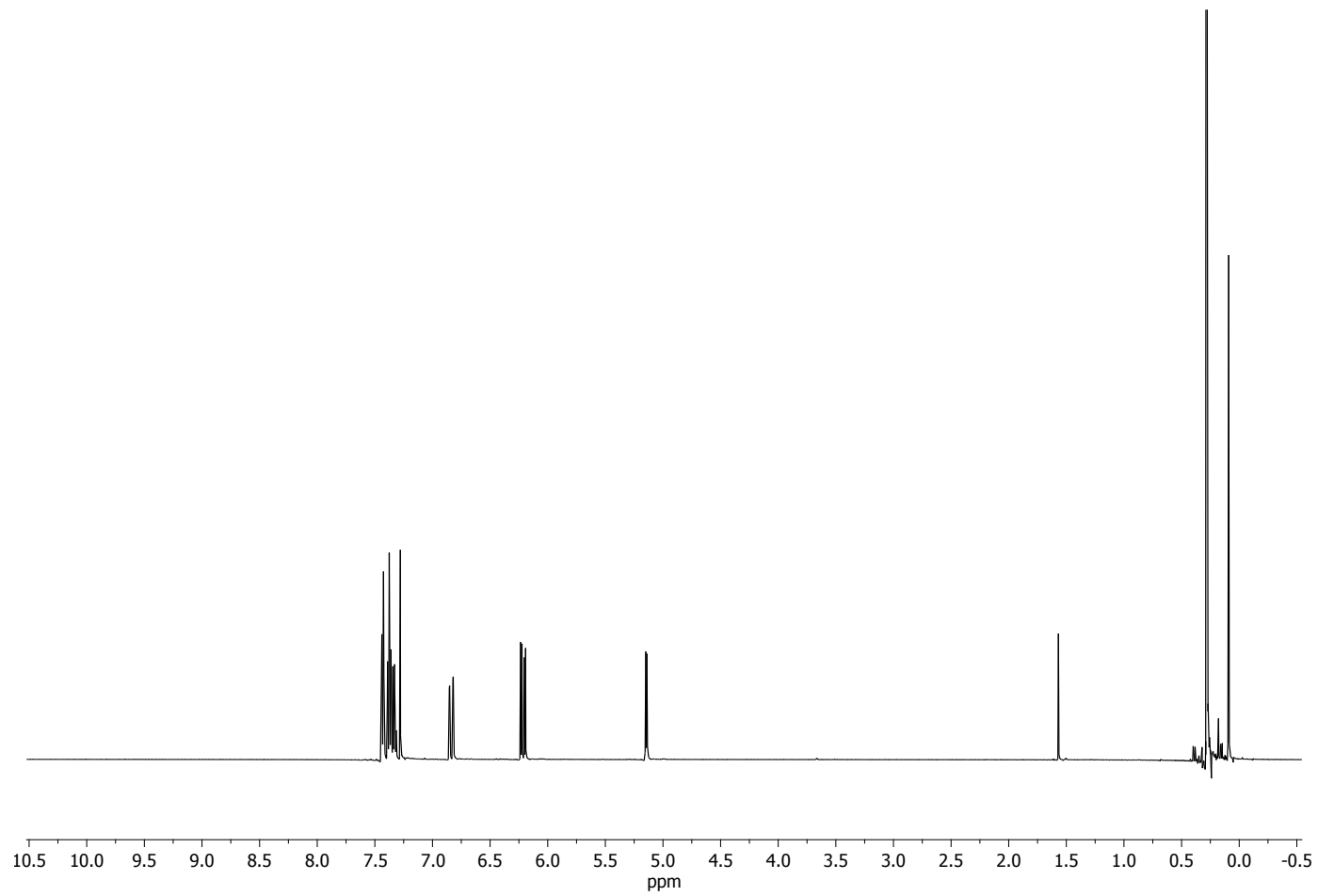


(Table 2 Entry 4)

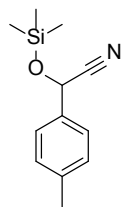




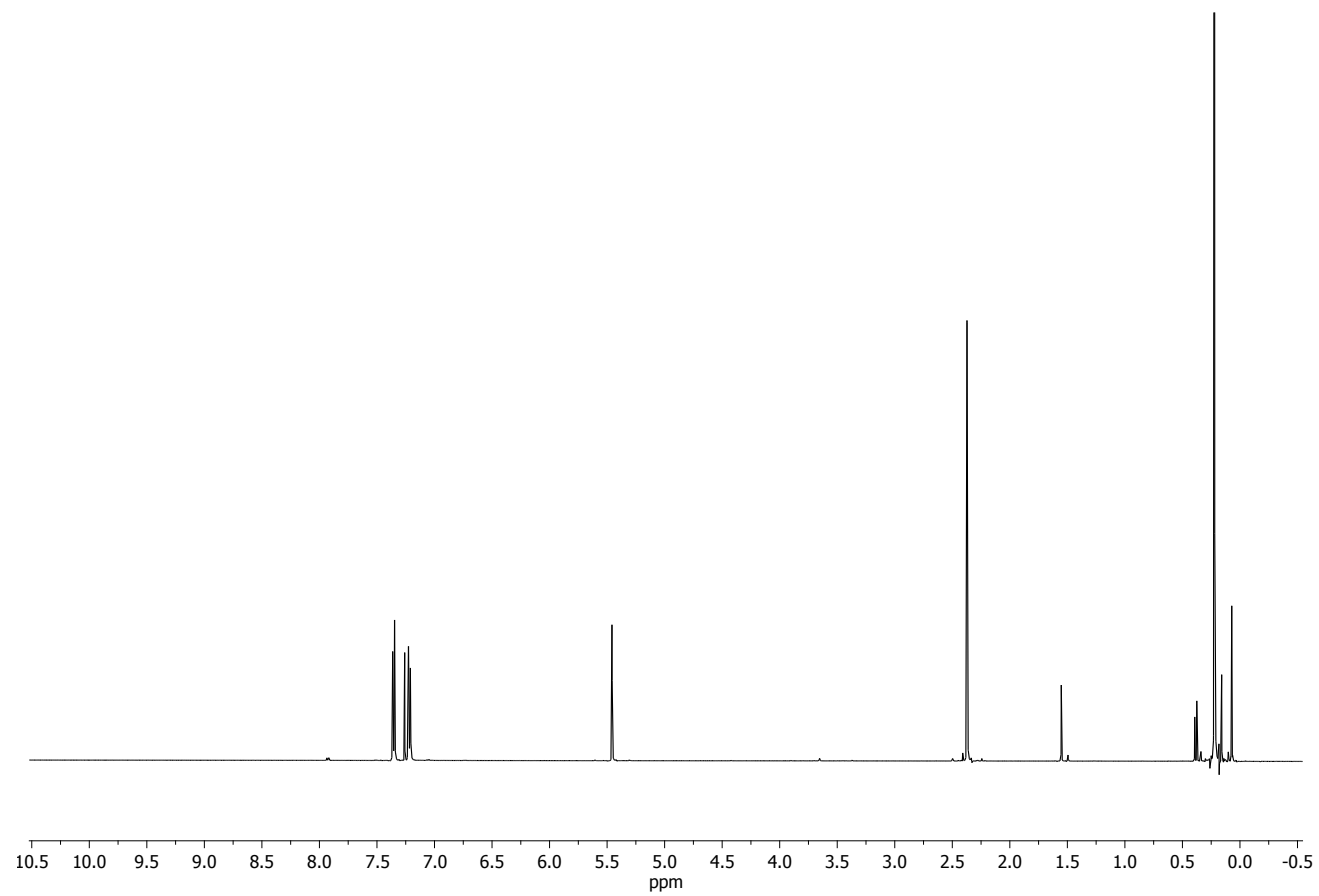
(Table 2 Entry 5)

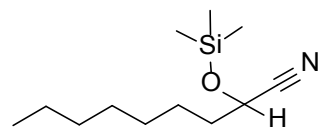




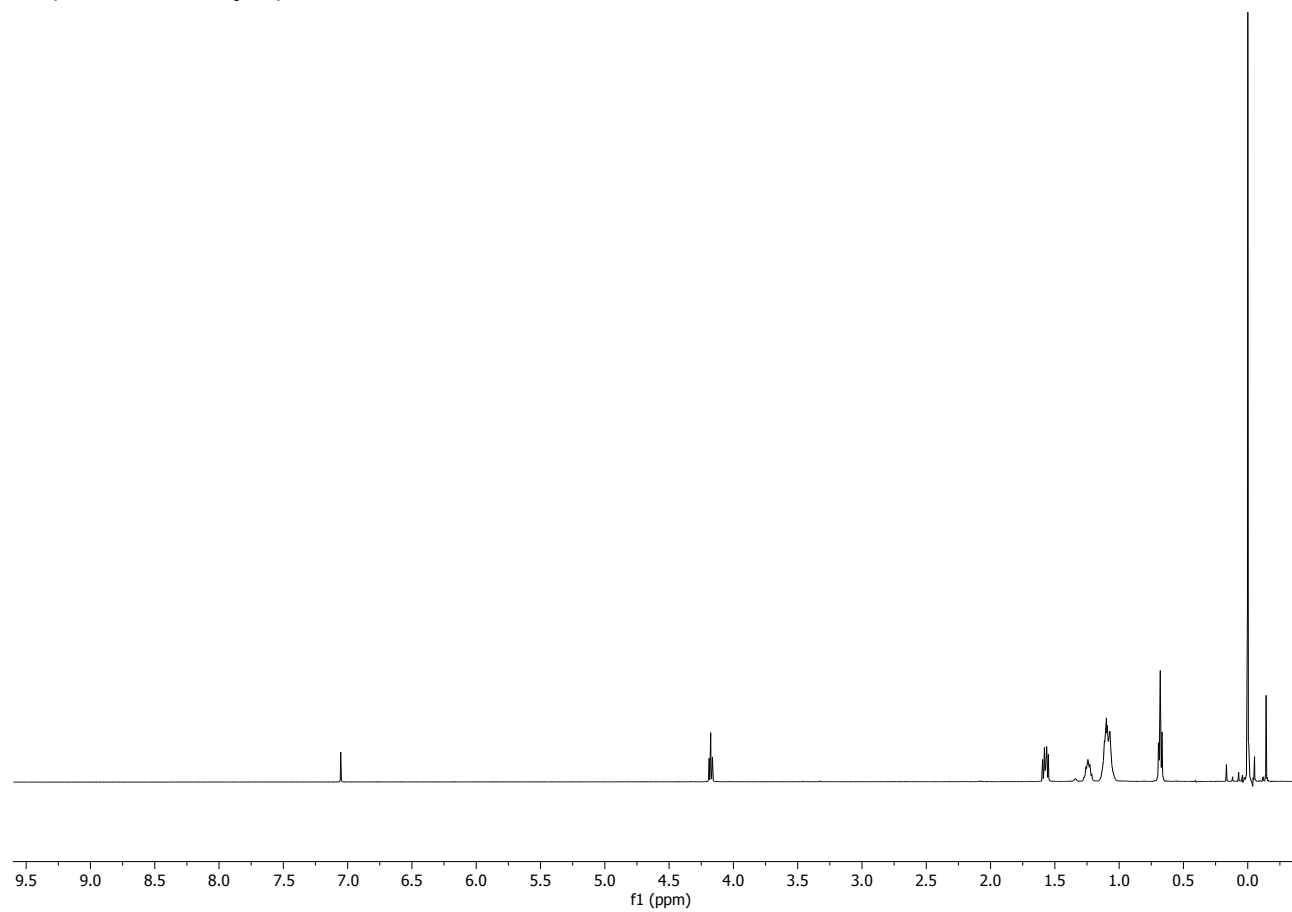


(Table 2 Entry 6)





(Table 2 Entry 7)



**Supported Ionic Liquid-Like  
Phases (SILLPs) as immobilised  
catalysts for the multistep and  
multicatalytic continuous flow  
synthesis of chiral cyanohydrins**

**CHAPTER 4**



## Chapter 4. Supported Ionic Liquid-Like Phases (SILLPs) as immobilised catalysts for the multistep and multicatalytic continuous flow synthesis of chiral cyanohydrins

### 4.1 RESUMEN DEL MANUSCRITO

Las cianohidrinas quirales representan intermedios sintéticos o moléculas clave de elevado valor en la química orgánica en general y en la química farmacéutica en particular (Figura 4.1).

En este capítulo se describe el desarrollo de una metodología sintética sencilla para la obtención de cianohidrinas quirales en condiciones de flujo continuo. Esta metodología se basa en el acoplamiento sucesivo de diferentes transformaciones sintéticas de manera telescópica, es decir, sin necesidad de purificar o separar los reactivos y productos obtenidos en las reacciones sucesivas (Figura 4.2). El empleo de SILLPs funcionalizados con propiedades catalíticas es un elemento esencial para llevar a cabo las transformaciones sintéticas requeridas. La combinación de estos sistemas catalíticos con un proceso de resolución enzimática permite obtener los correspondientes derivados de forma sencilla y con una elevada pureza óptica.

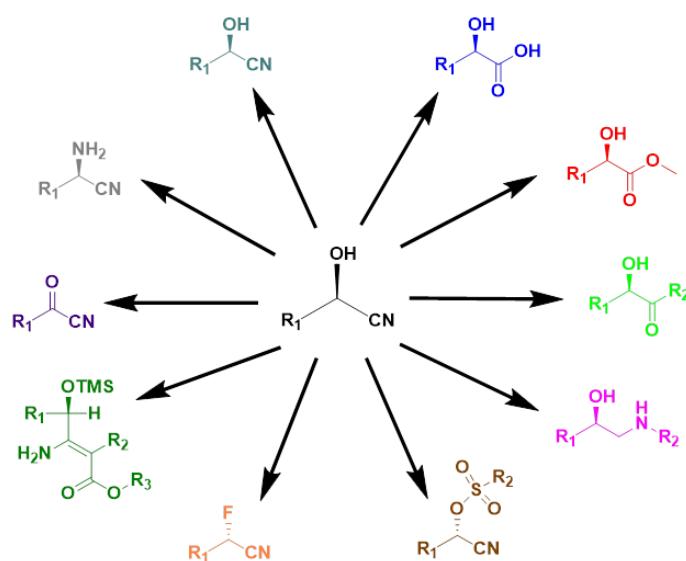


Figura 4.1. Algunas de las transformaciones sintéticas de las cianohidrinas quirales.

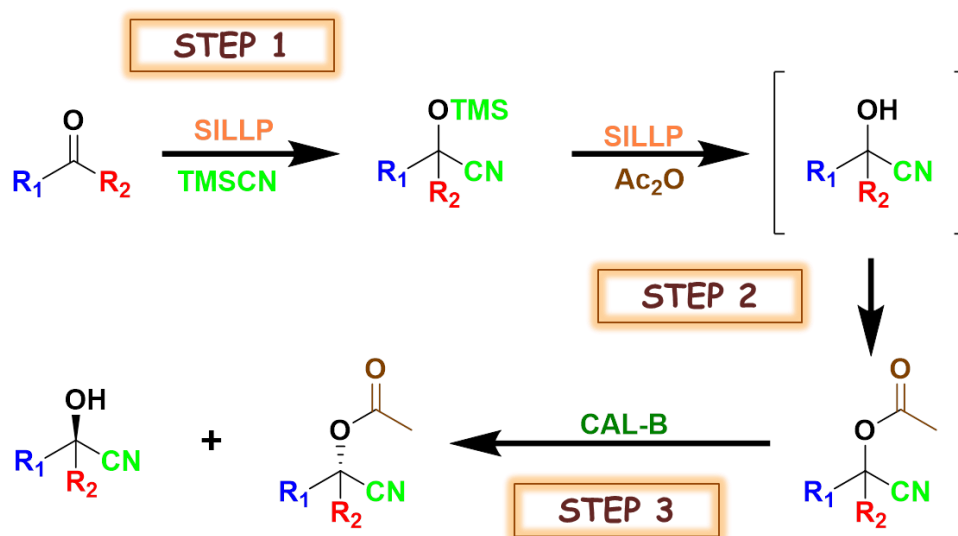


Figura 4.2. Estrategia sintética para la obtención de cianohidrinas quirales.

El proceso planteado consta de tres pasos sintéticos, que corresponden con cuatro transformaciones químicas consecutivas (Figura 4.2). El primer paso de esta estrategia sintética es la cianosililación de un compuesto carbonílico con TMSCN para obtener la correspondiente cianohidrina O-sililada racémica. Este proceso ha sido desarrollado y descrito con éxito en el tercer capítulo de este trabajo empleando un SILLP como organocatalizador soportado. El segundo paso consiste en la hidrólisis (desililación) de este derivado y su posterior acetilación. La Figura 4.3 recoge la familia de catalizadores que se evaluaron para llevar a cabo esta reacción, incluyendo diferentes SILLPs funcionalizados con diferentes unidades catalíticas así como distintos catalizadores ácidos comerciales.

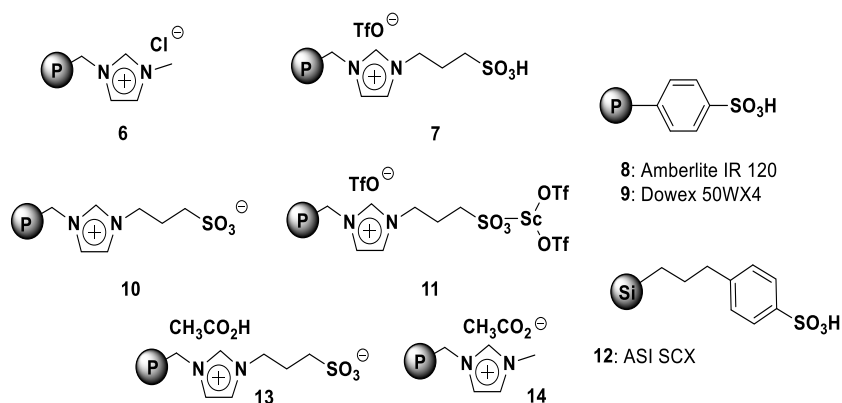
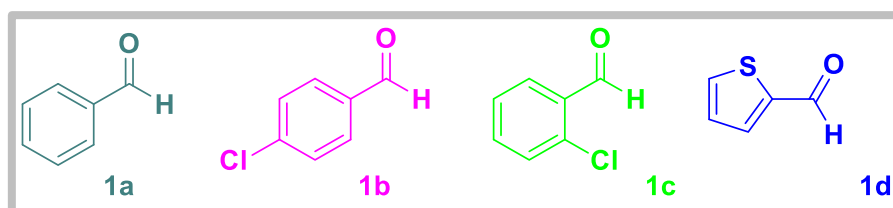


Figura 4.3. Diferentes catalizadores soportados empleados para el primer y segundo paso.

Un cribado inicial, empleando la cianohidrina O-sililada derivada del benzaldehído como sustrato y anhídrido acético, demostró que los catalizadores soportados **11**, **12**, **13** y **14** son efectivos para llevar a cabo la reacción de la desililación y acetilación consecutivas en un único paso.

Por último, la resolución cinética enzimática de la cianohidrina acetilada derivada del benzaldehído nos permitió obtener la cianohidrina enantiopura correspondiente, mediante el empleo de una Lipasa de *Candida Antarctica* tipo B inmovilizada como catalizador enzimático (Novozym 435).

Esta metodología se aplicó con éxito a tres aldehídos para probar la viabilidad de la estrategia sintética propuesta (Figura 4.4). Estos sustratos fueron escogidos por su estructura, ya que las correspondientes cianohidrinas quirales son moléculas clave en la síntesis de diferentes Principios Activos de la industria farmacéutica.



**Figura 4.4. Sustratos utilizados para la síntesis en 3 pasos consecutivos de cianohidrinas quirales.**

Las tres etapas fueron realizadas con éxito por separado en discontinuo (batch) para los cuatro sustratos empleando los catalizadores **6**, **11** y Novozym 435, para los pasos 1, 2 y 3 respectivamente. En estas reacciones el producto del primer paso se empleó en los pasos consecutivos sin necesidad de purificación, simplemente separando el catalizador inmovilizado. Los rendimientos para los dos primeras etapas fueron >95% independientemente del sustrato empleado. El rendimiento para la resolución enzimática estuvo cerca del 50% con purezas ópticas >99% ee.

Una vez desarrollada la estrategia sintética se evaluó la posibilidad de llevar a cabo la síntesis en un proceso único (“one-pot”), es decir que sea capaz de realizar las tres reacciones de forma consecutiva en el mismo reactor discontinuo (batch) y en presencia de los tres catalizadores. Bajo estas condiciones no fue posible conseguir la cianohidrina quiral correspondiente derivada del benzaldehído, debido a

problemas de compatibilidad entre los sustratos, productos y catalizadores empleados.

Así pues, se planteó como alternativa a un sistema o reactor multicatalítico, un sistema catalítico multireactor, es decir realizar las reacciones de forma consecutiva en tres reactores diferentes conectados en flujo continuo de manera telescópica. Este sistema, empleando diferentes mini reactores de lecho fijo, nos ofrece una compartimentalización que permite que cada reacción se pueda llevar a cabo en unas condiciones idóneas para cada proceso, separando los diferentes catalizadores a emplear. La inspiración para desarrollar estos procesos catalíticos consecutivos y compartimentalizados proviene de la naturaleza. En ella, numerosas transformaciones químicas potencialmente incompatibles están compartimentalizadas mediante membranas, paredes celulares, etc. La Figura 4.5 representa de forma esquemática el sistema de reactores para el proceso telescópico multicatalítico en continuo desarrollado para la síntesis de cianohidrinas quirales a partir de compuestos carbonílicos.

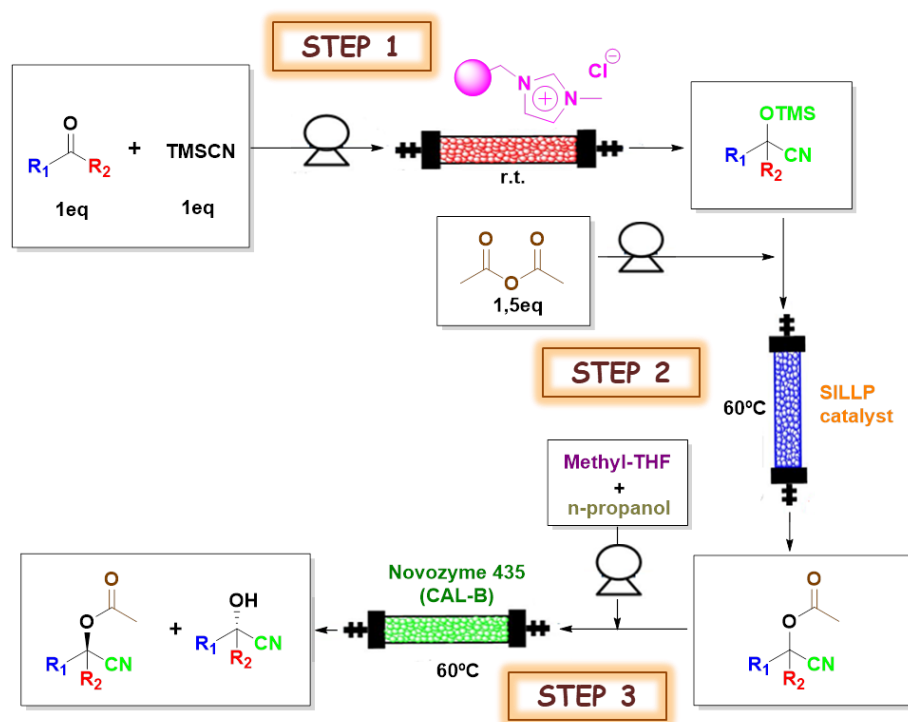
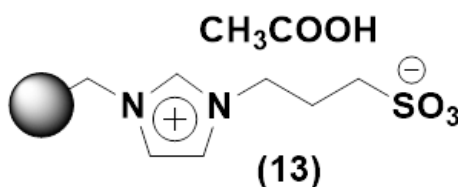


Figura 4.5. Esquema del sistema catalítico multireactor en continuo para la obtención de cianohidrinas quirales a partir de compuestos carbonílicos.

El proceso telescópico en continuo se implementó usando benzaldehído como sustrato de partida. El primer paso se llevó a cabo como se ha



descrito en el capítulo anterior. Un reactor de lecho fijo, relleno del SILLP **6**, demostró ser activo y estable durante al menos 50 horas para la obtención de la cianohidrina O-sililada con rendimientos superiores al 95%. El principal problema encontrado es la estabilidad en continuo de los catalizadores del segundo paso, que incluye la hidrólisis y acetilación de la cianohidrina O-sililada racémica. Aunque se disponía de una serie de catalizadores que se habían mostrado activos incluso durante varios ciclos consecutivos de reacción en discontinuo, su empleo en un sistema de flujo continuo demostró su falta de estabilidad debido a la participación de mecanismos de desactivación diferentes. El SILLP **11** redujo su actividad catalítica de un 99% a un 30% antes de 24 horas, mientras que la resina **12** pasó de 95% a 70% a las 5 horas de uso en continuo. Finalmente, el SILLP **13** mantuvo su actividad en el 65% desde el primer momento durante más de 40 horas en continuo utilizando las condiciones estándar de reacción. El hecho de mantener la actividad desde el primer momento resultó crucial, ya que el rendimiento pudo ser elevado fácilmente a valores aproximados al 90% modificando las condiciones experimentales tales como los equivalentes de anhídrido acético o el flujo empleado. Este catalizador es de tipo zwitteriónico con un grupo sulfonato en la cadena alquílica del SILLP y cuenta con moléculas de ácido acético adsorbidas (Figura 4.6), puede que en muy pequeña cantidad, pero que le confieren unas propiedades ácidas decisivas para el desarrollo la reacción sin pérdida de actividad. Una activación dual electrófilo-nucleófilo ocurre a través de un sistema complejo de interacciones por enlaces de hidrógeno. Este mecanismo de activación, que se ha reportado para los líquidos iónicos en solución, puede tener lugar de forma análoga en el SILLP **13**. Estos resultados muestran una vez más que los líquidos iónicos soportados en forma de SILLPs presentan propiedades catalíticas análogas a sus homólogos líquidos.



**Figura 4.6. Catalizador ácido tipo SILLP desarrollado para el segundo paso del proceso telescópico de obtención de cianohidrinas quirales en continuo.**

La resolución cinética enzimática del tercer paso se pudo llevar a cabo en condiciones de flujo continuo con buenos resultados y alta estabilidad. Así, fue posible desarrollar el proceso telescópico acoplado para los 3 pasos sintéticos que requieren 4 reacciones en total sin

necesidad de aislar o purificar ningún intermedio. El sistema demostró ser estable en uso continuo durante al menos 48 horas.

Cabe destacar el hecho de que se consigue combinar organocatalizadores y biocatalizadores (todos ellos soportados) en un mismo sistema catalítico, consiguiendo obtener cianohidrinas enantioméricamente puras en un proceso catalítico totalmente libre de metales. La ausencia de disolventes en los dos primeros casos también es un factor a tener muy en cuenta. La combinación de estos factores nos proporciona un factor E, tanto de cada uno de los procesos individuales como de la suma global de todos ellos, muy bajo y con una comparación muy favorable respecto a otros procesos empleados para obtener cianohidrinas quirales descritos recientemente. Además, con el proceso telescópico ideado y desarrollado se consigue una productividad, tanto de los procesos separados como del global, comparable o superior a la de otros procesos recientemente publicados.

# Supported Ionic Liquid-Like Phases (SILLPs) as immobilised catalysts for the Multistep and Multicatalytic Continuous Flow Synthesis of Chiral Cyanohydrins.

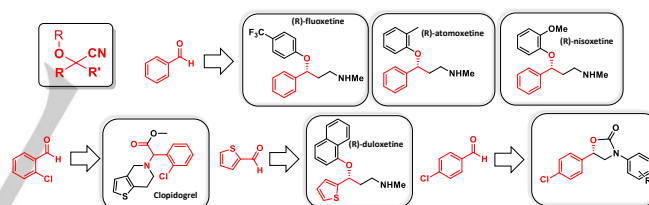
Edgar Peris, Raúl Porcar, María Isabel Burguete, Eduardo García-Verdugo\* and Santiago V. Luis\*.

**Abstract:** Supported Ionic Liquid-Like Phases have been found to be efficient organocatalysts for the synthesis of cyanohydrin esters under solvent-free conditions by an “electrophile–nucleophile dual activation” based on hydrogen bond formation. The combination of multiple and consecutive multicatalytic steps in a single and integrated cascade process of organocatalytic SILLPs with commercially available supported CAL-B has allowed developing an efficient process for the multicatalytic synthesis of enantiopure cyanohydrins under flow conditions.

## Introduction

Ionic Liquids (ILs) have emerged as exceptionally interesting systems in many fields, including their use as reaction media for catalytic processes.<sup>1,2,3</sup> In this context, a great effort has been devoted to develop ILs with modified functionalities (Task-Specific ILs-TSILs) in order to introduce groups providing Brønsted and Lewis acidic or basic behaviour, organocatalytic or organometallic properties, all of which can display a catalytic activity.<sup>4</sup> In the search of practical applications of these catalytically active TSILs, the full recovery of the catalytic system needs to be always considered. Therefore, the use of supported IL-phases has gained importance in this field.<sup>5,6,7,8</sup> For this purpose, the covalent attachment of IL-phases to an organic polymeric support has been demonstrated to transfer to the surface of the polymer some of the main features of ILs at the molecular level (stability, tuneable polarity, etc.) while avoiding the possibility of leaching.<sup>9,10,11</sup> On the other hand, the presence of the polymeric backbone offers an additional design vector to optimise the macroscopic and process properties of the overall catalytic system.<sup>12,13</sup> Indeed, these supported ionic-liquid like phases (SILLPs) can be applied as “solid ionic solvents” for catalytic processes in an analogous way to bulk ILs but simplifying product isolation and recycling of the catalyst-IL-phase. As for bulk ILs, structural changes/modifications in both cation and anion result in widely varying properties of the supported ILs, allowing their tuning for the specific needs of a given catalytic process.<sup>14,15</sup> This approach combines the advantages of ILs as catalyst supports and modifiers with the

use of solid phase chemistry, enabling not only flow processes,<sup>16,17,18,19,20,21,22,23,24,25,26</sup> but the development of one-pot multicatalytic multi-component transformations integrating several synthetic reactions in a single process.<sup>27,28</sup> The inspiration for this strategy is the biosynthetic machinery operating in nature, where potentially incompatible chemical transformations are separated by compartmentalisation, with reactive intermediates being passed from one unit to the next one. Although past decades have seen a significant progress in this direction, one-pot multicatalytic reactions are still not of general application.<sup>29</sup> The one-pot combination of catalytic and biocatalytic processes is an even more challenging issue. Although different strategies have been assayed to circumvent their mutual inactivation,<sup>30,31</sup> the strong potential negative interferences between the components of both systems (reagents, products and catalysts) and the conditions needed for both processes have often hampered the development of one-pot sequential telescoped synthetic processes of this nature.



**Figure 1.** Structure of drugs synthesisable through cyanosilylation of different aldehydes.

Here we report a simple methodology for the continuous flow synthesis of cyanohydrins based on the combination of multiple and consecutive multicatalytic steps in a single and integrated cascade process, where organocatalysts based on so-called Supported Ionic Liquid-Like Phases play a key role. The combination of organocatalytic SILLPs with commercially available supported CALB has allowed developing an efficient process for the multicatalytic synthesis of enantiopure cyanohydrins under flow conditions.

## Results and Discussion

Cyanohydrins have considerable synthetic potential as chiral building blocks allowing their transformation into a large number of chiral molecules, especially in the field of pharmaceuticals and agrochemicals.<sup>32</sup> Different methodologies have been developed for their synthesis in both racemic and enantiopure forms. A majority of methods reported for the preparation of

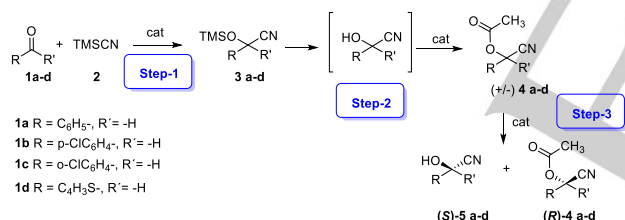
[a] Prof. S. V. Luis, Dr. E. García-Verdugo  
Department of Inorganic and Organic Chemistry, Supramolecular and Sustainable Chemistry Group, Universitat Jaume I, Avda Sos Baynat s/n, E-12071-Castellón. Spain.  
E-mail: [luis@uji.es](mailto:luis@uji.es), [cepeda@uji.es](mailto:cepeda@uji.es)

Supporting information for this article is given via a link at the end of the document.

enantiopure cyanohydrins are based on the asymmetric addition of a cyanide derivative, such as a silyl cyanide, a cyanophosphate, a cyanophosphate, or an acyl cyanide, to a prochiral carbonyl compound by using a (chiral) Lewis acid or a Lewis base catalyst or a combination of both types of catalysts.<sup>33,34</sup> Alternatively, HCN biocatalytic addition has been shown to provide high selectivity to a variety of prochiral aldehydes. These two methods, however, present some limitations. The first one requires the use of expensive chiral organometallic systems, while for the biocatalytic approach, albeit being more environmentally friendly,<sup>35</sup> the reversibility of the reaction may cause deterioration of the enantiomeric excess.<sup>36,37</sup> Thus, the design of simple and highly enantioselective processes with a low environmental footprint is still needed.

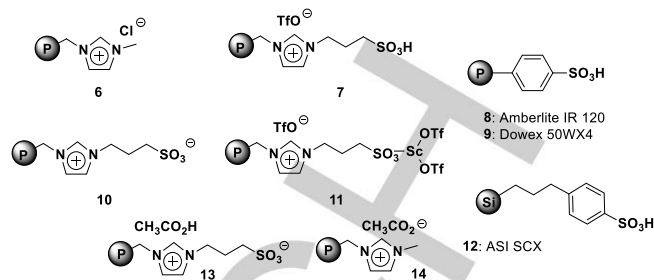
In this study, four specific different aldehydes (**1-4**) for which the corresponding cyanohydrins are key intermediates for the total synthesis of different commercial drugs (Figure 1) were selected as the starting materials.<sup>38</sup>

Scheme 1 depicts the general synthetic methodology proposed to obtain the corresponding chiral cyanohydrins from simple available aldehydes. The process requires three consecutive steps involving four catalytic reactions: 1) organocatalytic cyanosilylation of the aldehydes; 2) transformation into the corresponding methyl ester, which requires two consecutive reactions, first the hydrolysis of the cyanosilyl ether and then the formation of the corresponding ester; 3) the enzymatic kinetic resolution of the resulting cyanohydrin ester by transesterification in presence of alcohol. In this way, at least three different catalysts are required to develop a single-pot process.



**Scheme 1.** Synthesis of chiral cyanohydrins by multiple catalytic cascade reactions.

It has been recently reported that Supported Ionic Liquid-Like Phases (SILLPs) can efficiently catalyse the cyanosilylation reaction of aldehydes and ketones (step-1).<sup>39</sup> Table 1 shows that by using **6** (Figure 2) as a simple supported organocatalyst the four aldehydes considered could be converted into the corresponding cyanosilyl ethers (**3a-d**) with excellent yields. This methodology allows the first synthetic step to proceed with excellent yield, 100% atom economy, no waste regarding the side-products formation and unconverted reactants, use of solvent-free conditions, excellent catalytic activity, and no requirement for purification before performing the next step.



**Figure 2.** Catalysts assayed for the different steps of the overall process.

Step-2 involving the consecutive hydrolysis of the cyanosilyl ether and the formation of the corresponding acetyl ester requires a catalyst able to facilitate both reactions. Figure 2 illustrates the structure of the catalysts **7-14** evaluated for this step under batch conditions. The screening was performed in the absence and presence of acetic anhydride (Ac<sub>2</sub>O) to evaluate the intrinsic activity of the catalyst for the silyl ether hydrolysis (in the absence of Ac<sub>2</sub>O) and, alternatively, for the two consecutive reactions (in the presence of 2 eq. of Ac<sub>2</sub>O). The trimethylsilyl cyano ether (**3a**) derived from benzaldehyde (step-1) was used as the model substrate for such screening under solvent free conditions.<sup>40</sup> The commercially available polymeric supported sulfonic acids assayed (**8** and **9**) were able to promote the quantitative hydrolysis of the silyl ether group, but not the acetylation of the resulting cyanohydrin (< 10%). The water absorbed on the catalyst is likely to favour the hydrolysis of the silyl ether while inhibiting ester formation (Table S1, entries 1 and 3). Indeed, the opposite trend was observed when these catalysts (**8** and **9**) were vacuum dried for 24 hours. The reaction performed in the absence of Ac<sub>2</sub>O was inhibited (< 15%), while in the presence of Ac<sub>2</sub>O the consecutive catalysed desilylation and ester formation took place (>90%, Table S1, entries 2 and 4). The related silica-immobilised sulfonic catalyst (**12**) was also an active catalyst displaying a good performance for the two tested reactions (> 90%, Table S1, entry 5).

In the search of alternative catalytic systems, ILs and task specific ILs have been used to catalyse both ester formation,<sup>41,42</sup> and the desilylation reaction.<sup>43</sup> It has been also reported that Sc(OTf)<sub>3</sub>/Ac<sub>2</sub>O mixtures can be efficient systems for the consecutive desilylation and acetylation of sugars and this mixture was also very efficient in our case (entry 6 in Table S1).<sup>44,45</sup> In view of these precedents, we prepared a series of task-specific SILLPs (**7**, **10**, **11**, **13**, **14** Figure 2) as potential catalysts for the second step. Unfortunately, the initial screening of the catalyst **7** indicated that it was neither efficient for the hydrolysis nor for the esterification in the presence of Ac<sub>2</sub>O (Table S1, entry 8). However, the related Sc complex formed by reaction with Sc(OTf)<sub>3</sub> and the zwitterionic SILLP **10** led to moderate results for the consecutive desilylation and acetylation reactions (Table S1, entry 7). In the case of catalyst **13**, prepared by treating SILLP **10** with acetic acid, initial results showed also a moderated activity (Table S1, entry 9) for both coupled reactions. Interestingly, while for catalyst **10** a significant loss of activity was observed with reuse (Figure S1b), the reuse of catalyst **13** under the same conditions showed an

increase in its activity in such a way that after four reuses yields > 95 % were obtained for the synthesis of the corresponding cyano ester (Figure S1a). The catalyst **14** was also active for synthesis of the cyano ester **4a** (Table S1, entry 11). Summarising, at least four supported catalytic systems (**11**, **12**, **13** and **14**) were effective for the consecutive desilylation and acetylation reactions required for the step 2 of our proposed telescoping synthesis.

We also evaluate the direct preparation of cyanohydrin acetal ester (**4a**) by the reaction of benzaldehyde with acetyl cyanide under solvent free conditions and using different catalysts (Table S3, SI). The catalysts tested were less efficient providing lower yields than the two step reaction using TMSCN and Ac<sub>2</sub>O as reagents and the catalysts based on SILLPs.

The final step can be achieved by the use of an enzymatic catalyst.<sup>46</sup> Thus, the enantioselective hydrolysis of the racemic mandelonitrile acetate ((±)-**4a**) in the presence of *n*-propanol and using 2-methyl-tetrahydrofuran (2-Me-THF) as the solvent was considered. The immobilised commercially available Lipase B from *Candida Antarctica* (Novozym 435) could be used to transform the racemic cyanohydrin acetate into a mixture of (*S*)-cyanohydrin and (*R*)-mandelonitrile acetate (> 99.9 % ee), with a conversion slightly higher than 50% (Table 1, entry 1). The effect of the concentration of the racemic mandelonitrile acetate was then investigated (Table S2). Concentrated solutions, up to 1 M, of *rac*-mandelonitrile acetate could be used with good conversions (55%) and enantioselectivities (> 99% ee for **4a**, Table S2, entry 2). The use of more concentrated solutions of *n*-propanol (2 M in 2-Me-THF), however, produced a decrease on the enantioselectivity of the kinetic resolution (KR) (52% ee for **4a**, Table S2, entry 3).

**Table 1.** Batch multistep consecutive synthesis of cyanohydrins

Entry	Substrate		Step-1 <sup>[e]</sup>	Step-2 <sup>[f]</sup>	Step-3 <sup>[g]</sup>	% ee
	R	R'	Yield (%) <sup>[a]</sup>	Yield (%) <sup>[b]</sup>	Yield (%) <sup>[c]</sup>	
1	C <sub>6</sub> H <sub>5</sub> -	H	99	99	56	>99
2	<i>p</i> -ClC <sub>6</sub> H <sub>4</sub> -	H	95	99	57	>99
3	<i>o</i> -ClC <sub>6</sub> H <sub>4</sub> -	H	95	99	51	>99
4	C <sub>4</sub> H <sub>9</sub> S-	H	95	99	52	>99

[a] Conditions: 1 eq R'COR, 1.2 eq TMSCN; rt, 24 h, Cat: 25 mg per mmol of R'COR. [b] Conditions: 1 eq substrate, 2 eq Ac<sub>2</sub>O, 40°C, 24 h, 50 mg of cat. per mmol of substrate. [c] Conditions: 9.8 mL 2-Me-THF, 0.15 mL *n*-propanol and 100 mg CAL-B (Novozym 435) per mmol of substrate, 60°C, 24h, yield for **5a-d**. [d] e.e. for **4a-d**; e.e.>95 % for **5a-d**. [e] Catalysed by **6**. [f] Catalysed by **11**. [g] Catalysed by Novozym 435.

Table 1 summarises the results obtained when the catalysts **6**, **11** and Novozym 435 were applied for the synthesis, under batch conditions, of the corresponding cyanohydrins from aldehydes **1-4**. The results demonstrate that it is possible to obtain the corresponding cyanosilyl ethers (**3a-d**) and the corresponding racemic cyanohydrin esters (**4a-d**) with excellent yields (>90%) independently of the aldehyde used. Noteworthy, the first and second steps were performed under solvent-free conditions, where the single purification performed before the subsequent step was the filtration of the corresponding solid

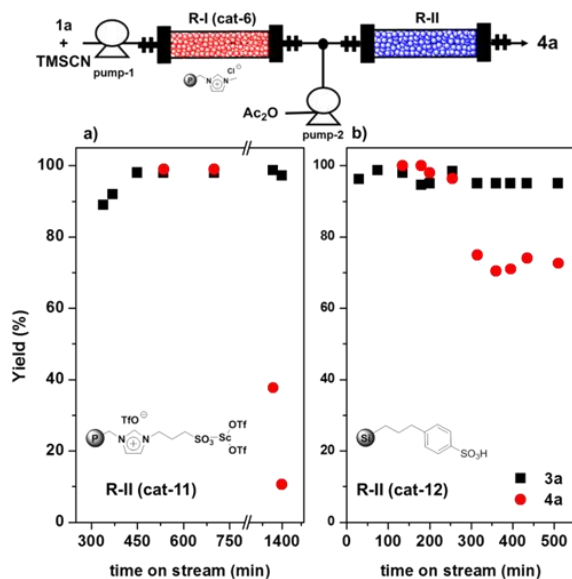
catalysts. The kinetic enzymatic resolution of the cyanohydrin esters was able to selectively hydrolyse the racemic esters to yield the (*S*)-enantiomer of the cyanohydrins and leaving the corresponding (*R*)-cyanohydrin acetates (with an enantiomeric excess >99.9 %).

These results demonstrate that it is possible to perform the synthesis of the enantiopure cyanohydrins by three consecutive catalytic steps under batch conditions. However, when the single-pot multistep catalytic cascade reaction was evaluated, using a combination of the different catalytic systems, the single process fail. Indeed, even when different protocols were assayed for the consecutive addition of the catalysts and/or reagents, the global process proceeded with low conversion and/or low enantioselection. Thus, the single-pot multistep catalytic process is not feasible under batch conditions due to the incompatibility between the enzymatic catalyst and some of the reagents and/or catalysts involved in the global synthetic sequence.

A simple approach to enable cascade or concurrent chemoenzymatic reactions to occur without mutual inactivation is to compartmentalise the different catalytic systems. This approach shields the catalytic centers from one another.<sup>30,31,47,48</sup>

The use of consecutive fixed-bed reactors can provide the required isolation of the catalysts by compartmentalisation and to favor the simple and continuous production of the chiral target without the need for isolation of any intermediates and without requiring the separation of any catalysts, co-products, by-products, and excess reagents.<sup>16,27,28,49,50</sup>

Thus, the use of a continuous flow process using benzaldehyde as the starting material to perform a telescoping synthesis of the corresponding cyanohydrin was evaluated. Accordingly, the continuous synthesis of the cyanohydrin esters using two fixed-bed reactors coupled together in-line was initially evaluated. The first reactor (**R-I**) was packed with catalyst **6**, and a neat mixture of benzaldehyde and TMSCN (1:1.1 molar ratio) was pumped at 0.01 mL min<sup>-1</sup>. A second reactor (**R-II**) filled with catalyst **11** was connected at the exit of **R-I** by means a T-piece, which also allowed to mix the silyl ether coming out from **R-I** with a stream containing acetic anhydride. The flow of this stream was adjusted to a flow rate (0.009 mL min<sup>-1</sup>) matching to 2 equivalents of Ac<sub>2</sub>O per each equivalent of the silyl ether coming out from **R-I**. Although catalyst **11** was able to simultaneously hydrolyse the silyl ether and to form the corresponding ester yielding the desired *rac*-mandelonitrile acetate, it did not show a long-term stability. A strong deactivation of **11** was observed after 24 hours of continuous use on stream (Figure 3a). After this time, the main product collected at the outlet of the two reactors was the cyanosilyl ether, indicating that though the second reactor was not stable enough, **R-I** was still active. Indeed, this reactor (**R-I**) was stable for at least 50 hours, with > 95 % yields, with the productivity for this period being ca. 24 g of product / g of catalyst.



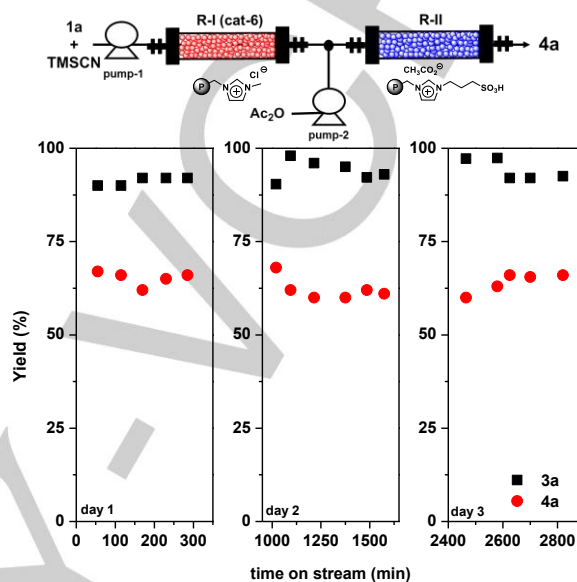
**Figure 3.** Evaluation of the catalyst stability for the two-step synthesis of racemic mandelonitrile acetate (**4a**) under continuous flow conditions. Black squares: yield for step-1 after R-I; Red dots: yield for step-2 after R-II. a) step 1: R-I: 1 g catalyst **6**, 0.01 mL min<sup>-1</sup>, r.t.; step 2: R-II: 1 g catalyst **11**, 0.019 mL min<sup>-1</sup>. b) step 1: R-I: 1 g catalyst **6**, 0.01 mL min<sup>-1</sup>, r.t.; step 2: R-II: 1 g catalyst **12**, 0.02 mL min<sup>-1</sup> 1a:TMSCN:Ac<sub>2</sub>O 1:1.1:1.2 (molar ratio).

In order to confirm the deactivation suffered by the catalyst **11**, a mixture of the cyanosilyl ether (**3a**) and Ac<sub>2</sub>O (1:1.2 eq.) was pumped directly through R-II at 0.02 mL min<sup>-1</sup>. The catalyst was stable during the 3 first hours with yields >99%. However, after an additional period of 24 hours on stream, the yield dropped to < 30%. These results highlight the importance of assessing the long term stability of the catalyst for flow processes. Even catalysts that are active for consecutive runs under batch conditions might be not suitable for prolonged used under continuous flow. In the light of the former results, other active catalysts were evaluated for step-2 taking into consideration the results previously discussed (according to results in Table S1). Thus, an alternative R-II fix-bed reactor was prepared with the commercially available silica-based sulfonic acid catalyst **12** and the reaction mixture was pumped through it at a flow rate of 0.02 mL min<sup>-1</sup>. The catalyst was still active after 20 hour of continuous use, although after 5 hours on stream the activity dropped from > 95% to 70% (Figure 3b).

Finally, catalyst **13** displayed a constant catalytic performance with a stable yield for **4a** of ca. 65% for more than 40 hours of continuous use under flow conditions (Figure 4). At the view of the stable performance of this catalyst, the improvement in the obtained yield was assayed by adjusting the experimental conditions. Indeed, an increase of the excess of the Ac<sub>2</sub>O used from 1.2 to 2 equivalents rendered an improvement of the yield from ca. 65% to ca. 90%, suggesting SILLP **13** as a suitable catalyst for step-2.

The different stability of the catalysts can be rationalised attending their differences at the molecular level. The catalyst **11** is a metallic salt with Lewis acid properties that in the presence

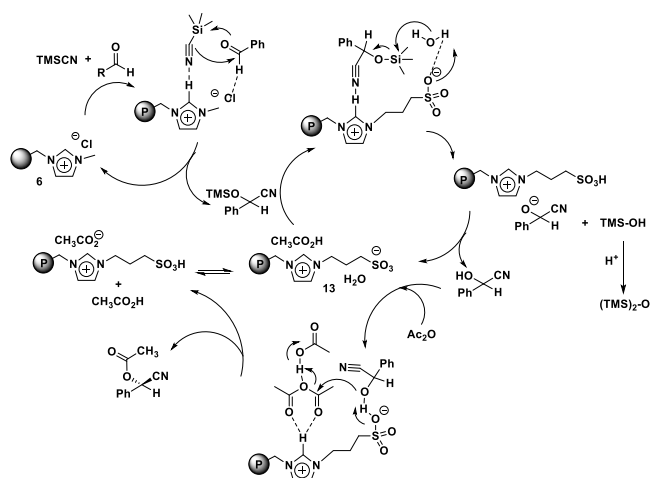
of an excess of acetic acid can lead to a significant scandium leaching. Indeed, an increase in the amount of Ac<sub>2</sub>O used in the reaction from 1.2 to 2 equivalents led to a faster catalyst deactivation. Regarding the solid sulfonic acid catalyst **12**, its partial deactivation can be associated to the lack of efficient regeneration of the Brønsted acidity in the catalytic cycle.



**Figure 4.** Evaluation of the catalyst stability for the two-step synthesis of racemic mandelonitrile acetate (**4a**) under continuous flow conditions. Black squares: yield for step-1 after R-I; Red dots: yield for step-2 after R-II. a) step-1: R-I: 1 g catalyst **6**, 0.01 mL min<sup>-1</sup>, r.t.; step-2: R-II: 1 g catalyst **13**, 0.019 mL min<sup>-1</sup>. 1a:TMSCN:Ac<sub>2</sub>O 1:1.1:1.2.

On the contrary, the bifunctional SILLP **13** can work as a dual catalyst with a dramatic anion–cation cooperative effect and a catalytically efficient combination of acidic and basic sites. As detected by TGA SILLP **13** contains ca. 5% of water and ca. 2% of acetic acid (see Figure S2). The acid sites, in the presence of some water, can hydrolyse the cyanosilyl ether to yield the corresponding alcohol.<sup>51</sup> On the other hand, the C-2 hydrogen at the imidazolium moiety can also contribute to the electrophilic activation of the carbonyl group of Ac<sub>2</sub>O through hydrogen bond formation. The efficient transformation of the initially formed trimethyl silyl alcohol (TMSOH) into the corresponding ether (TMS<sub>2</sub>O) is essential to regenerate the catalytic water needed for the hydrolysis, which seems to be facilitated by the presence of acetic acid molecules in **13**. An acetic acid molecule can also play a key role in the acylation step by activating the Ac<sub>2</sub>O through hydrogen bonding.<sup>52,53</sup> Therefore, the cation of the SILLP and the acetic acid activate the electrophile, as hydrogen bond donors, while the anion activates the nucleophile, as hydrogen bond acceptor. The importance of the dual nature of catalyst **13** is demonstrated by comparing its catalytic activity with the one for a mixture of **8** and **14**, a SILLP containing acetate as the counteranion. The mixed system is catalytically active but its activity decreases with the

reuse (Figure S3a) and the same is observed for **14** (Figure S3b).



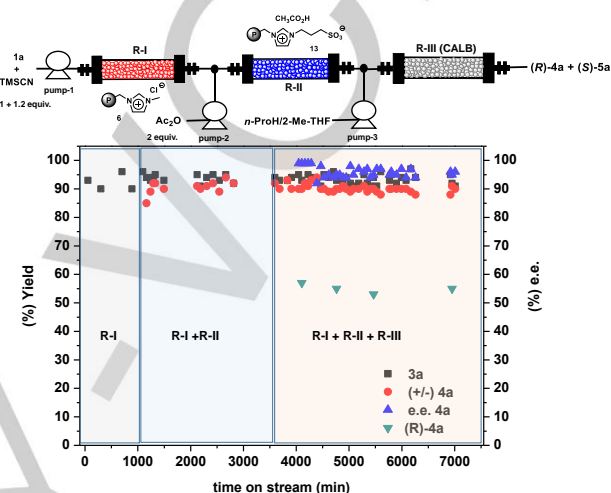
**Figure 5.** Mechanistic model for the consecutive processes involved in the synthesis of cyanohydrin catalysed by SILLPs **6** and **13**.

A plausible reaction mechanism is presented in Figure 5 based on this dual activation effect. Here the SILLP is acting in a similar fashion than related ILs in solution by an “electrophile–nucleophile dual activation” through a cooperative hydrogen-bonded network.<sup>54,55,56,57</sup> These results confirmed that supported ionic liquid phases are able to mimic the catalytic behavior found for bulk ILs with the additional advantages of needing a smaller amount of IL, an easier isolation and recycling and the possibility to work under continuous flow conditions.

The last step to complete the process is the continuous kinetic resolution of the cyanohydrin ester obtained after the second step. This process is a well established reaction under batch conditions.<sup>58</sup> A bioreactor was prepared as a fix bed reactor with Novozyme 435 (**R-III**) to evaluate the feasibility of this approach. A solution of the racemic cyanohydrin ester **4a** in 2-Me-THF (0.1 M) and *n*-propanol as the transesterification agent (2 equiv., 0.2 M) was pumped through the catalytic bed (**R-III**) at 60 °C and 40 bar. Thus, for a total flow rate of 0.35 mL/min, an excellent and selective conversion of the cyanohydrin ester to the corresponding alcohol (ca. 48% yield for the alcohol) was found, with excellent enantiopurities for both the (*R*)-acetylated mandelonitrile (95% e.e.) and the hydrolyzed (*S*)-mandelonitrile (>99% e.e., Figure S4). Thus, these results demonstrated the feasibility of the KR of the racemic acetylated mandelonitrile under continuous conditions. At the view of these results, the telescoped synthesis of cyanohydrin was assayed by using three consecutive fix bed reactors (**R-I**, **R-II** and **R-III**) packed respectively with the organocatalytic SILLPs **6** and **13** and with Novozym 435 as the supported biocatalyst. The results obtained for this set-up are summarized in Figure 6.

The reactors were coupled sequentially after each reactor had reached the steady state without including any separation step. Thus, the reactor **R-II** was connected to **R-I** after 1000 min, when the first reaction was taking place with yields > 90% to

afford the cyanosilyl ether **3a**. In a similar way, **R-III** was attached to the two previous ones after 3700 min, when the corresponding acetate ((±)-**4a**) was obtained with > 90% conversion. In the last reactor, the racemic acetate was kinetically resolved by the action of the enzyme, which selectively hydrolysed the racemic esters to yield the (*S*)-enantiomer of the cyanohydrin **5a** and the corresponding (*R*)-cyanohydrin acetate (**4a**) (with an enantiomeric excess >99 % for a conversion to **5a** slightly higher than 50%).



**Figure 6.** Evaluation of the catalyst stability for the multicatalytic synthesis of enantiopure mandelonitrile acetate ((*R*)-**4a**) under continuous flow conditions. Black squares: yield for step-1 after **R-I**; red dots: yield for step-2 after **R-II**; green triangles: yield for step-3 after **R-III**; blue triangles: enantioselectivity for the final product ((*R*)-**4a**) after **R-III**. Step-1: **R-I**: 1 g catalyst **6**, 0.01 mL min<sup>-1</sup>, rt; step-2: **R-II**: 1 g catalyst **13**, 0.019 mL min<sup>-1</sup>. **1a**: TMSCN:Ac<sub>2</sub>O 1:1.1:2; step-3: **R-III**: 1 g Novozym 435 (CALB), 60°C, flow 0.35 mL min<sup>-1</sup>, 0.1 M **4a** in Me-THF:IPA (0.85:0.15).

Noteworthy, it was possible to achieve efficiently a coupled process involving four consecutive reactions, which was not feasible as a single-pot process under batch conditions. The system was stable at least for two days (> 3000 minutes) of continuous use. Our results suggest that the combination of continuous flow processes, SILLPs as organocatalytic phases and biocatalysts can lead to an efficient process in terms of catalytic efficiency but also regarding the process productivity and sustainability. In this context, it should be mentioned that step-1 and its combination with step-2 (step1 + step-2) have remarkably low E factors (0.1 and 0.93 respectively, Table S4), which highlight the greenness of these two steps performed under solvent free conditions. The use of an additional organic solvent required in the KR step is reflected in the significant increase of the E factor (21.8 without considering solvent recovery). These values are however lower than those reported for other catalytic and biocatalytic methods (see Tables S5 and S6 in the SI) being inferior to the usual E values for a pharmaceutical product ranging from 25 to 100.<sup>59</sup> Regarding productivity, the obtained values for the individual steps range from 100 to 200 mg g<sup>-1</sup> h<sup>-1</sup>, being the biocatalytic step the one displaying the higher productivity. Overall, the space-time-yield

(STY) for the final step of the process, including the two chiral products of interest formed, is  $124 \text{ g g}^{-1}\text{cat. h}^{-1} \text{ L}^{-1}$ , a value that compares well for related biocatalytic processes described for the synthesis of cyanohydrins using hydroxynitrile liases and HCN, a more hazardous chemical reagent than TMSCN.<sup>60, 61</sup>

## Conclusions

In summary, the right combination of organocatalysts based on Supported Ionic Liquid-Like Phases with a biocatalyst allows successfully developing a valuable flow protocol for the multicatalytic, multistep, single-pot and metal-free synthesis of chiral cyanohydrins with good yield and enantioselectivity. Our studies also highlight the potential for catalytic applications of SILLPs designed with specific functionalities. An “electrophile–nucleophile dual activation” through a complex network of hydrogen bonding seems to be essential, in a similar way to that observed in bulk ILs. Hence, SILLPs might be regarded as “solid ionic solvents” or as nanostructured materials with microenvironments displaying the same characteristics, at molecular level, than their analogous ILs phases. Besides, their insoluble nature enables their use under continuous flow, allowing the possibility of combining organocatalytic and biocatalytic successive reactions to facilitate complex synthetic syntheses to occur in a single process, avoiding deactivation/incompatibility issues found in the related single-pot batch syntheses.

## Experimental Section

Experimental details are provided in the electronic supplementary information

## Acknowledgements

This work was partially supported by G. V. (PROMETEO 2016-071) and MINECO (CTQ2015-68429R). E. Peris thanks MICINN for the financial support (FPU13/00685).

**Keywords:** continuous flow • supported ionic liquids • biocatalyst • organocatalyst • cyanohydrin

- [1] *Ionic Liquids in Synthesis* (Eds.: P. Wasserscheid, T. Welton), Wiley-VCH, Weinheim, **2008**  
 [2] J. P. Hallett, T. Welton, *Chem. Rev.* **2011**, *111*, 3508–3576.  
 [3] J. Dupont, *Acc. Chem. Res.* **2011**, *44*, 1223–1231.  
 [4] C. Chiappe, C. S. Pomelli, *Eur. J. Org. Chem.* **2014**, 6120–6139.  
 [5] *Supported Ionic Liquids: Fundamentals and Applications* (Eds.: R. Fehrmann, A. Riisager, M. Haumann), Wiley-VCH, Weinheim, **2014**.  
 [6] F. Giacalone, M. Gruttadauria, *ChemCatChem* **2016**, *8*, 664–684.  
 [7] H. Li, P. S. Bhadury, B. Song, S. Yang, *RSC Adv.* **2012**, *2*, 12525–12551.  
 [8] C. Van Doorslaer, J. Wahlen, P. Mertens, K. Binnemans, D. De Vos, *Dalton Trans.* **2010**, 39, 8377–8390.  
 [9] M. I. Burguete, F. Galindo, E. García-Verdugo, N. Karbass, S. V. Luis, *Chem. Commun.* **2007**, 3086–3088.  
 [10] S. Zhang, K. Dokko, M. Watanabe, *Chem. Sci.* **2015**, *6*, 3684–3691.

- [11] V. Sans, N. Karbass, M. I. Burguete, V. Compañ, E. García-Verdugo, S. V. Luis, M. Pawlak, *Chem. Eur. J.* **2011**, *17*, 1894–1906.  
 [12] B. Altava, M. I. Burguete, J. M. Fraile, J. I. García, S. V. Luis, J. A. Mayoral, M. J. Vicent, *Angew. Chem. Int. Ed.* **2000**, *39*, 1503–1506.  
 [13] B. Altava, M. I. Burguete, E. García-Verdugo, S. V. Luis, M. J. Vicent, J. A. Mayoral, *React. Funct. Polym.* **2001**, *48*, 25–35.  
 [14] K. L. Luska, J. Julis, E. Stavitski, D. N. Zakharov, A. Adams, W. Leitner, *Chem. Sci.* **2014**, *5*, 4895–4905.  
 [15] K. L. Luska, P. Migowski, S. El Sayed, W. Leitner, *Angew. Chem. Int. Ed.* **2015**, *54*, 15750–15755.  
 [16] E. García-Verdugo, B. Altava, M. I. Burguete, P. Lozano, S. V. Luis, *Green Chem.* **2015**, *17*, 2693–2713.  
 [17] *Chemical Reactions and Processes under flow conditions* (Eds.: S. V. Luis, E. García-Verdugo), RSC Green Chemistry Series, **2010**.  
 [18] J. Britton, C. L. Raston, *Chem. Soc. Rev.* **2017**, *6*, 1250–1271.  
 [19] B. Gutmann, D. Cantillo, C. O. Kappe, *Angew. Chem. Int. Ed.* **2015**, *54*, 6688–6728.  
 [20] M. Baumann, I. R. Baxendale, *Beilstein J. Org. Chem.* **2015**, *11*, 1194–1219.  
 [21] S. V. Ley, D. E. Fitzpatrick, R. M. Myers, C. Battilocchio, R. J. Ingham, *Angew. Chem. Int. Ed.* **2015**, *54*, 10122–10136.  
 [22] M. I. Burguete, E. García-Verdugo, S. V. Luis, *Beilstein J. Org. Chem.* **2011**, *7*, 1347–1359.  
 [23] C. Rodríguez-Escrich, M. A. Pericàs, *Eur. J. Org. Chem.* **2015**, 1173–1188.  
 [24] F. G. Finelli, L. S. Miranda, R. O. M. A. de Souza, *Chem. Commun.* **2015**, 3708–3722.  
 [25] I. Atodiresei, C. Vila, M. Rueping, *ACS Catal.* **2015**, *5*, 1972–1985.  
 [26] R. Munirathinam, J. Huskens, W. Verboom, *Adv. Synth. Catal.* **2015**, *357*, 1093–1123.  
 [27] D. T. McQuade, P. H. Seeberger, *J. Org. Chem.* **2013**, *78*, 6384–6389.  
 [28] R. L. Hartman, J. P. McMullen, K. F. Jensen, *Angew. Chem. Int. Ed.* **2011**, *50*, 7502–7519.  
 [29] M. J. Climent, A. Corma, S. Iborra, M. J. Sabater, *ACS Catal.* **2014**, *4*, 870–891.  
 [30] C. A. Denard, J. F. Hartwig, H. Zhao, *ACS Catal.* **2013**, *3*, 2856–2864.  
 [31] M. Hönl, P. Sondermann, N. J. Turner, E. M. Carreira, *Angew. Chem. Int. Ed.* **2017**, *56*, 8942–8973.  
 [32] C. Moberg, E. Wingstrand, *Synlett* **2010**, 3, 355–367.  
 [33] M. North, *Tetrahedron: Asymmetry* **2003**, *14*, 147–176.  
 [34] N. H. Khan, R. I. Kureshy, S. H. R. Abdi, S. Agrawal, R. V. Jasra, *Coord. Chem. Rev.* **2008**, *252*, 593–623.  
 [35] G. Torrelo, N. van Midden, R. Stloukal, U. Hanefeld, *ChemCatChem* **2014**, *6*, 1096–1102.  
 [36] M. M. E. Delville, K. Koch, J. C. M. van Hest, F. P. J. T. Rutjes, *Org. Biomol. Chem.* **2015**, *13*, 1634–1638.  
 [37] A. Brahma, B. Musio, U. Ismayilova, N. Nikbin, S. B. Kamptmann, P. Siegert, G. E. Jeronim, S. V. Ley, M. Pohl, *Synlett* **2016**, 27, 262–266.  
 [38] R. K. Rej, T. Das, S. Hazra, S. Nanda, *Tetrahedron Asymmetry* **2013**, *24*, 913–918.  
 [39] S. Martín, R. Porcar, E. Peris, M. I. Burguete, E. García-Verdugo, S. V. Luis, *Green Chem.* **2014**, *16*, 1639–1647.  
 [40] R. D. Crouch, *Tetrahedron* **2013**, *69*, 2383–2417.  
 [41] J. Fraga-Dubreuil, K. Bourahl, M. Rahmounic, J. P. Bazureau, J. Hamelina, *Cat. Commun.* **2002**, *3*, 185–190.  
 [42] I. López, K. Bravo, M. Caraballo, J. L. Barneto, G. Silvero, *Tetrahedron Lett.* **2011**, *52*, 3339–3341.  
 [43] A. H. Jadhav, H. Kim, *Tetrahedron Lett.* **2012**, *53*, 5338–5342.  
 [44] W. Ke, D. M. Whitfield, *Carbohydr. Res.* **2004**, *339*, 2841–2850.  
 [45] S. Lee, J. H. Park, *J. Mol. Cat. A: Chem.* **2003**, *194*, 49–52.  
 [46] J. Holt, U. Hanefeld, *Curr. Org. Synth.* **2009**, *6*, 15–37.  
 [47] P. Lozano, E. García-Verdugo, N. Karbass, K. Montague, T. De Diego, M. I. Burguete, S. V. Luis, *Green Chem.* **2010**, *12*, 1803–1810.  
 [48] M. I. Burguete, E. García-Verdugo, F. Gelat, N. Karbass, S. V. Luis, V. Sans, *Adv. Synth. Cat.* **2010**, *352*, 3013–3021.  
 [49] T. Tsubogo, H. Oyamada, S. Kobayashi, *Nature* **2015**, *520*, 329–332.  
 [50] J. C. Pastre, D. L. Browne, S. V. Ley, *Chem. Soc. Rev.* **2013**, *42*, 8849–8869.  
 [51] S. Iimura, K. Manabe, S. Kobayashi, *J. Org. Chem.* **2003**, *68*, 8723–8725.  
 [52] A. Sarkar, S. R. Roy, N. Parikh, A. K. Chakraborti, *J. Org. Chem.* **2011**, *76*, 7132–7140.  
 [53] A. K. Chakraborti, S. R. Roy, *J. Am. Chem. Soc.* **2009**, *131*, 6902–6903.  
 [54] A. Aggarwal, N. L. Lancaster, A. R. Sethi, T. Welton, *Green Chemistry* **2002**, *4*, 517–520.  
 [55] A. Sarkar, S. R. Roy, A. K. Chakraborti, *Chem. Commun.* **2011**, *47*, 4538–4540.  
 [56] L. Zhang, X. Fu, G. Gao, *ChemCatChem* **2011**, *3*, 1359–1364.  
 [57] S. R. Roy, A. K. Chakraborti, *Org. Lett.* **2010**, *12*, 3866–3869



[58] L. Veum, M. Kuster, S. Telalovic, U. Hanefeld, T. Maschmeyer, *Eur. J. Org. Chem.* **2002**, 1516-1522.

[59] R. A. Sheldon, *Green Chem.* **2017**, *19*, 18-43.

[60] T. Purkarthofer, W. Skranc, C. Schuster, H. Griengl, *Appl. Microbiol. Biotechnol.* **2007**, *76*, 309-320.

[61] P. Bracco, H. Busch, J. von Langermann, U. Hanefeld, *Org. Biomol. Chem.* **2016**, *14*, 6375-6389.

WILEY-VCH

WILEY-VCH

## Electronic Supporting information

# Supported Ionic liquid-like Phases (SILLPs) as immobilised catalysts for the Multistep and Multicatalytic Continuous Flow Synthesis of Chiral Cyanohydrins

Edgar Peris, Raúl Porcar, María Isabel Burguete, Eduardo García-Verdugo,\* and Santiago V. Luis\*

Universitat Jaume I, Departamento de Química Inorgánica y Orgánica, Campus del Riu Sec, E-12071 Castellón, Spain

### Table of Contents

#### 1. General procedures.

#### 2. Tables.

**Table S.1.** Batch screening of the immobilized catalysts for the step-2.

**Table S.2.** Effect of the concentration on the KR of *rac*-mandelonitrile acetate with Novozyne-435 and *n*-propanol in 2-Me-THF.

**Table S.3.** Alternative one-step synthesis of cyanohydrins esters.

**Table S.4.** E factor calculation for the multistep and multicatalytic continuous flow synthesis of chiral cyanohydrins.

**Table S.5.** E factor comparison between our process and other ones described on the literature in the recent years.

**Table S.6.** E factor comparison between our global process and other enzymatic resolutions of racemic mandelonitrile described on the literature in the recent years.

#### 3. Figures.

**Figure S.1.** Stability catalyst evaluation for the synthesis of racemic mandelonitrile acetate **4a**.

**Figure S.2.** TGA for **10** and **13**.

**Figure S.3.** Stability catalyst evaluation for the synthesis of the racemic mandelonitrile acetate **4a** (step 2). a) catalysed by **8** + **14**. b) Catalyzed by **14**.

**Figure S.4.** Stability catalyst evaluation for Kinetic Resolution of racemic mandelonitrile acetate (**4a**) under continuous flow conditions.

**Figure S.5.** Setup used for the multistep and multicatalytic continuous flow synthesis of chiral cyanohydrins.

**4. Synthesis of Polymer-supported. Catalysts and Characterization.**

**5. General procedure for reactions.**

**6. NMR Spectra, HPLC and GC conditions.**

## 1. General procedures.

Reagents were supplied by Aldrich and were used without further purification.  $^1\text{H-NMR}$  experiments were obtained using Varian INOVA 500 ( $^1\text{H}$ , 500 MHz) or Varian MERCURY 300 ( $^1\text{H}$ , 300 MHz) spectrometer. The chemical shifts are given in delta ( $\delta$ ) values (ppm). Samples were analysed by GC VARIAN 3900. FTIR spectra were acquired with a MIRacle single-reflection ATR diamond/ZnSe accessory or KBr. High performance liquid chromatography (HPLC) analyses were carried out in a Merck HITACHI LaChrom chromatograph UV detector at 210 nm using a Daicel CHIRALCEL OD-H column (25 cm  $\times$  4.6 mm I.D.).

## 2. Tables.

**Table S.1.** Batch screening of immobilised catalysts for the step-2.

Entry	Cat.	Hydrolysis <sup>a</sup>	Hydrolysis+ Acetylation <sup>b</sup>
1	<b>8</b>	99	n.t.
2	<b>8<sup>c</sup></b>	15	96
3	<b>9</b>	99	10
4	<b>9<sup>c</sup></b>	7	93
5	<b>12</b>	99	99
6	Sc(OTf) <sub>3</sub>	n.t.	100
7	<b>11</b>	0	100
8	<b>7</b>	14	10
9	<b>10</b>	n.t.	70
10	<b>13</b>	99	64
11	<b>14</b>	n.t.	99

<sup>a</sup> Solvent free conditions, 50 mg of cat. per mmol of cyanosilyl ether, 60°C, 24 hours.

<sup>b</sup> Solvent free conditions, 50 mg of cat. per mmol of cyanosilyl ether and 2 eq. of Ac<sub>2</sub>O, 60°C, 24 hours.

<sup>c</sup> Catalyst dried at 40 °C and high vacuum till constant weight.

n.t. = not tested.

**Table S.2.** Effect of the concentration on the KR of *rac*-mandelonitrile acetate with Novozym-435 and *n*-propanol in 2-Me-THF.

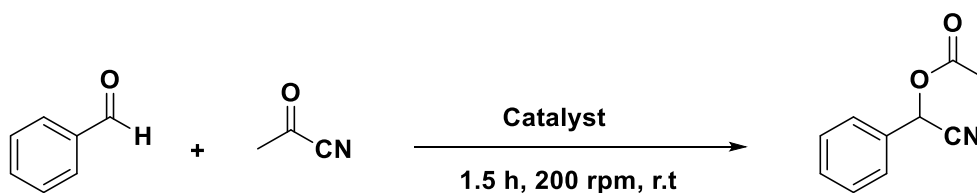
Entry	Concentration (M)	Conversion (%)	e.e.(%) (R)-ROAc-X
1	0.1 <sup>a</sup>	65	>99
2	1 <sup>b</sup>	55	>99
3	2 <sup>b</sup>	<50	52

<sup>a</sup> Conditions: 10 mL 2-Me-THF, 0.15 mL *n*-propanol and 100 mg CAL-B (Novozym 435) per mmol of substrate, 60 °C, 24 hours.

<sup>b</sup> Conditions: 1 mL 2-Me-THF, 0.15 mL *n*-propanol and 100 mg CAL-B (Novozym 435) per mmol of substrate, 60 °C, 24 hours.

<sup>c</sup> Conditions: 0.5 mL 2-Me-THF, 0.15 mL *n*-propanol and 100 mg CAL-B (Novozym 435) per mmol of substrate, 60 °C, 24 hours.

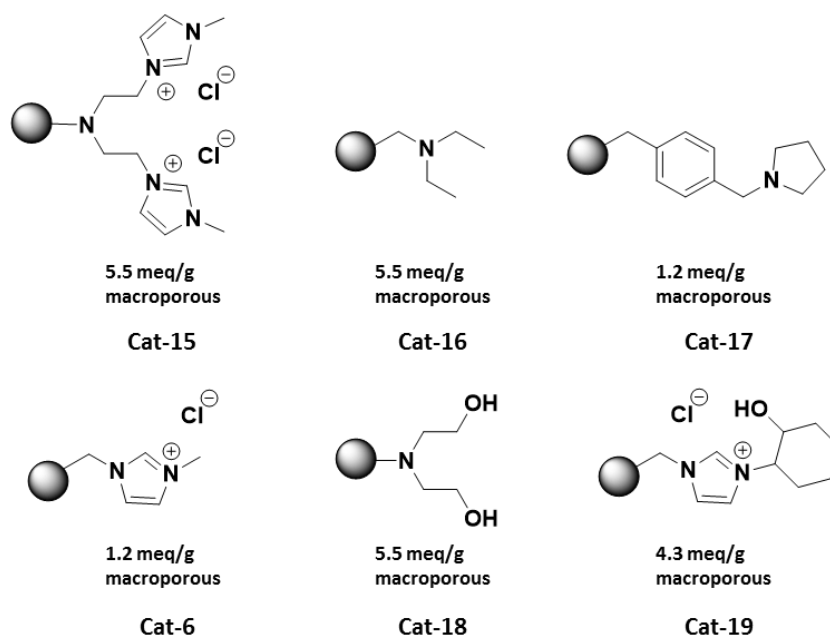
**Table S.3.** Alternative one-step synthesis of cyanohydrins esters.



Conditions: 1eq benzaldehyde (3 mmol, 306  $\mu$ L), 1.1eq acetyl cyanide (3.33 mmol, 236  $\mu$ L).

Catalyst	Amount (mg)	Yield(%) <sup>a</sup>
Et <sub>3</sub> N	31	68
Cat-15	55.5	0
Cat-16	57.6	56
Cat-17	258.2	36
Cat-6	256.5	0
Cat-18	55.5	26
Cat-19	133.2	0
CAL-B	103.3	0

<sup>a</sup> Yields were calculated by <sup>1</sup>H-NMR (CDCl<sub>3</sub>)



**Table S.4.** E factor calculation for the multistep and multicatalytic continuous flow synthesis of enantiopure mandelonitrile acetate ((*R*)-4a) (Figure 6 from the main paper).

Step	mmol waste/min	mmol product/min	E factor <sup>c</sup>
1	0.0015	0.015	0.1
1+2	0.037	0.04	0.93
1+2+3	0.436	0.02 <sup>a</sup>	21.8 <sup>b</sup>

<sup>a</sup> The calculation included as waste solvent used in the synthesis, side products and unreacted reagents. Only the product mandelonitrile acetate ((*R*)-4a) is considered for the calculation of the E factor.

<sup>b</sup> Lower than the average value for the pharmaceutical industry (25-100).

<sup>c</sup> E factor = (mmol waste/min) / (mmol product/min).

**Table S.5.** E factor comparison between our process and another ones described on the literature in the recent years. For comparison synthetic methods for the asymmetric synthesis of **3a** and **4b** were selected from the literature

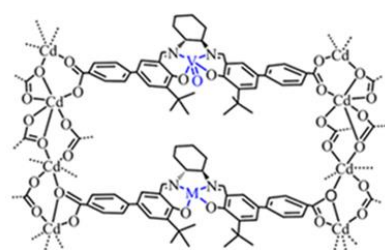
Process reference	Catalyst	e.e. (%)	E factor
this paper	SILLPs/CALB	99 ( <b>4a</b> )	21.8
ACS Catal., 2016, 6, 7590-7596 <sup>a</sup>	VO-Salen-MOF (Cat-20)	86 ( <b>3a</b> )	76.2
Chem. Commun., 2000, 1963-1964 <sup>b</sup>	N-sulfonylated $\beta$ -amino alcohols- Ti(O <i>i</i> -Pr) <sub>4</sub> (Cat-21)	68 ( <b>3a</b> )	69.0
Angew. Chem., Int. Ed. 2010, 49, 6746-6750 <sup>c</sup>	Salen-Ti (Cat-22)	96 ( <b>4a</b> )	25
J. Org. Chem., 2004, 69, 7910-7913 <sup>d</sup>	$\beta$ -amino-alcohol-Ti(O <i>i</i> -Pr) <sub>4</sub> (Cat-23)	92 ( <b>3a</b> )	33.0

<sup>a</sup> 0.25mmol benzaldehyde, 0.375mmol TMSCN (1.5eq), 1ml toluene, 0.5%mol catalyst at -78°C

<sup>b</sup> 0.5mmol benzaldehyde, 1.5mmol TMSCN (3eq), 2ml DCM, 0.05mmol catalyst at 0°C

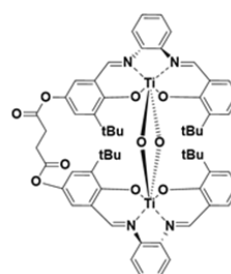
<sup>c</sup> 2.5mmol benzaldehyde, 2.75mmol TMSCN (1.1eq), 3ml DCM, 0.05% mol catalyst at 25°C

<sup>d</sup> 0.25mmol benzaldehyde, 0.5mmol TMSCN (2eq), 0.5ml DCM, 0.0125ml toluene, 10% mol catalyst at -20°C.

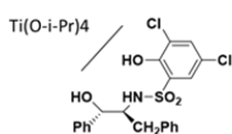


M = VO

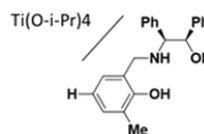
**Cat-20**



**Cat-21**



**Cat-22**



**Cat-23**



**Table S.6.** E factor comparison between our global process and other enzymatic resolutions of racemic mandelonitrile described on the literature in the recent years.

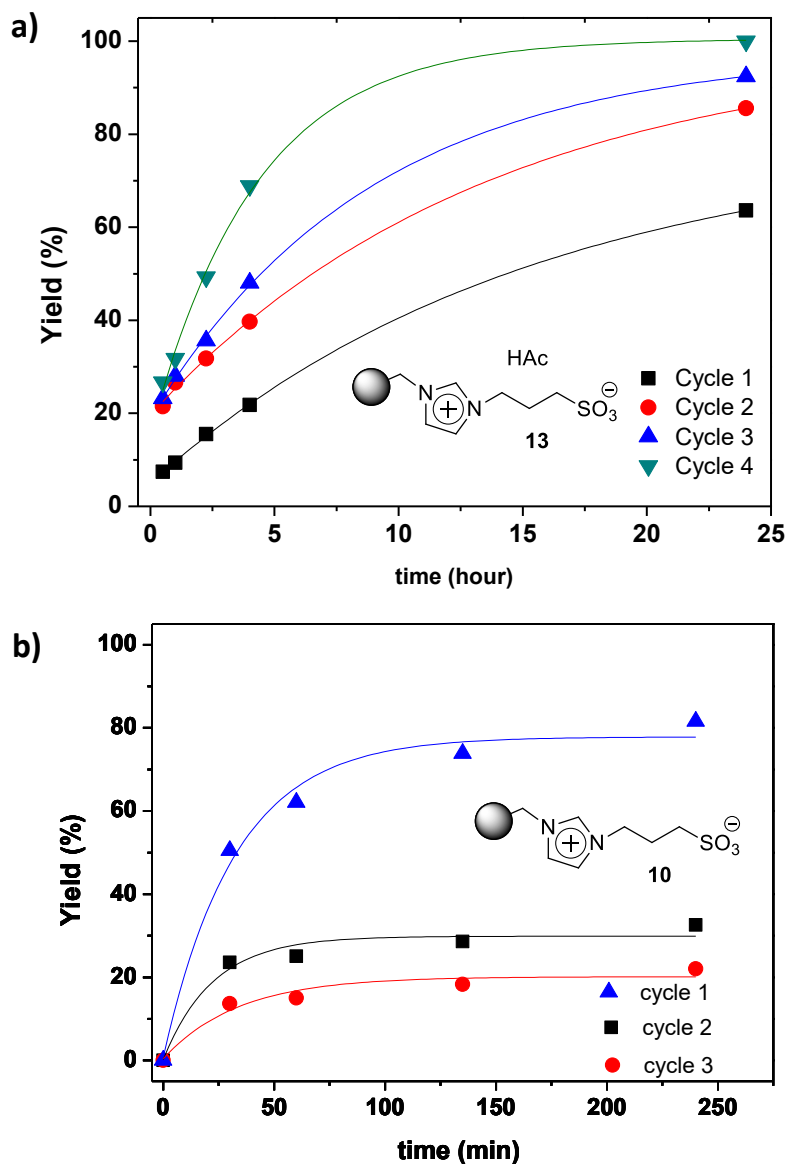
Process reference	E factor
this paper	21.8
Synlett., 2000, 1775-1776 <sup>a</sup>	95.0
Tetrahedron Asymmetry, 2002, 13, 739-743 <sup>b</sup>	95.5
Eur. J. Org. Chem., 2002, 1516-1522 <sup>c</sup>	93.0

<sup>a</sup> 0.5mmol racemic mixture, 1mmol propanol (2eq), 50mg CAL-B, 5ml toluene, N<sub>2</sub> atm.

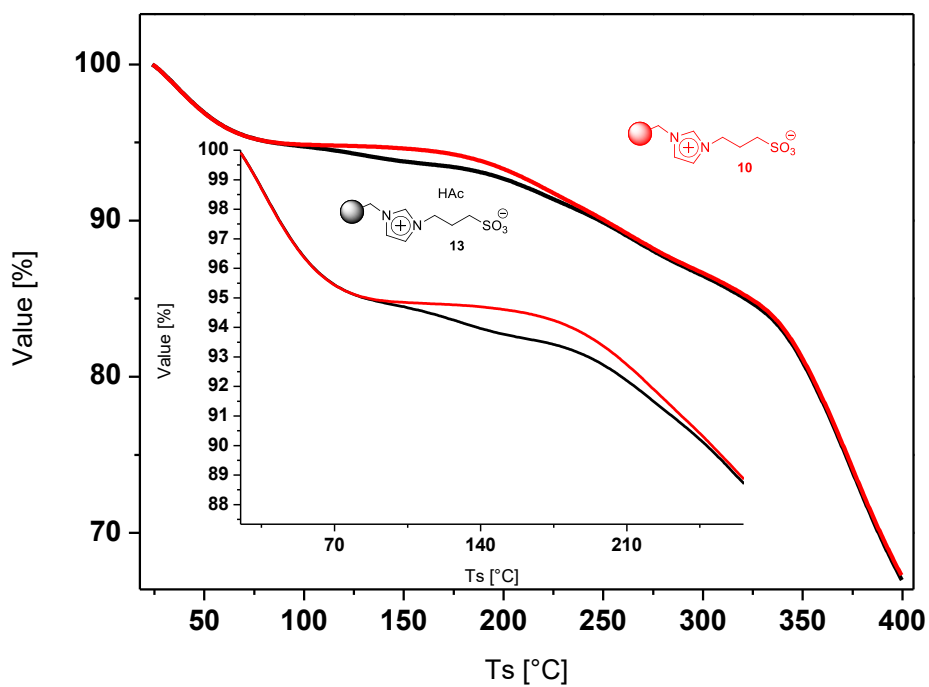
<sup>b</sup> 0.5mmol racemic mixture, 1.25mmol isopropenyl acetate (2.5eq), 50mg CAL-B, 5ml dry toluene.

<sup>c</sup> 3.68mmol racemic mixture, 7.36mmol propanol, 368mg CAL-B, 36ml toluene, N<sub>2</sub> atm

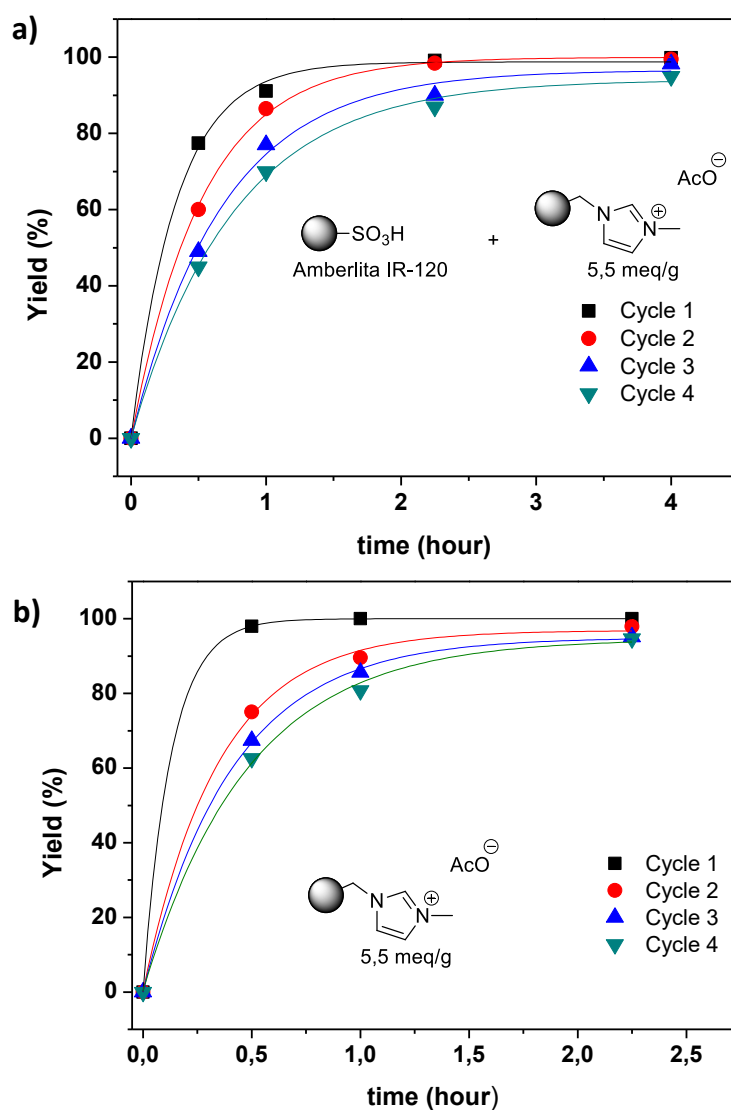
### 3. Figures.



**Figure S.1.** Stability catalyst evaluation for the synthesis of the racemic mandelonitrile acetate **4a** (step 2). **a)** Catalysed by **13**. **b)** Catalysed by **10**. Solvent free conditions, 50 mg of cat. per mmol of cyanosilyl ether and 2 eq. of  $\text{Ac}_2\text{O}$ ,  $60^\circ\text{C}$ .

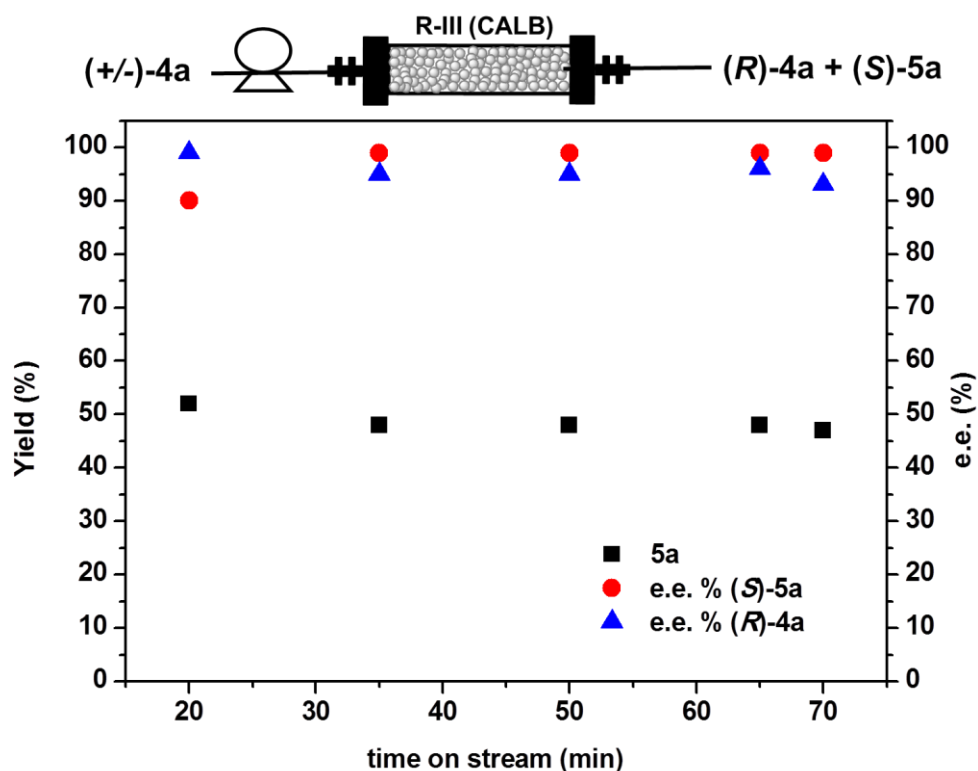


**Figure S.2.** TGA for **10** (red) and **13** (black) obtained from 25 to 600 °C at constant heating rate of 10 °C/min, purge gas N<sub>2</sub> at 50 ml/min.



**Figure S.3.** Stability catalyst evaluation for the synthesis of the racemic mandelonitrile acetate **4a** (step 2). **a)** Catalysed by **8** + **14**. **b)** Catalysed by **14**. Solvent free conditions, 50 mg of cat. per mmol of cyanosilyl ether and 2 eq. of Ac<sub>2</sub>O, 60°C.

Evaluation biocatalysts stability step-3.



**Figure S.4.** Stability catalyst evaluation for Kinetic Resolution of racemic mandelonitrile acetate (**4a**) under continuous flow conditions. Conditions: 0.1 M AcOR in Me-THF:IPA (0.85:0.15), **RIII**: 1 g CAL-B packed in a Omnifit glass column (1 cm x 10 cm), 60°C, flow 0.35 mL/min. Conversion calculated by <sup>1</sup>H-NMR. Enantiomeric excess calculated by chiral GC column Cyclodexb and HPLC Daicel Chiralcel OD-H.

Setup used for the multistep and multicyclic continuous flow synthesis of chiral cyanohydrins.



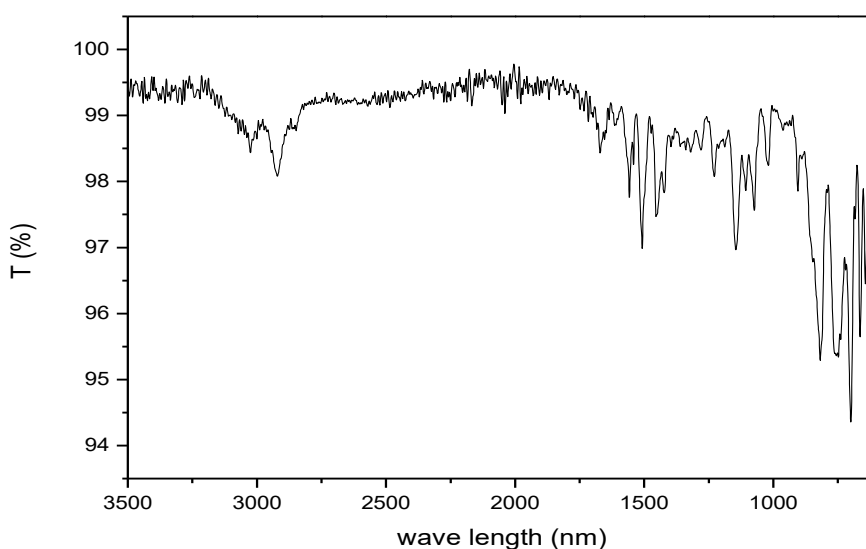
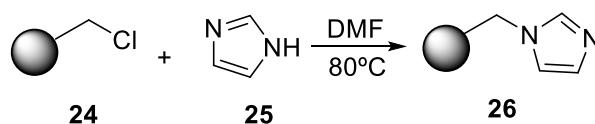
**Figure S.5.** Syringe pumps from kdScientific and Hamilton syringes were used for the three steps. The reactors were glass Omnifit columns 006RG-10-10 (0.7854 cm diameter x 10 cm length). Temperature reached when needed with a *i*-PrOH reflux. Syringe 1 was filled with benzaldehyde:TMSCN (1:1.1). Reactor was 1 filled with cat **6**. Syringe 2 was filled with Ac<sub>2</sub>O. Reactor 2 was filled with cat **10**. Syringe 3 was filled with n-propanol:Me-THF (0.15:0.85). Reactor 3 was filled with CAL-B. Samples were collected with a Fraction Collector Frac-920.

#### 4. Synthesis of Polymer-supported catalysts and characterisation.

**Synthesis of compound 6.** 5 g of Merrifield resin **24** (5.5 mmol Cl/g, 27.5 mmol) were suspended in 25 mL of N-methylimidazolium (304.7 mmol). The mixture was heated under stirring for 2 hours at 80°C. Then the polymer was filtered and washed with THF (3 x 5 mL), CH<sub>2</sub>Cl<sub>2</sub> (3 x 5 mL) and MeOH (3 x 5 mL). The resultant SILLP (**6**) was dried in a vacuum oven till constant weight. FT-IR (cm<sup>-1</sup>) KBr: 3422, 2921, 2580, 1571, 1512, 1492, 1224, 1112, 1019, 824, 762, 704. Raman (cm<sup>-1</sup>): 1603, 1404, 1377, 1178, 1081, 1012, 992, 824, 753, 611. Elemental analysis, experimental: %N 8.37. Calculated: %N 8.50. Loading of compound **6**: 3.03 meq/g.

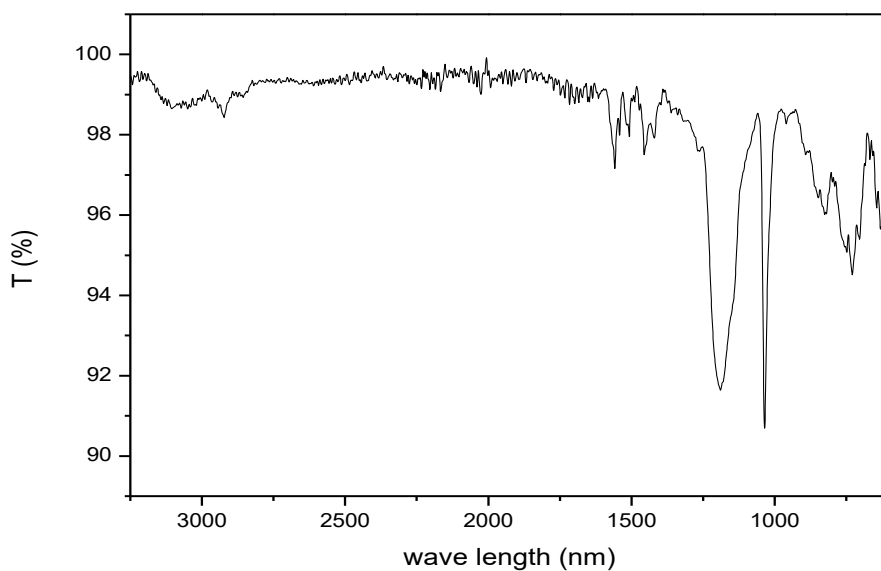
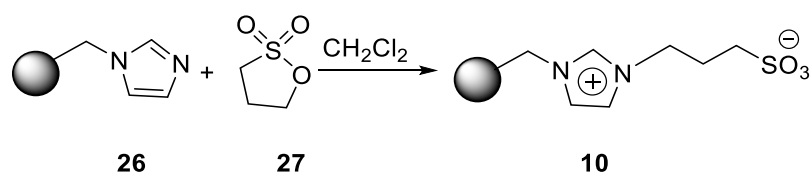
#### Synthesis of compound 10.

**Step 1. Synthesis of compound 17.** 5.5 g of the Merrifield resin **24** (macroporous resin 5.5meq/g, 1 mmol) were suspended in a 100 mL of imidazole (**25**) solution in DMF (0.03 M, 3 eq., 3 mmol). The mixture was stirred at 80°C for 24 hours. Then the polymer was filtered over vacuum and washed with THF (3 x 20 mL), CH<sub>2</sub>Cl<sub>2</sub> (3 x 20 mL) and MeOH (3 x 20 mL). The polymer obtained (**26**) was dried in a vacuum oven at 50 °C till constant weight. FTIR-ATR (cm<sup>-1</sup>): 3026, 2921, 2848, 1670, 1558, 1508, 1454, 1423, 1228, 1145, 1107, 1074, 1021, 905, 819. Elemental analysis, experimental: %N 10.1. Loading of compound **26**: 3.6 meq/g.



**Figure S.6.** IR spectra of compound **26**.

**Step 2. Synthesis of compound 10.** 3.6 g of polymer **26** (1 eq., 1mmol) were suspended in 90 mL of dichloromethane and a 4.3 mM solution of 1,3-propanesultone (**27**) solution in DCM (70 mL, 3 eq.) was added dropwise under stirring at room temperature to the polymer suspension. After 24 hours, the polymer was filtered under vacuum and washed with THF (3 x 20 mL), CH<sub>2</sub>Cl<sub>2</sub> (3 x 20 mL) and MeOH (3 x 20 mL). The Polymer obtained (**10**) was dried overnight in vacuum oven at 50 °C. FTIR-ATR (cm<sup>-1</sup>): 3102, 2924, 2856, 1558, 1542, 1508, 1456, 1420, 1262, 1182, 1036, 960, 892. Elemental analysis, experimental: %N 6.7. Loading of compound **10**: 2.4 meq/g.



**Figure S.7.** IR spectra of compound **10**.



### Synthesis of compound 13.

0.33 g of polymer **10** (0.792 mmol) were suspended in 10 mL of MeOH. Then 4.8 mL of a aqueous solution of acetic acid (37.5 % vol) were added to the polymer suspension. The mixture was stirred at room temperature for 3 hours. After that, the polymer was filtered over vacuum and washed with THF (3 x 20 mL), CH<sub>2</sub>Cl<sub>2</sub> (3 x 20 mL ) and MeOH (3 x 20 mL). The polymer obtained (**13**) was dried in a vacuum oven at 50 °C till constant weight. FTIR-ATR (cm<sup>-1</sup>): 3454, 3082, 2924, 2851, 1733, 1643, 1614, 1561, 1512, 1452, 1423, 1357, 1317, 1179, 1035, 962, 850, 823, 751, 732. Elemental analysis, experimental: %N 6.68. Loading of compound **13**: 2.39 meq/g.

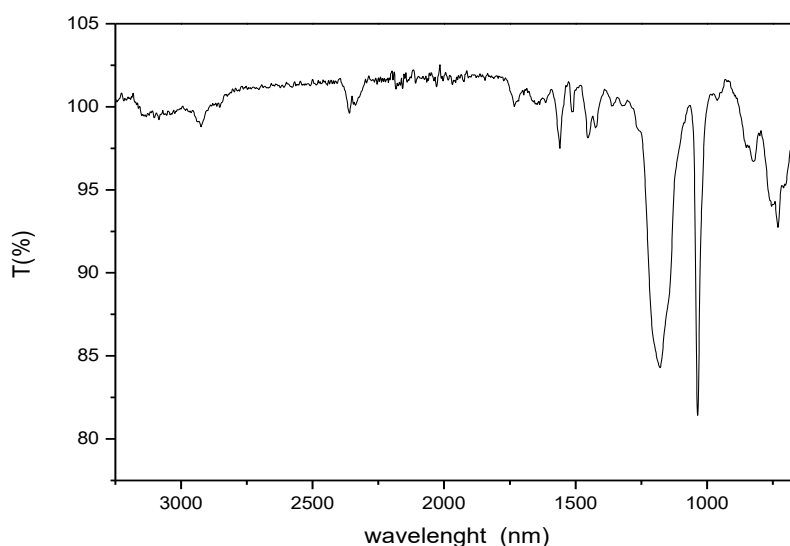


Figure S.8. IR spectra of compound **13**.

### Synthesis of compound 7.

600 mg of the polymer **13** (0,49 mmol) were suspended in a 3.5 mL solution of CF<sub>3</sub>SO<sub>3</sub>H (130 μL, 1.47 mmol) in MeOH:H<sub>2</sub>O (6:1) (420 mM). The mixture was stirred for 24 hours at room temperature. After that, the polymer was filtered and washed with THF (3 x 5 mL), CH<sub>2</sub>Cl<sub>2</sub> (3 x 5 mL) and MeOH (3 x 5 mL). The solid obtained was dried in a vacuum oven at 50 °C till constant weight. IR (cm<sup>-1</sup>) FTIR-ATR: 3025, 2924, 1685, 1492, 539, 1451, 1199, 759, 700. Elemental analysis, experimental: %N 2.06. Calculated: %N 2.09. Loading of compound **7**: 0.74 meq/g.

### Synthesis of compound 11.

The dried polymer **10** (1g, 2.4 mmol) was suspended in MeOH (20 mL) and 1.77 mg of  $\text{Sc}(\text{OTf})_3$  (1.5 eq., 3.6 mmols) were added to this suspension. The mixture was stirred at room temperature for 24 hours. Then the polymer was filtered and washed with MeOH (3 x 20 mL) and dried in vacuum oven at 50 °C till constant weight. IR( $\text{cm}^{-1}$ ) FTIR-ATR: 3144, 2927, 2861, 1654, 1558, 1542, 1508, 1456, 1425, 1336, 1254, 1223, 1211, 1150, 1028, 826. Elemental analysis, experimental: %N 5.9; Loading of compound **11**: 2.11 meq/g.

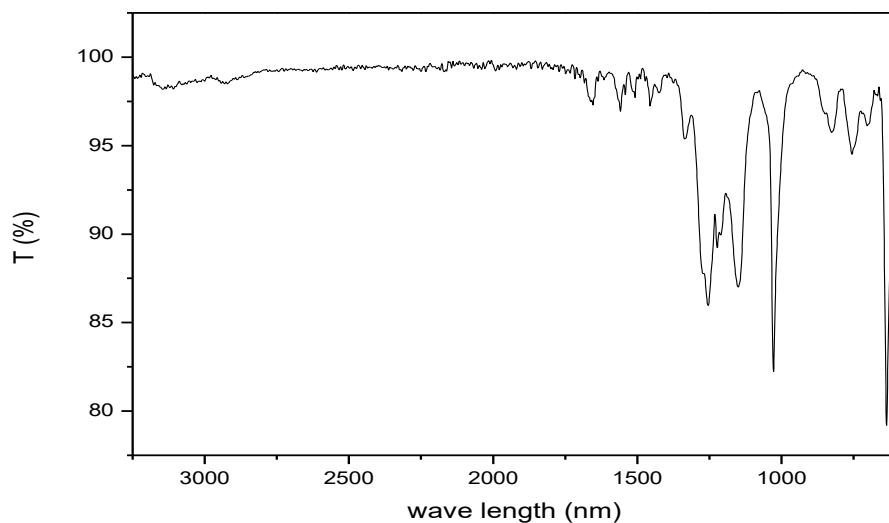
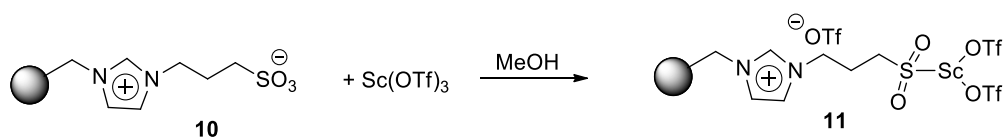


Figure S.9. IR spectra of compound **11**.

## 5. General procedure for reactions.

### General procedure for cyanosilylation reactions using cat6.

Aldehyde (1 eq., 1 mmol) and TMSCN (1,2 eq., 1,2 mmol) were combined in a 10 mL vial. Then 25 mg of **6** per mmol of aldehyde were added. The mixture was stirred at room temperature for 24 hours. After that, the reaction mixture was filtered with a microfilter and no purification was required. Products were characterised by <sup>1</sup>H-NMR.

### General procedure for acetylation reactions using catalysts 7-14.

Cyanosilyl ether (**3a-d**) (1 eq., 1mmol) and acetic anhydride (2 eq., 2mmol) were combined in a 10 mL vial. Then 50 mg of cat (**7-14**) per mmol of substrate were added. The mixture was stirred at 60°C for 24 hours. After that, the reaction mixture was filtered with a microfilter and no purification was needed for the next step. Products were characterized by <sup>1</sup>H NMR, GC and HPLC.

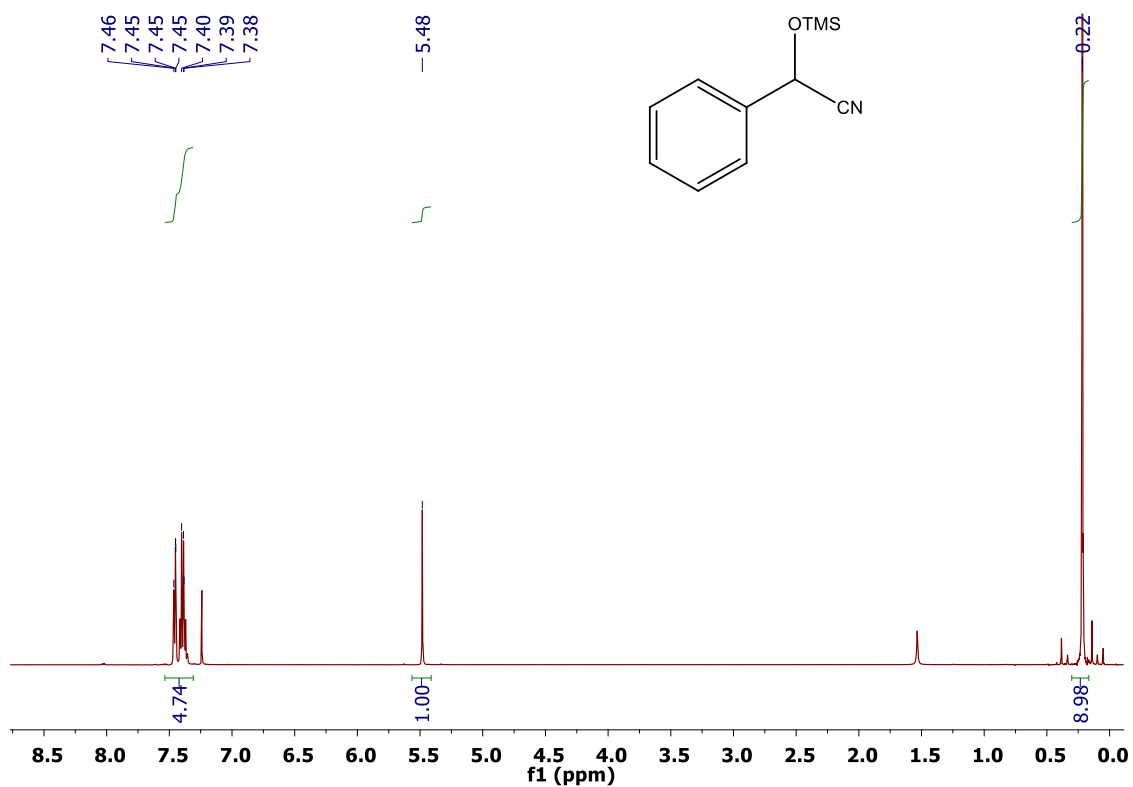
### General procedure for the kinetic resolution of the cyanohydrin esters using Novozym 435

Cyanohydrin esters (**4a-d**) (1 mmol) were solved in a mixture of 2-MeTHF (10 mL per mmol of substrate) and n-propanol (0,15 mL per mmol of substrate). Then CAL-B (Novozym 435) (100 mg per mmol of substrate) was added. The mixture was stirred at 60°C for 24 hours. After that, the solvent was evaporated and the crude was dried in vacuum pump. Enantiomeric excess of (*R*)-cyanohydrin esters was determined by HPLC and GC.

## 6. NMR Spectra, HPLC and GC conditions.

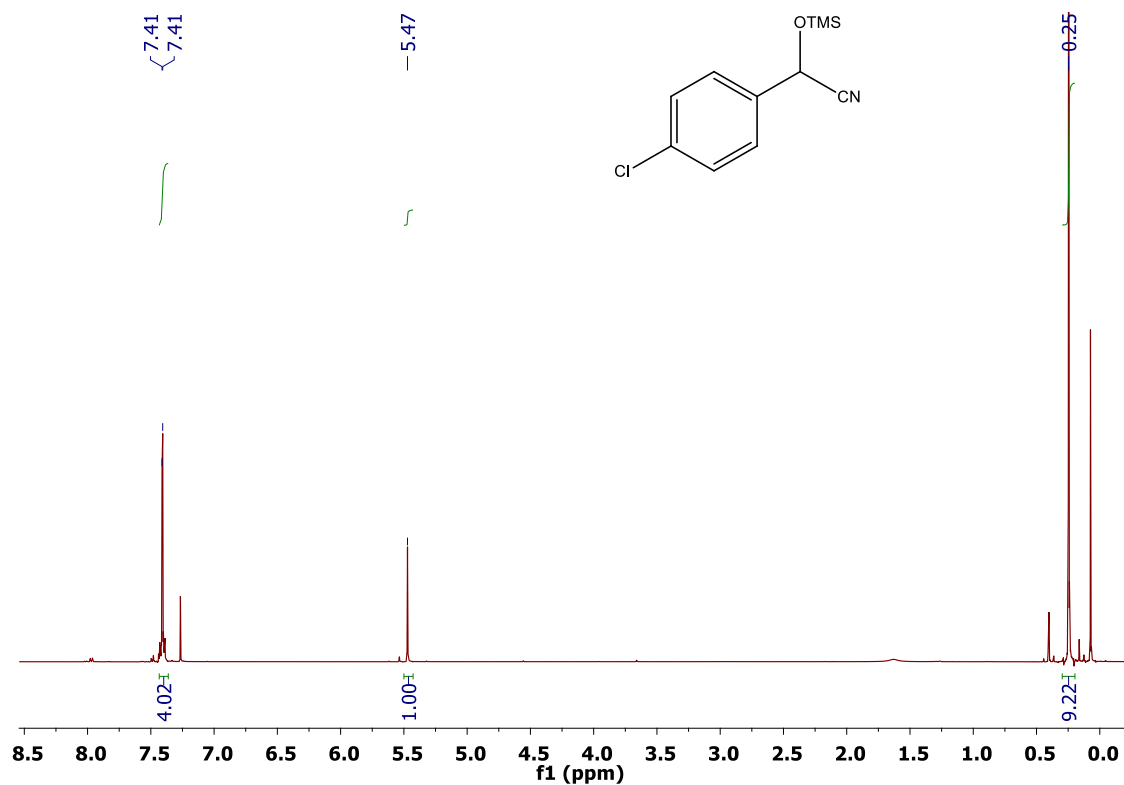
All the products here synthesised were previously reported and characterised according to the bibliography. The  $^1\text{H-NMR}$  ( $\text{CDCl}_3$ ) correspond to the reaction crude. These crudes were used in the consecutive reaction step without any further purification.

### Spectroscopical data of 2-phenyl-2-((trimethylsilyl)oxy)acetonitrile



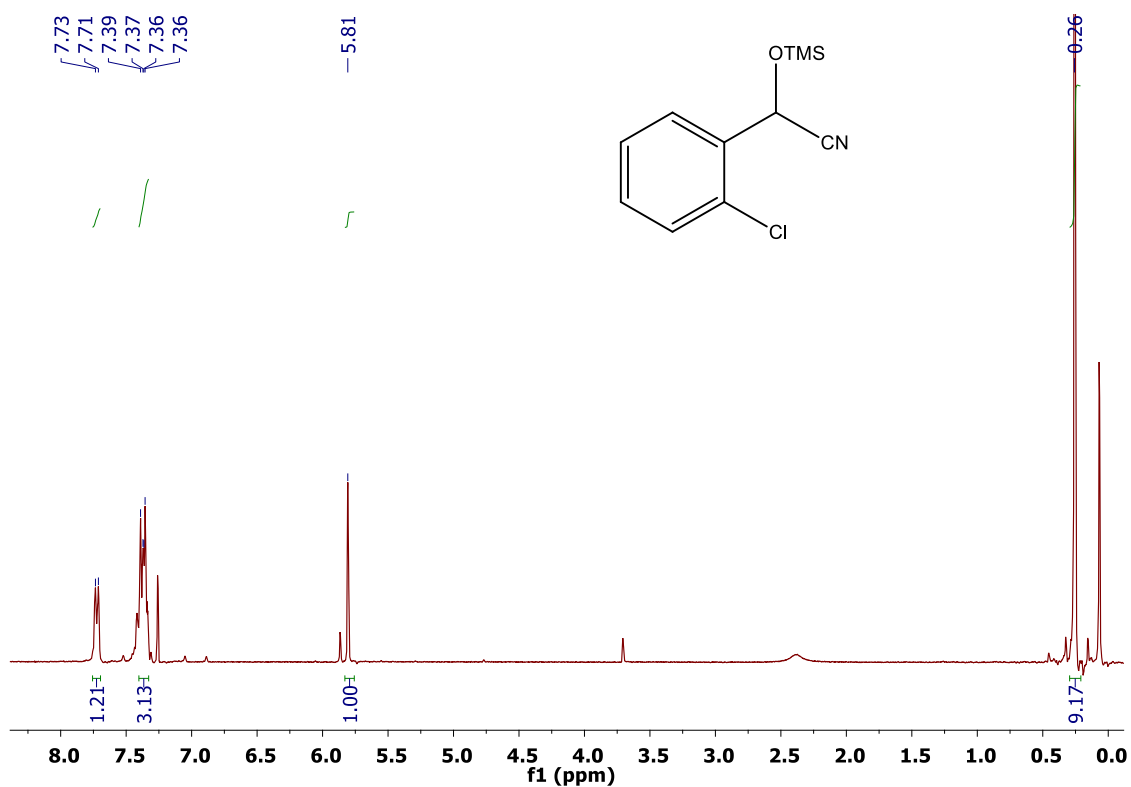
$^1\text{H-NMR}$  (500 MHz,  $\text{CDCl}_3$ )  $\delta$  7.46-7.38 (m, 5H), 5.48 (s, 1H), 0.22 (s, 9H) ppm.

Spectroscopical data of 2-(4-chlorophenyl)-2-((trimethylsilyl)oxy)acetonitrile



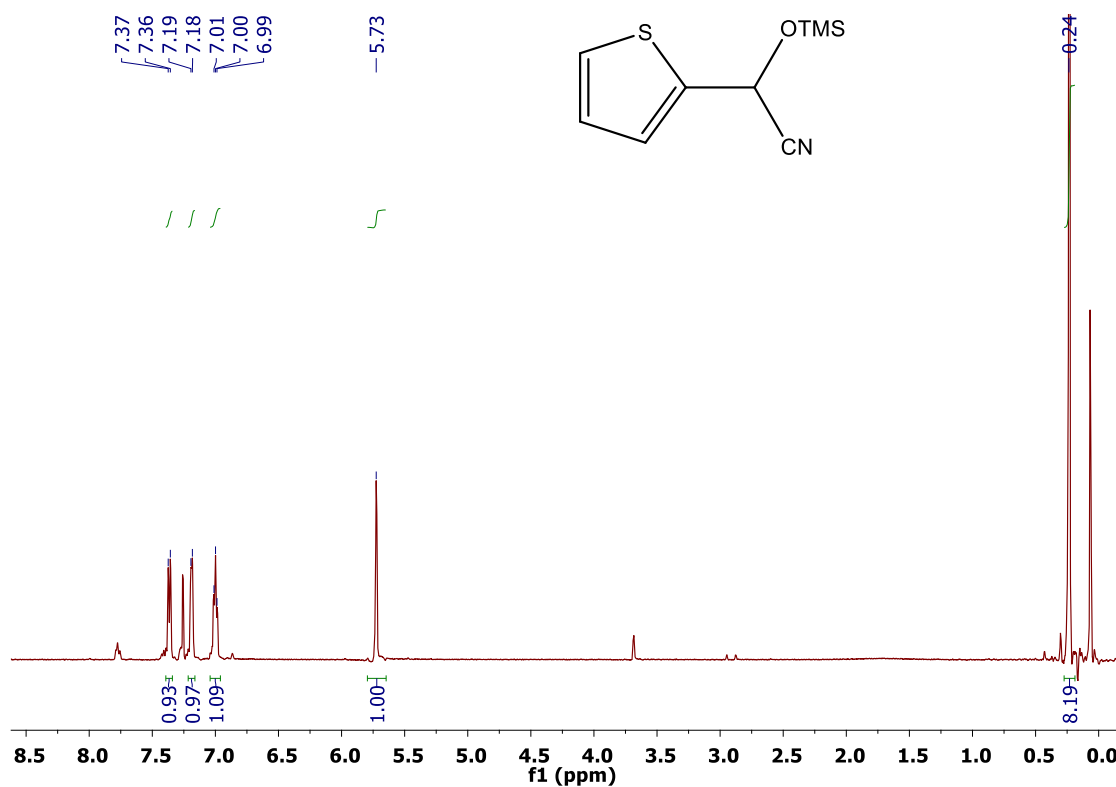
<sup>1</sup>H-NMR (500 MHz, CDCl<sub>3</sub>) δ 7.41 (m, *J* = 2.6 Hz, 4H), 5.47 (s, 1H), 0.25 (s, 9H) ppm.

Spectroscopical data of 2-(2-chlorophenyl)-2-((trimethylsilyl)oxy)acetonitrile



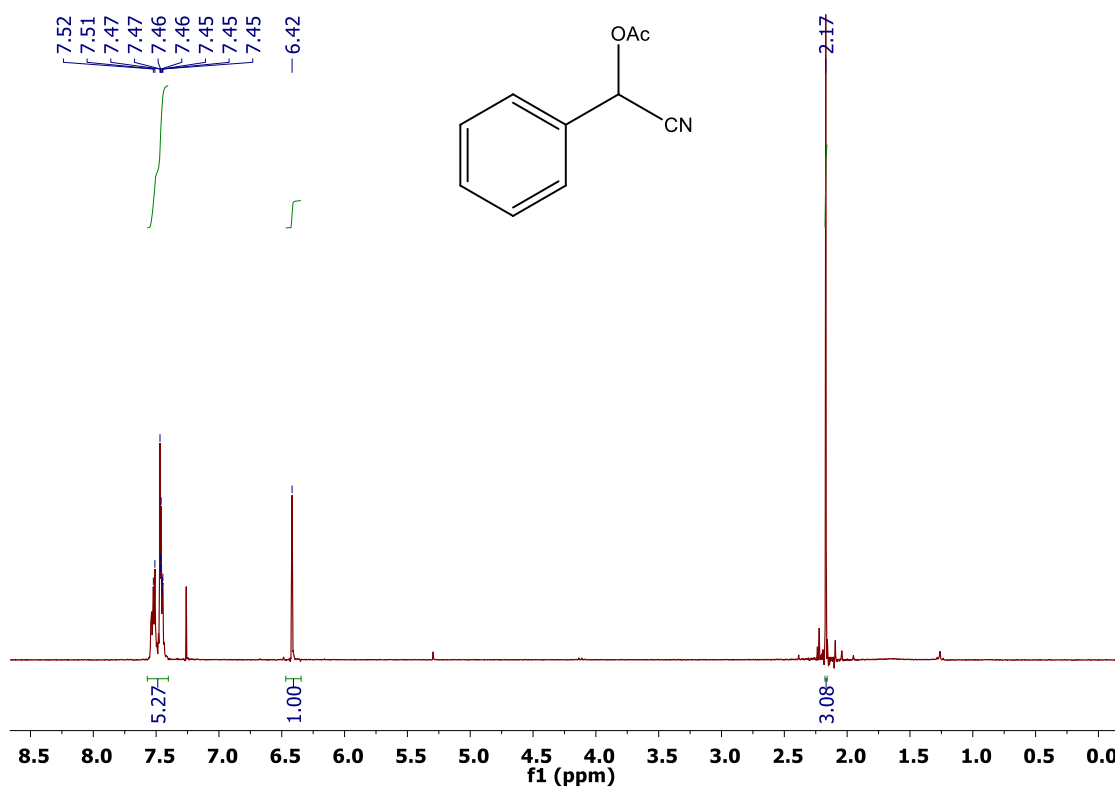
$^1\text{H-NMR}$  (300 MHz,  $\text{CDCl}_3$ )  $\delta$  7.71 (d,  $J = 6.7$  Hz, 1H), 7.37 (dd,  $J = 6.2, 4.2$  Hz, 3H), 5.81 (s, 1H), 0.26 (s, 9H) ppm.

Spectroscopical data of 2-(thiophen-2-yl)-2-((trimethylsilyl)oxy)acetonitrile



<sup>1</sup>H-NMR (300 MHz, CDCl<sub>3</sub>) δ 7.37 (d, *J* = 5.1 Hz, 1H), 7.19 (d, *J* = 3.5 Hz, 1H), 7.00 (t, *J* = 3.5 Hz, 1H), 5.73 (s, 1H), 0.24 (s, 9H) ppm.

### Spectroscopical data of Cyano(phenyl) methyl acetate

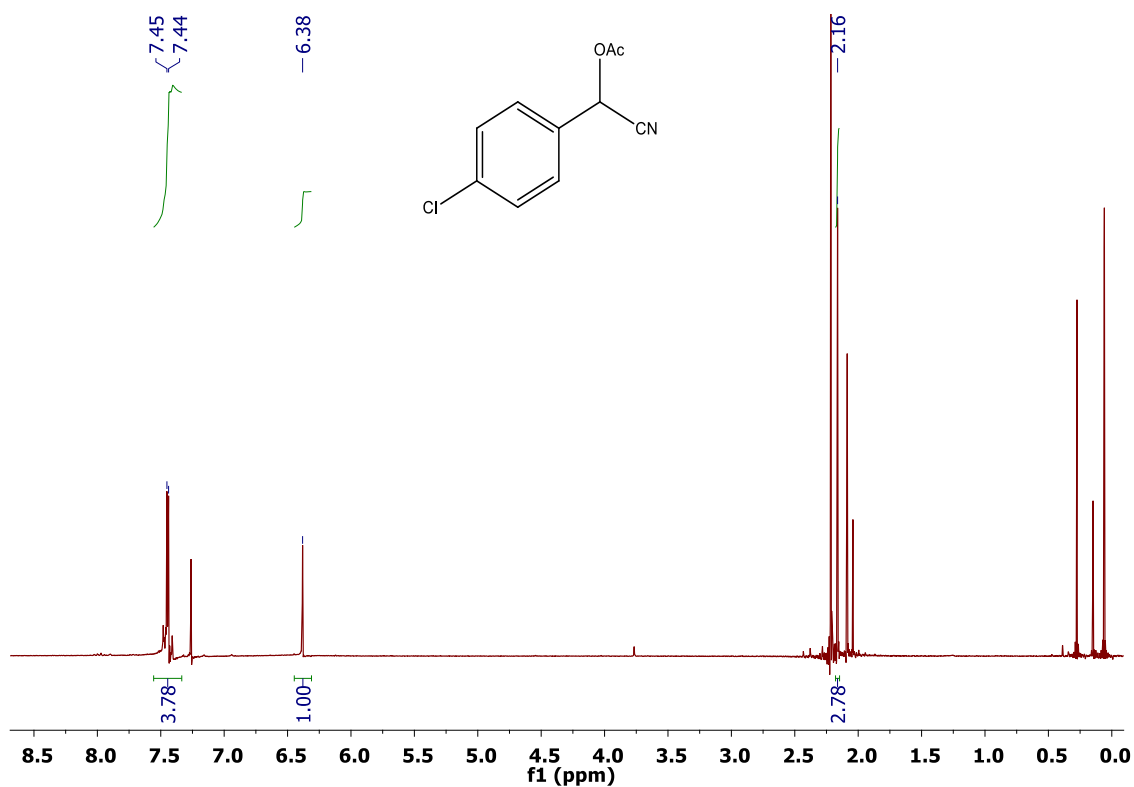


<sup>1</sup>H NMR (300 MHz, CDCl<sub>3</sub>) δ 7.52-7.45 (m, 5H), 6.42 (s, 1H), 2.17 (s, 3H) ppm.

CG: Column Cyclodexb, Injector: 230 °C, Oven: 60 °C (step1), 60-130 °C (10 °C/min, step2), 130 °C (30 min, step3), Pressure: 15.00 Psi, Detector: 300 °C, Helium flow: 25mL/min, Nitrogen flow: 30mL/min, Air flow: 300mL/min,  $t_R = 29.31$  min (R),  $t_R = 32.26$  min (S).



## Spectroscopical data of (4-chlorophenyl) cyano methyl acetate

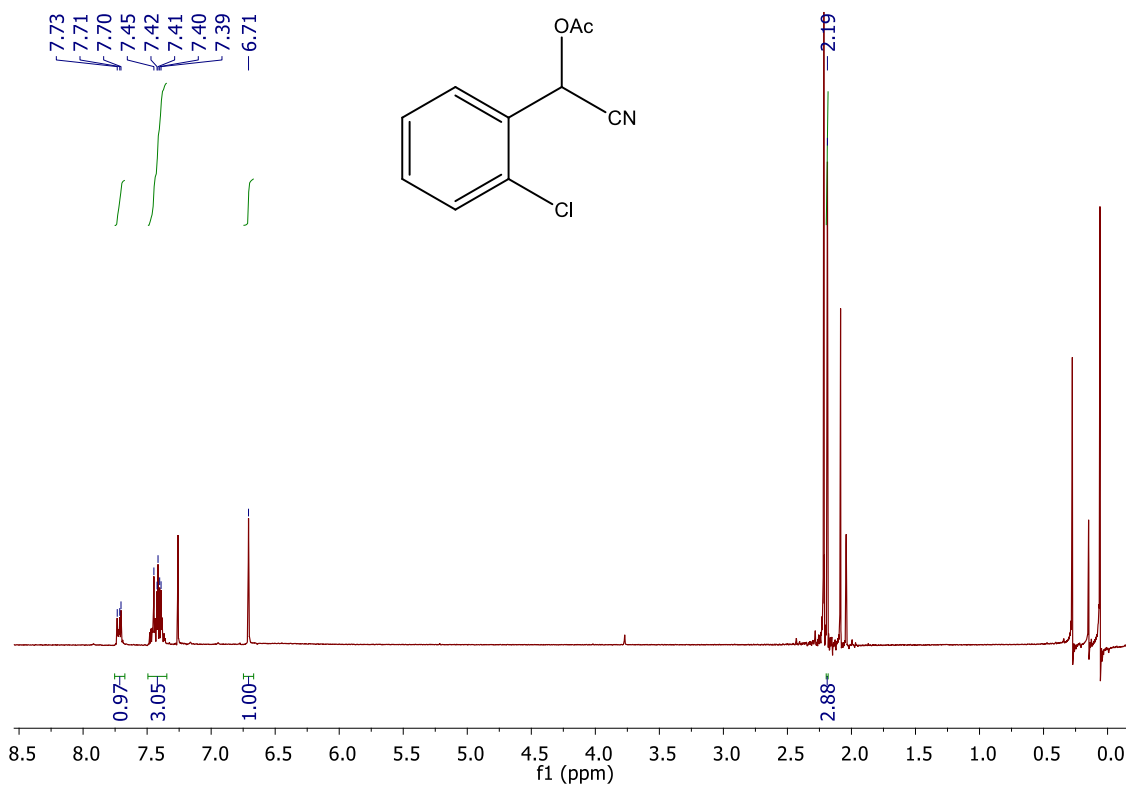


<sup>1</sup>H-NMR (300 MHz, CDCl<sub>3</sub>) δ 7.45–7.44 (m, 4H), 6.38 (s, 1H), 2.16 (s, 3H) ppm.

Discussion: No purification was needed for the next step so we can see more signals due to the excess of Ac<sub>2</sub>O (~2 ppm) and the –OTMS leaving our molecule (~0 ppm).

HPLC Daicel Chiralcel OD-H, hexane/*i*-PrOH = 95/5, T = 30 °C, flow rate = 1 mL/min, λ = 210 nm, *t*<sub>R</sub> = 9.08 min (*R*), *t*<sub>R</sub> = 9.96 min (*S*).

## Spectroscopical data of (2-chlorophenyl) cyano methyl acetate

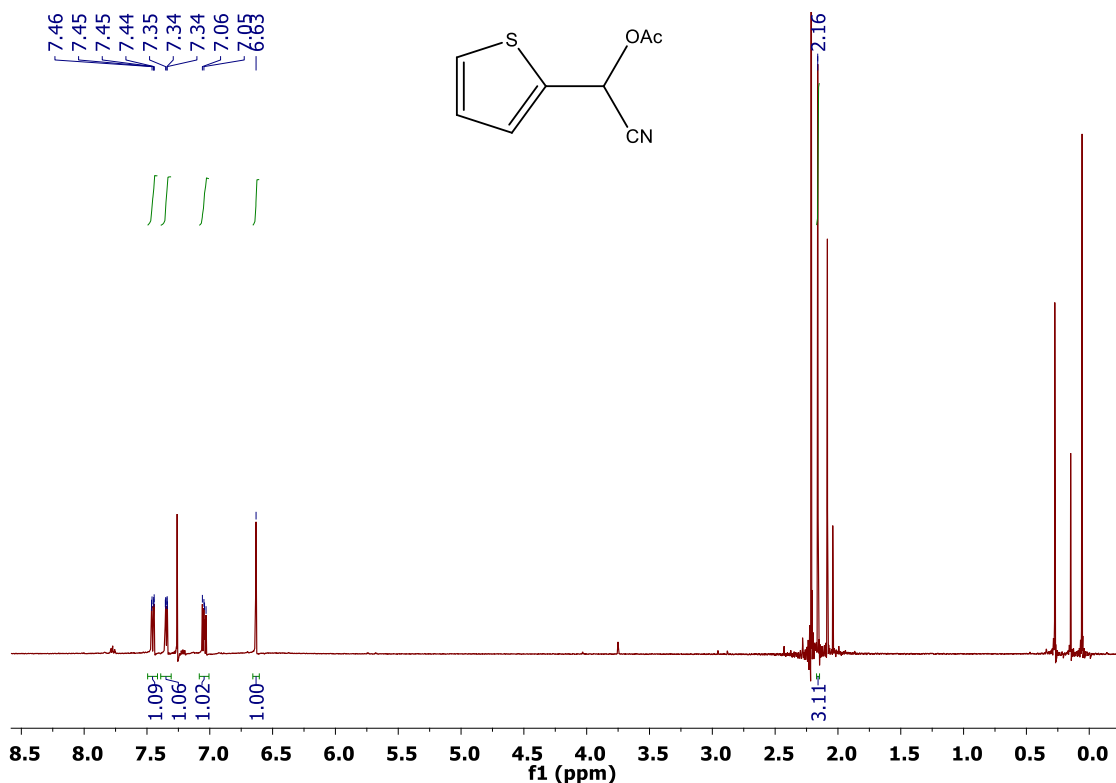


<sup>1</sup>H-NMR (300 MHz, CDCl<sub>3</sub>) δ 7.73-7.70 (m, 1H), 7.45-7.39 (m, 3H), 6.71 (s, 1H), 2.19 (s, 3H) ppm.

Discussion: No purification was needed for the next step so we can see more signals due to the excess of Ac<sub>2</sub>O (~2 ppm) and the -OTMS leaving our molecule (~0 ppm).

HPLC: Daicel Chiralcel OD-H, hexane/*i*-PrOH = 95/5, T = 30 °C, flow rate = 1 mL/min, λ = 210 nm, *t*<sub>R</sub> = 6.57 min (S), *t*<sub>R</sub> = 7.19 min (R).

## Spectroscopical data of Cyano(thiophen-2-yl)methyl acetate



<sup>1</sup>H-NMR (300 MHz, CDCl<sub>3</sub>) δ 7.46-7.44 (m, 1H), 7.35 (ddt, 1H), 7.05 (dd, 1H), 6.63 (s, 1H), 2.16 (s, 3H) ppm.

Discussion: No purification was needed for the next step so we can see more signals due to the excess of Ac<sub>2</sub>O (~2 ppm) and the -OTMS leaving our molecule (~0 ppm).

CG: Column Cyclodexb, Injector: 230 °C, Oven: 60 °C (step1), 60-130 °C (10 °C/min, step2), 130 °C (30 min, step3), Pressure: 15.00 Psi, Detector: 300 °C, Helium flow: 25mL/min, Nitrogen flow: 30mL/min, Air flow: 300mL/min, *t<sub>R</sub>* = 29.65 min (*R*), *t<sub>R</sub>* = 31.81 (*S*).



**Divergent multistep continuous  
synthesis enabled by immobilised  
catalysts on IL-phases**

**CHAPTER 5**



## Chapter 5. Divergent multistep continuous synthesis enabled by immobilised catalysts on IL-phases

### 5.1 RESUMEN DEL MANUSCRITO

En este capítulo se presenta la combinación de diferentes plataformas catalíticas basadas en el empleo de líquidos iónicos de manera divergente y empleando condiciones de flujo continuo. El objetivo fue desarrollar una metodología que permita, a partir de un único producto inicial, obtener nuevos productos de forma divergente en función de la presencia de diferentes tipos de catalizadores y reactivos. Así pues, se planteó que a partir de alcoholes alílicos, estos se puedan isomerizar a cetonas que, a su vez, pueden evolucionar bien a cianohidrin O-sililadas, mediante cianosililación, o alternativamente a  $\alpha$ -amino nitrilos mediante la reacción de Strecker (Figura 5.1).

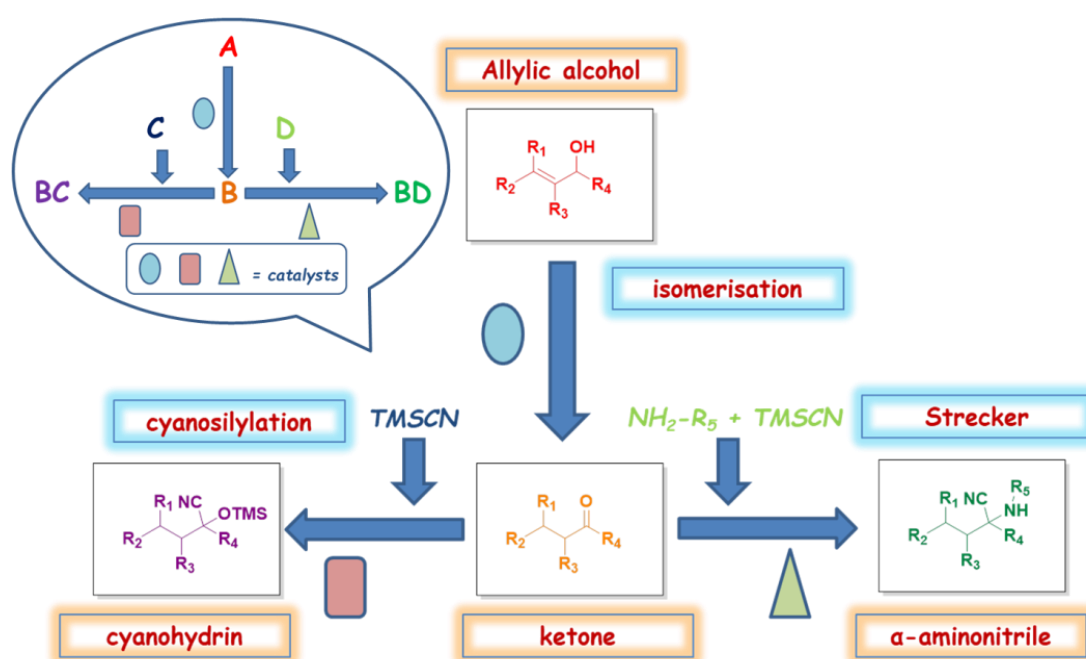


Figura 5.1. Esquema general para un sistema sintético divergente multicatalítico (arriba a la izquierda) y esquema del sistema que queremos desarrollar.

En la reacción de Strecker, partiendo de compuestos carbonílicos (aldehídos y cetonas), introducimos el grupo nitrilo en el carbono

contiguo al grupo carbonilo original. El grupo nitrilo se introduce empleando TMSCN en lugar de otros reactivos como HCN ó KCN por las ventajas ya expuestas en los capítulos anteriores. La diferencia respecto a la cianosililación es que ahora el grupo carbonilo no se transforma en un alcohol (dando una cianohidrina) sino en un grupo amino gracias a la formación, en presencia de una amina, de la correspondiente imina (ver Figura 5.2), dando como producto  $\alpha$ -amino nitrilos.

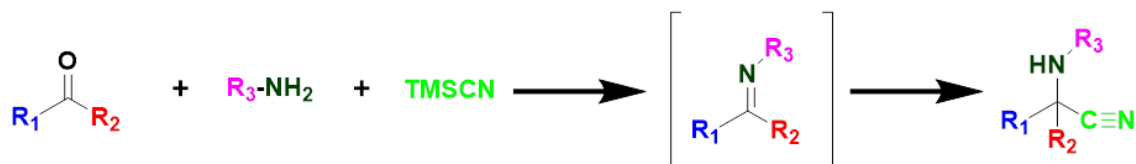


Figura 5.2. Esquema general de la reacción de Strecker estudiada empleando TMSCN como fuente de nitrilo.

Los  $\alpha$ -amino nitrilos, del mismo modo que las cianohidrinás, representan intermediarios sintéticos clave de elevado valor en síntesis orgánica, sobre todo para compuestos biológicamente activos. (Figura 5.3). Además, estos grupos funcionales nitrilo y amina pueden participar en interacciones importantes con objetivos o dianas biológicas. Podemos encontrar un ejemplo representativo de la importancia de los  $\alpha$ -amino nitrilos en la obtención de  $\alpha$ -aminoácidos mediante hidrólisis del nitrilo de los correspondientes  $\alpha$ -amino nitrilos.

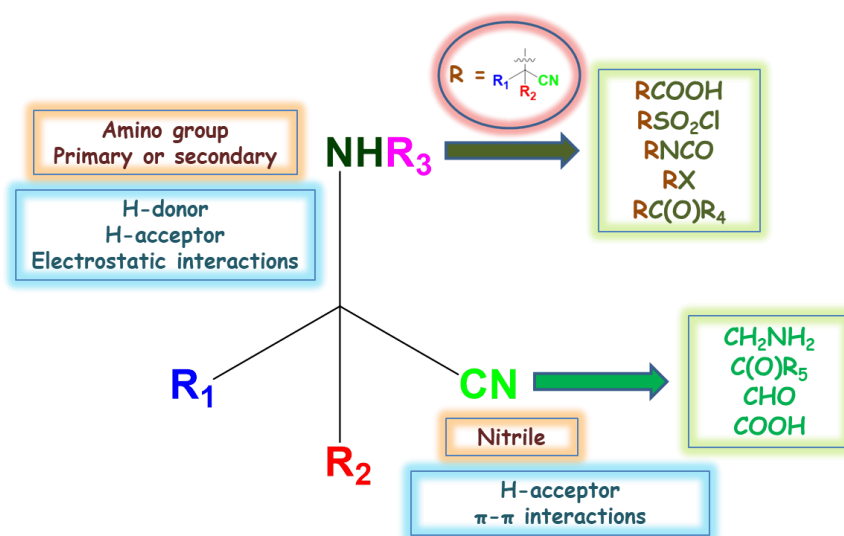
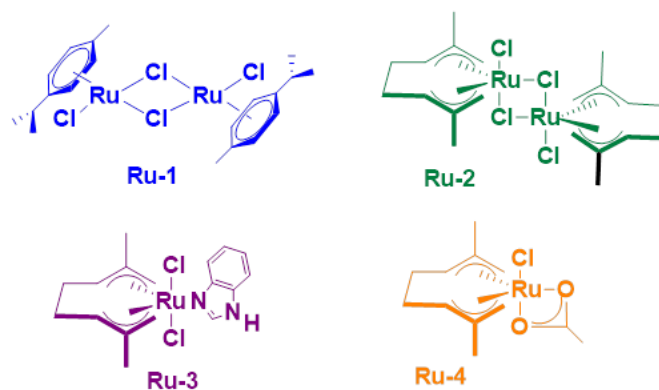


Figura 5.3. Versatilidad e importancia de los  $\alpha$ -aminonitrilos como “building blocks”. Propiedades como compuestos bifuncionales.



La **primera plataforma catalítica** consistió en la isomerización catalítica de alcoholes alílicos a cetonas. Para ello, se estudiaron como posibles catalizadores los complejos de rutenio que se muestran en la Figura 5.4. Estos compuestos son altamente efectivos (y solubles en general) en el seno de líquidos iónicos.



**Figura 5.4. Complejos de rutenio utilizados como catalizadores para la isomerización de alcoholes alílicos a cetonas.**

La reacción de isomerización de 1-octen-3-ol a 3-octanona fue elegida como reacción modelo para estudiar esta primera plataforma catalítica. Las pruebas iniciales en discontinuo mostraron que los catalizadores **Ru-4** y **Ru-2** eran los más eficientes para la reacción de isomerización empleando [BMIM][NTf<sub>2</sub>] como disolvente.

Así, se planteó el desarrollo de un sistema bifásico ILs-scCO<sub>2</sub> en continuo. El scCO<sub>2</sub> es soluble en el IL (líquido iónico) pero el IL no es soluble en el scCO<sub>2</sub>, lo que permite la inmovilización del catalizador de Ru en la fase homogénea IL. El scCO<sub>2</sub> se emplea para liberar el reactivo (alcohol alílico, soluble en scCO<sub>2</sub>) al medio de reacción y para extraer posteriormente el producto (cetona, soluble en scCO<sub>2</sub>) como se muestra en la Figura 5.5.

Mediante ciclos de alimentación de 1-octen-3-ol, reacción (15 h) y posterior extracción de la 3-octanona con scCO<sub>2</sub> (1.5 mL/min) se desarrolló un sistema semicontinuo para la reacción de isomerización. El sistema es estable durante 48 horas con rendimientos > 95% empleando el catalizador **Ru-4** inmovilizado en [BMIM][NTf<sub>2</sub>]. El producto se aísla después de la descompresión del CO<sub>2</sub> sin necesidad de ninguna purificación. El catalizador **Ru-2** mostró una menor eficiencia catalítica para este proceso.

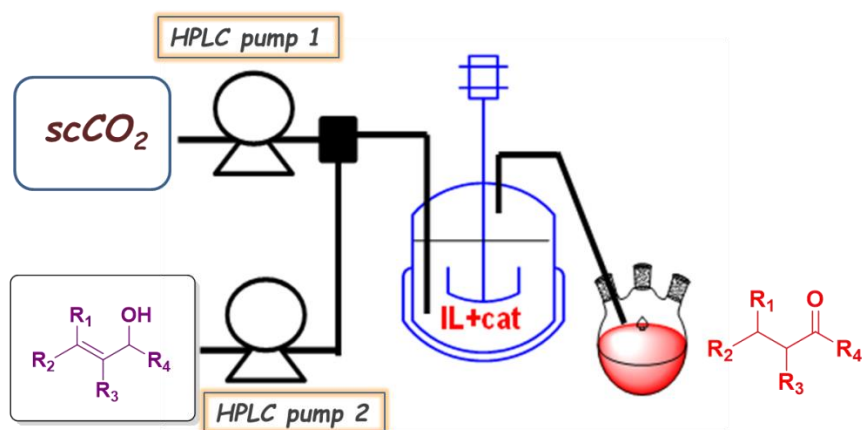


Figura 5.5. Esquema de la plataforma catalítica I: isomerización del alcohol alílico a cetona. Una llave de paso regula que al reactor entre alcohol alílico para cargar el sistema o  $scCO_2$  para extraer el producto formado. En el interior del reactor de presión se encuentra el catalizador de rutenio inmovilizado en el líquido iónico.

La **segunda plataforma catalítica** consiste en la reacción de cianosililación de la 3-octanona con TMSCN en condiciones de flujo continuo para dar la correspondiente cianohidrina O-sililada. Para ello, se rellenó un reactor de lecho fijo con el SILLP (**8**) descrito en el tercer capítulo (Figura 5.6), dónde esta reacción ha sido implementada. De nuevo se obtiene el producto correspondiente sin necesidad de disolvente, a temperatura ambiente y con excelentes rendimientos (>99%) y productividad (0.12 g cianohidrina O-sililada por gramo de catalizador por minuto).

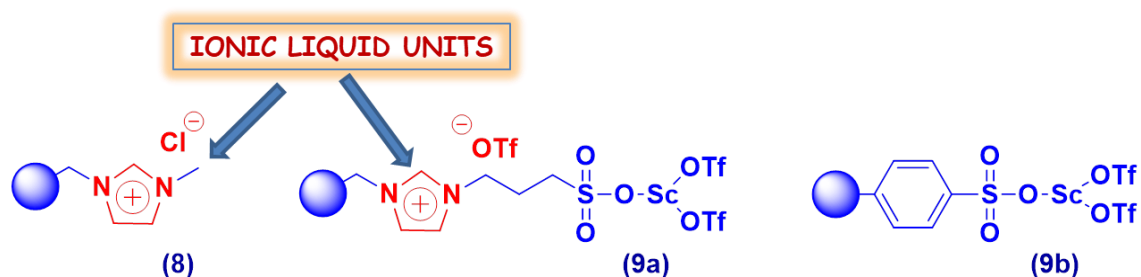


Figura 5.6. Catalizadores soportados empleados para las plataformas catalíticas II (**8**) y III (**9a** y **9b**)

En la **tercera plataforma catalítica** se pretende obtener el correspondiente  $\alpha$ -amino nitrilo mediante la reacción de Strecker. Para esta transformación se ideó un líquido iónico soportado de funcionalidad específica con grupos sulfónico capaces de complejar triflato de scandio ( $Sc(OTf)_3$ ) (**9a**) (Figura 5.6), ya que los triflatos de

lantánidos han sido descritos como excelentes catalizadores para la reacción de Strecker. En este catalizador tipo SILLP, la presencia de unidades de IL proporciona una activación dual electrófilo-nucleófilo mediante interacciones por enlace de hidrógeno aumentando la actividad catalítica del ácido de Lewis. Tanto el catión imidazolio como el anión OTf contribuyen a esta activación.

Esto se demostró comparando la actividad catalítica del SILLP **9a** con la del catalizador de scandio soportado análogo sin unidades de IL (**9b**), es decir, triflato de scandio soportado en un polímero de poliestireno-divinilbenceno con grupos sulfónicos (amberlita) (Figura 5.6).

El catalizador SILLP **9a** con unidades de líquido iónico en su estructura dio a lugar mejores resultados para la reacción de Strecker, con TMSCN y anilina, tanto para el benzaldehído como para la acetofenona, que los obtenidos para **9b**.

El empleo de disolvente también se estudió para estas transformaciones mostrando que un disolvente como acetonitrilo (CH<sub>3</sub>CN), con grupos –CN, puede competir con el TMSCN disminuyendo la activación de éste y dificultando la reacción. Sin embargo, eso no ocurre con 2-Me-THF, que además es un disolvente más sostenible. La reacción sin disolvente, que proporcionó un buen resultado, tiene una importante limitación cuando el α-amino nitrilo resultante es sólido, sobre todo para su aplicación en condiciones de flujo continuo.

Una vez identificado un catalizador eficiente, se evaluó la reacción de Strecker entre benzaldehído, TMSCN y anilina en condiciones de flujo continuo. Este proceso se llevó a cabo a temperatura ambiente, empleando el SILLP **9a** como catalizador (en un reactor de lecho fijo) y 2-Me-THF como disolvente. Bajo estas condiciones, la reacción alcanzó rendimientos > 95% siendo el catalizador estable durante al menos 75 horas, permitiendo incluso flujos relativamente altos que dieron lugar a una productividad de 2.5 g de α-amino nitrilo por hora y gramo de catalizador. Este resultado demostró la idoneidad del SILLP **9a** para reacciones de Strecker en condiciones de flujo continuo.

Sin embargo, al realizar en continuo la reacción de Strecker entre la 3-octanona (resultante de la plataforma catalítica 1), el TMSCN y la anilina, empleando el mismo SILLP **9a**, en ausencia de disolvente, los rendimientos obtenidos fueron del orden del 45% con una selectividad del 80-85%. Esta reducción de la eficiencia está relacionada con la menor reactividad de la 3-octanona que, en presencia del SILLP y TMSCN, dio lugar a la correspondiente cianohidrina O-sililada. La reacción de Strecker transcurre a través de un intermedio tipo imina,

cuya formación es el paso limitante. En el caso de la 3-octanona, menos reactiva, la formación de la imina necesaria es más costosa.

En consecuencia, se evaluaron diferentes alternativas con el fin de mejorar la eficiencia y selectividad de la reacción: i) reducir el flujo, ii) bombear juntos la 3-octanona y la anilina a través de un reactor tubular previo a la inyección de TMSCN y iii) hacer reaccionar durante toda la noche la 3-octanona y la anilina antes de introducirlos en el sistema. Todas ellas pretendían aumentar el tiempo de contacto entre la 3-octanona y la anilina para favorecer la formación del intermedio imínico en mayor medida. En general, estas estrategias consiguieron mejorar la selectividad con valores cercanos al 95% pero los rendimientos no fueron mayores del 55%.

Finalmente, la solución se encontró mediante la introducción de un reactor de lecho fijo previo al que contiene el SILLP **9a**, el cual se rellena con dos agentes deshidratantes, como  $P_2O_5$  y tamiz molecular de 4Å, más un catalizador ácido como la Montmorillonita K10. Este reactor permitió favorecer la formación de imina previa a la introducción del TMSCN. Este sistema con dos reactores consecutivos permitió obtener el  $\alpha$ -amino nitrilo correspondiente con un rendimiento  $>70\%$ , una selectividad  $>95\%$  y una productividad de 1.9 g / (g cat h) durante al menos 36 horas.

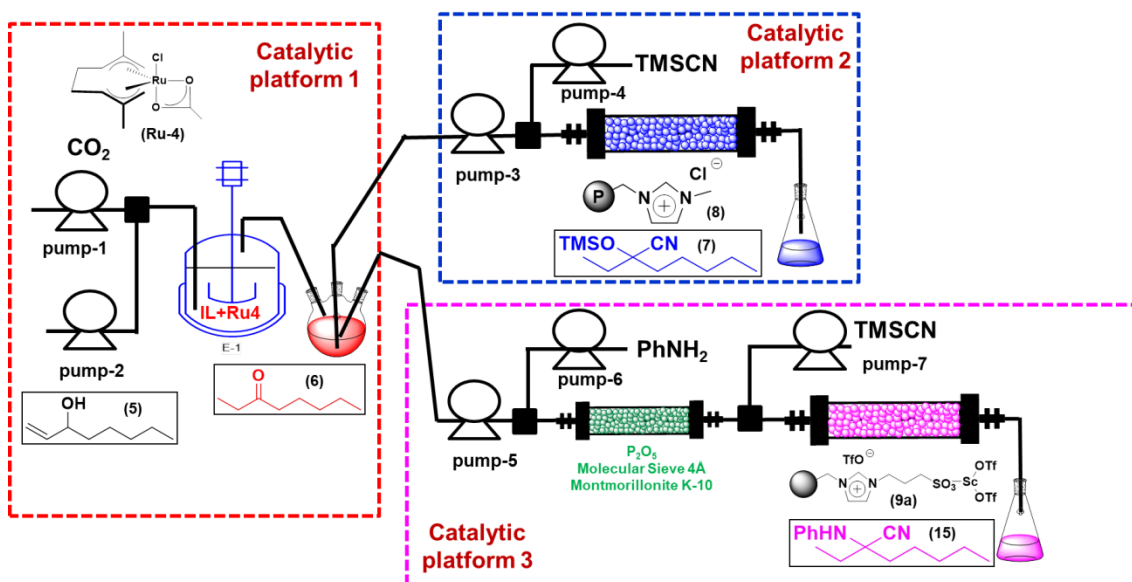


Figura 5.7. Sistema multicatalítico divergente en continuo desarrollado.

El acoplamiento de las plataformas catalíticas II y III con la primera demostró ser posible dando lugar a un **sistema multicatalítico divergente** en continuo que permite la obtención de cianohidrinas O-sililadas o  $\alpha$ -amino nitrilos, ambos de elevado valor sintético, empleando líquidos iónicos, tanto soportados como en fase homogénea, para la catálisis y únicamente disolventes neutéricos como el propio líquido iónico o CO<sub>2</sub> supercrítico (Figura 5.7).



# Divergent multistep continuous synthesis enabled by immobilised catalysts on IL-phases.

Edgar Peris<sup>[a]</sup>, Raúl Porcar<sup>[a]</sup>, Joaquín García-Álvarez<sup>[b]</sup>, María Isabel Burguete<sup>[a]</sup>, Eduardo García-Verdugo<sup>\*[a]</sup> and Santiago V. Luis<sup>\*[a]</sup>

**Abstract:** Two distinct and individual catalytic platforms (metal- and organo-catalysed) based in the use of ILs have been successfully integrated. The right combination of different single continuous flow processes has enabled the access to the divergent preparation of two alternative interesting intermediate compounds from the same starting material.

## Introduction

Sustainability is not only a challenge, but also an opportunity to radically transforming processes for the synthesis of organic products by adapting them to the new emerging technologies.<sup>1</sup> In this context, there is a need to develop alternative synthetic approaches mimicking natural processes that integrate multiple and consecutive catalytic sequences.<sup>2,3,4,5</sup> These catalytic transformations can be performed, in order to reduce environmental impact, under alternative reaction conditions using neoteric solvents such as water, dimethyl carbonate, ionic liquids (ILs) or supercritical fluids.<sup>6</sup> Indeed, these solvents can contribute to not only reducing human health problems and the environment footprint of the synthetic process, but in some cases, to modify the catalytic system enhancing its activity, recyclability, stability and / or selectivity. At the same time, these new synthetic methodologies should also face challenges related to the paradigm shifts that the chemical industry is experiencing. They include replacing the large volume discontinuous processes requiring multiple unit operations by highly flexible and integrated continuous flow catalytic processes.<sup>7,8,9,10,11</sup> In this regard, the development of synthetic platforms integrating multicatalytic systems into sequential and controllable processes, leading to complex syntheses through reduced external intervention and minimal environmental impact, are highly desirable.<sup>12,13,14,15,16</sup> These platforms allow: i) greater

reproducibility of reactions; ii) easy scaling, which facilitates the direct transfer of laboratory results to production; iii) a reduction in environmental impact; iv) improved safety; v) the synthesis of new high-value chemical entities; vi) intensification of the process, allowing the use of smaller size systems that offer cost reduction and higher productivity. Furthermore, the assembly of these synthetic platforms in a divergent telescopic sequential fashion can lead to systems able to produce molecules with wide structural diversity.<sup>17,18</sup>

In the search of such systems, here we report our efforts to develop ILs-based catalytic platforms, as liquid phases or supported on solid polymeric materials, which can be combined in a single continuous flow process to provide alternatively two different families of intermediate compounds. Besides, they allow the reduction of the environmental impact and enable the simple separation and reuse of the catalysts, providing products not contaminated by traces of either catalyst or solvent.

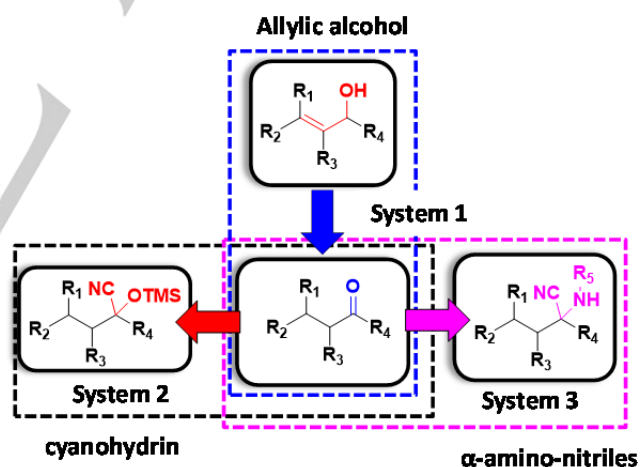


Figure 1. Divergent synthesis based on continuous flow catalytic platforms.

## Results and Discussion

The main aim of the work has focused in the divergent synthesis of  $\alpha$ -cyano-amine and cyanohydrin trimethylsilyl ethers.  $\alpha$ -Cyano-amines are very useful synthetic intermediates for the preparation of a wide variety of organic molecules with relevant pharmacological properties.<sup>19,20</sup> They can be obtained by the three-component Strecker reaction using an aldehyde or ketone, an amine and a cyanide source. In a similar way, in absence of the amine and with the selection of the proper catalyst the same reactants can be alternatively transformed in cyanohydrin

[a] Mr. E. Peris, Dr. R. Porcar, Prof. M. I. Burguete, Dr. E. García-Verdugo\* and Prof. S. V. Luis\*  
Department of Inorganic and Organic Chemistry,

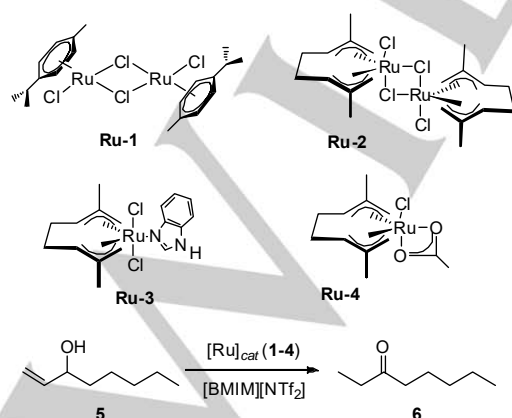
Universitat Jaume I,  
Avda Sos Baynat s/n, E-12071, Castellón, Spain.  
E-mail: cepeda@uji.es, luiss@uji.es

[b] Dr. J. García-Álvarez  
Departamento de Química Orgánica e Inorgánica, Instituto Universitario de Química Organometálica "Enrique Moles" (Unidad asociada al CSIC),  
Facultad de Química,  
Universidad de Oviedo,  
E-33071 Oviedo, Spain

Supporting information for this article is given via a link at the end of the document.

trimethylsilyl ethers.<sup>21</sup> These two reactions generally require HCN or alkali metal cyanides such as KCN or NaCN as cyanide sources.<sup>20</sup> To overcome problems associated with those cyanide sources in terms of safety and waste after completion of the reaction, TMSCN has proven to be an effective, relatively safe, and easily handled cyanide anion source for the synthesis of both types of functional molecules. As it has been mentioned both reactions used as starting materials ketones or aldehydes that can be obtained from the isomerisation of readily accessible allylic alcohols in a ruthenium-catalysed process. In this way, the combination of appropriate catalytic platforms can provide, by a single process divergent synthesis, the aforementioned two different families of intermediate compounds starting with the isomerisation of readily available allylic alcohols.

**Catalytic Platform 1. Ruthenium-catalysed isomerisation of allylic alcohols into ketones:** Ru-complexes are highly efficient catalysts for the isomerisation of different allylic alcohols under mild conditions and using neoteric solvents such as water,<sup>22</sup> deep eutectic solvents,<sup>23</sup> or ILs like [BMIM][BF<sub>4</sub>].<sup>24,25</sup> In the case of ILs, the catalysts can be recovered at least during five consecutive batches, using hexane as the extractive solvent. However, the catalyst activity showed certain degree of deactivation upon recycling. In order to develop a catalytic platform based on a Ru-catalyst able to efficiently working for multiple cycles and allowing a simple recycling of the catalyst, the combination of ILs with supercritical CO<sub>2</sub> (scCO<sub>2</sub>) provides a relatively simple and straightforward technological solution.<sup>26</sup> Generally, the IL-phase is used for the homogeneous immobilisation of the catalyst (metal complexes, enzymes, nanoparticles, etc), while the scCO<sub>2</sub> phase is intended to favor the delivery of substrates to the catalytic sites on the IL phase and to facilitate the extraction and separation of the final products. Very often, this combination allows optimising the efficiency of a given process leading to good yields and productivities by the fine tuning of the contact time of the scCO<sub>2</sub>/IL-phases using either the pressure or the flow rates. These catalytic platforms exclude the need of other additional solvents and facilitate the isolation and separation of the products from the catalyst, being able to work 24/7, requiring less work force for operation, reducing the equipment size and maximising the productivity.



**Scheme 1.** Model isomerisation reaction and Ru catalysts used.

In order to develop such a catalytic platform, four different Ru-complexes were initially screened for the batch isomerisation of 1-octen-3-ol in a IL phase. The reaction was performed using a solution of 0.5% weight of the Ru-complexes in [BMIM][NTf<sub>2</sub>] and with 1% mol of the catalyst with respect to the alcohol. The reaction was monitored at 1 and 17 hours. The results obtained are summarised in Table 1. The Ru(IV)-acetate complex **Ru-4** was the organometallic catalyst showing a higher activity, reaching > 99% of isomerisation yield of **5** in only one hour. The rest of the Ru(IV)-catalysts (**Ru-2** and **Ru-3**) led to lower yields in one hour (67% and 73%, respectively), while the Ru(II)-complex (**Ru-1**) showed almost no activity (< 10%) during the same period. The three Ru-complexes yielded from excellent to good levels of isomerisation when the reaction was performed for 17 hours. These results are in agreement with previous results, showing that the ruthenium(IV)-acetate complex **Ru-4** was an efficient catalyst for this reaction in both water (0.2 mol%, > 99%, 5 min, TOF 6000 h<sup>-1</sup>) and [BMIM][BF<sub>4</sub>] (1 mol%, > 99%, 5 min, TOF 1200 h<sup>-1</sup>).<sup>25</sup> The slight decay in activity here observed is likely to be associated with the less polar nature of [BMIM][NTf<sub>2</sub>].

**Table 1.** Isomerisation of 1-octen-3-ol (**5**) in [BMIM][NTf<sub>2</sub>] with 1% mol of Ru catalysts.<sup>[a]</sup>

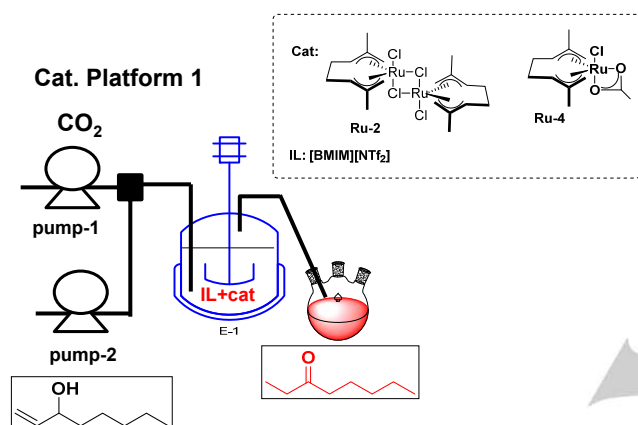
Entry	Catalyst	Yield (%) <sup>[b]</sup>	
		1 h	17 h
1	<b>Ru-1</b>	< 7	> 99
2	<b>Ru-2</b>	67	> 99
3	<b>Ru-3</b>	73	87
4	<b>Ru-4</b>	> 99	--

[a] 2 mmol of **5**. 1 gram of IL per mmol of reagent. 1% mol catalyst. Room temperature. [b] Determined by GC.

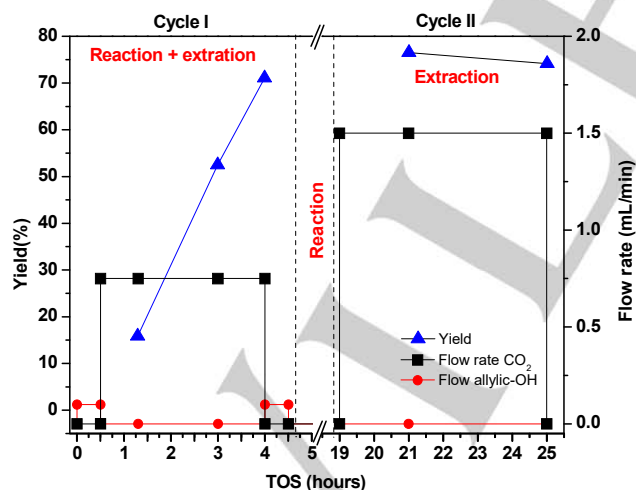
Once demonstrated the catalytic efficiency of the Ru(IV)-acetate complex (**Ru-4**) for the isomerisation of allylic alcohols in [BMIM][NTf<sub>2</sub>], the reaction was assayed using a ILs/scCO<sub>2</sub> system, which enabled the semi-continuous production of the ketone without the use of any additional organic solvent. The IL-phase was used simultaneously as reaction solvent and homogenous media for catalyst immobilisation. Initial experiments were performed with the dimeric complex **Ru-2**, as it can be obtained commercially or easily prepared and had shown good levels of activity for the isomerisation reaction. The reactor set-up is depicted in Fig. 2. The allylic alcohol was delivered by a HPLC pump, while a refrigerated head scCO<sub>2</sub> pump was used to feed the CO<sub>2</sub>. A stainless steel autoclave (100 mL) equipped with a magnetic stirring bar was used as the reactor unit. The reactants/scCO<sub>2</sub> flow was introduced in the reactor through a capillary (1/16 inch) into the IL-phase and the out-coming flow was connected to the upper part of the autoclave. The total pressure in the system was controlled via a backpressure regulator. The product was collected from the effluent CO<sub>2</sub> flow, after decompression, in a refrigerated glass



collector. The commercially available Ru(IV)-complex **Ru-2** (154 mg) was dissolved in 10.5 g of [BMIM][NTf<sub>2</sub>] (1.5% by weight). Initially the flow rates were set to 0.1 mL/min of 1-octen-3-ol (**5**) and 1.5 mL/min of CO<sub>2</sub> at 75 °C and 10 MPa. The reaction was performed by first feeding 3 mL of **5** to the reactor at a flow rate of 0.1 mL/min. After this, the system was filled with CO<sub>2</sub> until reaching a 10 MPa pressure and then, maintaining a constant flow rate of 1.5 mL/min, samples were collected at different times and analysed by GC. The initial samples showed a low degree of isomerisation due to the short contact time of the allylic alcohol with the complex. The degree of isomerisation increased with time, reaching ca. 50% and 70% after 3 and 4 hours, respectively (Cycle I, Fig. 3).



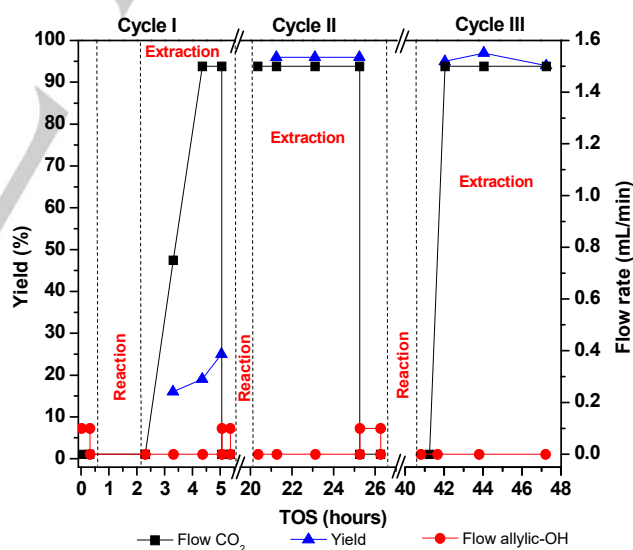
**Figure 2.** Schematic representation of the IL/scCO<sub>2</sub> set-up used for the isomerisation of **5** catalysed by **Ru-2** and **Ru-4**.



**Figure 3.** Results obtained for the isomerisation of **5** catalysed by **Ru-2** in a [BMIM][NTf<sub>2</sub>]/scCO<sub>2</sub> system at 75 °C and 10 MPa.

These results, demonstrated the feasibility of the isomerisation using the Ru complex immobilised in the homogenous liquid IL-

phase and the need of longer reaction times. Thus, the reactor was charged again in a second cycle with 3 mL of **5** (Cycle II; Fig 3). Then the reactor was filled with CO<sub>2</sub> until reaching 10 MPa and 75 °C. Once reached this pressure, the CO<sub>2</sub> flow was stopped and the reaction was left to proceed during 15 h at 10 MPa. After this period, the CO<sub>2</sub> pumping was restarted at 0.75 mL/min during 7 hours and the out-effluent collected and analysed. The GC and NMR of the oil obtained showed 95% of conversion of the allylic alcohol into the corresponding ketone. An additional cycle was repeated under the same conditions leading to comparable results (93% of the product was ketone). However, when the overall mass balance was analysed, a significant mass loss was observed. This can be associated with the evaporation of the product during the decompression process or with a low extraction efficiency of the product from the IL-phase. In order to evaluate the second possibility, the reactor was open and the catalyst/IL-phase recovered and extracted with Et<sub>2</sub>O. The organic layer showed a significant mass of the ketone (718 mg) confirming the low efficiency in the extraction under the conditions assayed. Noteworthy, a significant colour difference was observed between the product extracted either by scCO<sub>2</sub> or ether (Fig S.1). The product obtained by ether extraction clearly showed traces of the catalyst (coloured solution). Besides, the <sup>1</sup>H-NMR spectra revealed the presence in this product of traces of the IL-phase, while the one obtained with scCO<sub>2</sub> was a clear uncoloured oil without any trace of IL or catalyst.



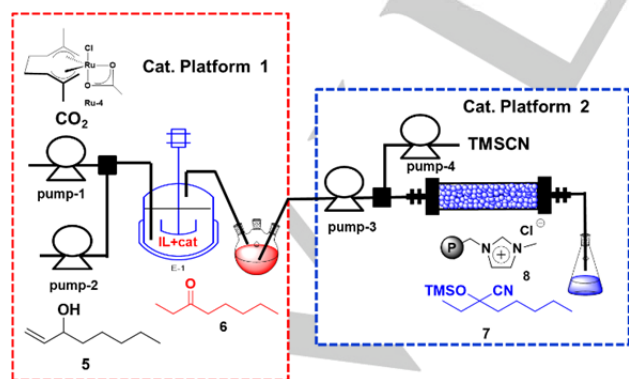
**Figure 4.** Results obtained for the isomerisation of **5** catalysed by **Ru-4** in a [BMIM][NTf<sub>2</sub>]/scCO<sub>2</sub> system at 75 °C and 10 MPa.

Encouraged by these results, the catalyst **Ru-4** was assayed under similar conditions. Fig. 4 gathers the results obtained. In a first cycle the reactor was loaded with 2 mL of the allylic alcohol corresponding with a 0.27% mol catalyst loading and left during ca. two hours at 75 °C and 10 MPa. Under these conditions the product was extracted with low conversion (<30%, Cycle I).

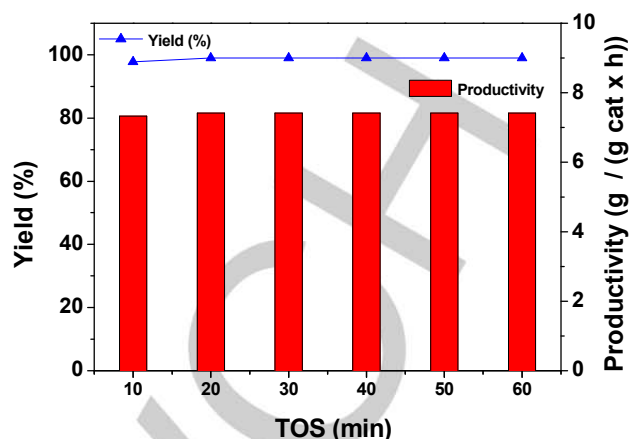
When the reactor was loaded with 2 mL of **5** and left to react overnight, the extract obtained under these conditions (1.5 mL/min flow rate of CO<sub>2</sub>) showed full conversion of the allylic alcohol into the corresponding ketone (Fig. 4, Cycle II). In order to push further the efficiency of the system, the reactor was loaded, in a third cycle, with 6 mL of **5**, corresponding with a catalyst loading of 0.09% mol and left to react overnight. Regardless of the catalyst loading reduction, the extract obtained corresponded with > 95% of conversion. Noteworthy, cycles II and III altogether provided a TON of 1425 moles of **6** per mol of **Ru-4**. Hence, the IL/scCO<sub>2</sub> system with the catalyst **Ru-4** provided a simple and efficient system for the synthesis of **6**, allowing the simple separation between the catalytic phase and the product and the recovery and reuse of the catalyst and the IL-phase.

**Catalytic Platforms 1 + 2. From allylic alcohols to cyanohydrins:** Once established that the combination **Ru-4** / IL / scCO<sub>2</sub> can efficiently transform the allylic alcohol **5** into ketone **6**, the further transformation of **6** into its cyanohydrin trimethylsilyl ether (**7**) by reaction with TMSCN was evaluated using an organocatalytic system (catalytic platform 2). A highly efficient catalyst has been reported by our group for this transformation, based on the use of supported ionic liquid-like systems.<sup>27</sup> Thus, the conversion of the ketone **6** obtained by the catalytic platform 1 into **7** was evaluated by pumping this product through a fixed-bed reactor containing the catalyst **8** (Fig. 5).

Figure 6 summarises the results obtained using a flow rate of 0.1 mL/min of a mixture of one equivalent of ketone **6** and 1.2 equivalents of TMSCN at room temperature and under solvent free conditions. Under this experimental set-up, 6 mL of the ketone **6** (obtained with the metal-based catalytic platform 1) were transformed under solvent-free conditions into the corresponding cyanohydrin **7** with an excellent yield (99%). Hence, the combination of these two systems can be used for the efficient synthesis of cyanohydrins starting from allylic alcohols with excellent productivity by unit of volume for both synthetic transformations, 18 g of **6**·g<sup>-1</sup> cat **Ru-4**·min<sup>-1</sup>·L<sup>-1</sup> and 0.12 g of **7**·g<sup>-1</sup> cat **8**·min<sup>-1</sup> highlighting the efficiency of the system.

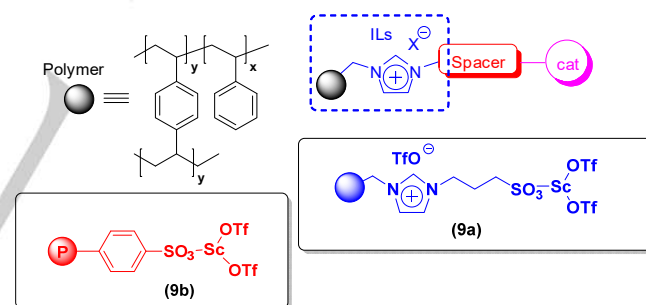


**Figure 5.** Schematic representation of the set-up combining the catalytic platforms 1 + 2 for the conversion of **5** into **7** catalysed by **Ru-4** and **8**.



**Figure 6.** Catalytic platform 2. Solventless conversion of the ketone **6** obtained with the catalytic platform 1 into **7**. Flow rate: 0.1 mL/min. **6**:TMSCN 1:1.2 mol ratio. Residence time: 20 min. 600 mg of catalyst **8**.

**Catalytic Platforms 1 + 3. From allylic alcohols to  $\alpha$ -aminonitriles:** The classical Strecker reaction is one of the simplest and most economical methods for the synthesis of racemic  $\alpha$ -aminonitriles, which can be further converted into other useful products such as  $\alpha$ -amino acids or other intermediates of pharmacological interest either via hydrolysis or by nucleophilic additions to the nitrile group.<sup>28</sup>



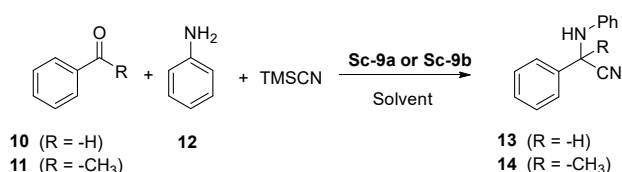
**Figure 7.** PS-DVB Task specific supported ionic liquid like phases for Sc complexation (**9a**) and related non-IL-like system (**9b**).

Among the cyanide sources, trimethylsilyl cyanide (TMSCN) is relatively easy to handle and highly soluble in organic solvents. Being the same reagent leading to cyanohydrins, TMSCN can be used to induce further diversity in the presence of an amine and the suitable catalyst.

Polystyrene-immobilised catalysts, with either Ru or Sc as the Lewis acid site, readily promote the three-component reaction of aldehydes and amines with TMSCN to afford  $\alpha$ -aminonitriles with excellent conversions.<sup>29</sup> The analogous reactions with ketones required catalysts being significantly more active. For instance, a polystyrene-supported gallium triflate (PS-Ga(OTf)<sub>2</sub>) has been reported to efficiently catalyse the ketonic Strecker

reaction, in which the target  $\alpha$ -aminonitriles were obtained in high yield and purity.<sup>30</sup> Furthermore, this catalyst showed a good activity under continuous flow conditions.

Previous work in our group allowed developing a catalyst based on task specific supported ionic liquid-like phases modified with sulfonic groups able to complex lanthanide triflates, in particular scandium triflate ( $\text{Sc}(\text{OTf})_3$ ).<sup>31,32</sup> Fig. 7 illustrates the structure of this catalyst (**9a**). In **9a**, the presence of the extra imidazolium IL-like units on the polymeric support can achieve, as in related ILs, an “*electrophile–nucleophile dual activation*”. The presence of a cooperative hydrogen-bonded network can contribute to improve the catalytic activity provided by the Lewis acid units.<sup>33,34,35,36</sup> The analogous Sc-supported catalyst **9b**, lacking the IL-like units, was also prepared from a commercially available sulfonic polystyrene-divinylbenzene polymer (Amberlyst® 15) and  $\text{Sc}(\text{OTf})_3$ .<sup>37</sup>



**Scheme 2.** Three-component benchmark Strecker reaction catalysed by **9a** and **9b**.

**Table 2.** Three-component Strecker reaction of benzaldehyde (**10**) or acetophenone (**11**), aniline (**12**) and TMSCN catalysed by **9a** or **9b** (r.t.).<sup>[a]</sup>

Entry	Catalyst	Substrate	Solvent	R	Yield
1	<b>9a</b>	<b>10</b>	Solvent free	-H	89
2	<b>9a</b>	<b>10</b>	CH <sub>3</sub> CN	-H	99
3	<b>9a</b>	<b>10</b>	2-Me-THF	-H	98
4	<b>9a</b>	<b>10</b>	DMC	-H	95
5	<b>9b</b>	<b>10</b>	CH <sub>3</sub> CN	-H	84
6	<b>9b</b>	<b>10</b>	2-Me-THF	-H	17
7	<b>9a</b>	<b>10</b>	CH <sub>3</sub> CN	-CH <sub>3</sub>	20
8	<b>9a</b>	<b>10</b>	2-Me-THF	-CH <sub>3</sub>	69
9	<b>9b</b>	<b>11</b>	CH <sub>3</sub> CN	-CH <sub>3</sub>	< 5
10	<b>9b</b>	<b>11</b>	2-Me-THF	-CH <sub>3</sub>	< 5

[a] 1 eq benzaldehyde (**10**) or acetophenone (**11**) (5 mmol), 1 eq aniline (**12**) (5 mmol), 1.2 eq TMSCN (6 mmol); 50 mg cat. **9a** or **9b** per mmol of **10/11**; 1 mL of solvent per mmol of **10/11**. Room temperature.

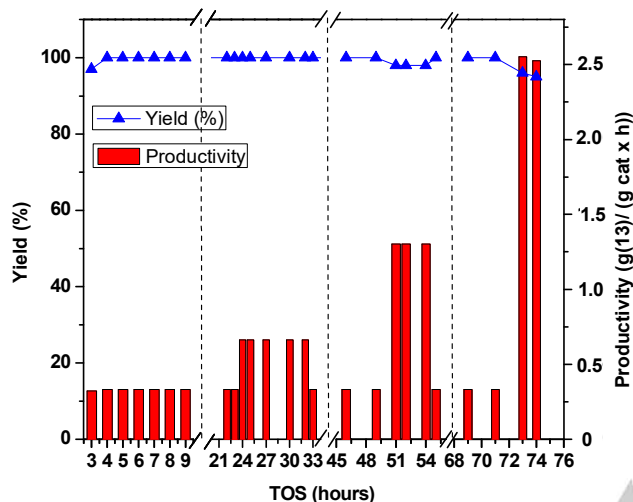
Both catalysts, **9a** and **9b**, were evaluated for the Strecker reaction between benzaldehyde (**10**), aniline (**12**) and trimethylsilyl cyanide (TMSCN) (Scheme 2).<sup>38</sup> Under solvent free conditions, benzaldehyde was smoothly converted in the corresponding  $\alpha$ -aminonitrile in the presence of the catalyst **9a** (Entry 1, Table 2). Near quantitative yields were achieved when the reaction was performed in the presence of an additional

solvent (Entries 2-4, Table 2). Excellent yields were observed when 2-methyl-tetrahydrofuran (2-Me-THF) and dimethylcarbonate (DMC) were evaluated as alternative more benign solvents than acetonitrile. In order to elucidate the possible role of the IL-like units, the reaction between **10**, **12** and TMSCN was also carried out in the presence of **9b** using either CH<sub>3</sub>CN or 2-Me-THF as solvents. The yields obtained under these conditions (Entries 5 and 6, Table 2) were significantly lower than those observed for **9a** having IL-like units. When the reaction was performed in 2-Me-THF, the catalyst **9a** led to 98% yield for **13** in 24 hours, while the yield was only 17% with **9b** (Entries 3 vs. 6, Table 2). This difference was lower for the reactions carried out in CH<sub>3</sub>CN (99 vs. 84%, entries 2 and 5, Table 2). These differences were even more pronounced, when the less reactive acetophenone (**11**) was used instead of benzaldehyde. The Strecker reaction catalysed by **9a** afforded moderate yields of **14** in 2-Me-THF (69%, Entry 8, Table 2) while in CH<sub>3</sub>CN the yield was 20% (Entry 7, Table 2). Noteworthy, the catalyst **9b** was not active for this reaction in either of the solvents evaluated (Entries 9 and 10, Table 2).

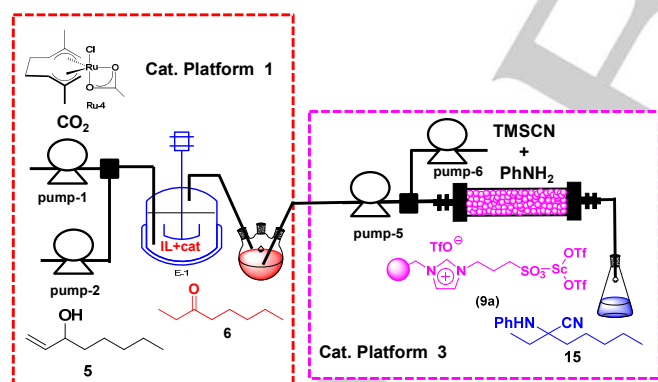
The very different behaviour of catalysts **9a** and **9b** highlights the key role played by the presence of IL-like fragments in **9a**. A cooperative effect seems to exist between the scandium sites and the IL-like units leading to a more efficient catalyst. The substrates can be activated through hydrogen bonding with both the imidazolium cation and the OTf<sup>-</sup> anion, which is not feasible in **9b**. As could be expected, this effect is more important in 2-Me-THF as CH<sub>3</sub>CN can compete with TMSCN minimising the “*electrophile–nucleophile dual activation*” of the reactants with the IL-like units.

The long-term stability of the catalyst **9a**, the continuous flow reaction between benzaldehyde (**10**) aniline (**12**) and TMSCN in 2-Me-THF was studied using a fixed bed reactor. This allows evaluating the catalyst stability in the absence of any physical abrasion of the polymeric beads associated to their extensive use and recycling produced after multiples cycles under batch conditions.<sup>39</sup> Different flow rates were evaluated (Figure 8). Firstly, the reactants were pumped through a reactor packed with 0.85 g of catalyst at a constant flow of 15  $\mu\text{L}/\text{min}$ . For this flow, the yield obtained was > 99% without any apparent activity decay during more than 24 hours. Therefore, the flow rate was increased from 15  $\mu\text{L}/\text{min}$  to 30  $\mu\text{L}/\text{min}$ . The analysed samples still showed very good activity (yield > 95%). The flow rate was again reduced to 15  $\mu\text{L}/\text{min}$  to confirm the results previously obtained and again yields > 99% were observed. No leaching of scandium was detected in the liquid phase by ICP-MS. These results confirmed the stability of the catalyst for more than 50 hours of continuous use. Then, the flow rate was increased further to 60  $\mu\text{L}/\text{min}$ . Once again excellent results were found when the samples were analysed (yield > 95%). Once more, the flow rate was set back to 15  $\mu\text{L}/\text{min}$  achieving again to the same initial results, thus, not observing any catalytic decay during 71 hours of continuous use. Finally, the flow rate was increased to 120  $\mu\text{L}/\text{min}$  showing yields again around 95%. Altogether, these results suggest that **9a** is a very stable catalyst for the Strecker reaction under continuous flow conditions, with no detectable indication of catalyst deactivation after long periods of time.

It should also be mentioned that the increase in the flow rate provides important improvements in the productivity of this catalytic platform. Thus, for the higher flow rate used (120  $\mu\text{L}/\text{min}$ ) ca. 2.5 grams of **13** per hour and gram of catalyst are produced, keeping a high conversion of the initial reactants (95%). Accordingly, with a small lab reactor (volume lower than 2.5 mL) loaded with ca. 2 g of catalyst and using a flow rate of 0.12 mL/min, ca. 121 g of **13** can be obtained in only 24 hours.



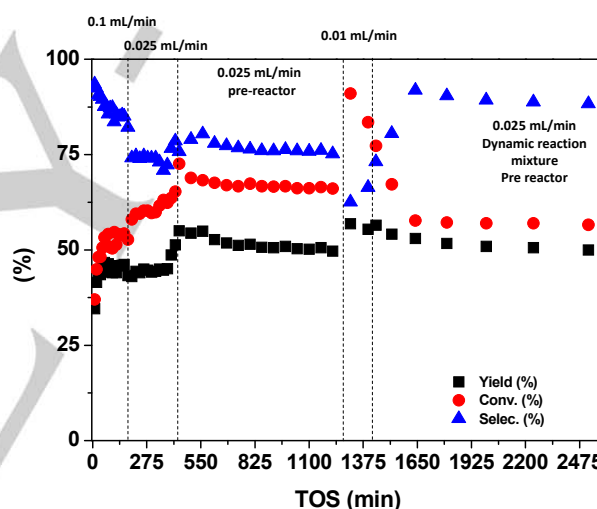
**Figure 8.** Yield of **13** vs. time on stream (TOS) for the three-component Strecker reaction of benzaldehyde (**10**), aniline (**12**) and TMSCN catalysed by **9a**. 1.5 M in 2-Me-THF, 0.850 g of catalyst **9a**, 2.4 mL reactor volume.



**Figure 9.** Schematic representation of the reactor set-up combining catalytic platforms 1 + 3 for the conversion of **5** into **15** catalysed by **Ru-4** and **9a**.

The combination of catalyst **9a** (Cat. Platform 3) with the **Ru-4**/IL/ $\text{scCO}_2$  system (Cat. platform 1) was then studied to transform the allylic alcohol **5** into the ketone **6** and this into the corresponding  $\alpha$ -aminonitrile **15**. The reaction of **6** with aniline (**11**) and TMSCN was firstly evaluated under batch and solvent free conditions. Noteworthy, the corresponding  $\alpha$ -aminonitrile **15** was obtained with a 99% yield (no traces of **7** were observed), confirming the selectivity of the reaction. Therefore, it seems

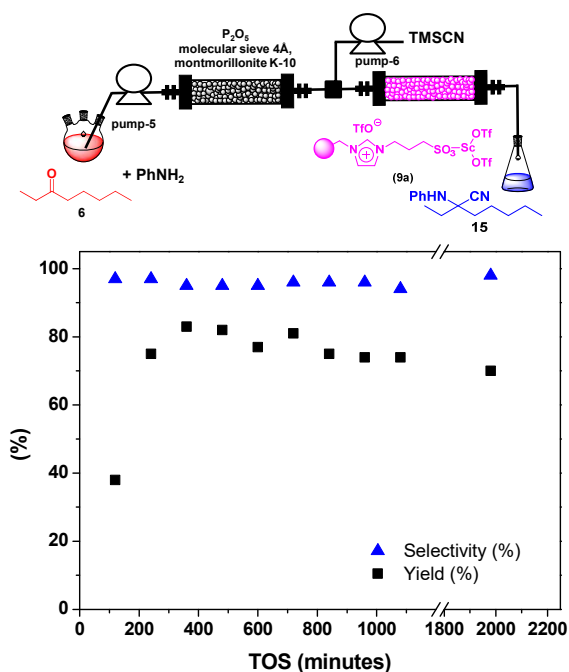
feasible to connect together the two catalytic platform 1 and 3 (Fig. 9). In this way, the product extracted from the system 1 was pumped through a catalytic fixed-bed reactor containing 0.6 g of **9a** at 0.1 mL/min. The results are summarised in Fig. 10. Initial results revealed modest yields (ca. 40-45%) of product **15** and low selectivities (80-85%) due to the formation of the corresponding cyanohydrin (obtained by direct reaction of **7** and TMSCN). A reduction in the flow rate to 25  $\mu\text{L}/\text{min}$  led to similar product yields, but the formation of the side product was enhanced leading to an increase of the ketone conversion and a decay in selectivity (ca. 70%). These results suggest that ketimine formation, under the conditions assayed, was the limiting factor. It must be noted that although the reaction in batch conditions was very selective, flow experiments are performed under different conditions. The actual substrate/catalyst ratio in the flow system is much higher than under batch conditions, which can additionally promote both the cyanosilylation and the Strecker reaction rates as to be higher than the one for ketimine formation, reducing selectivity.



**Figure 10.** Results obtained combining the catalytic platforms 1 and 3. Conversion, yield and selectivity of **15** vs. time on stream (TOS) for the three-component Strecker reaction of ketone **6**, aniline (**12**) and TMSCN catalysed by **9a**. 0.6 g of catalyst **9a**, 1.9 mL reactor volume.

An alternative to improve imine formation was to pump the ketone and the amine together in a coil reactor (0.2 mL, 8 min residence time) located before the fixed-bed reactor loaded with **9a**. Increasing the contact of ketone and aniline can favour the formation of the ketimine prior to the action of the catalyst **9a**. Under these conditions and using a 25  $\mu\text{L}/\text{min}$  flow rate, only a slight improvement in selectivity (75-77%) and yield of **15** (50-55%) was observed. A further increase of the residence time reducing the flow rate to 10  $\mu\text{L}/\text{min}$  did not improve the results. To avoid the problem associated to the slow formation of the ketimine, the ketone (**7**) and the aniline (**12**) were mixed together under solvent free conditions for 12 hours and then this mixture was pumped into the reactor at 25  $\mu\text{L}/\text{min}$ . The results obtained

were similar in terms of yield (50-55%) but the selectivity was clearly improved (ca. 90-92%).



**Figure 11.** Yield and selectivity for **15** vs. time on stream (TOS) for three-component Strecker reaction of ketone **6**, aniline (**12**) and TMSCN catalysed by **9a** and set-up used for the reaction. Reactor I: 1.2 g of molecular sieve 4A, 1.2 g  $P_2O_5$  and 1.2 g of MMK10, 3.9 mL reactor volume. Reactor II: 0.6 g of catalyst **9a**, 1.9 mL reactor volume.

To further implement the formation of the ketimine, a new fixed-bed reactor packed with a mixture of dehydrating agents and an acid catalyst was inserted before the reactor loaded with catalyst **9a** (Fig. 11).<sup>40,41</sup> This new reactor contained equal amounts of  $P_2O_5$ , 4A molecular sieves, and montmorillonite K-10 (MM K10). Thus, ketone **6** and aniline (**12**) were mixed together under solvent free conditions during 12 hours and then pumped through the first reactor heated at 60 °C using a 12  $\mu$ L/min flow rate. The solution at the outlet of this reactor was mixed with a flow of TMSCN (15  $\mu$ L/min) before entering the second fixed-bed reactor maintained at room temperature and packed with **9a**. Under these conditions, the yield was higher than 70% and the selectivity excellent (> 95%). Once again the final product (**15**) was obtained with excellent productivities as the reaction was performed under solvent free conditions (1.9 g of **15**  $g^{-1}$  of **9a**  $h^{-1}$ ). Thus, the combination of the catalytic platform 1 (metal-catalysed) and 3 (organo-catalysed) demonstrated to be suitable for the formation of  $\alpha$ -cyano-amines derived from aliphatic ketones.

## Conclusions

By the right combination of three different catalytic continuous flow platforms, a divergent synthetic flow system for the preparation of both protected cyanohydrin (**8**) and  $\alpha$ -amino nitrile (**15**) from allylic alcohol (**5**) has been achieved. The long term stability and the activity of each catalytic platform has been evaluated and optimised. In all of the catalytic platforms ILs-related species, as reaction media and / or as supported catalysts (SILLPs) played a key role. The results obtained for the Strecker reaction highlight the potential for catalytic applications of task specific functionalities (imidazolium-sulfonic acid in this case). The three component Strecker reaction of a non-reactive aliphatic ketone (**6**) has been achieved using a combination of dehydrating agents and supported catalysts in telescoped consecutive flow mini-reactors. Thus, the combination of allylic alcohol isomerisation with the cyanosilylation and Strecker reactions, both for aldehydes and ketones, gives access to a broad scope of valuable synthetic building blocks as are protected cyanohydrins and  $\alpha$ -amino nitriles with good yields in long-term stable continuous flow procedures. It is worth to comment that catalytic platforms 2 and 3 work under solventless conditions being the neoteric solvents  $scCO_2$  and [BMIM][NTf<sub>2</sub>] used in platform 1 the only solvent employed. Moreover, no purification step is needed between catalytic platforms and therefore a waste minimisation is reached in the whole process reported. High productivities can be obtained for the different catalytic and multicatalytic systems developed in the order of grams  $g^{-1}$  cat  $h^{-1}$ .

## Experimental Section

Ruthenium complexes (**Ru-1** to **Ru-4**) were obtained as previously described,<sup>24</sup> as well as SILLPs **8** and **9a-b**.<sup>27,31</sup>

**Batch isomerisation of 1-octen-3-ol (**5**) into 3-octanone (**6**).** 0.315 mL (2 mmol) of 1-octen-3-ol (**5**) were dissolved in 2 g of [BMIM][NTf<sub>2</sub>]. 0.02 mmol (1% mol) of ruthenium catalysts (**Ru-1** to **Ru-4**) were added and the mixture was left at 80 °C under orbitalic stirring (220 rpm) for 1 hour. Samples were periodically analysed by GC.

**Batch three-component Strecker reaction of benzaldehyde (**10**) or acetophenone (**11**), aniline (**12**) and TMSCN catalysed by **9a** or **9b**.** 0.515 mL (5 mmol) of benzaldehyde (**10**) or 0.590 mL (5 mmol) of acetophenone (**11**), 0.456 mL (5 mmol) of aniline (**12**) and 0.758 mL (6 mmol) of TMSCN were mixed. 5 mL of solvent (except solvent free cases) and 250 mg of catalysts **9a** or **9b** were added (50 mg/mmol **10** or **11**). The mixture was stirred for 24 hours at room temperature. The samples were analysed by <sup>1</sup>H-NMR.

**Continuous flow three-component Strecker reaction of benzaldehyde (**10**), aniline (**12**) and TMSCN catalysed by **9a**.** The reactor was set-up by introducing the SILLP-**9a** (850 mg) in a glass Omnifit® column 006RG-10-10 (0.7854 cm x 10 cm), which was connected at its head to a KdScientifics model of syringe pump. A 25 mL Hamilton syringe filled with benzaldehyde (**10**), aniline (**12**) and TMSCN (1:1:1.2) was used. The mixture of reagents was pumped through the catalytic bed at different flow rates going from 0.015 to 0.12 mL/min. Aliquots were taken at constant time intervals and analysed by <sup>1</sup>H-NMR.

**Continuous flow cyanosilylation reaction of 3-octanone (6).** The reactor was set-up by introducing the SILLP-8 (600 mg) in a glass Omnifit® column 006RG-10-10 (0.7854 cm x 10 cm), which was connected at its head to a KdScientifics model of syringe pump. A 25 mL Hamilton syringe filled with 3-octanone (6) and TMSCN (1:1.2) was used. The mixture of reagents was pumped through the catalytic bed at 0.1 mL/min. Aliquots were taken at constant time intervals and analysed by GC.

**Continuous flow three-component Strecker reaction of 3-octanone (6), aniline (12) and TMSCN catalysed by 9a** The reactor was set-up by introducing the SILLP-9a (600 mg) in a glass Omnifit® column 006RG-10-10 (0.7854 cm x 10 cm). The reagents mixture was pumped through the reactor using Hamilton syringes in KdScientifics syringe pumps. Several different strategies were used in order to favour the previous formation of the ketimine. Method i) a mixture of 3-octanone (6), aniline (12) and TMSCN (1:1:1.2) was pumped through a coil reactor at 0.025 mL/min (1 m, 0.2 mL, 8 min residence time) set-up before the fixed-bed reactor loaded with 9a. Aliquots were taken at constant time intervals and analysed by GC. Method ii) a mixture of 3-octanone (6) and aniline (12) (1:1) was stirred at r.t. overnight (15 h). Then, TMSCN was added (1.2 molar eq.) and the mixture was pumped through the fixed bed reactor loaded with 9a using a 25 mL Hamilton syringe and a KdScientifics model of syringe pump. Aliquots were taken at constant time intervals and analysed by GC. Method iii) a Omnifit® column 006RG-10-10 (0.7854 cm x 10 cm) was packed with 4Å molecular sieves (1.2 g), P<sub>2</sub>O<sub>5</sub> (1.2 g) and montmorillonite K10 (1.2 g). The reactor was heated at 60 °C using a *i*-PrOH reflux and was connected at the head to a KdScientifics model of syringe pump. A mixture of 3-octanone (6) and aniline (12) (1:1) was pumped through the reactor at 0.012 mL/min. After this reactor a T-piece was connected and TMSCN was pumped at 0.013 mL/min joining the previous reagents mixture before entering the reactor packed with 9a. Aliquots were taken at the exit of the second reactor and analysed by <sup>1</sup>H-NMR.

## Acknowledgements

Financial support has been provided by MINECO of Spain (CTQ2015-68429-R, CTQ2016-81797-REDC and CTQ2016-75986-P) Generalitat Valenciana (PROMETEO/2016/071) and the Gobierno del Principado de Asturias (Project GRUPIN14-006). Technical support from SCIC-UJI is also acknowledged.

E. Peris thanks MICINN for the financial support (FPU13/00685).

**Keywords:** Ionic liquid • Supported ionic liquid • supercritical CO<sub>2</sub> • catalysis • continuous flow

- [1] H. C. Erythropel, J. B. Zimmerman, T. M. de Winter, L. Petitjean, F. Melnikov, C. H. Lam, A. W. Lounsbury, K. E. Mellor, N. Z. Janković, Q. Tu, L. N. Pincus, M. M. Falinski, W. Shi, P. Coishac, D. L. Plata, P. T. Anastas, *Green Chem.* **2018**, *20*, 1929-1961.
- [2] G. Szöllösi, *Catal. Sci. Technol.* **2018**, *8*, 389-422.
- [3] M. Hönic, P. Sondermann, N. J. Turner, E. M. Carreira, *Angew. Chem. Int. Ed.* **2017**, *56*, 8942-897.
- [4] *Metal Catalyzed Cascade Reactions*, (Ed.: T. J. J. Müller), Springer, Berlin, **2006**.
- [5] S. Schmidt, K. Castiglione, R. Kourist, *Chem. Eur. J.* **2018**, *24*, 1755-1768.
- [6] R. A. Sheldon, *Green Chem.* **2005**, *7*, 267-278.
- [7] *Chemical Reactions and Processes under Flow Conditions*, (Eds.: S. V. Luis, E. Garcia-Verdugo), RSC, Green Chemistry Series, **2009**.
- [8] M. B. Plutschack, B. Pieber, K. Gilmore, and P. H. Seeberger, *Chem. Rev.* **2017**, *117*, 11796-11893.
- [9] J. A. M. Lummiss, P. D. Morse, R. L. Beingsner and T. F. Jamison, *Chem. Rec.* **2017**, *17*, 667-680.
- [10] D. Dallinger, C. O. Kappe, *Curr. Opin. Green Sustain. Chem.* **2017**, *7*, 6-12.
- [11] L. Vaccaro, D. Lanari, A. Marrocchi and G. Strappaveccia, *Green Chem.* **2014**, *16*, 3680-3704.
- [12] V. Sans, L. Cronin, *Chem. Soc. Rev.* **2016**, *45*, 2032-2043.
- [13] S. Kobayashi, *Chem. Asian J.* **2016**, *11*, 425-436.
- [14] S. V. Ley, D. E. Fitzpatrick, R. M. Myers, C. Battilocchio, R. J. Ingham, *Angew. Chem. Int. Ed.* **2015**, *54*, 10122-10136.
- [15] E. García-Verdugo, B. Altava, M. I. Burguete, P. Lozano, S. V. Luis, *Green Chem.* **2015**, *17*, 2693-2713.
- [16] D. E. Fitzpatrick, S. V. Ley, *Tetrahedron* **2018**, *74*, 3087-3100.
- [17] D. Ghislieri, K. Gilmore, P. H. Seeberger, *Angew. Chem. Int. Ed.* **2015**, *54*, 678-682.
- [18] T. Nobuta, G. Xiao, D. Ghislieri, K. Gilmore, P. H. Seeberger, *Chem. Commun.* **2015**, *51*, 15133-15136.
- [19] F. F. Fleming, L. Yao, P. C. Ravikumar, L. Funk, B. C. Shook, *J. Med. Chem.* **2010**, *53*, 7902-7917.
- [20] D. Enders, J. P. Shilvock, *Chem. Soc. Rev.* **2000**, *29*, 359-373.
- [21] R. J. Gregory, *Chem. Rev.* **1999**, *99*, 3649-3682.
- [22] J. García-Álvarez, S. E. García-Garrido, P. Crochet, V. Cadierno, *Curr. Top. Catal.* **2012**, *10*, 35-56.
- [23] C. Vidal, F. J. Suárez, J. García-Álvarez, *Catal. Commun.* **2014**, *44*, 76-79.
- [24] J. García-Álvarez, J. Gimeno, F. J. Suárez, *Organometallics* **2011**, *30*, 2893-2896.
- [25] F. J. Suárez, C. Vidal, J. García-Álvarez, *Curr. Green Chem.* **2014**, *1*, 121-127.
- [26] U. Hintermair, G. Franciò, W. Leitner, *Chem. Commun.* **2011**, *47*, 3691-3701.
- [27] S. Martín, R. Porcar, E. Peris, M. I. Burguete, E. García-Verdugo, S. V. Luis, *Green Chem.* **2014**, *16*, 1639-1647.
- [28] V. V. Kouznetsov, C. E. Puerto Galvis, *Tetrahedron* **2018**, *74*, 773-810.
- [29] S. Kobayashi, *Eur. J. Org. Chem.* **1999**, 15-27.
- [30] C. Wiles, P. Watts, *ChemSusChem* **2012**, *5*, 332-338.
- [31] R. Porcar, P. Lozano, M. I. Burguete, E. Garcia-Verdugo, S. V. Luis, *React. Chem. Eng.* **2018**, *3*, 572-578.
- [32] Y. Gu, C. Ogawa, J. Kobayashi, Y. Mori, S. Kobayashi, *Angew. Chem. Int. Ed.* **2006**, *45*, 7217-7220.
- [33] A. Aggarwal, N. L. Lancaster, A. R. Sethi, T. Welton, *Green Chem.* **2002**, *4*, 517-520.
- [34] A. Sarkar, S. R. Roy, A. K. Chakraborti, *Chem. Commun.* **2011**, *47*, 4538-4540.
- [35] L. Zhang, X. Fu, G. Gao, *ChemCatChem* **2011**, *3*, 1359-1364.
- [36] S. R. Roy, A. K. Chakraborti, *Org. Lett.* **2010**, *12*, 3866-3869.
- [37] S. Iimura, K. Manabe, S. Kobayashi, *Tetrahedron* **2004**, *60*, 7673-7678.
- [38] F. Rajabi, S. Nourian, S. Ghiassian, A. M. Balu, M. R. Saidi, J. C. Serrano-Ruiz, R. Luque, *Green Chem.* **2011**, *13*, 3282-3289.
- [39] B. Altava, M. I. Burguete, E. García-Verdugo, S. V. Luis, *Chem. Soc. Rev.* **2018**, *47*, 2722-2771.
- [40] L. Abahmane, A. Knauer, J. M. Köhler J.M., G. A. Gross, *Chem. Eng. J.* **2011**, *167*, 519-526.
- [41] L. Abahmane, A. Knauer, U. Ritter, J. M. Köhler, G. A. Groß, *Chem. Eng. Technol.* **2009**, *32*, 1799-1805.

## Electronic Supporting Information

### **Divergent multistep continuous synthesis enabled by immobilised catalysts on IL-phases**

Edgar Peris<sup>a</sup>, Raúl Porcar<sup>a</sup>, Joaquín García-Álvarez<sup>b</sup>, María Isabel Burguete<sup>a</sup>, Eduardo García-Verdugo<sup>a\*</sup>, and Santiago V. Luis<sup>a\*</sup>

<sup>a</sup> Universitat Jaume I, Departamento de Química Inorgánica y Orgánica, Campus del Riu Sec, E-12071 Castellón, Spain

<sup>b</sup> Universidad de Oviedo, Departamento de Química Orgánica e Inorgánica, Instituto Universitario de Química Organometálica “Enrique Moles”, E-33071 Oviedo, Spain.

#### Table of Contents

1. *scCO*<sub>2</sub> *vs.* Et<sub>2</sub>O extraction
2. Set-up used for 1-octen-3-ol (5) isomerisation in *scCO*<sub>2</sub>.
3. Kinetic study of the batch Strecker reaction of benzaldehyde (10), aniline (12) and TMSCN catalysed by 9a.
4. Set-up used for the continuous flow three-component Strecker reaction of benzaldehyde (10), aniline (12) and TMSCN catalysed by 9a.
5. Different set-ups/strategies used for the continuous flow three-component Strecker reaction of 3-octanone (6), aniline (12) and TMSCN catalysed by 9a.
6. NMR Spectra.

## 1. $scCO_2$ vs $Et_2O$ extraction

The product of the isomerisation of 1-octen-3-ol (**5**), 3-octanone (**6**), was extracted with  $scCO_2$  in a continuous flow system. The catalytic ruthenium complex was dissolved in the IL [BMIM][NTf<sub>2</sub>] inside the reactor where the reaction takes place. 1-octen-3-ol (**5**) was pumped inside the reactor and finally the product 3-octanone (**6**) was extracted using  $scCO_2$ . This allowed to extract only the product (colourless) remaining intact the IL+Ru catalyst for the next catalytic cycle. In order to compare and confirm the suitability of the choice of  $scCO_2$ , an extraction with diethyl ether was performed. As could be seen in Figure S.1, with diethyl ether not only the product was extracted, but also part of the ionic liquid and the Ru catalyst dissolved in it. The colouration of the colourless diethyl ether is a proof (see Figure S1). Moreover, <sup>1</sup>H-NMR studies were done (see Figure S2) confirming this hypothesis. The top spectrum only contains the signals from 3-octanone (**6**), but the spectrum on the bottom shows additional signals.



Figure S1.  $Et_2O$  (left) vs  $scCO_2$  (right) extraction of the 3-octanone (**6**)



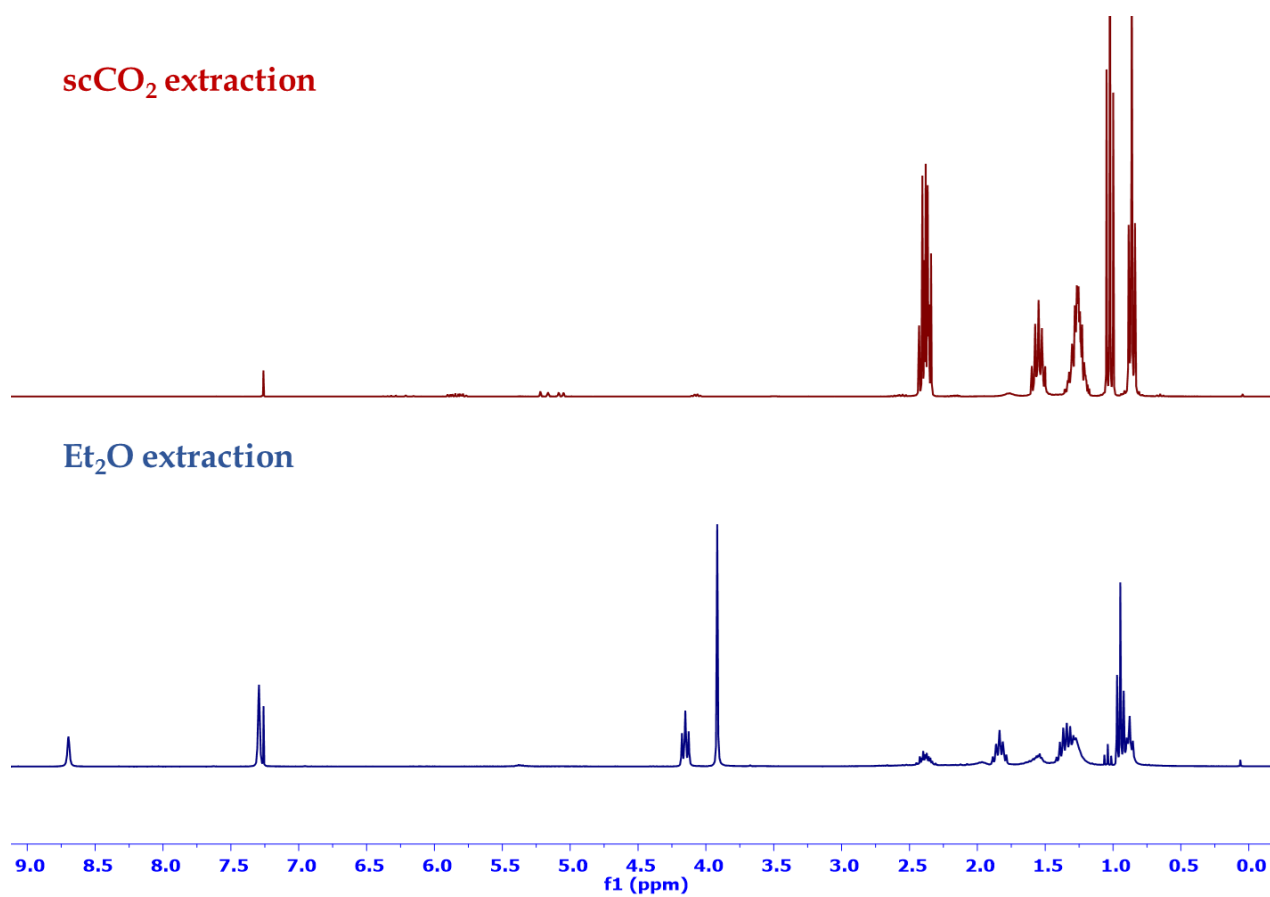


Figure S2. <sup>1</sup>H-NMR comparative study of the extraction of 3-octanone with scCO<sub>2</sub> or Et<sub>2</sub>O

## 2. Set-up used for 1-octen-3-ol (5) isomerisation in scCO<sub>2</sub>.

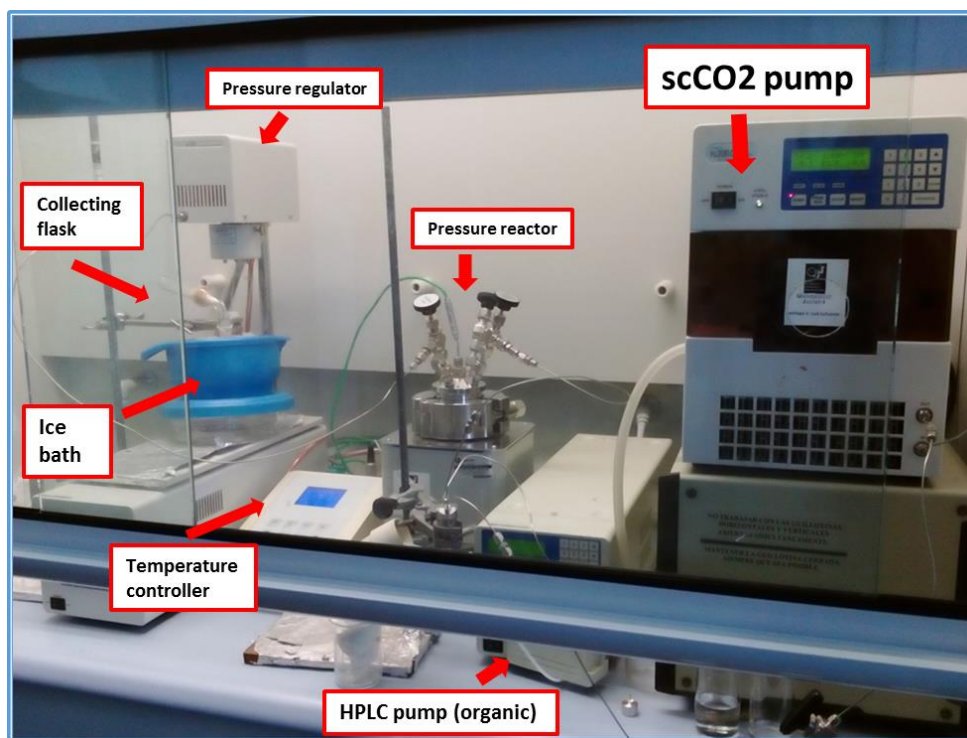


Figure S3. Set-up used for the continuous flow isomerisation of 1-octen-3-ol (5) into 3-octanone (6) using scCO<sub>2</sub>

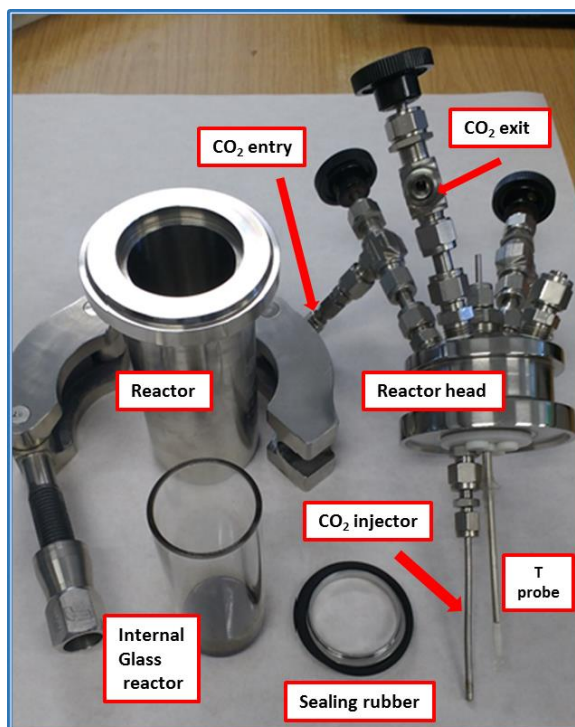
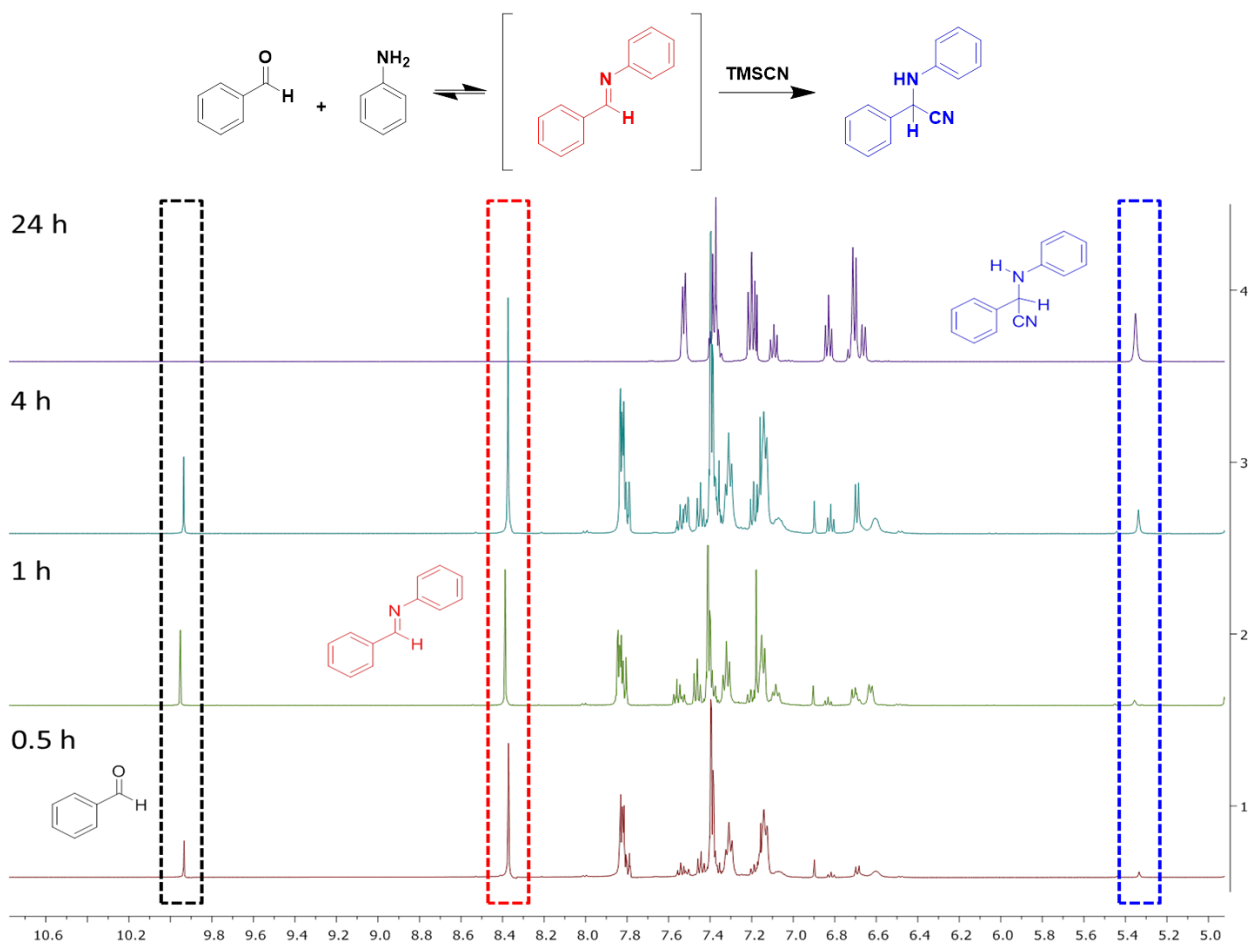


Figure S4. Parts of the pressure reactor used

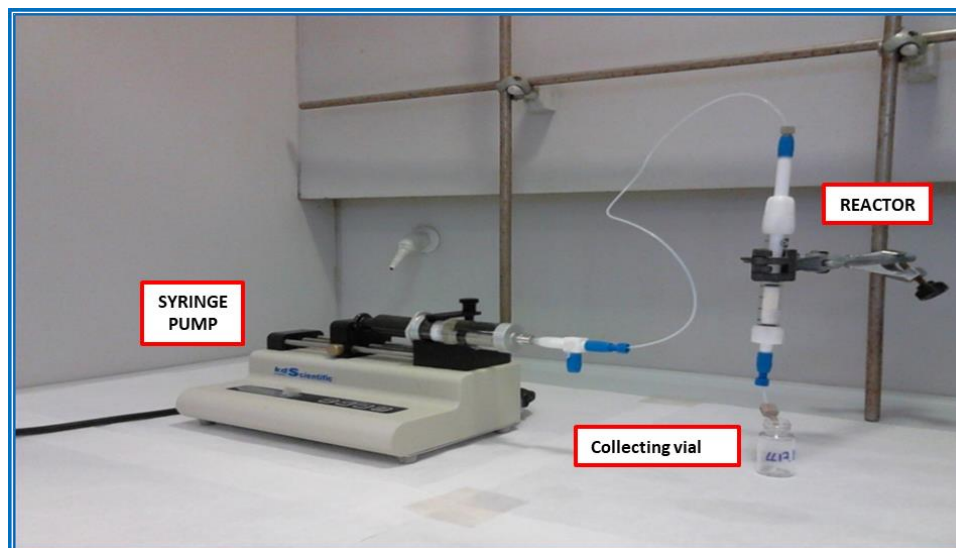
~ SI.4 ~

### 3. Kinetic study of the batch Strecker reaction of benzaldehyde (10), aniline (12) and TMSCN catalysed by 9a.



**Figure S5.** Kinetic study by  $^1\text{H-NMR}$  ( $\text{CDCl}_3$ ) of the batch Strecker reaction of benzaldehyde (10), aniline (12) and TMSCN. Conditions: 1 eq benzaldehyde (10) (5 mmol), 1 eq aniline (12) (5 mmol), 1.2 eq TMSCN (6 mmol), 250 mg cat-9a, 5 mL 2-MeTHF, r.t. The benzaldehyde singlet proton signal is observed at 9.9 ppm. The imine intermediate singlet proton signal is observed at 8.4 ppm. The Strecker product singlet proton signal is observed at 5.3 ppm. The evolution of the reaction with the appearing of the imine intermediate and posterior disappearing could be observed.

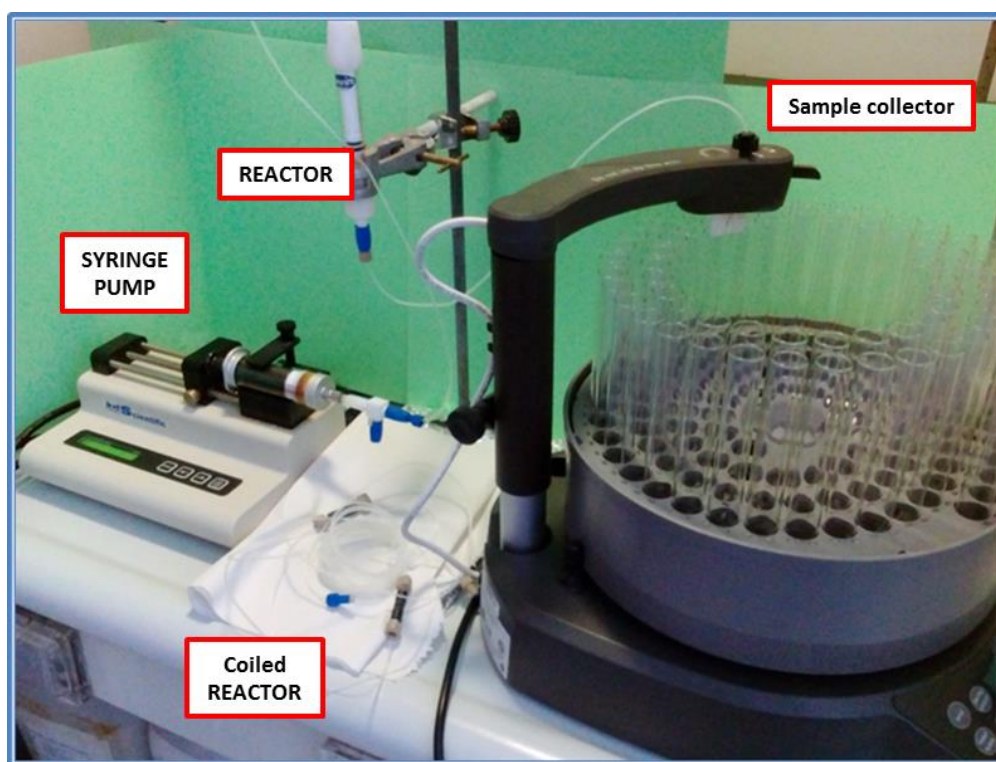
4. Set-up used for the continuous flow three-component Strecker reaction of benzaldehyde (**10**), aniline (**12**) and TMSCN catalysed by **9a**.



**Figure S6.** Set-up used for the continuous flow Strecker reaction of benzaldehyde (**10**). Syringe pump from kdScientific and Hamilton 25 mL syringe were used. Glass Omnifit column 006RG-10-10 (0.7854 cm diameter x 10 cm length) was used as reactor. The syringe was filled with a mixture of benzaldehyde (**10**), aniline (**12**) and TMSCN (1:1:1.2) 1.5 M in 2-MeTHF. The reactor was packed with 850 mg of SILLP-**9a**. The samples were collected in 12 mL glass vials.

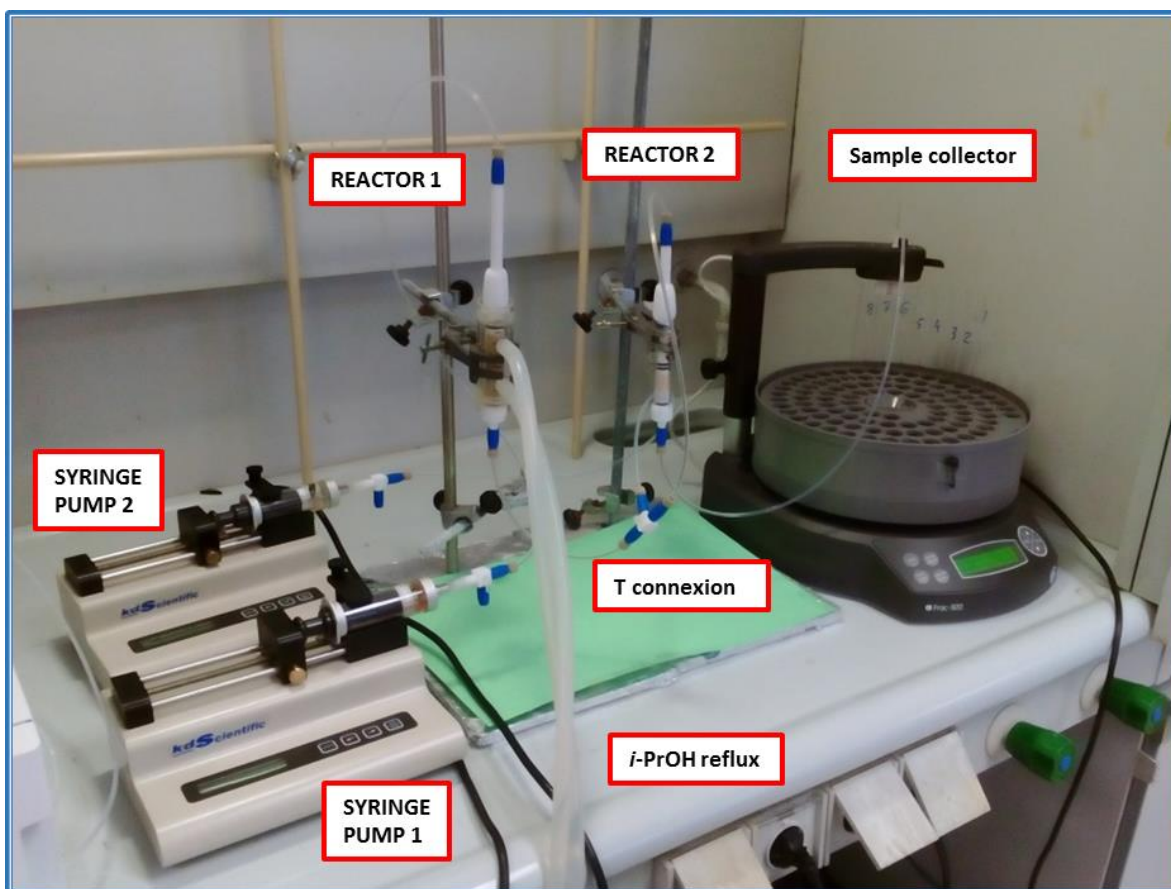
## 5. Different set-ups/strategies used for the continuous flow three-component Strecker reaction of 3-octanone (6), aniline (12) and TMSCN catalysed by 9a.

Imine intermediate formation showed to be the yield limiting step in the continuous flow Strecker reaction of the 3-octanone (6). One strategy tested to improve imine formation was to pump the ketone and the amine together in a coil reactor (0.2 mL, 8 min residence time) set-up before the fixed bed reactor loaded with 9a (see Figure S7). Increasing the contact time of ketone and aniline can favor the formation of the ketamine prior to the action of the catalyst 9a.



**Figure S7.** Set-up used to perform the Strecker reaction of 3-octanone (6) with a previous coil reactor to favor the imine intermediate formation. Syringe pump from kdScientific and Hamilton 25 mL syringe were used. Glass Omnifit column 006RG-10-10 (0.7854 cm diameter x 10 cm length) was used as reactor. Syringe was filled with a mixture of 3-octanone (6), aniline (12) and TMSCN (1:1:1.2). The coil reactor was 1 m length and 0.2 mL volume. Omnifit column reactor was filled with 600 mg of SILLP 9a. Fractions were collected at the exit of the column reactor using a Collector "GE Healthcare Frac-920".

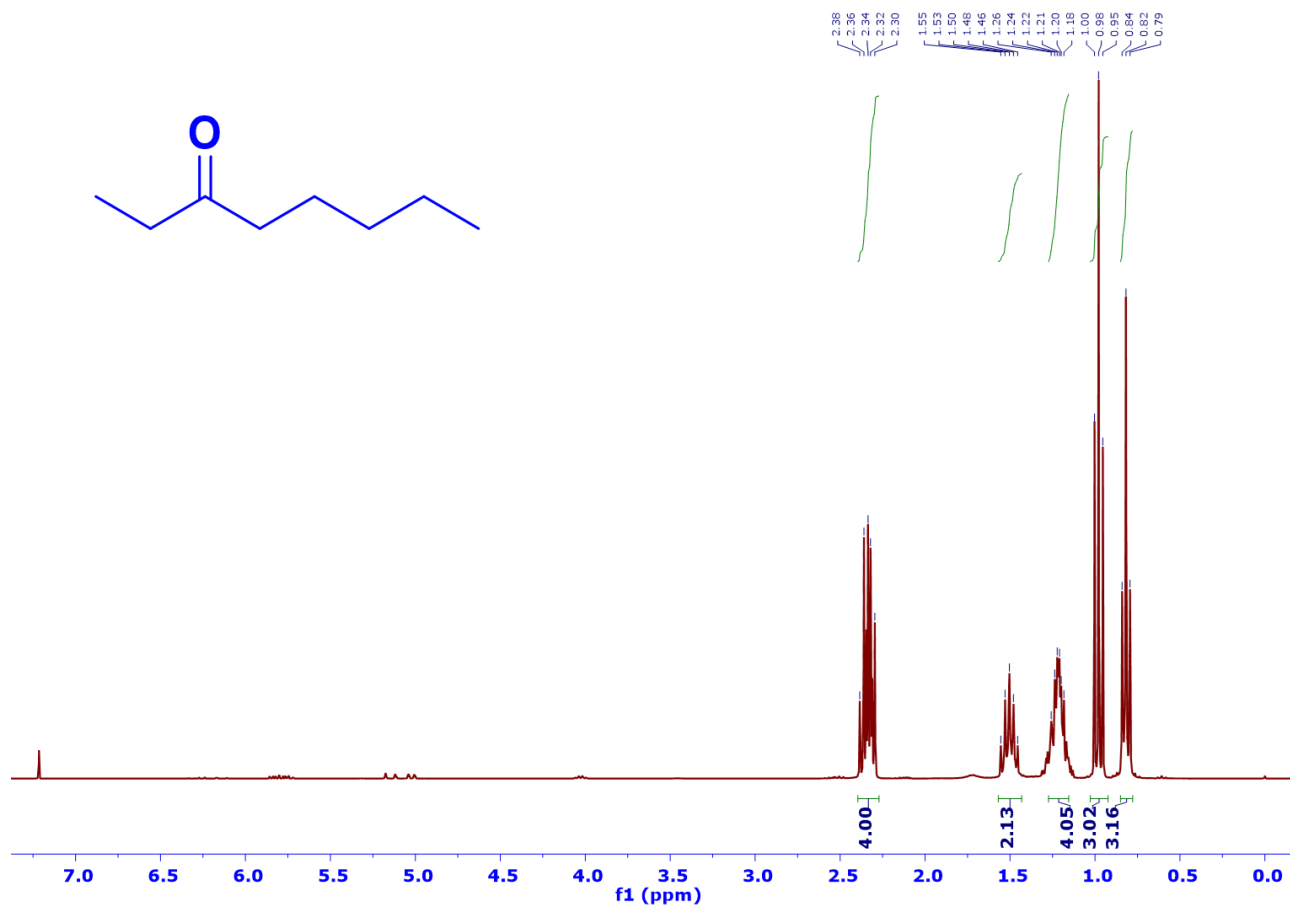
The second strategy used in order to push further the formation of the selectivity limiting ketamine, was to build a previous dehydrating catalytic reactor to favour the formation of the imine (see Figure S8).



**Figure S8.** Set-up used to perform the three-component Strecker reaction of 3-octanone (**6**) with a previous dehydrating catalytic fixed-bed reactor to favour the formation of the imine intermediate. Syringe pumps from kdScientific and Hamilton 25 mL syringes were used. Glass Omnifit columns 006RG-10-10 (0.7854 cm diameter x 10 cm length) were used as fixed-bed reactors. Syringe 1 was filled with a mixture of 3-octanone (**6**) and aniline (**12**) (1:1). Syringe 2 was filled with TMSCN. Reactor 1 was packed with 4Å molecular sieves (1.2 g), P<sub>2</sub>O<sub>5</sub> (1.2 g) and montmorillonite K10 (1.2 g). Reactor 1 was heated at 60 °C with a *i*-PrOH reflux. Reactor 2 was packed with 600 mg of SILLP **9a**. Fractions were collected at the exit of reactor 2 using a sample collector “GE Healthcare Frac-920”.

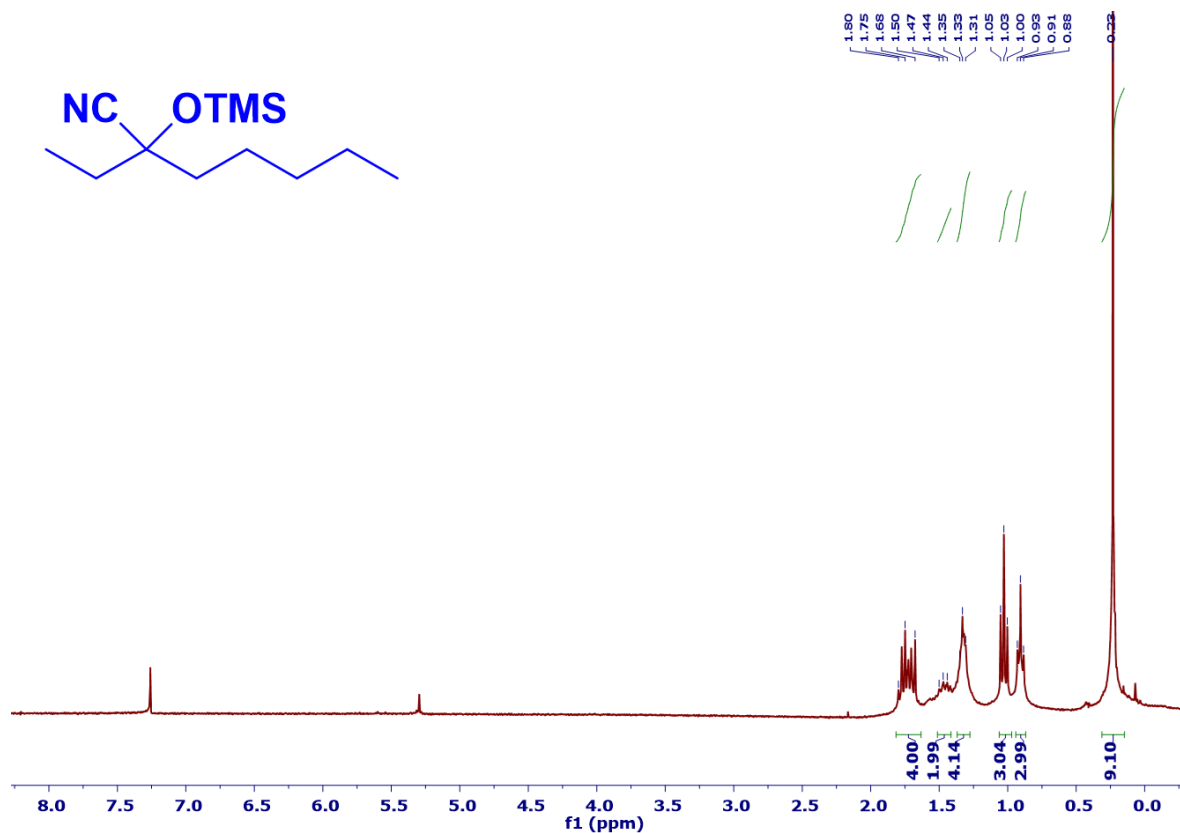
## 6. RMN spectra

### $^1\text{H-NMR}$ of 3-octanone (6)



$^1\text{H-NMR}$  (300 MHz,  $\text{CDCl}_3$ )  $\delta$  2.38-2.30 (m, 4H), 1.50 (q, 2H), 1.26-1.18 (m, 4H), 0.98 (t, 3H), 0.82 (t, 3H)

<sup>1</sup>H-NMR data of 2-ethyl-2-((trimethylsilyl)oxy)heptanenitrile (7)

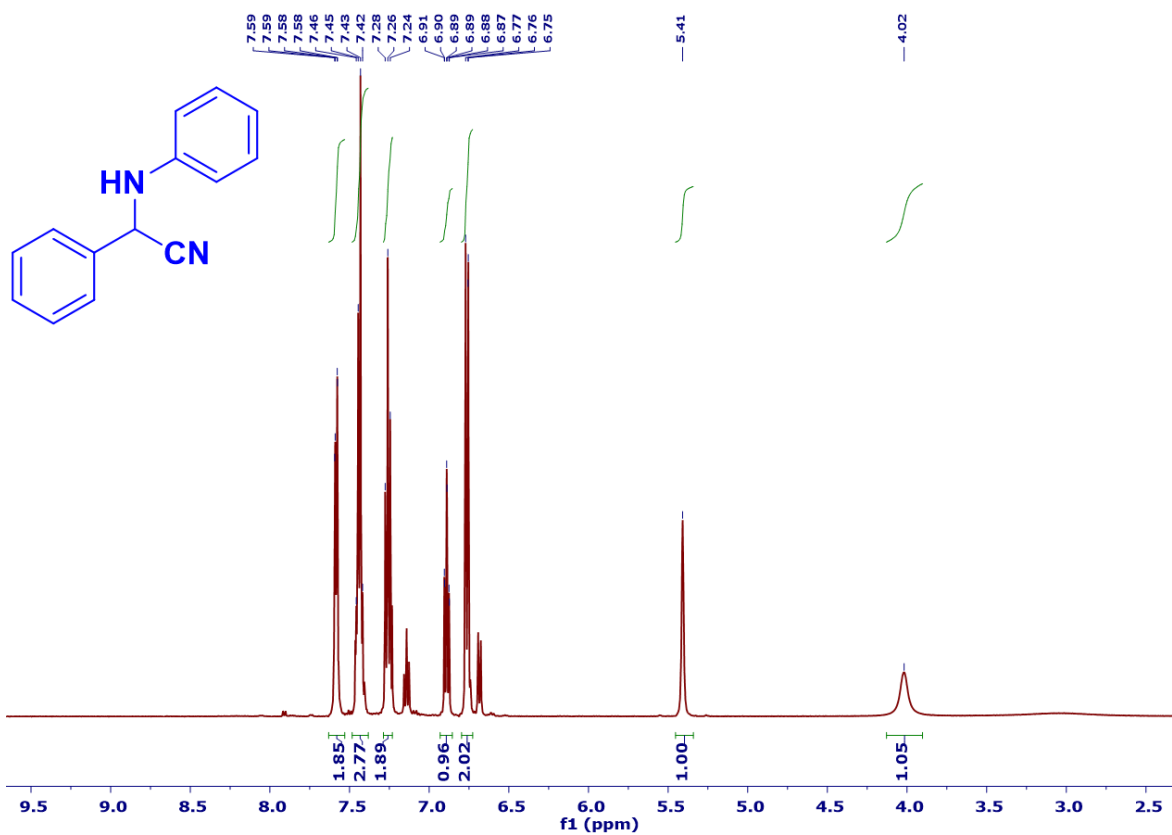


<sup>1</sup>H-NMR (300 MHz, CDCl<sub>3</sub>) δ 1.80-1.68 (m, 4H), 1.50-1.44 (m, 2H), 1.35-1.31 (m, 4H), 1.03 (t, 3H), 0.91 (t, 3H), 0.23 (s, 9H)

~ SI.10 ~



**<sup>1</sup>H-NMR data of 2-phenyl-2-(phenylamino)acetonitrile (13)**



<sup>1</sup>H-NMR (300 MHz, CDCl<sub>3</sub>) δ 7.58 (dd, 2H), 7.47-7.40 (m, 3H), 7.26 (t, 2H), 6.89 (td, 1H), 6.76 (dd, 2H), 5.41 (s, 1H), 4.02 (bs, 1H)



**Synergy between Supported Ionic  
Liquid-Like Phase and  
immobilised Palladium N-  
Heterocyclic Carbene Phosphine  
complexes for the Negishi  
reaction under flow conditions**

**CHAPTER 6**



## Chapter 6. Synergy between Supported Ionic Liquid-Like Phase and immobilised Palladium N-Heterocyclic Carbene Phosphine complexes for the Negishi reaction under flow conditions

### 6.1 RESUMEN DEL MANUSCRITO

Los complejos carbeno N-heterocíclico-paladio (NHC-Pd) se han empleado como catalizadores homogéneos eficientes para las reacciones de Negishi. La inmovilización de estos complejos metálicos en soportes poliméricos facilita su separación y recuperación. En este capítulo se resumen nuestros esfuerzos en el estudio del efecto de los SILLPs en la mejora de la eficiencia catalítica de los carbenos N-heterocíclicos de paladio (NHC-Pd) soportados en las reacciones de acoplamiento carbono-carbono de tipo Negishi y su evaluación en sistemas de flujo continuo.

En primer lugar se sintetizaron dos complejos NHC-Pd inmovilizados (**4a-b**) mediante alquilación de los correspondiente aril-imidazoles (**2a-b**) con resinas macroporosas preformadas de tipo Merrifield (**1**, PS-DVB clorometiladas, 20% DVB, 1.2 mmol Cl/g). Su reacción con Pd(OAc)<sub>2</sub> en medio básico dio lugar a los correspondientes complejos inmovilizados (Figura 6.1).

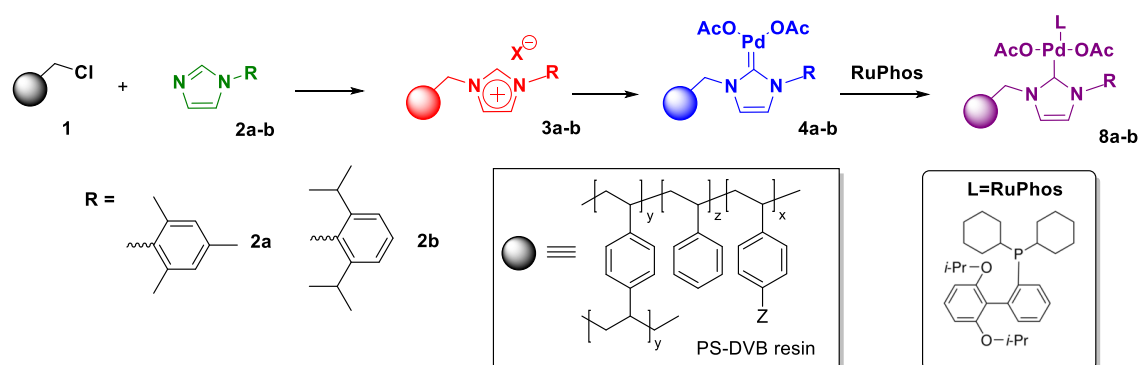


Figura 6.1. Secuencia de obtención de los NHC-Pd-SILLPs sintetizados

La reacción de acoplamiento de Negishi modelo elegida para evaluar la actividad catalítica de estos sistemas fue el acoplamiento entre bromuro de bencilzinc (**5**) y 4-bromobenzoato de metilo (**6**) (Figura 6.2).

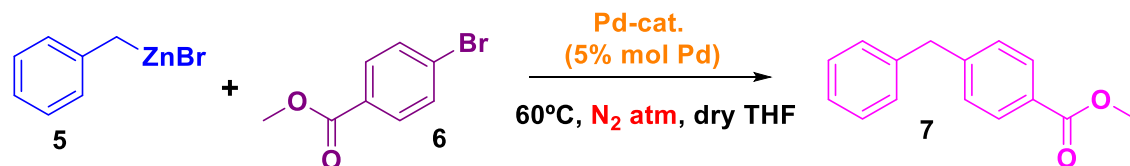


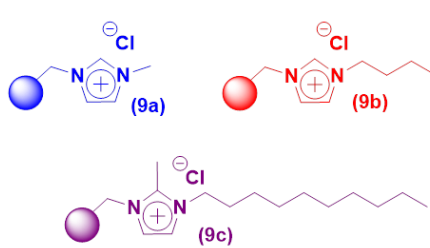
Figura 6.2. Reacción de acoplamiento de Negishi modelo.

Al evaluar la actividad catalítica de estos sistemas, el NHC-Pd-SILLP con sustituyentes metilo (**4a**) demostró muy poca actividad (< 10%) mientras que el catalizador con los sustituyentes isopropilo (**4b**) alcanzó una conversión del 67% en 2 horas. Con el fin de aumentar la reactividad de estos sistemas se evaluó la adición de una fosfina, ya que se ha descrito, en solución, que la presencia de ligandos conteniendo átomos de C, N o P coordinantes puede modular la reactividad de estos sistemas. En particular, se adicionó RuPhos como fosfina, ya que esta había sido empleada previamente como ligando de paladio en la reacción de Negishi. En ambos casos, la presencia de la fosfina incrementó sensiblemente la actividad del catalizador, confirmado el efecto sinérgico de la fosfina en la reactividad del NHC-Pd inmovilizado

Al intentar trasladar estos resultados a condiciones de flujo continuo, empleando reactores de lecho fijo rellenos con los catalizadores NHC-Pd-RuPhos-SILLP **8a** y **8b** (Figura 6.1), se observaron buenas reactividades iniciales si bien la actividad decayó, con una disminución de la actividad hasta alrededor del 50%, con el uso prolongado del sistema. Esto se puede explicar en función del lixiviado de paladio encontrado en las muestras recogidas y analizadas por ICP-MS. Así pues, los resultados sugieren que, bajo las condiciones de reacción empleadas, los complejos de NHC-Pd no son estables y en realidad actúan como pre-catalizadores liberando al medio de reacción especies de paladio catalíticamente activas.

Los líquidos iónicos soportados (SILLPs) pueden actuar, en principio, como scavengers de estas especies de paladio liberadas al medio de reacción. De este modo pueden evitar o minimizar el lixiviado de paladio y consecuentemente minimizar la pérdida de actividad de estos sistemas catalíticos. Por este motivo, se evaluó el posible papel de tres SILLPs con diferentes sustituyentes alquílicos como scavengers en la

reacción modelo, empleando la proporción 1:3 en peso del catalizador NHC-Pd con respecto al SILLP. Los resultados obtenidos sugieren que los SILLPs sí actúan como scavengers ya que en su presencia el nivel de paladio lixiviado a la reacción se redujo (Figura 6.3). La estructura del SILLP ejerció un papel tanto en el nivel de lixiviado como en la reactividad del sistema. Así, a menor longitud de la cadena alquílica, menor reactividad pero también menor lixiviado de paladio (Figura 6.3). Los análisis por TEM de los polímeros obtenidos después de la reacción mostraron, en todos los casos, la presencia de nanopartículas de paladio (PdNPs). La diferencia de reactividad observada puede atribuirse a la diferencia de tamaño observado para las PdNPs. A mayor longitud de cadena alquílica en el scavenger, menor tamaño de partícula presentan las PdNPs formadas y por ello una mayor reactividad.



	% conversion at 30 min	Leaching (ppm)
8a	40	22.4
8a + 9a	60	2.7
8a + 9b	78	14.4
8a + 9c	82	17.1

**Figura 6.3.** SILLPs utilizados como scavengers y resultados de su evaluación para la reacción de Negishi modelo entre bromuro de bencilzinc (5) y 4-bromobenzoato de metilo (6).

Estos estudios, junto a los resultados de estabilidad obtenidos en los estudios de flujo, parecen indicar que hay un mecanismo de liberación y recaptura de las diferentes especies de paladio y que, dependiendo de la naturaleza del NHC-Pd y del SILLP, se puede llegar a controlar la actividad y estabilidad de estos sistemas complejos. Con el fin de validar esta hipótesis, se inmovilizaron y evaluaron como catalizadores diferentes especies de Pd(II) y Pd(0) sobre SILLPs. Los resultados mostraron que estos sistemas son activos en la reacción de Negishi, siendo activos incluso durante varios ciclos consecutivos de reacción, siempre que esté presente el ligando tipo fosfina.

A la vista de estos estudios, se evaluó el uso conjunto del catalizador NHC-Pd-SILLP **4a** y del scavenger derivado de metilimidazolio (**9a**). Para ello, se diseñaron diferentes reactores de lecho fijo para su uso en continuo, demostrándose que un empaquetado homogéneo permite mantener la actividad de manera constante, mientras que para un

empaquetamiento en dos capas se produjo una desactivación significativa de la actividad catalítica (ver Figura 6.4).

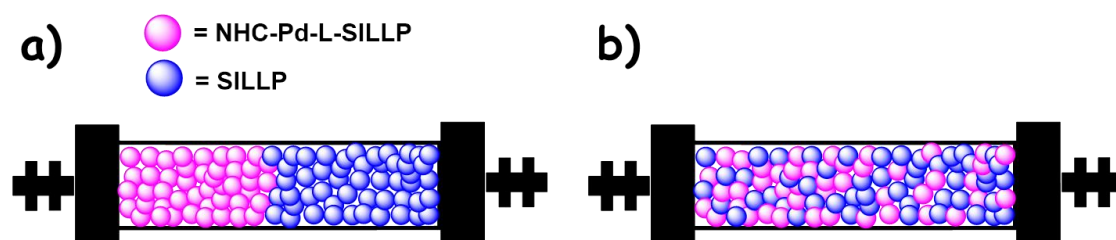


Figura 6.4. a) Llenado en dos capas de un reactor de lecho fijo, b) llenado homogéneo mezclando por completo los dos componentes.

Así pues, se diseñaron dos reactores de lecho fijo empleando este tipo de llenado:

- i) NHC-Pd-RuPhos-SILLP (**8a**) + SILLP (**9c**) (1:3): Conversión inicial del 100% pero rápida caída hasta un 50% antes de llegar a los 100 minutos de funcionamiento en continuo. Estos datos confirmaron lo esperado. El scavenger con el sustituyente decilo proporciona mayor reactividad pero poca estabilidad y la actividad decae.
- ii) NHC-Pd-RuPhos-SILLP (**8a**) + SILLP (**9a**) (1:3): Una conversión inicial del 85% cayó hasta el 70% a los 70 minutos pero se mantuvo estable así, con una producción de aproximadamente 5 g del producto acoplado (**7**)/g catalizador h. Encontramos, según lo previsto, una menor reactividad pero un sistema mucho más estable donde las especies catalíticas liberadas se recapturan de una manera más eficiente prolongando la estabilidad del sistema.

El trabajo desarrollado en este capítulo ha puesto de manifiesto las posibilidades de uso de los SILLPs para obtener sistemas catalíticos soportados de Pd más activos y estables para la reacción de acoplamiento de Negishi. El empleo de SILLPs modulables como soporte y scavenger, junto con el empleo de ligandos tipo fosfina, proporciona un efecto favorable en combinación con los complejos NHC-Pd tradicionalmente empleados.



# Synergy between Supported Ionic Liquid-Like Phase and immobilized Palladium N-Heterocyclic Carbene Phosphine complexes for the Negishi reaction under flow conditions.

*Edgar Peris,<sup>a</sup> Raul Porcar,<sup>a</sup> Jesús Alcázar,<sup>b</sup> Eduardo García-Verdugo,<sup>a</sup> Santiago V. Luis.<sup>a</sup>*

a) Dpt. of Inorganic and Organic Chemistry, Supramolecular and Sustainable Chemistry Group, University Jaume I, Avda Sos Baynat s/n, E-12071-Castellon. Spain, [luiss@uji.es](mailto:luiss@uji.es), [cepeda@uji.es](mailto:cepeda@uji.es)

b) Janssen Pharmaceutical Companies of J&J, Janssen-Cilag, S.A., Jarama 75A, 45007 Toledo, Spain, [jalcazar@its.jnj.com](mailto:jalcazar@its.jnj.com)

KEYWORDS. NHC complex, palladium, Negishi, supported ionic liquid, ionic liquid, immobilized catalyst.

## ABSTRACT

The combination of supported ionic liquid and immobilized NHC-Pd-RuPhos led to active and more stable immobilized systems for the Negishi reaction under continuous flow conditions than those solely based on NHC-Pd-RuPhos. The fine tuning of the NHC-Pd catalyst and SILLPs is a

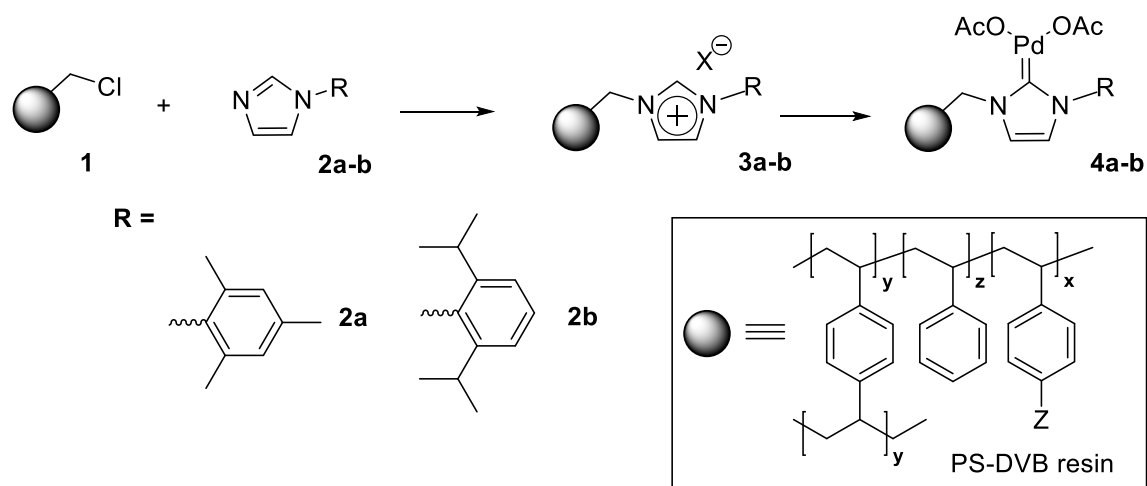
key factor for the optimization of the release and catch system leading to easily recoverable and reusable for a large number of catalytic cycles enhancing the long term catalytic performance.

## **Introduction.**

N-heterocycle carbenes (NHC) are known as efficient coordination ligands for different type of metals. The main feature of NHC-complexes is their structural tunability.<sup>1</sup> Thus, their catalytic efficiency can be easily modulated through systematic variations of the steric and electronic design vectors of the NHC-ligand.<sup>2</sup> These complexes have been used as highly efficient catalyst of a wide variety of C-C and C-X cross-coupling reactions.<sup>3</sup> Among others, different NHC-Pd complexes have been designed as efficient homogeneous catalysts for Negishi reactions.<sup>4</sup> Although these systems are highly efficient, their homogeneous nature hamper the separation of the products and recovery of the excess of the palladium from the reaction solution. A possible solution to this issue, it is the preparation of the related immobilized complex enabling a simpler recovery and reuse of the catalysts by filtration.<sup>5</sup> Furthermore, the immobilized NHC-complexes can be easily adapted to flow processes using a fix-bed reactor set-up increasing simultaneously the sustainability and the efficiency of the C-C coupling reactions.<sup>6,7</sup> In the pursuit of NHC immobilized metal complexes many different materials of organic and inorganic nature have been used as supports.<sup>5</sup> A number of reports describe the synthesis of supported palladium-NHC complexes (Pd-NHC) and their application in cross-coupling reactions.<sup>8,9,10</sup> The main flaw of this type of systems is related with the mechanistic aspect of most C-C formation reactions catalyzed by palladium.<sup>11</sup> Careful studies of the reaction mechanism have revealed that, under certain conditions, the palladium supported species can act as mere pre-catalysts leading to a complex cocktail of active species.<sup>12,13</sup> In the case of immobilised catalyst, these palladium species can be

released from the support reacting in the homogeneous medium transformed from Pd<sup>0</sup> to Pd<sup>II</sup>. In this way, a “cocktail” of catalyst including molecular complex, cluster and nanoparticles may be responsible for the catalytic activity.<sup>14</sup> In a continuous system, in order to avoid a loss of activity by this leaching process, the role of the ligand and the support on the evolution of the catalytic systems should be carefully considered. We and others have showed that the immobilization of Pd-catalyst or precatalyst onto supported ionic liquid like materials can facilitate the recapture of the active species by the support at the end of the reaction, in what has been called a “boomerang” mechanism.<sup>15</sup> Here, we report our efforts aiming a rational development for Negishi catalysts based on NHC-Pd complexes in conjunction with Supported Ionic Liquid-Like Phases to enhance their catalytic stability under continuous flow conditions.

**Results and discussion.** The synthesis of the different functionalized polymers considered in this work was carried out using commercial macromolecular Merrifield resins (macroporous chloromethylated PS-DVB, 20% DVB, 1.2 meq Cl /g, **1**).<sup>16,17</sup> The synthetic routes assayed are outlined in the Scheme 1. The introduction of the imidazolium subunit involves the reaction of the corresponding N-aryl imidazole (**2a** and **2b**) with a polymer-bound alkylating agent (Scheme 1). The modification of the modified resins was monitored by different techniques, such as FT-ATR-IR, Raman micro-spectroscopy and the NBP test.<sup>18,19</sup> All the polymers synthesized were then functionalized with Pd(OAc)<sub>2</sub> in the presence of a strong base to yield the corresponding supported Pd-NHC complexes (**4a-b**, Scheme 1). The amount of immobilized NHC ligand was determined by elemental analysis, while the palladium loaded on the polymer was determined by ICP analyses (see Table 1).

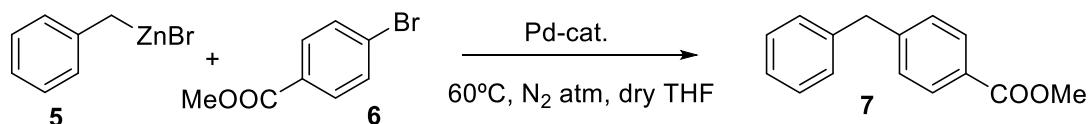


**Scheme 1.** Synthesis of NHC supported catalysts.

**Table 1.** Pd Loading for the different NHC-Pd synthesized.

Entry	Polymer	NHC Loading <sup>a</sup>	Pd Loading <sup>b</sup>
1	<b>4a</b>	0.764	0.7
2	<b>4b</b>	0.660	0.6

<sup>a</sup> As determined by elemental analysis (mmol functional group/g resin). <sup>b</sup> As determined by ICP analysis (mmol Pd/g resin).

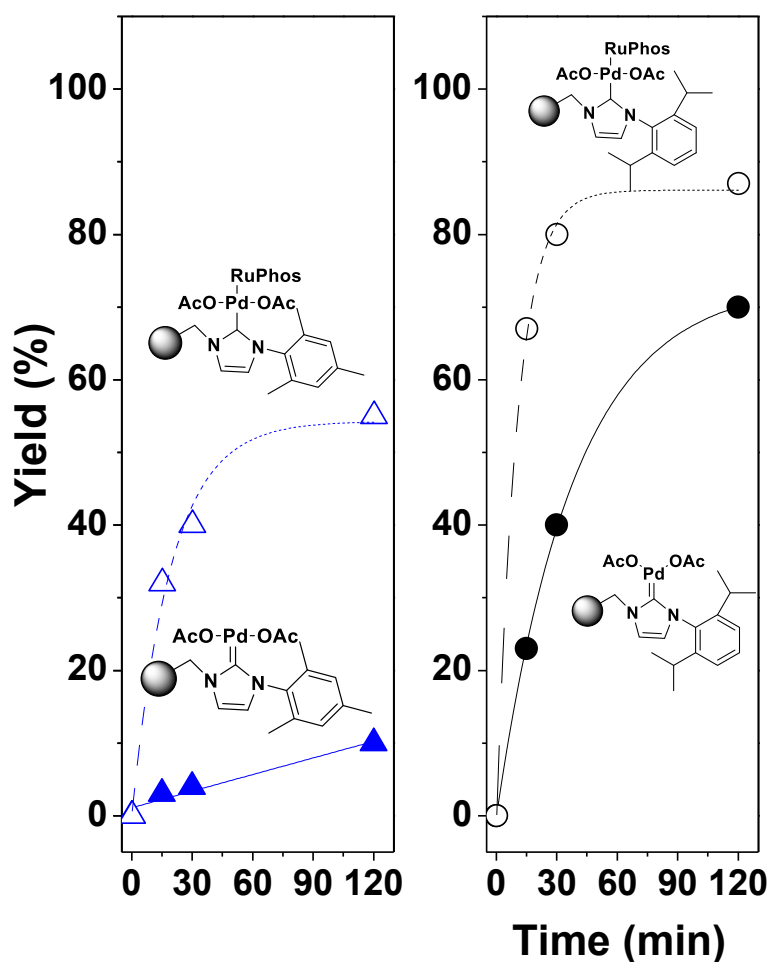


**Scheme 2.** Negishi benchmark reaction.

The catalytic activity of the polymer supported Pd species was tested for the Negishi reaction between benzylzinc bromide (**5**) and methyl 4-bromobenzoate (**6**) (Scheme 2). The Negishi reaction is a powerful cross-coupling reaction in organic synthesis, especially important for the synthesis of pharmaceuticals and for the fine chemistry industry.<sup>20</sup> The conditions selected for

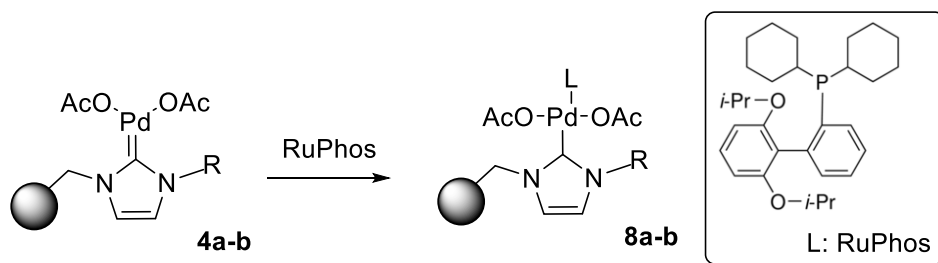
the benchmark reaction were the use of THF as the solvent, 60°C and a catalyst loading based on the introduction of 5 mol% of Pd.

The kinetic plots for this model reaction are represented in Figure 1. The catalytic behavior of the NHC-Pd catalysts **4a** showed little activity (less 10% after two hours), while the catalyst bearing *i*-Propyl moieties in the aromatic ring **4b** yielded to an increase on the catalytic activity reaching a 67% of conversion at 120 min (Figure 1).



**Figure 1.** Negishi reaction catalyzed by immobilized NHC-Pd complexes. 1eq 4-methylbromobenzoate (0.25 mmol), 2 eq Benzylzinc bromide (0.5 mmol, 1 mL of 0.5 M in THF), 5% mol Pd catalyst (0.0125 mmol) in dry THF (1 mL). N<sub>2</sub> atmosphere.

In order to improve the catalytic performance of these systems, we evaluate the cooperative effect between NHC and additive ligand. Organ and coworkers have demonstrated that the introduction of pyridine can be used to enhance the activity of NHC complexes (pyridine enhance precatalyst preparation, stabilization and initiation, PEPPSI).<sup>21,22</sup> In addition to pyridine ligands, other compounds with coordinating atoms such as C, N or P have been reported to tune the catalytic activity of NHC-Pd complexes.<sup>23</sup> We select, for the activation of NHC complex, a ligand containing P as coordinating atom. In particular, RuPhos (2-Dicyclohexylphosphino-2',6'-diisopropoxybiphenyl) as it has been used as palladium ligand for the Negishi reaction.<sup>24</sup> The preparation of the NHC-Pd-RuPhos complexes (**8a-b**) was carried out by putting in contact a suspension of **4a-b** with a solution of RuPhos during 2 hours (Scheme 3). The corresponding modified immobilized NHC-Pd-RuPhos were isolated by filtration and washed to remove the non-coordinated RuPhos (0.37 and 0.57 meq of Pd /g for **8a** and **8b**, respectively).



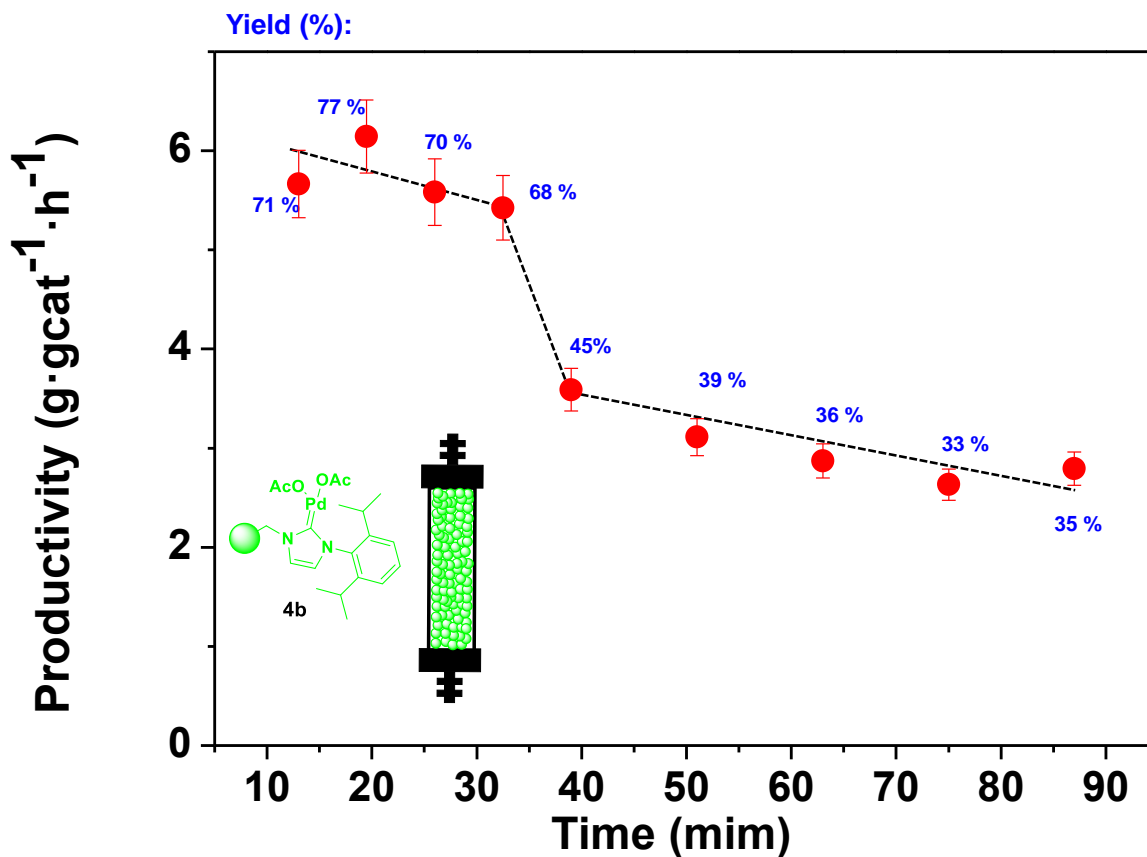
**Scheme 3.** Synthesis of immobilized NHC-Pd-RuPhos.

The introduction of the additional phosphine ligand produced a clear positive effect on the activity, enhancing the catalytic performance of the immobilized NHC-Pd complexes assayed as clearly showed in the kinetics profiles depicts in Figure 1. The catalysts NHC-Pd-RuPhos showed an activity increased of *ca.* 10 fold for **9a** and *ca.* 2.9 fold for the case **9b** attending to the TOF values calculated at 15 minutes.

At the view of the initial screening under batch condition with the both NHC-Pd (**4a-b**) and NHC-Pd-RuPhos (**8a-b**), we started to evaluate the activity and stability of these complexes under flow conditions. Thus, we prepared the corresponding fixed-bed reactors. It should be mentioned that the catalyst **4a** showed, as in batch process, low activity (< 5% yield) under flow conditions. However, the catalyst **4b** yielded to **7** under flow condition using a flow rate of 0.214 mL/min (Figure 2). The initial samples revealed yield of **7** even higher than those obtained in the batch process considering the short residence time used (2.5 min). However, a strong deactivation was observed under prolonged use (Figure 2). The catalytic activity decay calculated as productivity (g of **7** / g of Pd·h) accounts for *ca.* 50% of the initial one in only 2 hour of continuous used. This decay in activity *ca* be associated with the leaching of the palladium from the heterogeneous phase.<sup>25</sup> The initial samples collected showed an elevated concentration of leached soluble palladium species calculated by ICP-MS of the sample solutions (> 15 ppm of Pd). The elemental analysis of the catalyst after its use is consistent with the initial ligand loading suggesting a loss of the Pd from NHC-complex.

Additionally, the catalyst **8a** was also tested under continuous flow conditions. Although, this time a fivefold larger fixed bed reactor (2.9 mL *vs* 0.5 mL) leading to larger residence time (29 min *vs* 2.5 min) was used. An increase in the residence time may favor the re-adsorption of the active species into the support limiting in some extent the catalyst leaching. The results obtained under these conditions are depicted in the Figure 3. As expected, the use of larger residence time led to a high yield, indeed 100% of yield was achieved under these conditions with a productivity of 1.73 g **7** / g Pd·h. This level of activity was kept constant during at least 5.5 hours of continuous used. However, after this time a strong deactivation of the catalyst took place. An

activity loss of *ca.* 50% of the initial value was observed. After this decay, between 8 and 15 hours under continuous used, the value of activity was maintained around 0.8 g 7/ g Pd·h.

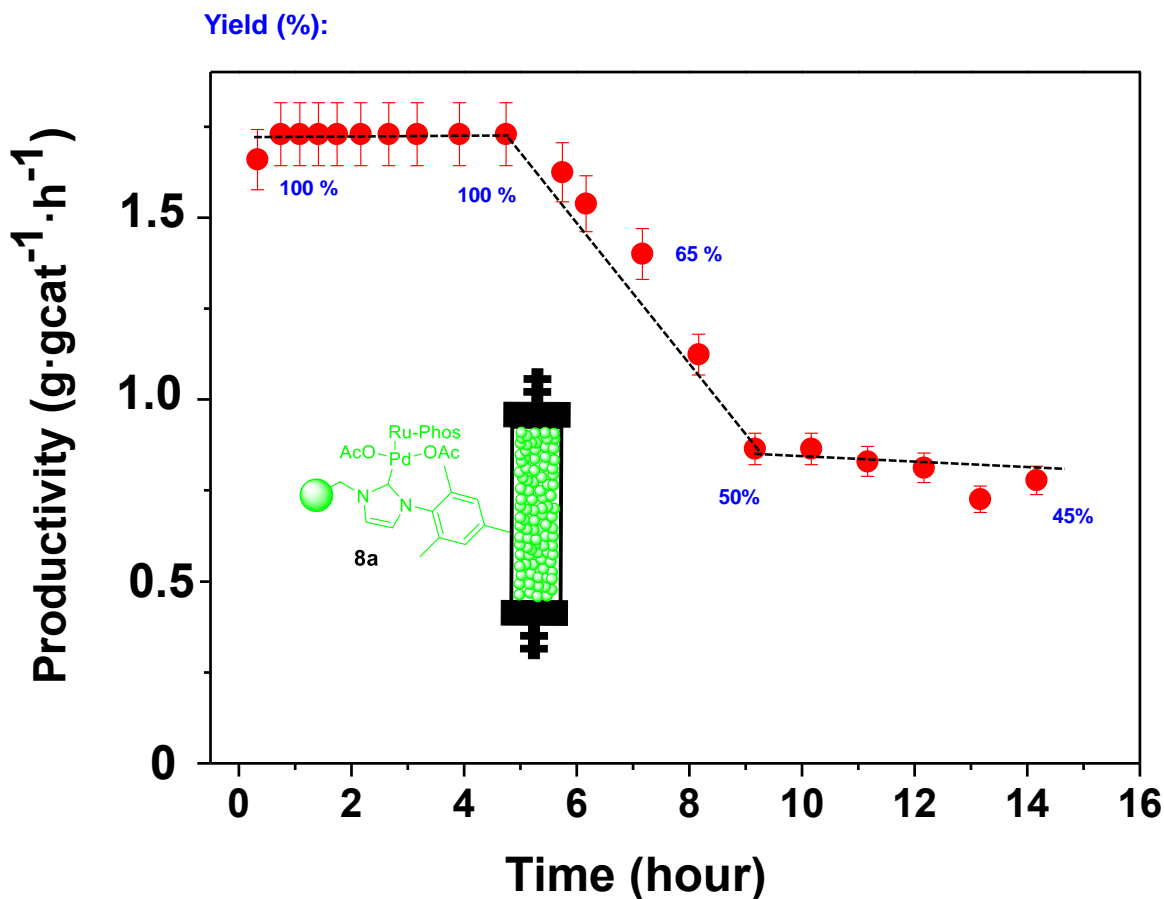


**Figure 2.** Negishi model reaction between **5** and **6** under flow conditions catalyzed by **4b**. V = 0.535 mL, 363 mg of **4b**. Residence time= 2.5 min, total flow rate 0.214 mL/min. Productivity max: 7.97 g 7 / g Pd h.

These results are in agreement with the observed by G. Organ and coworkers, who have developed silica-immobilized Pd-PEPPSI-*IPr*-SiO<sub>2</sub><sup>26</sup> and Pd-PEPPSI-*IPent*-SiO<sub>2</sub><sup>27</sup> catalysts. They observed a gradual catalyst death due to the slow release of palladium over time. However,



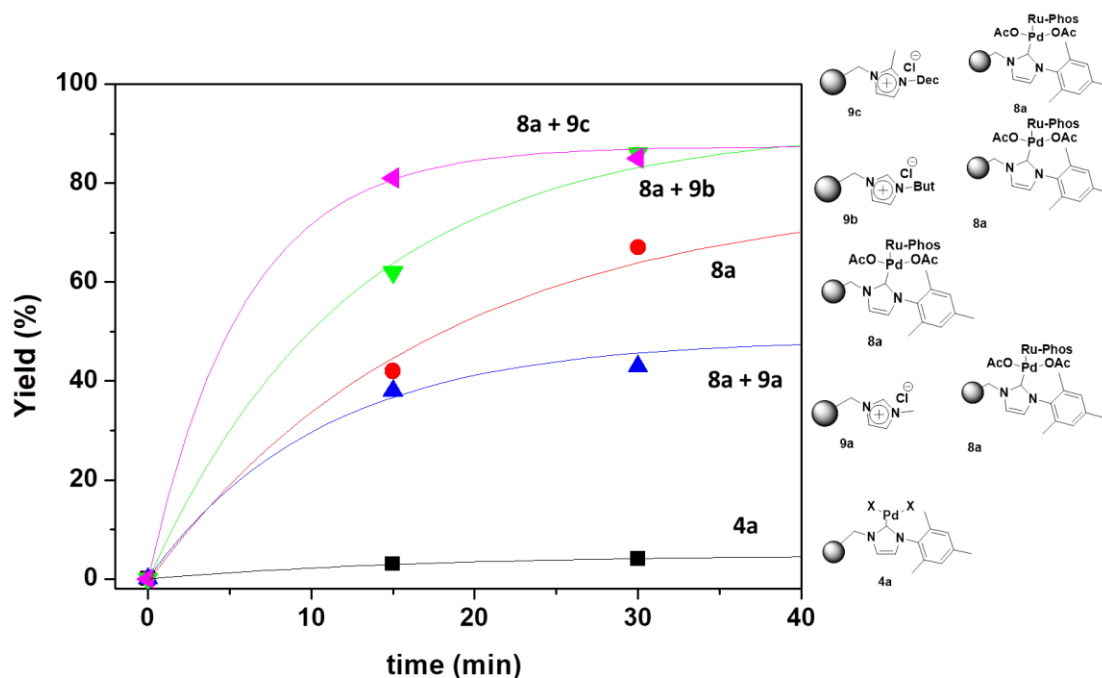
the high of the reactivity, especially for Pd-PEPPSI-IPent-SiO<sub>2</sub>, offsets the loss of catalyst, half of palladium loading over time, still allows relatively long-term flow runs.



**Figure 3.** Negishi model reaction under flow conditions catalyzed by **8a**. V = 2.9 mL, 1.25 g of cat, Residence time= 29 min, Total flow rate: 1 mL/min, productivity max: 1.73 g Product / g Pd ·h.

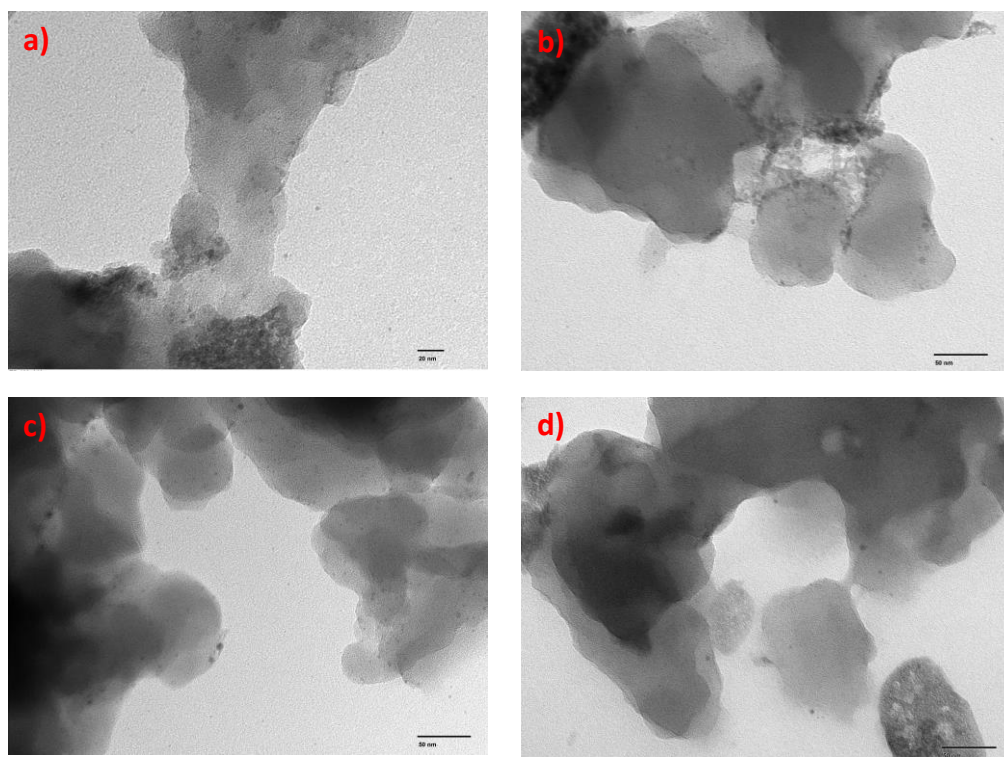
We have evaluated different strategies to develop supported precatalysts/catalysts immobilized onto supported ionic liquid-like phases (SILLPs).<sup>28,29,30,31</sup> In these systems, the microenvironment of the catalyst provided by the ionic liquid-like units has a remarkable influence on the overall process, especially on the catalytic activity and recyclability of the

supported species. Indeed, the appropriate design of the SILLPs is a key factor for the optimization of the release and catch system leading to easily recoverable and reusable for a large number of catalytic cycles without any loss in performance.<sup>28,29</sup> We decided to evaluate the effect of the presence of different type of SILLPs in the catalytic behavior of complexes here prepared. In this way, the benchmark Negishi reaction between **5** and **6** was performed using a polymeric mixture of two components: the immobilized NHC-Pd-RuPhos and polymeric SILLPs in weight ratio of 1:3. The first component can efficiently act as a catalyst but also will generate and release a series of Pd species accounting for the leaching. The second component, the SILLP, can act as scavenger of those species leached to the solution not only eliminating them from the solution but also contributing to their stabilization avoiding the formation of inactive species and keeping their activity for further catalytic cycles. Three different SILLPs were evaluated having different imidazolium substitution pattern and a loading of IL-like loading of 13-24 % by weight. The Figure 4 summarized the results obtained for this study. The presence of the SILLP induced an effect in both activity and Pd leaching. Regarding the activity, the presence of methyl imidazole SILLPs **9a** slightly reduce the catalytic activity, while the presence of SILLPs bearing butyl and methyl-decyl imidazolium units (**9b** and **9c**, respectively) led to more active systems. In absence of the SILLP, solely using **8a** as catalyst, the observed leaching was 22.4 ppm, corresponding with a leaching of ca. 7%. In presence of the SILLPs this leaching was reduced to 2.7, 14.4 and 17.1 for the polymeric mixtures **8a** + **9a**, **8a** + **9b** and **8a** + **9c**, respectively. Thus, the leaching in presence of SILLPs was lower than without it confirming that the SILLPs acts as scavenger for the leached Pd species. Noteworthy the larger palladium leaching did not lead to higher activity suggesting that in absence of the SILLP some deactivation of the leached species was taking place.



**Figure 4.** Negishi reaction between **5** and **6** catalyzed by **8a** in presence of SILLPs. 1eq 4-methylbromobenzoate (0.25 mmol), 2 eq Benzylzinc bromide (0.5 mmol, 1 mL of 0.5 M in THF), 2.4 % mol Pd catalyst (0.0125 mmol) in dry THF (1 mL). N<sub>2</sub> atmosphere

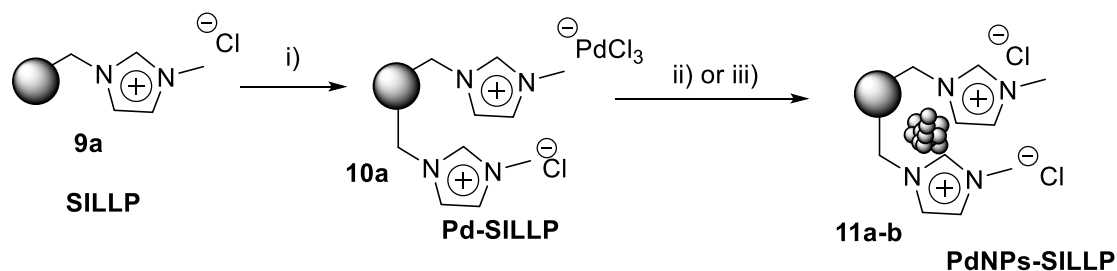
The TEM analysis of the polymers after the reactions showed the presence of palladium nanoparticles (Figure 5) confirming that during the reaction part of the leached palladium was converted into. The higher reactivity of the cocktails based on **9b** and **9c** can be associated with the presence of PdNPs with smaller size distributions. Our previous results obtained for AuNPs SILLPs indicated that for the macroporous resins the NP size decreased when the size of the aliphatic residue of the imidazolium units was increased with decyl N-substitution leading to smaller size particles.<sup>32</sup> The analysis of the polymeric samples revealed similar trend for the case of PdNPs. The decyl N-substituted SILLPs (**9c**) and the butyl one (**9b**) presented the smallest size distributions being also the most reactive ones.



**Figure 5.** TEM images of the polymer after the Negishi reaction between **5** and **6**. a) **8a** bar scale 20 nm, PdNPs particle size distribution  $4.91 \pm 1.26$  nm. b) **8a** + **9a** bar scale 50 nm, PdNPs particle size distribution  $4.23 \pm 1.65$  nm. c) **8a** + **9b** bar scale 50 nm, PdNPs particle size distribution  $3.61 \pm 1.36$  nm. d) **8a** + **9c** bar scale 50 nm, PdNPs particle size distribution  $3.23 \pm 0.81$  nm.

At the view of these experiments, it can be concluded that the NHC-Pd-RuPhos acts as both catalyst and a system releasing a series of soluble Pd species, which can be partially catch by the SILLP acting as scavenger. The key is to find out if these recaptured species onto SILLP are still active for the Negishi reaction. The leaching of the NHC-Pd-RuPhos is in agreement with previous studies for C-C palladium catalyzed reaction.<sup>28-30</sup> Recently, P. Ananikov and co-workers reported that for Pd-NHC systems the reactivity of the systems is mainly determined by the cleavage of the metal-NHC bond, while the catalyst performance is strongly affected by the

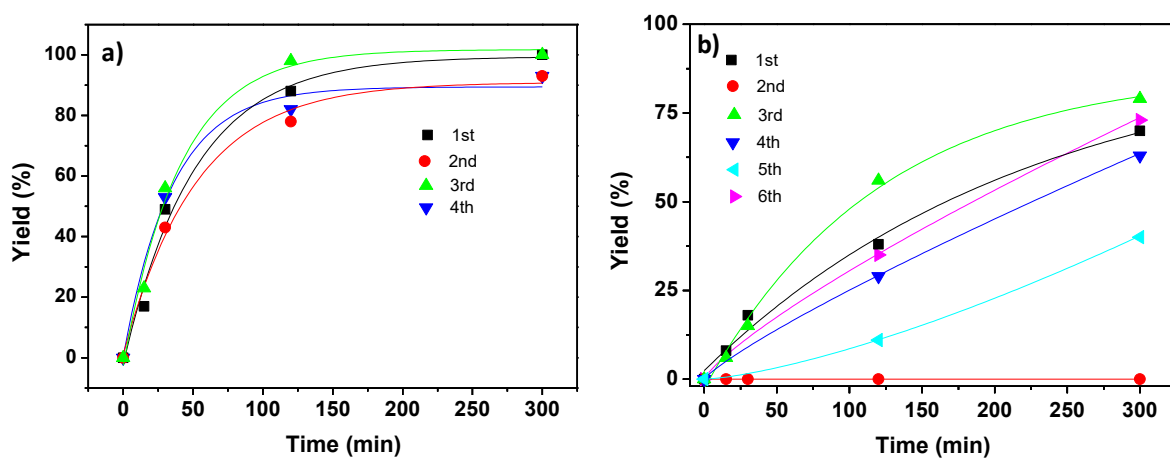
stabilization of in situ formed metal clusters.<sup>14,25</sup> They hypothesized a mechanism including two different pathways to connect Pd-NHC complexes to “cocktail”-type catalysis: (i) reductive elimination from a Pd(II) intermediate and the release of NHC-containing byproducts and (ii) dissociation of NHC ligands from Pd intermediates, where metal clusters and nanoparticles can be readily formed from M-NHC complexes after formation of new M–C or M–H bonds followed by C–NHC or H–NHC coupling. Thus, a combination of a classical molecular mode of operation and a cocktail-type mode of operation can be also be involved in the Negishi reaction, in which two different palladium species released from the NHC-complex can act as catalyst for the Negishi reaction: i) soluble Pd(II) species or ii) palladium nanoparticles (PdNPs). The SILLPs are able to scavenger and stabilize these two type of palladium species. We decided to evaluate the possible catalytic effect of these Pd species immobilized onto SILLPs for the Negishi reaction. Firstly, a solution of Pd(II) was adsorbed in the SILLP **9a** with high loading of methyl imidazolium units leading to a Pd(II)-SILLP system **10a** with 0.56 meq of Pd / g of SILLP and 3.79 meq of IL-like units /g of SILLP (Scheme 4). This system was treated with NaBH<sub>4</sub> solution and, alternatively, with EtOH under microwave irradiation to lead to corresponding PdNPs immobilized onto SILLPs (**11a-b**).



**Scheme 4.** Pd species immobilized onto SILLPs. i) 1 g SILLP **9a**, 100 mg PdCl<sub>2</sub> in H<sub>2</sub>O miliQ (100 mL 1% HCl, 1000 ppm Pd), orbitalic stirring, r.t., 5h. ii) 250 mg Pd-SILLP **10a**, 0.2 g NaBH<sub>4</sub> in 12 mL EtOH/H<sub>2</sub>O 1:4, r.t., 3h. iii) 250 mg Pd-SILLP **10a**, 4 mL EtOH, MW (2h, 200°C, 300 psi, 120 W).

These systems **10a** and **11a-b** were tested as potential catalyst for the benchmark Negishi reaction. The Pd(II) adsorbed by ionic exchange yielded to 73% of **7** after 120 minutes of reaction under standard conditions suggesting that the soluble Pd(II) species released from the immobilized systems and scavenged by the SILLPs are active catalyst for the Negishi reaction. The reaction was also evaluated in presence of 0.05 equivalent of RuPhos, as some of this ligand should be released from the NHC-Pd-RuPhos complex together with the palladium (Fig 6a). Under such conditions, the reaction took place with yields for **7** of *ca.* 90% for the first cycle. Noteworthy the levels of leaching were lower than the observed for the **8a** (0.49 ppm vs. 22.4 ppm for **8a**). The reaction was also assayed in presence of one equivalent of RuPhos using a mixture of **10a** and SILLP **9a** as scavenger in a 1:3 weight ratio (Figure 6b). Under these conditions, the reaction was less active, however the leaching was reduced even further reaching a 0.04 ppm for the polymeric mixture **10a** + **9a** in presence of one equivalent of RuPhos. The recyclability of the systems were also tested. In general, the catalysts assayed maintained the catalytic activity as far as RuPhos was added in the additional cycle. Thus, the activity of **10a** with addition of 0.05 equivalents of RuPhos was kept constant for at least four catalytic cycles

being the leaching for each cycle around 0.4 ppm. The catalyst **10a** in presence of additional scavenger **9a** was also active in successive cycles, although the activity suffered from more fluctuations, probably due to the heterogeneity of the systems formed by two different polymers. In any case, the systems were still active until six consecutive cycles being the leaching per cycle between 0.04-0.12 ppm.



**Figure 6.** Negishi reaction between **5** and **6** catalyzed by **10a**. 1eq 4-methylbromobenzoate (0.25 mmol), 2 eq Benzylzinc bromide (0.5 mmol, 1 mL of 0.5 M in THF), 5 % mol Pd catalyst in dry THF (1 mL). a) **10a** in presence of RuPhos, Pd:RuPhos 1:0.05 mol. RuPhos added each cycle. b) **10a** + **9a**, ratio by weight 1:3, in presence of RuPhos, Pd:RuPhos 1:1 mol, RuPhos added each cycle except 2<sup>nd</sup> cycle. N<sub>2</sub> atmosphere.

Regarding the activity of the PdNP-SILLPs **11a-b**, the systems showed non activity with yield lower than 1% in absence of RuPhos, while they provided good catalytic performance in the presence of one equivalent of the phosphine. The catalysts prepared by NaBH<sub>4</sub> reduction were slightly less reactive than with EtOH as reducing agent. Noteworthy, the active supported

catalysts were active in further catalytic cycles after separation of the product by filtration and washing of the supported catalyst.<sup>33</sup> The **11a-b** were also recycled being **11a** even more active in a second than in the first cycle.

**Table 2.** Negishi reaction between **5** and **6** catalyzed by **11a-b**.<sup>a</sup>

Entry	Catalyst	Pd:RuPhos	Cycle	Yield (time, min)		
				15	30	120
1	<b>11a</b>	1:0	1	n.f.	n.f.	n.f.
2	<b>11b</b>	1:0	1	n.f.	n.f.	n.f.
3	<b>11a</b>	1:1	1	12	31	73
4	<b>11b</b>	1:1	1	42	50	73
5	<b>11a</b>	1:1	2	84	83	85
6	<b>11b</b>	1:1	2	11	21	66

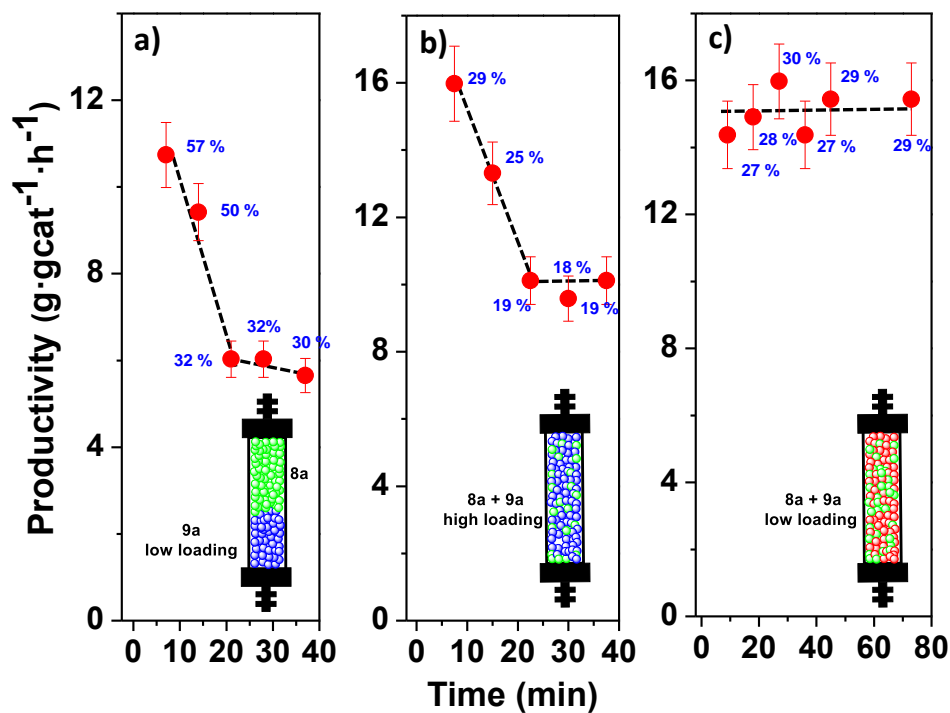
a: 1eq 4-methylbromobenzoate (0.25 mmol), 2 eq Benzylzinc bromide (0.5 mmol, 1 mL of 0.5 M in THF), 5 % mol Pd catalyst in dry THF (1 mL). n.f. product not found.

All these results suggest that the SILLP can be used as scavenger for the palladium leached species released from NHC-Pd-RuPhos complexes limiting the leaching and possibly improving the long-term system stability. In order to screen the effect of the SILLP under continuous flow conditions small flow fix-bed reactors were prepared and evaluated. The first system was prepared by packing two layers one on the top of the other of 200 mg of the catalyst **8a** and 200 mg of **9a**, where the first layer was the catalyst and the second one the SILLP to act as scavenger of the released species from **8a** (Figure 7a). This configuration did not contribute to improve the stability of the system, indeed a strong catalyst deactivation was again observed with *ca.* 47% activity decay. We consider that a homogeneous distribution of the catalyst and the scavenger within the fixed bed reactor may lead to better performance. In this case, two different fixed bed

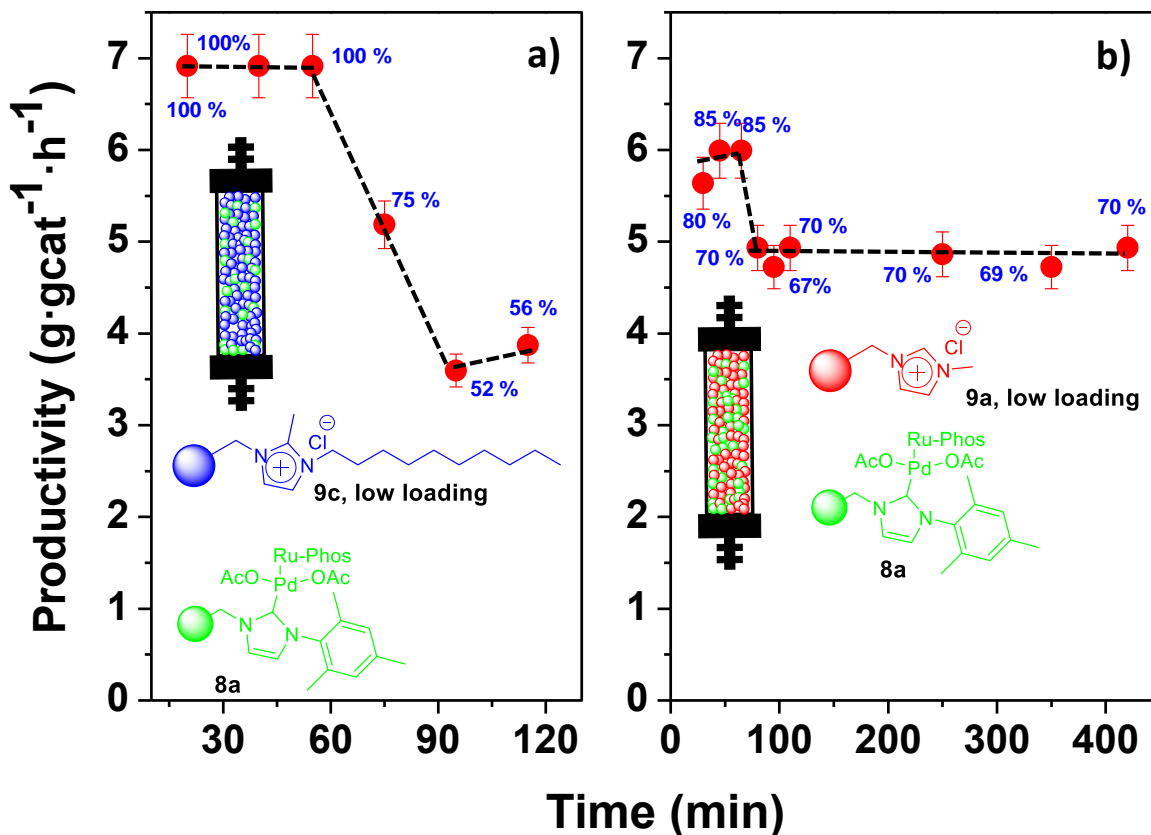


reactors were prepared with a well-disperse mixture formed by 50 mg of the catalyst **8a** and 150 mg of SILLP **9a**. Two different SILLPs **9a** were used, one with low loading of the IL-like units (1.09 meq/g, 13 %weight) and alternatively one with high loading (3.79 meq/g, 37 %weight). In the case of the continuous reactor containing the high loading SILLP the activity decay was lower than the previously observed (ca. 35%). However the systems based on the use of the SILLP **9a** with low loading kept the activity level around 15 g of **7** / g Pd·h in comparison with the strong decay observed from the other two configuration.

At the view of these results, we prepared and evaluated the performance of two larger fixed bed reactors for the Negishi reaction between **5** and **6**. A first one filled with 250 mg of **8a** and 750 mg of the SILLP **8a** and a second one with the same amount of catalyst but using the SILLP **9c** in state of **9a**. The results are summarized in the Figure 8. In agreement with the observed in the batch experiments, the mixture of the polymers **8a** + **9c** led to more active systems reaching >99% yield of **7**. However, the activity strongly decays after 60 minutes of continuous use. This can be related with the leaching observed during this period with samples containing up to 10 ppm of leached palladium. The system based on **8a** and **9a** provided a more stable performance. Although the activity of the systems was slightly lower as observed in the batch experiments, it remained constant after an initial time. Thus, the initial samples corresponding with the yield of ca. 85 % of **7** , which is maintained until 80 minutes slightly decaying to a ca. 70% corresponding with a productivity of 4.87 g of **7** / g·h. This level of productivity was maintained during at least five hours of continuous use.

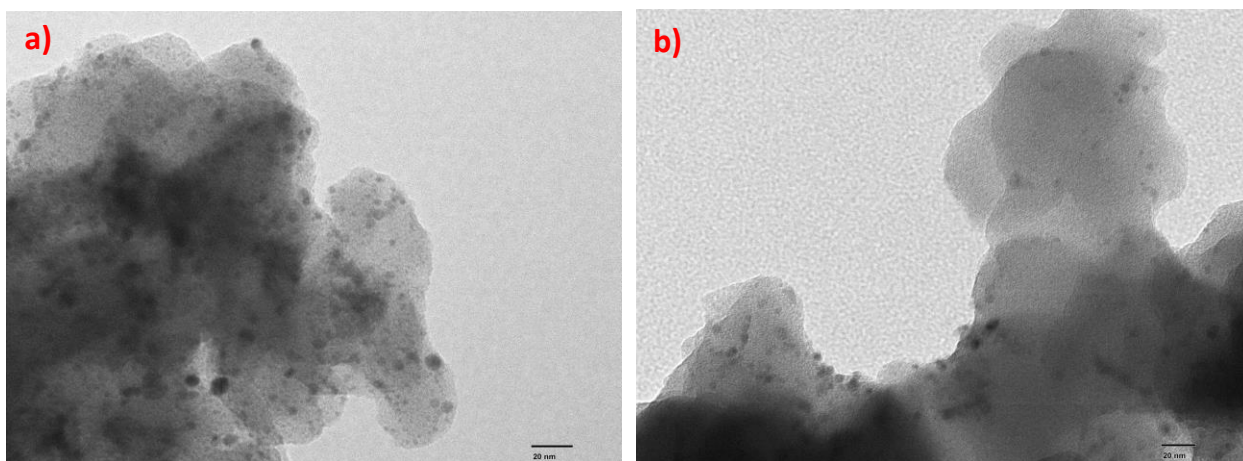


**Figure 7.** Effect of of SILLP **9a** as scavenger for Negishi between **5** and **6** under flow conditions catalyzed by **8a**. a) 200 mg of **8a** and 200 mg of **9a** SILLP low loading,  $V = 0.535$  mL, residence time = 2.5 min, Productivity max: 18.84 g **7** / g Pd·h. b) 50 mg of **8a** and 150 mg of **9a** SILLP high loading,  $V = 0.38$  mL, residence time = 2.5 min, Productivity max: 53.24 g **7** / g Pd·h. c) 50 mg of **8a** and 150 mg of **9a** SILLP low loading,  $V = 0.35$  mL, residence time = 2.5 min, Productivity max: 53.24 g **7** / g Pd·h.



**Figure 8.** Effect of type of SILLP as scavenger for Negishi between **5** and **6** under flow conditions catalyzed by **8a** in presence of SILLP as active scavenger. 60 °C. Total flow rate: 0.1 mL/min. 0.05 mL of 0.1 M of **5** in THF and 0.05 mL/min of 0.2 M of **6** in THF. V = 1.7 mL, residence time= 17 min, Productivity max: 7.08 g / g Pd·h. a) 250 mg of **8a** and 750 mg of **9c** SILLP low loading, b) 250 mg of **8a** and 750 mg of **9a** SILLP low loading.

The TEM images of the polymeric systems after their use under continuous flow conditions revealed again the presence of PdNPs (Fig. 9). For the systems **8a** + **9c** seems that the number of PdNPs and their size distribution are larger than for the **8a** + **9a**. This trend is different to the one observed in batch conditions.



**Figure 9.** TEM images of the polymer after the Negishi reaction between **5** and **6** under flow conditions. a) **8a** + **9c**, bar scale 20 nm, PdNPs particle size distribution  $4.72 \pm 1.44$  nm. b) **8a** + **9a** bar scale 20 nm, PdNPs particle size distribution  $3.12 \pm 0.97$  nm.

### **Conclusion.**

Our results suggest that it is possible to design systems formed by mixture of the supported NHC-Pd-RuPhos and SILLPs, where the last acts as scavenger of the palladium species released from the immobilized NHC-Pd-RuPhos leading to complex mixture of immobilized species still active for the Negishi reaction, while the leaching is minimized and the long term catalyst life improved. This provide an opportunity for the development of active and stable Pd systems to be used under flow conditions overcoming the limitations associated to the intrinsic mechanistic of the Negishi reaction, where a catch and released mechanism can be established thanks to the presence of the supported ionic liquid-like phase. SILLPs with low loading of methyl imidazolium units provided the most efficient systems to be used in conjunction with the immobilized NHC-Pd-RuPhos.

## Corresponding Author

\* [luiss@uji.es](mailto:luiss@uji.es), [cepeda@uji.es](mailto:cepeda@uji.es). Dpt. of Inorganic and Organic Chemistry, Supramolecular and Sustainable Chemistry Group, University Jaume I, Avda Sos Baynat s/n, E-12071-Castellon. Spain,

## ACKNOWLEDGMENT

This work was partially supported by G. V. (PROMETEO 2016-071) and MINECO (CTQ2015-68429R). E. Peris thanks MICINN for the financial support (FPU13/00685).

## References

- 
- 1 *Smart N-Heterocyclic Carbene Ligands in Catalysis*, E. Peris, *Chem. Rev.*, **2018**, *118*, 9988-10031.
  - 2 *Electronic Properties of N-Heterocyclic Carbenes and Their Experimental Determination*, H. V. Huynh, *Chem. Rev.*, **2018**, *118*, 9457–9492.
  - 3 *Designing Pd–N-Heterocyclic Carbene Complexes for High Reactivity and Selectivity for Cross-Coupling Applications*, R. D. J. Froese, C. Lombardi, M. Pompeo, R. P. Rucker, M. G. Organ, *Acc. Chem. Res.*, **2017**, *50*, 2244.
  - 4 *The Development of Bulky Palladium NHC Complexes for the Most-Challenging Cross-Coupling Reactions*, C. Valente, S. Çalimsiz, K. H. Hoy, D. Mallik, M. Sayah, M. G. Organ, *Angew. Chem. Int. Ed.*, **2012**, *51*, 3314-3332.
  - 5 *Reusable N-Heterocyclic Carbene Complex Catalysts and Beyond: A Perspective on Recycling Strategies*, W. Wang, L. Cui, P. Sun, L. Shi, C. Yue, F. Li, *Chem. Rev.*, **2018**, *118*, 9843-9929.

---

6 *Palladium-Catalyzed Cross-Coupling in Continuous Flow at Room and Mild Temperature*, C. Len, Chapter 7, 183-206, Sustainable Catalysis, Ed: R. Luque, F. L.-Y. Lam, **2018**, Wiley-VCH Verlag GmbH & Co.

7 *A Generalized Picture of C–C Cross-Coupling* Michael Busch, Matthew D. Wodrich, C. Corminboeuf, *ACS Cat.*, **2017**, 7, 5643-5653.

8 *Supported N-heterocyclic carbene complexes in catalysis*, W. J. Sommer, M. Weck, *Coord. Chem. Rev.*, **2007**, 251, 860-873.

9 *Immobilization of N-Heterocyclic Carbene Compounds: A Synthetic Perspective*, R. Zhong, A. C. Lindhorst, F. J. Groche, F. E. Kühn, *Chem. Rev.*, **2017**, 117, 1970-2058.

10 *Polymer-Supported Palladium(II) Carbene Complexes: Catalytic Activity, Recyclability, and Selectivity in C@H Acetoxylation of Arenes*, M. H. Majeed, P. Shayesteh, L. R. Wallenberg, A. R. Persson, N. Johansson, L. Ye, J. Schnadt, O. F. Wendt, *Chem. Eur. J.*, **2017**, 23, 8457-8465.

11 *Immobilized Transition Metals as Catalysts for Cross-Couplings in Continuous Flow—A Critical Assessment of the Reaction Mechanism and Metal Leaching*, D. Cantillo, C. O. Kappe, *ChemCatChem* **2014**, 6, 3286-3305.

12 *A unifying mechanism for all high-temperature Heck reactions. The role of palladium colloids and anionic species*, J.G. de Vries, *Dalton Trans.*, **2006**, 6, 421-429.

13 *Palladium Nanoparticles as Efficient Green Homogeneous and Heterogeneous Carbon–Carbon Coupling Precatalysts: A Unifying View*, D. Astruc, *Inorg. Chem.*, **2007**, 46, 1884-1894.

14 *Understanding active species in catalytic transformations: From molecular catalysis to nanoparticles, leaching, “Cocktails” of catalysts and dynamic systems*, D. B. Eremin, V. P. Ananikov, *Coord. Chem. Rev.*, **2017**, 346, 2-19.

- 
- 15 *A New Concept for the Noncovalent Binding of a Ruthenium-Based Olefin Metathesis Catalyst to Polymeric Phases: Preparation of a Catalyst on Raschig Rings*, A. Michrowska, K. Mennecke, U.; Kunz, A. Kirschning, K. Grela, *J. Am. Chem. Soc.*, **2006**, *128*, 13261-13267.
- 16 *Polymer-supported Pd-NHC complexes: Strategies for the development of multifunctional systems*, V. Sans, F. Gelat, M.I. Burguete, E. Garcia-Verdugo, S.V. Luis, *Cat. Today*, **2012**, *196*, 137-147.
- 17 *Base supported ionic liquid-like phases as catalysts for the batch and continuous-flow Henry reaction*, M.I. Burguete, H. Erythropel, E. García-Verdugo, S.V. Luis, V. Sans, *Green Chem.* **2008**, *10*, 401-407.
- 18 *The use of NIR-FT-Raman spectroscopy for the characterization of polymer-supported reagents and catalysts*, B. Altava, M.I. Burguete, E. Garcia-Verdugo, S.V. Luis, M.J. Vicent, *Tetrahedron*, **2001**, *57*, 8675-8683.
- 19 *A Sensitive Colorimetric Method for the Study of Polystyrene Merrifield Resins and Chloromethylated Macroporous Monolithic Polymers*, F. Galindo, B. Altava, M.I. Burguete, R. Gavara, S.V. Luis, *J. Comb. Chem.*, **2004**, *6*, 859-861.
- 20 *Recent Developments in Negishi Cross-Coupling Reactions*, D. Haas, J. M. Hammann, R. Greiner, P. Knochel, *ACS Catal.*, **2016**, *6*, 1540-1552.
- 21 *Negishi Cross-Coupling of Secondary Alkylzinc Halides with Aryl/heteroaryl Halides Using Pd-PEPPSI-IPent*, S. Çalimsiz, M. G. Organ, *Chem. Commun.*, **2011**, *47*, 5181-5183.
- 22 *Pd-PEPPSI-IHeptCl: A General-Purpose, Highly Reactive Catalyst for the Selective Coupling of Secondary Alkyl Organozincs*, B. Atwater, N. Chandrasoma, D. Mitchell, M. J. Rodriguez, M.I. G. Organ, *Chem. Eur. J.*, **2016**, *22*, 14531-14534.

---

23 (a) *Synergistic Ligand Effect between N-Heterocyclic Carbene (NHC) and Bicyclic Phosphoramidite (Briphos) Ligands in Pd-Catalyzed Amination*, M. Kim, T. Shin, A. Lee, H. Kim, *Organometallics* **2018** DOI: 10.1021/acs.organomet.8b00413. b) *Designing Pd and Ni Catalysts for Cross-Coupling Reactions by Minimizing Off-Cycle Species*, D. Balcells, A. Nova, *ACS Catal.*, **2018**, *8*, 3499-3515, c) *Heterocyclic Carbene-Palladium(II)-1-Methylimidazole Complex Catalyzed Direct C–H Bond Arylation of Benzo[b]furans with Aryl Chlorides*, S.-C. Yin, Q. Zhou, X.-Y. Zhao, L.-X. N- Shao, *J. Org. Chem.*, **2015**, *80*, 8916-8921, d) *Chelating N-Heterocyclic Carbene Alkoxide as a Supporting Ligand for PdII/IV C-H Bond Functionalization Catalysis*, P. L. Arnold, M. S. Sanford, S. M. Pearson, *J. Am. Chem. Soc.*, **2009**, *131*, 13912-13913.

24 *Much Improved Conditions for the Negishi Cross-Coupling of Iodoalanine Derived Zinc Reagents with Aryl Halides*, A. J. Ross, H. L. Lang, R. F. W. Jackson, *J. Org. Chem.*, **2010**, *75*, 245–248.

25 *Fast and Slow Release of Catalytically Active Species in Metal/NHC Systems Induced by Aliphatic Amines*, O.V. Khazipov, M.A. Shevchenko, A.Y. Chernenko, A. V. Astakhov, D. V. Pasyukov, D. B. Eremin, Y. V. Zubavichus, V. N. Khrustalev, V. M. Chernyshev, V. P. Ananikov, *Organometallics*, **2018**, *37*, 1483-1492.

26 *Continuous flow Negishi cross-couplings employing silica-supported Pd-PEPPSI-IPr precatalyst*, G. A. Price, A. R. Bogdan, A. L. Aguirre, T. Iwai, S. W. Djuric, M. G. Organ, *Catal. Sci. Technol.*, **2016**, *6*, 4733-4742.

27 *Pd-PEPPSI-IPent-SiO<sub>2</sub>:ASupported Catalyst for Challenging Negishi Coupling Reactions in Flow*, G. A. Price, A. Hassan, A. R. Bogdan, S. W. Djuric, M. G. Organ, *Angew. Chem. Int. Ed.*, **2017**, *56*, 13347-13350.



---

28 *Pd catalysts immobilized onto gel-supported ionic liquid-like phases (g-SILLPs): A remarkable effect of the nature of the support*, M. I. Burguete, E. García-Verdugo, I. Garcia-Villar, F. Gelat, P. Licence, S.V. Luis, V. Sans, *J. Catal.*, **2010**, 269, 150-160.

29 *Polymer Cocktail: A Multitask Supported Ionic Liquid-Like Species to Facilitate Multiple and Consecutive C-C Coupling Reactions*, V. Sans, F. Gelat, N. Karbass, M. I. Burguete, E. Garcia-Verdugo, S. V. Luis, *Adv. Synth. Catal.*, **2010**, 352, 3013-3021.

30 N. Karbass, V. Sans, E. García-Verdugo, M. I. Burguete, S. V. Luis, *Chem. Commun.*, **2006**, 29, 3095-3097.

31 *Supported N-heterocyclic carbene rhodium complexes as highly selective hydroformylation catalysts*, W. Gil , K. Boczon, A. M. Trzeciak, J. J. Ziólkowski, E. Garcia-Verdugo, S. V. Luis, V. Sans, *J. Mol. Cat. A: Chem.*, **2009**, 309, 131–136.

32 *Preparation of polymer-supported gold nanoparticles based on resins containing ionic liquid-like fragments: easy control of size and stability*, M. I. Burguete, E. Garcia-Verdugo, S. V. Luis, J. A. Restrepo, *Phys. Chem. Chem. Phys.* **2011**, 13, 14831-14838.

33 *Pd Metal Catalysts for Cross-Couplings and Related Reactions in the 21st Century: A Critical Review*, A. Biffis, P. Centomo, A. Del Zotto, M. Zecca, *Chem. Rev.*, **2018**, 118, 2249-2295.



## ELECTRONIC SUPPORTING INFORMATION

# Synergy between Supported Ionic Liquid-Like Phase and immobilized Palladium N-Heterocyclic Carbene Phosphine complexes for the Negishi reaction under flow conditions.

Edgar Peris,<sup>a</sup> Raúl Porcar,<sup>a</sup> Jesús Alcázar,<sup>b</sup> Eduardo García-Verdugo,<sup>a</sup> Santiago V. Luis.<sup>a</sup>

a) Dpt. of Inorganic and Organic Chemistry, Supramolecular and Sustainable Chemistry Group, University Jaume I, Avda Sos Baynat s/n, E-12071-Castellon. Spain, [luiss@uji.es](mailto:luiss@uji.es), [cepeda@uji.es](mailto:cepeda@uji.es)

b) Janssen Pharmaceutical Companies of J&J, Janssen-Cilag S.A., Jarama 75A, 45007 Toledo, Spain, [jalcazar@its.jnj.com](mailto:jalcazar@its.jnj.com)

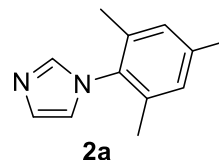
### Table of Contents

1. Catalysts synthesis.
2. Flow reactions set-up.
3. NMR spectra.

## 1. CATALYSTS SYNTHESIS

### 1.1. General procedure for the synthesis of ligands 2a-b

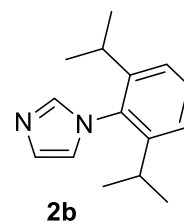
*1-mesityl-1H-imidazole (2a)*



An aqueous solution of glyoxal (30%, 6.2 mmol/mL, 0.1 mol) was added to a solution of 2,4,6-trimethylaniline (14.10 mL, 0.1 mol) in 50 mL of methanol. The mixture was stirred at r.t. for 24 hours. A yellow precipitate was formed during this time.  $\text{NH}_4\text{Cl}$  (10.70 g, 0.2 mol) followed by aqueous solution of formaldehyde 40% (10 mL, 0.2 mol) were added to this suspension and the resulting reaction mixture was diluted with MeOH (400 mL) and heated at reflux. Then, 14 mL of aqueous  $\text{H}_3\text{PO}_4$  85% was added drop-by-drop to the reaction mixture during 1 hour. The reaction was refluxed for 24 hours and followed by thin layer chromatography (hexane/ethyl acetate (1:1),  $R_f = 0.39$ ). When reaction was completed, the mixture was concentrated to dryness and the residue obtained added on ice water and neutralized with a solution of 40% KOH to pH = 9. Later, the resulting mixture was extracted with diethyl ether (5×150 mL). The organic phases were combined and washed with water saturated by NaCl. Finally, the resulting solution was dried with  $\text{Na}_2\text{SO}_4$ , concentrated to dryness and purified by flash chromatography on silica gel to afford a yellow solid.

Yield=65%. IR( $\text{cm}^{-1}$ ) ATR: 3095, 2964, 2926, 2869, 1645, 1495, 1066, 819, 810, 766, 669.  $^1\text{H}$  NMR (400 MHz,  $\text{CDCl}_3$ ):  $\delta$  1.98 (s, 6H, Ar- $\text{CH}_3$ ), 2.33 (s, 3H, Ar- $\text{CH}_3$ ), 6.88 (s, 1H,  $\text{H}_{\text{imid}}$ ), 6.96 (s, 2H, Ar-H), 7.23 (s, 1H,  $\text{H}_{\text{imid}}$ ), 7.43 (s, 1H,  $\text{H}_{\text{imid}}$ ).  $^{13}\text{C}$  RMN (400 MHz,  $\text{CDCl}_3$ ):  $\delta$  17.3 (2 $\text{CH}_3$ ), 21.5 ( $\text{CH}_3$ ), 120.5 ( $\text{C}_{\text{imid}}$ ), 129.5 (2 $\text{C}_{\text{aromatic}}$ ,  $\text{C}_{\text{imid}}$ ), 130.0 (2 $\text{C}_{\text{aromatic}}$ ), 136.0 ( $\text{C}_{\text{aromatic}}$ ), 138.0 ( $\text{C}_{\text{imid}}$ ), 139.3 ( $\text{C}_{\text{aromatic}}$ ). Elemental analysis found: %C 75.9; %H 7.3; %N 14.5; calculated for  $\text{C}_{12}\text{H}_{14}\text{N}_2$ : %C 77.4; %H 7.6; %N 15.

*1-(2,6-diisopropylphenyl)-1H-imidazole (2b)*



An aqueous solution of glyoxal (30%, 6.2 mmol/mL, 0.027 mol) was added to a solution of 2,6-diisopropylaniline (5.20 mL, 0.027 mol) in 25 mL of methanol. The mixture was stirred at r.t. for 24 hours. A yellow precipitate was formed

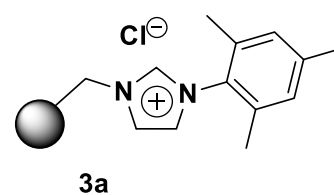
during this time.  $\text{NH}_4\text{Cl}$  (2.89 g, 0.054 mol) followed by aqueous solution of formaldehyde 40% (4.02 mL, 0.054 mol) were added to this suspension and the resulting reaction mixture was diluted with MeOH (85 mL) and heated at reflux. Then, 3.6 mL of aqueous  $\text{H}_3\text{PO}_4$  85% was added drop-by-drop to the reaction mixture during 1 hour. The reaction was refluxed for 24 hours and followed by thin layer chromatography (hexane/ethyl acetate (1:1),  $R_f = 0.32$ ). When reaction was completed, the mixture was concentrated to dryness and the residue obtained added on ice water and neutralized with a solution of 40% KOH to pH = 9. Later, the resulting mixture was extracted with diethyl ether (5×50 mL). The organic phases were combined and washed with water saturated by NaCl. Finally, the resulting solution was dried with  $\text{Na}_2\text{SO}_4$ , concentrated to dryness and purified by flash chromatography on silica gel to afford a yellow solid.

Yield=50%. IR( $\text{cm}^{-1}$ ) ATR: 3094, 2964, 2926, 2867, 1645, 1493, 1470, 1066, 908, 809, 767,669.  $^1\text{H}$  NMR (400 MHz,  $\text{CDCl}_3$ ):  $\delta$  1.99 (d, 12H,  $-\text{CH}(\text{CH}_3)_2$ ), 2.34 (m, 2H, Ar- $\text{CH}(\text{CH}_3)_2$ ), 6.89 (t, 2H,  $\text{H}_{\text{imid}}$ ), 6.97 (s, 2H, Ar-H), 7.23 (s, 1H,  $\text{H}_{\text{imid}}$ ), 7.44 (t, 1H, Ar-H). Elemental analysis found: %C 77.6; %H 8.6; %N 11.8; calculated for  $\text{C}_{15}\text{H}_{20}\text{N}_2$ : %C 78.9; %H 8.8; %N 12.3.

## 1.2. General procedure for the synthesis of Supported Ionic Liquid-like Phases (SILLPs) (3a-b)

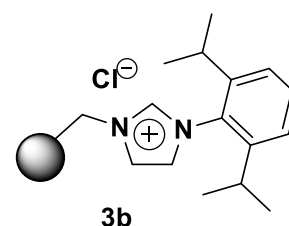
### *Synthesis of polymer 3a*

**2a** (4.93 g, 26.5 mmol) was dissolved in DMF (50 mL). Merrifield resin (7.36 g, 1.2 mmol Cl/g, 8.83 mmol) was then added. The mixture was stirred for 2 days at 80 °C. NBP test was positive. The resulting polymer was filtered and washed with THF (3X15 mL),  $\text{CH}_2\text{Cl}_2$  (3X15 mL), MeOH (3X15 mL) and dried in a vacuum oven. IR ( $\text{cm}^{-1}$ ) ATR: 3026, 2922,1603, 1541, 1491,1451, 759, 698. Elemental analysis found: %C 83.4; %H 7.3; %N 2.1. Loading N (mmol/g): 0.764.



### *Synthesis of polymer 3b*

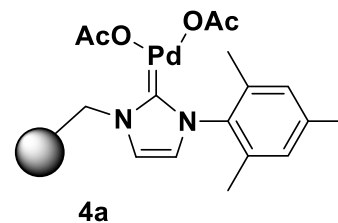
Same procedure than **3a**, employing **2b** (2.23 g, 9.76 mmol), DMF (22 mL), Merrifield resin (2.72 g, 1.2 mmol Cl/g, 3.25 mmol). IR ( $\text{cm}^{-1}$ ) ATR: 3026, 2925, 1542, 1494, 1453, 758, 697. Elemental analysis found: %C 81.9; %H 7.2; %N 1.8. Loading N (mmol/g): 0.655.



### 1.3. General procedure for the synthesis of Pd-NHC-SILLPs complexes (4a-b)

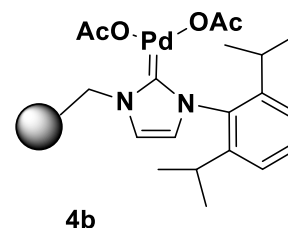
#### *Synthesis of supported Pd-NHC-SILLPs complex 4a*

Firstly, polymer **3a** (1.19 g, 0.925 mmol) was suspended in dry THF (20 mL). Later, potassium tert-butoxide (0.24 g, 1.85 mmol) was added and the system was stirred for 30 minutes. Pd(OAc)<sub>2</sub> (0.22 g, 0.925 mmol) was then added. The mixture was stirred for 2 hours at 50 °C. The resulting complex was filtered and washed with THF (3X15 mL), CH<sub>2</sub>Cl<sub>2</sub> (3X15 mL), MeOH (3X15 mL) and dried in a vacuum oven. IR (cm<sup>-1</sup>) ATR: 3026, 2918, 1602, 1492, 1451, 1030, 758, 697. Elemental analysis found: %C 79.2; %H 7.2; %N 1.2. Experimental Pd loading (mmol/g): 0.7



#### *Synthesis of supported Pd-NHC-SILLPs complex 4b*

Same procedure than **4a**, employing **3b** (1.09 g, 0.725 mmol), dry THF (20 mL), t-BuOK (0.195 g, 1.451 mmol), Pd(OAc)<sub>2</sub> (0.166 g, 0.725 mmol). IR (cm<sup>-1</sup>) ATR: 3025, 2923, 1600, 1490, 1451, 1182, 758, 698. Elemental analysis found: %C 80.2; %H 7.4; %N 1.3. Experimental Pd loading (mmol/g): 0.6



## 2. FLOW REACTIONS SET-UP

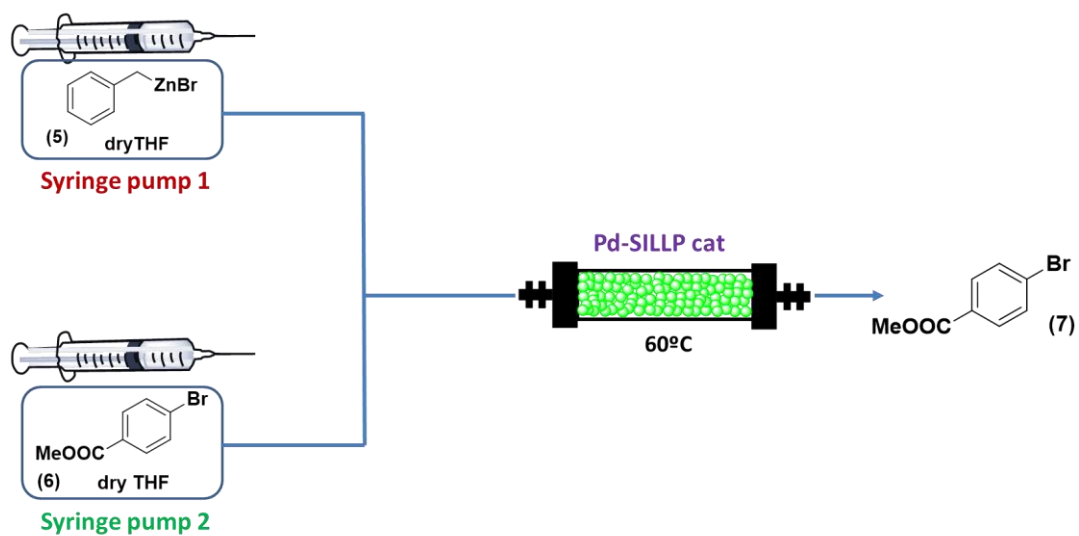


Figure S1. General scheme of the continuous flow Negishi cross-coupling reaction studied.

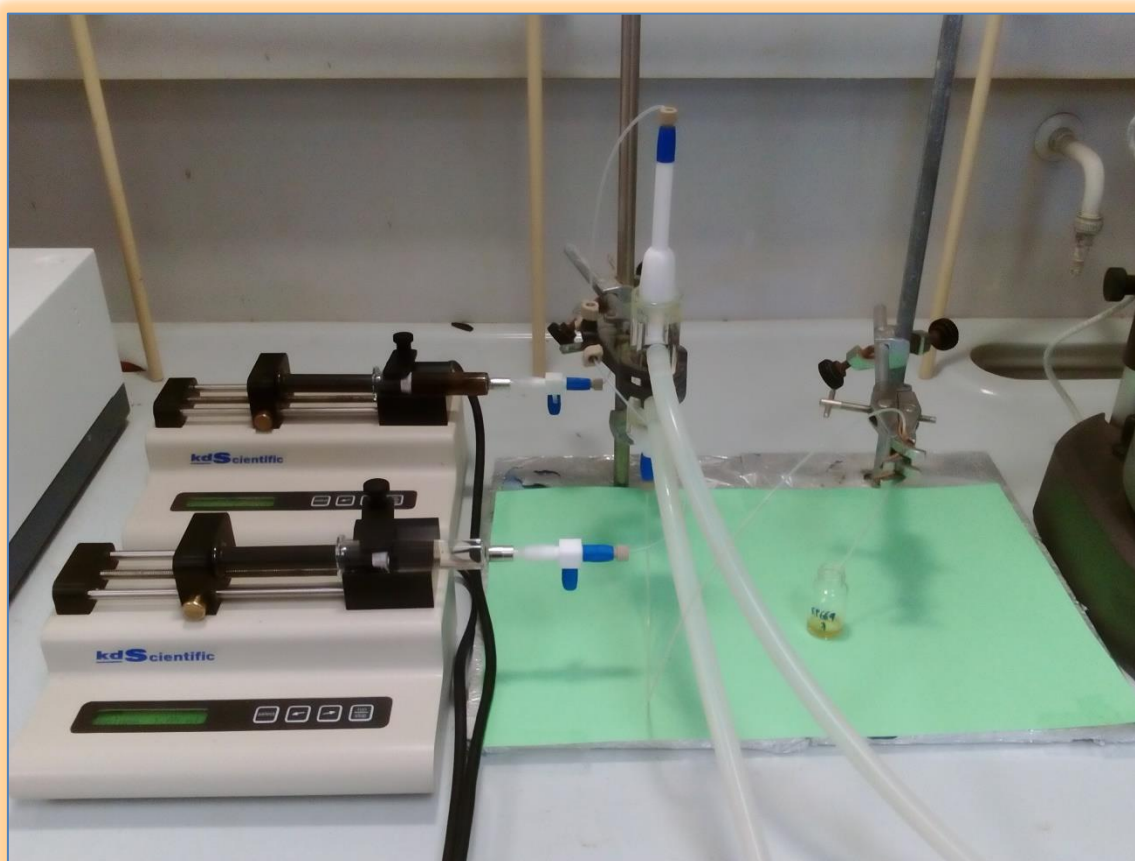
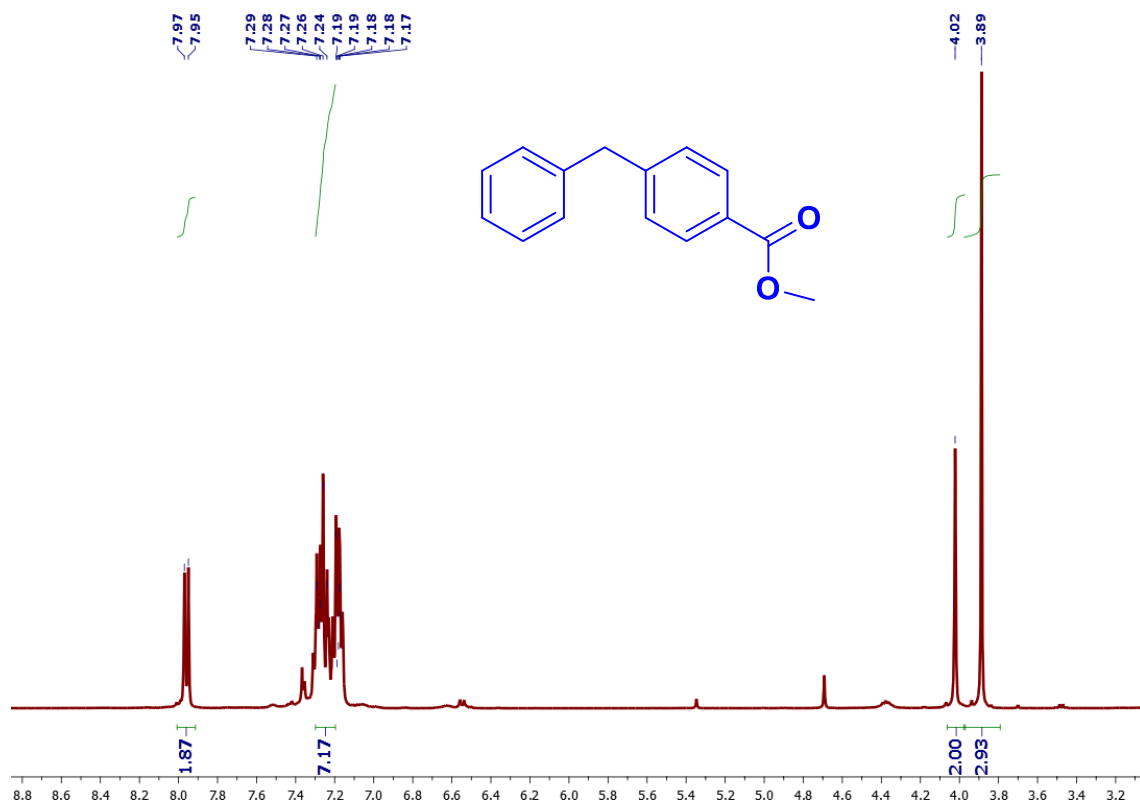


Figure S2. General set-up used to perform the Negishi cross-coupling reaction between benzylzinc bromide (5) and methyl 4-bromobenzoate (6). Syringe pumps from kdScientific and Hamilton 10 mL syringes were used. Glass Omnifit columns 006RG-10-10 (0.7854 cm diameter x 10 cm length) were used as fixed-bed reactors. The reactor was heated at 60 °C by i-PrOH reflux.

### 3. RMN SPECTRA

#### $^1\text{H-NMR}$ data of methyl 4-benzylbenzoate (7)



$^1\text{H-NMR}$  (300 MHz,  $\text{CDCl}_3$ )  $\delta$  7.96 (d, 2H), 7.29-7.17 (m, 7H), 4.02 (s, 2H), 3.89 (s, 3H)



**Tuneable 3D printed bioreactors  
for transaminations under  
continuous-flow**

**CHAPTER 7**



## Chapter 7. Tuneable 3D printed bioreactors for transaminations under continuous-flow

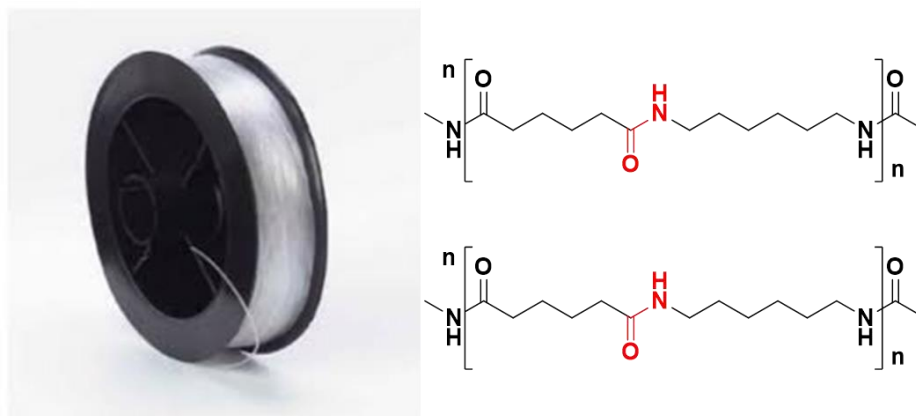
### 7.1 RESUMEN DEL MANUSCRITO

Este último capítulo se desvía ligeramente de la línea principal de la tesis, ya que aunque trata del desarrollo de un sistema catalítico en continuo, este no está basado en líquidos iónicos inmovilizados. Sin embargo, puede abrir la puerta a la inmovilización futura de líquidos iónicos en el tipo de sistema que se describe. Este trabajo se realizó durante la estancia predoctoral en la University of Nottingham (Reino Unido) bajo la dirección del Doctor Víctor Sans.

El trabajo viene inspirado por la creciente importancia que está adquiriendo la impresión 3D, también conocida como “additive manufacturing”, en el desarrollo de reactores químicos y demás material de laboratorio. Las impresoras 3D, cada vez más avanzadas, permiten el diseño y producción de reactores con un elevado grado de sofisticación. Por otra parte, el desarrollo de procesos biocatalíticos es cada vez más importante en la obtención sostenible de compuestos de alto valor añadido.

La estrategia que se va a emplear en este trabajo es el diseño, impresión 3D y posterior modificación química de reactores de flujo continuo para poder inmovilizar enzimas creando bioreactores catalíticamente activos.

Para la impresión de los dispositivos se eligió el Nylon como material debido a su bajo coste, a que es inerte químicamente, no tóxico, tiene buenas propiedades mecánicas y está comercialmente disponible (Figura 7.1).



**Figura 7.1.** A la izquierda, imagen de una bobina de Nylon como las que se utilizan en las impresoras 3D. Así sería la fuente de Nylon. A la derecha, la estructura polimérica del Nylon donde se aprecian los enlaces tipo amida.

La viabilidad de la estrategia propuesta se estudió en tres fases. En primer lugar, se estudió la posibilidad de llevar a cabo una modificación química de los sistemas impresos con la impresora 3D disponible (Lulzbot Taz 5). Para ello se imprimieron pequeñas piezas rectangulares de Nylon (1 x 0.6 x 0.2 cm) las cuales se modificaron como sigue (ver Figura 7.2):

- i) Hidrólisis ácida (HCl) de los grupos amida para obtener una superficie modificada con grupos  $-\text{NH}_2$  y  $-\text{COOH}$ .
- ii) Reacción de los  $-\text{NH}_2$  superficiales con un exceso de glutaraldehído formando los correspondientes enlaces tipo imina, quedando así la superficie decorada con grupos aldehído  $-\text{CHO}$ .
- iii) Por último, la reacción de los grupos aldehído con una poliamida permite incrementar la funcionalización en la superficie. Esta se puede modificar de nuevo con exceso de glutaraldehído dando lugar a una superficie multifuncional para la inmovilización de la enzima.

Estas modificaciones químicas o funcionalización de la superficie pudieron seguirse mediante ATR-FTIR gracias a la aparición, desaparición o incremento de la banda de aldehído a  $1719\text{ cm}^{-1}$ . Finalmente, una disolución de la enzima transaminasa comercial ATA-117 se utilizó para inmovilizar la enzima. La desaparición de la banda de aldehído confirmó que la enzima se había unido covalentemente formando un enlace tipo imina y un ensayo con la reacción de formación de acetofenona a partir de (*R*)-metilbencilamina (MBA) confirmó que la enzima inmovilizada conservaba su actividad biocatalítica.

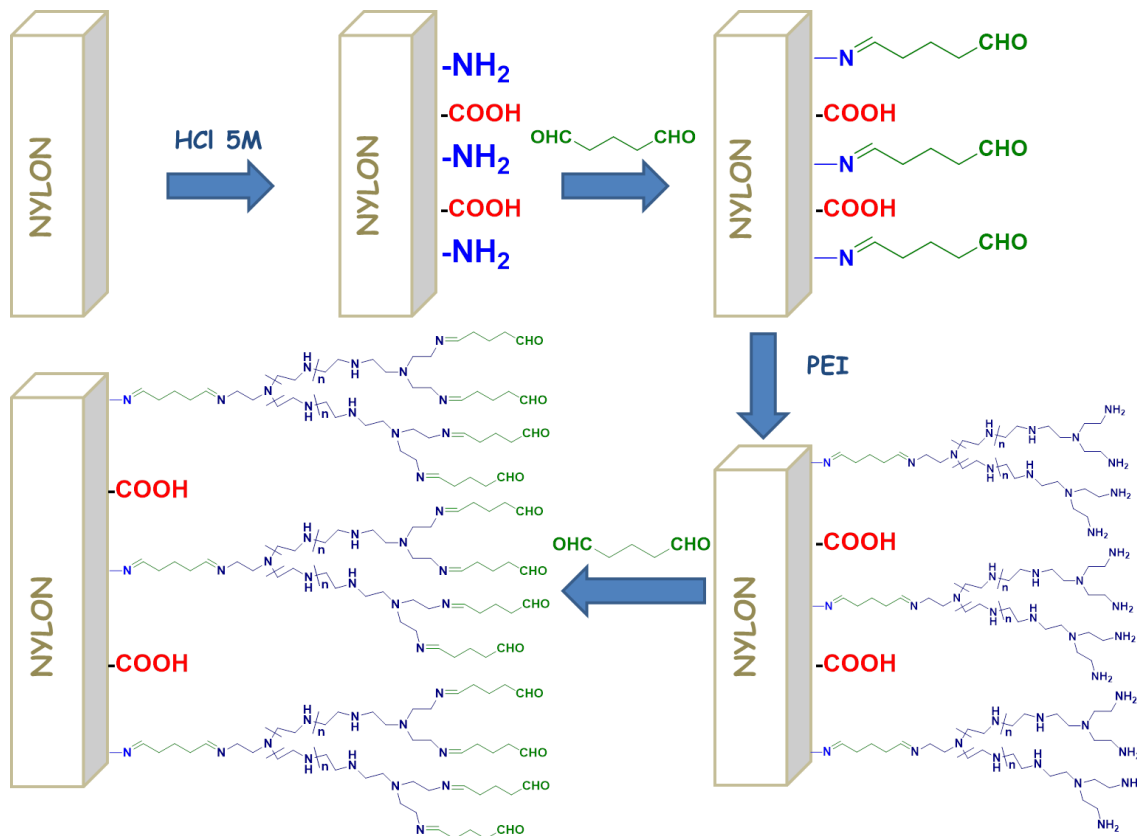


Figura 7.2. Esquema de la funcionalización o modificación química sobre la superficie del Nylon.

Una vez desarrollada la metodología sintética que permite la funcionalización del Nylon, se imprimió un dispositivo de múltiples pocillos “multiple-wells” (ver Figura 7.4). Este sistema nos permitió evaluar de forma rápida diferentes estrategias para la inmovilización de la enzima (absorción, iónica, covalente puntual, covalente multipunto), así como la actividad de diferentes transaminasas: i) ATA256, *S* selectiva y comercial; ii) ATA117, *R* selectiva y comercial; y iii) 3HMU, *S* selectiva. Para evaluar tanto la metodología de inmovilización como la enzima, se empleó la reacción de formación de acetofenona a partir de la correspondiente (*R*) o (*S*)-metilbencilamina (Figura 7.3).

Estos estudios iniciales nos permitieron establecer la inmovilización covalente puntual de la enzima como la metodología que daba lugar a sistemas más activos. Los otros modos de inmovilización evaluados producían una desactivación de la enzima perdiendo su actividad catalítica. Del mismo modo, este sistema de pocillos nos permitió discriminar entre las diferentes transaminasas disponibles. Así, la enzima ATA117 (*R*-selectiva) soportada mediante un proceso de inmovilización covalente puntual en el Nylon fue la que condujo a los mejores resultados en términos de actividad.

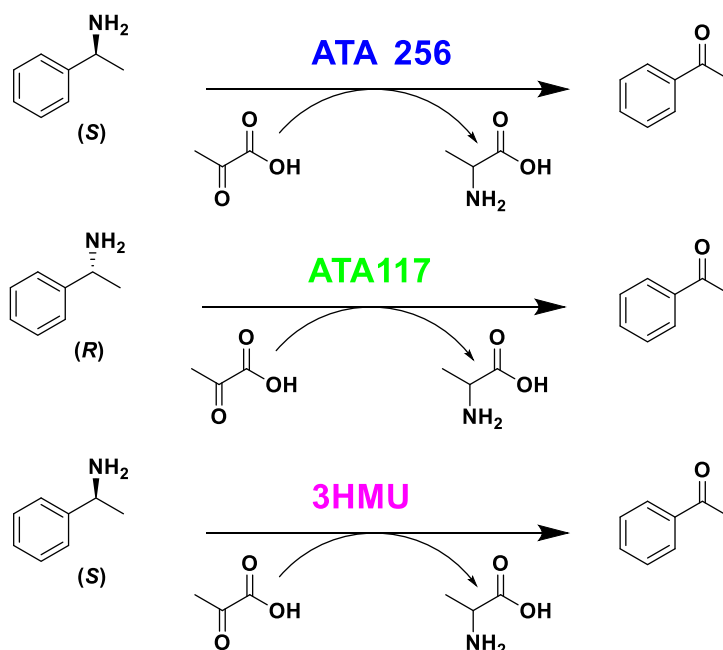


Figura 7.3. Reacciones empleadas para evaluar la metodología de inmovilización y la enzima a inmovilizar en el dispositivo de múltiples pocillos.

Establecido el método de modificación del Nylon y la metodología de inmovilización de la enzima, así como la naturaleza de la misma, se procedió a imprimir un reactor de Nylon para flujo continuo (ver Figura 7.4).



Figura 7.4. A la izquierda, pieza con los pocillos o “multi-plate Wells” para hacer ensayos. A la derecha, reactor de flujo continuo. Ambas piezas están impresas en Nylon.

La modificación de la superficie del canal interior del mismo, así como la inmovilización de la enzima, ambas realizadas en flujo, dieron lugar a un reactor biocatalítico. La eficiencia de este sistema se evaluó en la resolución cinética de la MBA racémica. La conversión total (>49%) de la *R*-MBA en acetofenona se observó empleando un flujo de 0.01

mL/min a temperatura ambiente, dando lugar a la S-MBA con un exceso enantiomérico >99% ee. El sistema mantuvo estos resultados durante 20 horas, luego fue guardado en nevera lleno de disolución tampón durante 48 horas antes de volver a utilizarlo durante 80 horas más con la misma eficiencia, demostrando una elevada estabilidad.

Cabe destacar que la enzima inmovilizada en el reactor presenta una actividad comparable a la de la enzima libre, por lo que su inmovilización no repercute en absoluto en la actividad catalítica. Además, la productividad del sistema se ve claramente favorecida bajo condiciones de flujo continuo.

Este trabajo abre nuevas posibilidades en el diseño y aplicación de reactores (bio)catalíticos, con el diseño que más se adapte a nuestras necesidades, a partir de un material económico que, tras ciertas modificaciones relativamente sencillas, permite inmovilizar catalizadores en su superficie sin que pierdan su actividad.

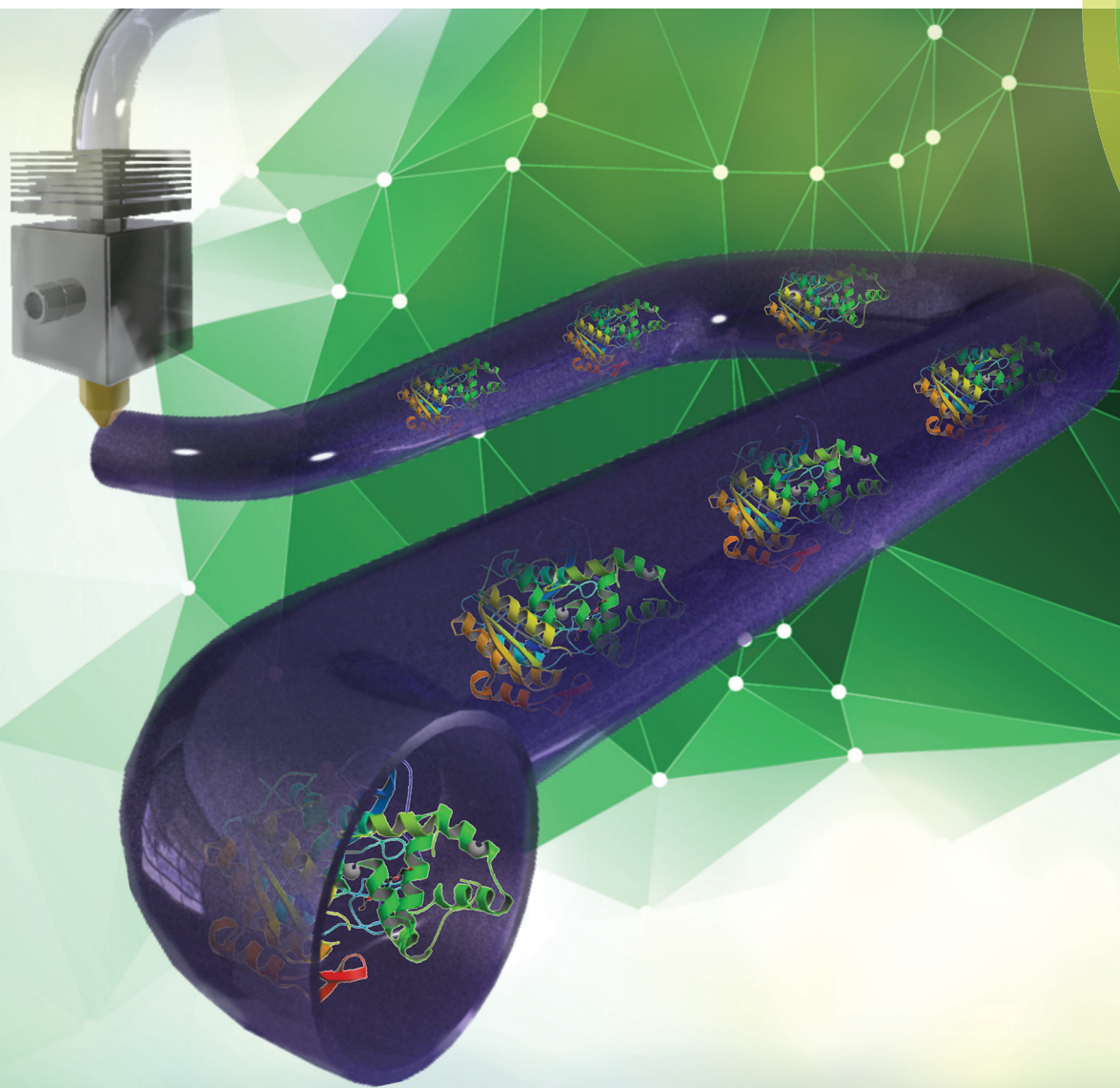




# Green Chemistry

Cutting-edge research for a greener sustainable future

[rsc.li/greenchem](http://rsc.li/greenchem)



ISSN 1463-9262



**COMMUNICATION**

Victor Sans *et al.*

Tuneable 3D printed bioreactors for transaminations under continuous-flow



## Tunable 3D printed bioreactors for transaminations under continuous-flow†

Cite this: *Green Chem.*, 2017, **19**, 5345

Received 9th August 2017,  
Accepted 3rd October 2017

DOI: 10.1039/c7gc02421e

rsc.li/greenchem

Edgar Peris,<sup>a</sup> Obinna Okafor,<sup>b,d</sup> Evelina Kulcinskaja,<sup>c</sup> Ruth Goodridge,<sup>b</sup> Santiago V. Luis,<sup>†a</sup> Eduardo Garcia-Verdugo,<sup>†a</sup> Elaine O'Reilly<sup>c</sup> and Victor Sans<sup>†a,b,d</sup>

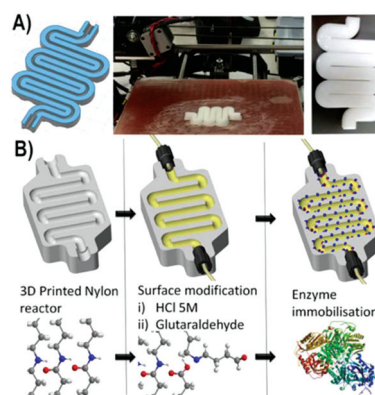
**A method to efficiently immobilize enzymes on 3D printed continuous-flow devices is presented. Application of these chemically modified devices enables rapid screening of immobilization mechanisms and reaction conditions, simple transfer of optimised conditions into tailored printed microfluidic reactors and development of continuous-flow biocatalytic processes. The bioreactors showed good activity (8–20.5  $\mu\text{mol h}^{-1} \text{mg}_{\text{enz}}^{-1}$ ) in the kinetic resolution of 1-methylbenzylamine, and very good stability (ca. 100 h under flow).**

The development of biocatalytic processes is emerging as a new paradigm in the sustainable manufacturing of high value chemicals for the pharmaceutical industry.<sup>1,2</sup> The application of biocatalysts can provide alternative synthetic approaches to those relying on more traditional chemistry, reducing the need for toxic reagents, transition-metal catalysts and avoiding costly purification steps and protecting group manipulations.<sup>3</sup> The immobilization of enzymes onto solid supports has facilitated the development of biocatalytic industrial processes, by simplifying the recovery and reuse of the enzymes and enabling their transition into continuous flow reactors.<sup>4–6</sup> However, the number of commercially available systems is currently limited, mainly due to the absence robust immobilization strategies.

Additive manufacturing, commonly known as 3D printing, has the potential to enable the rapid assembly of complex reaction system geometries, which is often challenging using traditional manufacturing techniques.<sup>7</sup> The development of 3D printed devices for chemical synthesis, coined “reactionware”, has gained a great deal of attention in recent years,<sup>8</sup> and continuous-flow reactors with varying degrees of sophistication

have been described in the literature for a variety of applications.<sup>9–13</sup> However, the chemical post-modification of printed devices has received much less attention.<sup>14</sup> The development of reliable methods for chemical modification has enormous potential to reduce cost and deliver functional devices for rapid screening of immobilized enzymes. Furthermore, the freedom of design inherent to 3D printing allows parallelized fast screening platforms to be combined with intensified continuous-flow reactors featuring advanced geometries and optimized mixing properties.

Here, we report the first example of modified 3D printed devices (Fig. 1A) for the immobilization and application of  $\omega$ -transaminase ( $\omega$ -TA) enzymes in continuous-flow. The sequential chemical functionalization of the printed devices (Fig. 1B) enables a fine control of the physico-chemical properties of the reactor surface, thus enabling diverse types of interaction with target enzymes and allowing rapid screening of experimental conditions. The strategy combines effective enzyme immobilization and reutilization with the efficiency of continuous-flow and represents a significantly more sustain-



**Fig. 1** Schematic representation of the preparation of 3D printed bioreactors. (A) Printing process of Nylon employing an FDM printer, including a CAD file of a simple fluidic device (left), the printing process (centre) and the device (right). (B) Schematic representation of the post-functionalisation of the printed reactor.

<sup>a</sup>Departamento de Química Inorgánica y Orgánica, Universitat Jaume I, 12071 Castellón de la Plana, Spain

<sup>b</sup>Faculty of Engineering, University of Nottingham, NG7 2RD Nottingham, UK

<sup>c</sup>School of Chemistry, University of Nottingham, NG7 2RD Nottingham, UK

<sup>d</sup>GSK Carbon Neutral Laboratory, University of Nottingham, Nottingham, NG8 2GA, UK. E-mail: victor.sansangorin@nottingham.ac.uk

† Electronic supplementary information (ESI) available. See DOI: 10.1039/c7gc02421e

able approach to the development of biocatalytic processes compared to those in traditional batch reactors.<sup>5b</sup>

An extrusion based 3D printing platform, Lulzbot Taz 5, with commercially available nylon 6 filaments was employed to fabricate bespoke devices. The surface was sequentially modified to enable the adhesion of enzymes, allowing the design of biocatalytic systems for screening in multiple well-plate and continuous-flow biocatalytic reactors. Nylon is a particularly convenient immobilization matrix for enzymes.<sup>15,16</sup> It is inexpensive, chemically inert, non-toxic, has good mechanical properties and is commercially available in multiple formats. Indeed, several studies report the immobilization of various enzymes like proteases, glucosidases, endocellulases and laccases onto different nylon matrices.<sup>15,17</sup> Various types of nylon are widely employed for additive manufacturing. Powder based nylon 11/12 is commonly employed material of choice for selective laser sintering (SLS) methods.<sup>18</sup> These platforms are capable of producing robust parts with highly intricate geometries and fine layer resolution of 100  $\mu\text{m}$ . Therefore, there is an untapped potential to develop 3D printed supported bioreactors fabricated in nylon.

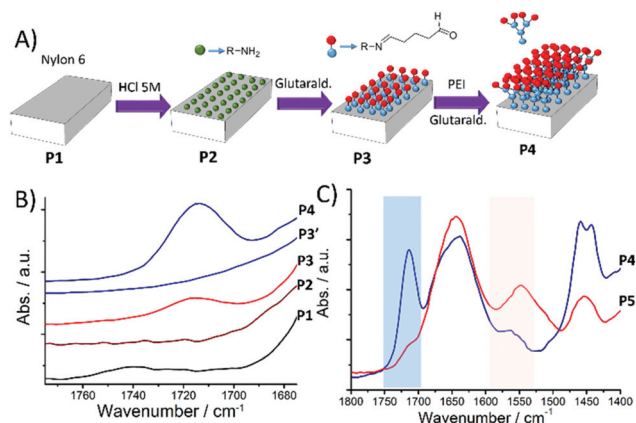
The initial goal was to functionalise 3D printed nylon. To this end, small pieces of commercially available Nylon Taulman 645 (1  $\times$  0.6  $\times$  0.2 cm) were printed and chemically modified following the scheme shown in Fig. 2A. After brief treatment with HCl (5 M), a functional surface was generated with glutaraldehyde, as evidenced by the presence of a characteristic aldehyde C=O band at 1719  $\text{cm}^{-1}$  in the ATR-IR spectra (Fig. 2B, P3). This modification was accompanied with a change of colour from white to light orange. In order to increase the functionality of the surface, polymer P3 was treated with polyethylenimine (PEI, 60k  $M_n$ ) to form the corres-

ponding imine leading to multiple free amines at the nylon surface (polymer P3'). The further reaction with glutaraldehyde led to a highly-functionalised polymer P4, characterized by the significant increase in the intensity of the C=O band associated with this functionality (Fig. 2B and C, spectra P4).

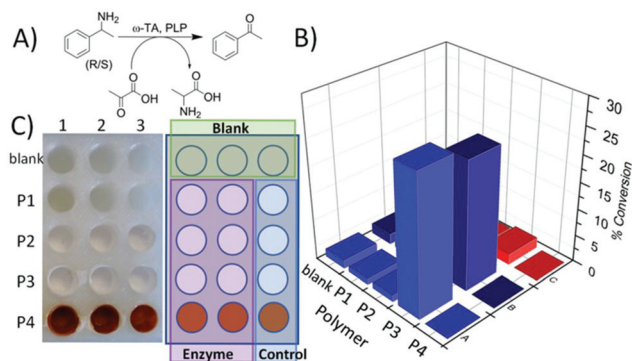
The application of transaminases for the synthesis of optically pure chiral amines from readily available ketones has received considerable attention from both the academic and industrial communities, due to the challenging nature of this transformation.<sup>19–24</sup> Additionally, there are only a handful of reports describing their successful application in continuous flow.<sup>25–28</sup> We selected the commercially available (*R*)- $\omega$ -TA, ATA117, to demonstrate our flow methodology. The enzyme was supported following a literature procedure (see ESI†) and the immobilization confirmed by ATR-FTIR (Fig. 2, polymer P5). An assay was used to confirm that the enzyme had retained activity (see ESI†).

A key advantage of the use of 3D printing is the ability to rapidly generate multiplexed reactors that can increase the experimental throughput, thus speeding up the discovery and optimization of new compounds or processes.<sup>29</sup> This can be invaluable for the rapid screening of immobilization conditions, which usually relies on trial and error approach, being time and resource intensive. Indeed, the use of microplate based immobilization techniques has been described to rapidly establish the best immobilization techniques for esterases.<sup>30</sup> Exploiting the same materials for enzyme immobilization and the development of 3D printed flow reactors has the potential to significantly speed up time and reduce labour intensive assays due to the rapid translation of immobilization conditions.

A multi-well plate (dimensions: 1 cm i.d.  $\times$  1 cm height, Fig. 3C) was manufactured in Nylon (Taulman 645). Four



**Fig. 2** Chemical modification of 3D printed material for enzyme immobilization. (A) A 3D printed nylon part (P1) was treated with HCl 5 M (P2) and then the superficial amine groups were reacted with glutaraldehyde (P3) to generate covalent link points for the enzyme. The reaction with polyethylenimine (PEI) (polymer P3') and glutaraldehyde led to a polymer with increased linkage points (P4). (B) Detail of the aldehyde region in the ATR-IR spectra from polymers P1–P4. (C) Disappearance of the aldehyde band (blue region) of polymer P4 in contact with a  $\omega$ -TA enzyme and amide-II bands observed at 1550  $\text{cm}^{-1}$  (brown region).



**Fig. 3** Evaluation of the effect of immobilisation on the enzymatic activity of an  $\omega$ -TA ATA117. (A) Reaction scheme for the benchmark reaction. (B) Experimental results obtained for the different immobilisation conditions. (C) Image and scheme of the chemically modified 3D printed wells (left) and the experimental design (right), consisting of a combination of blank reactors without chemical modification nor enzyme (green box), control reactions in chemically modified wells without enzyme (blue box) and chemically modified wells containing enzyme (purple). Reaction conditions: Each well was filled with a 785  $\mu\text{L}$  solution of methylbenzylamine (5 mM) ((*R*)-MBA in wells 1 & 2 and (*rac*)-MBA in well 3), pyruvate (5 mM) and PLP (0.1 mM) in potassium phosphate buffer, pH = 8.0. Reactions run at 30  $^{\circ}\text{C}$  for 17 hours.

different immobilization strategies were simultaneously screened (see ESI, Fig. S2† for the proposed immobilization mechanisms). The first row was left unmodified and without enzyme to function as a blank for the reaction. The wells of row 2 were maintained unmodified (*i.e.* with polymer P1) to study the possible non-covalent immobilization directly on the surface by weak interactions (hydrogen bonds, hydrophobic effects, *etc.*). Polymer P2 (Fig. 3C, row 3) provides a surface capable to immobilize the enzyme through ionic pairing and hydrogen bonds. Non-covalent immobilization is sometimes preferred to covalent immobilization as a minimal distortion of enzyme structures is expected. The covalent immobilization of the enzyme by polymer P3 in row 4 and multi-punctual covalent immobilization row 5. After the modifications, the wells of rows 2–5 and columns 1 and 2 were filled with a solution of a (*R*)- $\omega$ -TA (ATA117, 1 mg ml<sup>-1</sup> solution of the enzyme in 0.1 M K phosphate buffer pH = 8.0, with 0.1 mM PLP). Column 3 was employed as a control, containing only buffer and PLP. The plate was left overnight at 4 °C. After this period, the wells were emptied and washed with buffer. Wells in rows 4 and 5 were then additionally washed with a solution of NaCl (0.5 M) for 2 hours to remove any non-covalently immobilized enzyme.

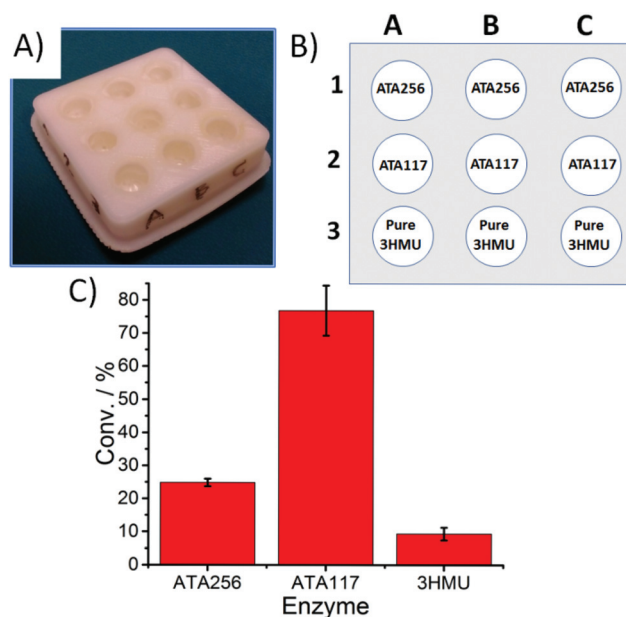
The conversion of (*R*)-methyl-benzylamine into acetophenone was selected as a model transamination reaction to evaluate the performance of the  $\omega$ -TA immobilized in the nylon wells (Fig. 3A). The wells were filled with 785  $\mu$ L of a solution containing the reagents required for the biotransformations (see Fig. 3 legend for details). After 17 hours, the solution was removed from the wells, extracted with ethyl acetate and analysed by GC/MS. The results obtained are summarized in the Fig. 3B. The control experiments (row 1 and column 3) showed only residual activity (<2%) indicating no catalytic activity from the different polymers without enzyme. Only polymer P4 (row 4, columns 1 and 2) showed some level of activity (*ca.* 25%). The  $\omega$ -TA immobilized on the modified surface with higher number of superficial aldehydes, which can potentially bind to the enzyme in multiple points (row-5) did not exhibited any level of activity. This was rather surprising, and it might be due to the presence of multiple covalent bonds between the enzyme and the support inducing changes in the structure of the enzyme or due to the adsorption of the substrates. In light of these results, polymer P4 (glutaraldehyde functionalized nylon) appeared to be the more efficient way to immobilize the  $\omega$ -TA tested. The diffusion of substrate outside the wells was visually observed, indicating an imperfect inter-bonding layer (see ESI Table S1†).

A new type of Nylon 6 (Taulman 618), which showed better inter-layer adhesion, was employed to manufacture a new set of well plates with the same dimensions and to evaluate the effect on a small panel of  $\omega$ -TAs. A plate containing 6 wells was printed and modified to generate the equivalent of polymer P4, called P4' for simplicity. Three different  $\omega$ -TAs, two of them (*S*) selective (256 and 3HMU) and one (*R*) selective (ATA117) were immobilized in triplicate under same conditions previously employed. The benchmark reaction, the conversion of

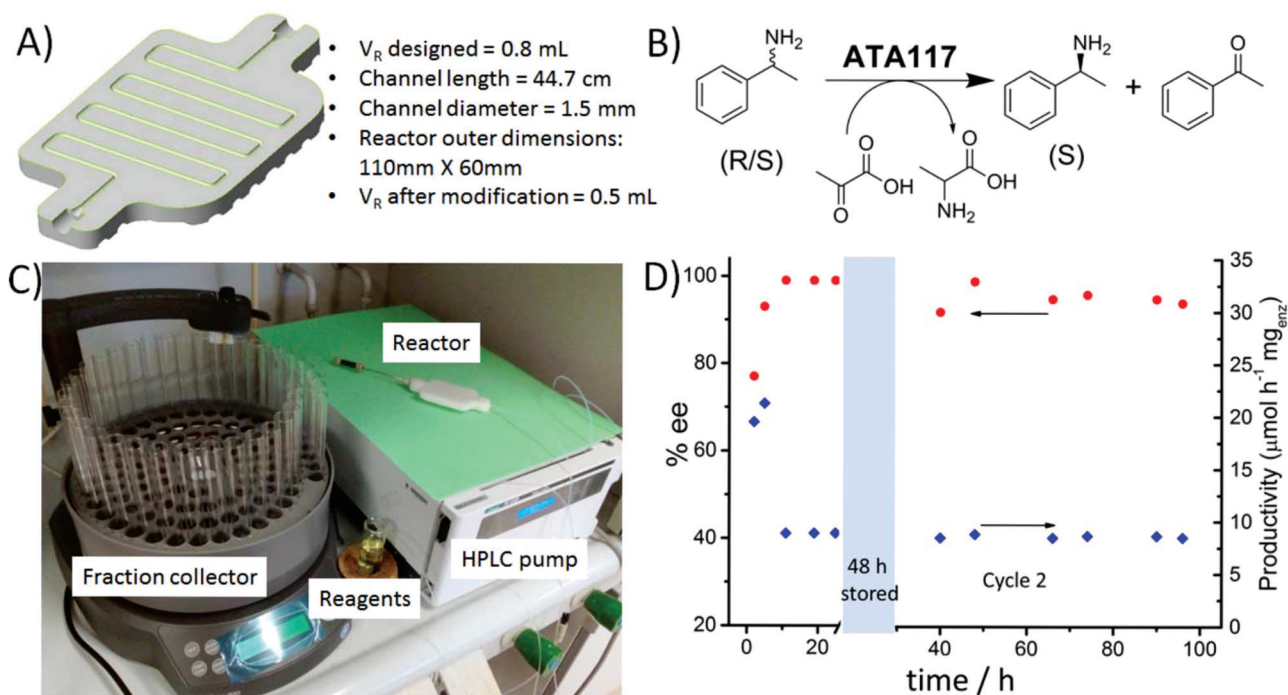
(*R*)- or (*S*)-methyl-benzylamine into acetophenone, was employed in order to compare the activity of the enzymes. The results demonstrated satisfactory reproducibility for the triplicate assays. The (*S*)-selective  $\omega$ -TAs displayed a lower activity than the (*R*)-selective enzyme (ATA117 > 256 > 3HMU) (Fig. 4). In summary, this simple screening highlighted ATA117 as the most suitable  $\omega$ -TA enzyme for immobilization by covalent attachment to 3D printing well-plate device (polymer P4').

Crucially, the results of the screening can be readily transferred into continuous-flow micro-structured devices. The bio-reactor devices were built in Nylon Taulman 618, Fig. 4A, using the same platform described for the fabrication of the test wells. An iterative approach described in the ESI† was employed to optimize the reactor manufacturing conditions. The nozzle temperature, build chamber temperature and model design were adjusted in order to produce robust leak-free devices. A 'track and hole' support structure (ESI, Table S1†) was incorporated into the design of the reactor to break up the large surface area of the part printed per layer, aiming to minimize warping. This design also reduces temperature build up at the mid regions of the part as allows air flow through these areas. The reactor device was connected with PTFE tubing using rheodyne metal connectors.

The reactor modification was performed under stop-flow conditions for the HCl and glutaraldehyde solutions (see ESI† for details). The immobilization of the enzyme was achieved *via* recirculation at 25  $\mu$ L min<sup>-1</sup> a 15 mL of solution of ATA117



**Fig. 4** (A) 3D-printed Nylon wells used to perform the screening of the different enzymes. (B) Representation of the enzyme distribution in the wells. (C) Average conversion and standard deviation (error bars) observed for the three experiments of each of the enzymes tested. Conditions: 5 mM (*R*)-MBA (in the case of ATA117) or *S*-MBA (in the case of ATA256 and 3HMU), 5 mM pyruvic acid, 0.1 mM PLP, r.t., 30 °C. 0.785 ml of a solution of the reagents in 0.1 M K phosphate buffer pH 8.0 was introduced in each well.



**Fig. 5** Continuous-flow biocatalytic reactors for the kinetic resolution of *rac*-methylbenzylamine. (A) CAD of the bioreactor and main reactor parameters. (B) Kinetic resolution of *rac*-methylbenzylamine employing ATA 117 supported on the 3D printed bioreactor. (C) Experimental set-up employed for the continuous-flow biocatalytic transformation. (D) Productivity and enantiomeric excess observed as a function of time. The first two data points correspond to experiments assayed at  $25 \mu\text{L min}^{-1}$ , while the rest were assayed at  $10 \mu\text{L min}^{-1}$ . The plot represents two separate runs under continuous-flow, the first of them for 24 h, followed by a 48 h storage in fresh buffer and a subsequent run for further 78 h. The results indicate the activity and stability of the enzyme, by keeping its activity over extended periods of time (ca. 100 h) under continuous-flow streams.

( $5 \text{ mg mL}^{-1}$  in 0.1 M of K phosphate buffer pH = 8.0 and 0.1 mM PLP) at r.t. for 24 h and washed with buffer solution afterwards. The analysis of the enzyme solution after the immobilization process indicated that  $170 \mu\text{g}$  of  $\omega$ -TA were attached to the surface of the reactor channel.

The results obtained for the kinetic resolution of *rac*-methylbenzylamine are summarized in Fig. 5D. At the initial flow rate assayed  $25 \mu\text{L min}^{-1}$  of a solution of 5 mM *rac*-methylbenzylamine, 5 mM pyruvic acid and 0.1 mM PLP and after 5 h of time on stream, a conversion of the 48% of the (*R*) enantiomer on the amine into ketone was observed. Thus, (*S*)-methylbenzylamine was obtained with an enantiomeric excess of  $93 \pm 2\%$  ee, as determined by HPLC. This corresponds to a remarkably low residence time of 20 min and a productivity of  $20.5 \mu\text{mol h}^{-1} \text{mg}_{\text{enz}}^{-1}$ . This is comparable to the batch experiment performed under similar conditions, thus indicating that the enzyme activity is retained. Then, the flow rate was reduced to  $10 \mu\text{L min}^{-1}$  in order to test the temporal stability of the bioreactor and the reaction was carried out for an additional 20 hours. At this flow rate, corresponding to a residence time of 50 min, almost full conversion of the (*R*)-enantiomer was observed ( $>49\%$ ) yielding the (*S*)-amine with an enantiomeric excess  $>99\%$  ee. In order to evaluate the stability of the biocatalytic system, the reactor was flushed with buffer and stored at  $4 \text{ }^\circ\text{C}$  for 48 hours. Afterwards, a second cycle was performed under the same experimental conditions ( $10 \mu\text{L min}^{-1}$ , 5 mM

*rac*-methylbenzylamine, 5 mM pyruvic acid, 0.1 mM PLP) and the flow system was maintained for a further 78 hours. During these period, the activity and enantioselectivity of the bioreactor was maintained with ee  $>94\%$ . These results demonstrate that the enzyme can be effectively immobilized on printed flow bioreactors, and the productivity of the system is greatly enhanced by the flow conditions. Indeed, a total of 105 catalytic cycles were performed with the same enzyme. This work has demonstrated the first example of enzyme immobilization on modified 3D printed continuous flow biocatalytic reactors and paves the way for numerous applications in industrial biotechnology. The possibility of rapidly testing different immobilization mechanisms and conditions, that are easily transferred to continuous-flow bioreactors with tailored geometries will allow for the development of numerous applications. Significantly, the  $\omega$ -TA enzymes tested showed a comparable activity to the free enzyme and were successfully recycled. Next steps will include demonstrating the approach on a diverse set of enzymes, employing different printing techniques and assessing alternative immobilisation methods by modifying the surface linking agents.

## Conflicts of interest

There are no conflicts to declare.

## Acknowledgements

The authors acknowledge the Royal Society (RG150021) for funding and the Research Priority Area (RPA) of UoN in Industrial Biotechnology for funding. Research leading to these results has also received funding from the BBSRC (BB/M021947/1) and from EPSRC (EP/I033335/2). This work was partially supported by G. V. (PROMETEO 2016-071) and MINECO (CTQ2015-68429R). E. Peris thanks MICINN for personal financial support (FPU13/00685).

## References

- 1 A. Schmid, J. S. Dordick, B. Hauer, A. Kiener, M. Wubbolts and B. Witholt, *Nature*, 2001, **409**, 258–268.
- 2 D. J. C. Constable, P. J. Dunn, J. D. Hayler, G. R. Humphrey, J. J. L. Leazer, R. J. Linderman, K. Lorenz, J. Manley, B. A. Pearlman, A. Wells, A. Zaks and T. Y. Zhang, *Green Chem.*, 2007, **9**, 411–420.
- 3 U. T. Bornscheuer, G. W. Huisman, R. J. Kazlauskas, S. Lutz, J. C. Moore and K. Robins, *Nature*, 2012, **485**, 185–194.
- 4 R. A. Sheldon and S. van Pelt, *Chem. Soc. Rev.*, 2013, **42**, 6223–6235.
- 5 (a) P. Lozano, *Green Chem.*, 2010, **12**, 555–569; (b) P. Lozano, E. Garcia-Verdugo, R. Piamtongkam, N. Karbass, T. De Diego, M. I. Burguete, S. V. Luis and J. L. Iborra, *Adv. Synth. Catal.*, 2007, **349**, 1077–1084.
- 6 R. C. Rodrigues, C. Ortiz, A. Berenguer-Murcia, R. Torres and R. Fernandez-Lafuente, *Chem. Soc. Rev.*, 2013, **42**, 6290–6307.
- 7 I. Gibson, D. W. Rosen and B. Stucker, *Additive Manufacturing Technologies: Rapid Prototyping to Direct Digital Manufacturing*, Springer-Verlag Berlin, Berlin, 2010.
- 8 M. D. Symes, P. J. Kitson, J. Yan, C. J. Richmond, G. J. T. Cooper, R. W. Bowman, T. Vilbrandt and L. Cronin, *Nat. Chem.*, 2012, **4**, 349–354.
- 9 S. Rossi, R. Porta, D. Brenna, A. Puglisi and M. Benaglia, *Angew. Chem., Int. Ed.*, 2017, **56**, 4290–4294.
- 10 O. Okafor, A. Weiland, J. A. Fernandes, E. Karjalainen, R. Goodridge and V. Sans, *React. Chem. Eng.*, 2017, **2**, 129–136.
- 11 V. Dragone, V. Sans, M. H. Rosnes, P. J. Kitson and L. Cronin, *Beilstein J. Org. Chem.*, 2013, **9**, 951–959.
- 12 P. J. Kitson, M. H. Rosnes, V. Sans, V. Dragone and L. Cronin, *Lab Chip*, 2012, **12**, 3267–3271.
- 13 A. K. Au, W. Huynh, L. F. Horowitz and A. Folch, *Angew. Chem., Int. Ed.*, 2016, **55**, 3862–3881.
- 14 Q. Guo, X. Cai, X. Wang and J. Yang, *J. Mol. Catal. B: Enzym.*, 2013, **1**, 6644–6649.
- 15 E. Fatarella, D. Spinelli, M. Ruzzante and R. Pogni, *J. Mol. Catal. B: Enzym.*, 2014, **102**, 41–47.
- 16 P. Lozano and J. L. Iborra, in *Immobilization of Enzymes and Cells*, ed. G. F. Bickerstaff, Humana Press, Totowa, NJ, 1997, pp. 27–40, DOI: 10.1385/0-89603-386-4:27.
- 17 F. H. Isgrove, R. J. H. Williams, G. W. Niven and A. T. Andrews, *Enzyme Microb. Technol.*, 2001, **28**, 225–232.
- 18 R. D. Goodridge, C. J. Tuck and R. J. M. Hague, *Prog. Mater. Sci.*, 2012, **57**, 229–267.
- 19 A. P. Green, N. J. Turner and E. O'Reilly, *Angew. Chem., Int. Ed.*, 2014, **53**, 10714–10717.
- 20 E. O'Reilly, C. Iglesias and N. J. Turner, *ChemCatChem*, 2014, **6**, 992–995.
- 21 E. O'Reilly, C. Iglesias, D. Ghislieri, J. Hopwood, J. L. Galman, R. C. Lloyd and N. J. Turner, *Angew. Chem., Int. Ed.*, 2014, **53**, 2447–2450.
- 22 L. Martinez-Montero, V. Gotor, V. Gotor-Fernandez and I. Lavandera, *Green Chem.*, 2017, **19**, 474–480.
- 23 M. Lopez-Iglesias, D. Gonzalez-Martinez, V. Gotor, E. Busto, W. Kroutil and V. Gotor-Fernandez, *ACS Catal.*, 2016, **6**, 4003–4009.
- 24 F. Guo and P. Berglund, *Green Chem.*, 2017, **19**, 333–360.
- 25 M. Planchestainer, M. L. Contente, J. Cassidy, F. Molinari, L. Tamborini and F. Paradisi, *Green Chem.*, 2017, **19**, 372–375.
- 26 N. Miložič, M. Lubej, M. Lakner, P. Žnidaršič-Plazl and I. Plazl, *Chem. Eng. J.*, 2017, **313**, 374–381.
- 27 W. Neto, M. Schürmann, L. Panella, A. Vogel and J. M. Woodley, *J. Mol. Catal. B: Enzym.*, 2015, **117**, 54–61.
- 28 L. H. Andrade, W. Kroutil and T. F. Jamison, *Org. Lett.*, 2014, **16**, 6092–6095.
- 29 P. J. Kitson, R. J. Marshall, D. L. Long, R. S. Forgan and L. Cronin, *Angew. Chem., Int. Ed.*, 2014, **53**, 12723–12728.
- 30 B. Brandt, A. Hidalgo and U. T. Bornscheuer, *Biotechnol. J.*, 2006, **1**, 582–587.

# Tuneable 3D printed enzymatic reactors for continuous-flow biotransformations

Edgar Peris,<sup>a</sup> Obinna Okafor,<sup>b,d</sup> Evelina Kulcinskaja,<sup>c</sup> Ruth Goodridge,<sup>b</sup> Santiago V. Luis,<sup>a</sup> Eduardo Garcia-Verdugo,<sup>a</sup> Elaine O'Reilly,<sup>c</sup> Victor Sans,<sup>b,d\*</sup>

\*Corresponding author

<sup>a</sup> *Departamento de Química Inorgánica y Orgánica, Universitat Jaume I, Castellón de la Plana, Spain*

<sup>b</sup> *Faculty of Engineering, University of Nottingham, University Park, NG7 2RD, Nottingham, UK.*

<sup>c</sup> *School of Chemistry, University of Nottingham, University Park, NG7 2RD, Nottingham, UK.*

<sup>d</sup> *GSK Carbon Neutral Laboratory, University of Nottingham, Nottingham, NG8 2GA, UK*

## Table of contents

<b>1</b>	<b>Fabrication of 3D printed reactor device .....</b>	<b>2</b>
<b>2</b>	<b>Experimental methods .....</b>	<b>4</b>
2.1	Enzyme expression and purification .....	4
2.2	Chemical modification of Nylon and enzyme immobilisation .....	4
2.3	Catalytic test with modified nylon part .....	5
2.4	Analytical methods .....	6
2.4.1	Nylon surface modifications .....	6
2.4.2	Catalytical test with pieces. Conditions and enzymes screening in wells. ....	6
2.5	Continuous-flow set-up .....	6
2.5.1	Functionalisation of the Nylon Reactor .....	6
2.5.2	Enzymatic enantiomeric resolution of MBA under continuous flow conditions .....	8
2.5.3	HPLC spectra .....	9
<b>3</b>	<b>References .....</b>	<b>11</b>

## 1 Fabrication of 3D printed reactor device

This platform has a minimum layer thickness 75 microns to 500 microns when coupled with a 0.5mm extruder nozzle. The minimum build layer thickness, although beneficial in creating near net-shaped parts and finer surface roughness, is largely dependent on processing conditions as well as utilised materials. Building with a controlled heated bed enhances the control of warping as well as layer of glue stick to ensure bonding with build bed.

The reactor device for the immobilisation of enzymes was fabricated on an extrusion based 3D printing platform, Lulzbot Taz 5, using off the shelf, Nylon 618 filament. Fabricating on such a platform allows the process parameters, such as the nozzle temperature, build plate temperature, layer height and the deposition patterns to be easily configured. It is evident from previous studies that a canvas processing parameter cannot be applicable for all geometries even when employing similar materials. The geometry and size of the build as well as the material play an important role in choosing the processing parameters, hence an iterative approach was used in the fabrication of the bioreactor devices. Producing materials having a high melt temperature is challenging, as there is a larger temperature difference between the extrudate and the already cooled deposited polymer. The pulling effect towards the warmer region of the build coupled with shrinkages cause the parts to warp. A glue stick was used to ensure the Nylon filament adhered to the build bed.

As fabricating on the selected platform was an inexpensive process, an iterative approach was used to optimise the fabricated geometry close to the intended design. The main parameters modified during the iterative process are highlighted in Table S1, while the intended reactor to be fabricated is shown in Figure S 1. The reactor device was designed featuring a 1.5mm channel diameter with a volume of 0.8ml and an all-round dimension of 110 x 60 x 11 mm.

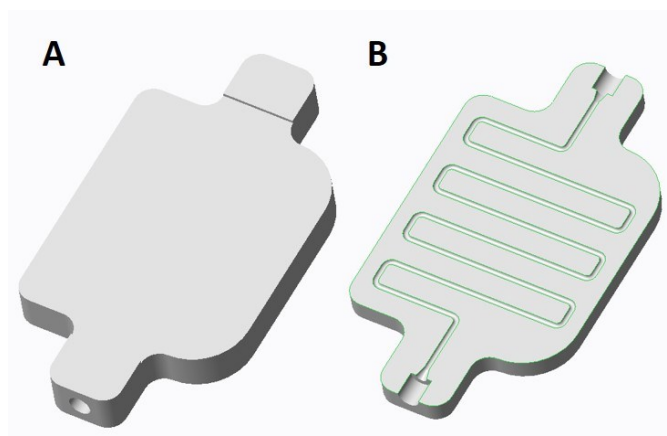
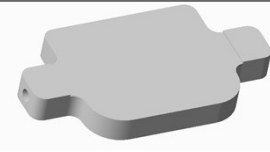



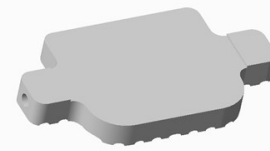
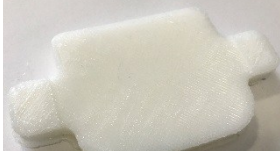
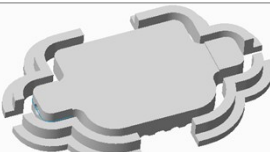

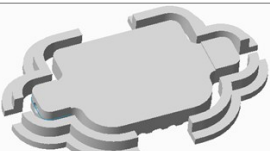



Figure S 1. (A) CAD model of 3D printed bioreactor (B) Section of the bioreactor device, showing the inner channel.



Table S 1 Optimisation of printing parameters for reactor manufacturing.

Entry	Print Conditions	CAD model	Fabricated part	Comments
1	Layer height: 0.3mm Nozzle temp: 235°C Build temp: 100°C			The designed reactor device was fabricated on the platform as designed without. The build warped and went off the build bed half way before completing. (Blocked reactor)
2	Layer height: 0.3mm Nozzle temp: 230°C Build temp: 100°C			'Track' were then added to the device to device, which aimed to break up the bottom layers and reduce warp. The build completed, however it still had a high degree of warpage causing the channels to block. (Blocked reactor)
3	Layer height: 0.3mm Nozzle temp: 230°C Build temp: 100°C			Increased the extraction flow rate of the fume cupboard to minimise build-up of temperature. This minimised warp and reduced the blistering effect see in the layers. (Blocked reactor)
4	Layer height: 0.3mm Nozzle temp: 230°C – 215°C Build temp: 100°C			Although the heated platform at 100 °C assisted adhesion of the build, this led to an over-heated bottom layers of the part noticed in previous builds. Two tactics were employed: (a) Edge temperature controllers around the part (b) A dynamic deposition temperature reduction from bottom layers to the top to compensate for the temperature of the build bed. (230-215 °C) (No blockage)
5	Layer height: 0.3mm Nozzle temp: 230°C – 215°C Build temp: 100 °C			Further increased the extraction flow rate of the fume cupboard with the parameters in test 4. Three further reactor devices were fabricated for experimentation using this condition without a blockages.

The final geometry obtained from the iterative process, Test 5, was then repeated three times. The devices were found to be leak free and similar. The track on the bottom of the print allowed for adhesion to the build bed, while the wall, designed around the build in test 4 & 5, assisted the retention of heat. This led to the fabrication of a device with minimal warp.

The selected conditions were a layer height of 0.3mm, build and nozzle temperature of 100 °C and 230 – 215 °C respectively. The reactor was designed to a total volume of 0.8mL and 1.5mm diameter with a single inlet-outlet configuration, see Figure 4A. The volume after fabrication was 0.5mL, due to the reduction in diameter as a result of larger XY resolution on the platform.

## 2 Experimental methods

### 2.1 Enzyme expression and purification

$\omega$ -transaminases ATA117 ((*R*)-selective) and ATA256 ((*S*)-selective) were purchased from Codexis, CA. The (*S*)-selective  $\omega$ -transaminase from *Silicibacter pomeroyi*, referred here by its PDB code 3HMU was expressed in *Escherichia coli* as described by Steffen-Munsberg *et al.*<sup>[1]</sup> The cell pellet was lysed by sonication on ice for 8 cycles of 15 s on, 30 s off in 50 mM Tris buffer pH 9.0, 0.3 M NaCl and 0.1 mM PLP, centrifuged for 30 min at 3 220 g at 4 °C and filtered through 0.45  $\mu$ m filters and loaded onto Ni-NTA superflow (IBA, Germany) and purified by gravity flow. The column was washed with wash buffer (100 mM Tris buffer pH 9.0, 0.3 M NaCl, 0.1 mM PLP, 12.5 mM imidazole) and the enzyme was eluted with elution buffer (100 mM Tris buffer pH 9.0, 0.3 M NaCl, 0.1 mM PLP, 250 mM imidazole). The buffer was exchanged to 100 mM Tris buffer pH 9.0, 0.1 mM PLP by the use of Vivaspin columns (GE Healthcare, Sweden) with 10 kDa molecular weight cut off.

Protein concentration was measured using the Bradford method and purity was assessed by SDS-PAGE, where a single band of the expected size of 50 kDa was visible.

### 2.2 Chemical modification of Nylon and enzyme immobilisation

The protocol described in Table S2 was used to functionalise the small pieces of Nylon (1cm x 0.6cm x 0.2cm) and the sets of wells. The pieces of Nylon were submerged in 5 mL of the solutions described and washed using tweezers (to catch the pieces) and pipettes. The wells were filled with these solutions and also filled with the washing solutions. In the case of the wells, the modification was stopped depending on the row.

Table S 2 Protocol for surface modification and enzymes immobilisation on Nylon

Step	Treatment
1	3D printed nylon was incubated for 15 min. at r.t. in 5M HCl, then washed profusely with H <sub>2</sub> O and 0.1M K phosphate buffer pH 8.0
2	Sample 1 was incubated for 2h at r.t. in Glutaraldehyde solution 25%(w/w) in H <sub>2</sub> O. Then washed profusely with H <sub>2</sub> O and 0.1M K phosphate buffer pH 8.0
3	Sample 2 was incubated for 2h at r.t. in 5%(w/v) polyethyleneimine in 0.1M K phosphate buffer pH 8.0. Then washed profusely with H <sub>2</sub> O and 0.1M K phosphate buffer pH 8.0
4	Step 2 was repeated and solution left overnight. Then washed as in previous steps.
5	Sample 3 and/or 4 were incubated in enzyme solution at 4 °C overnight. The enzyme concentration on 0.1M K phosphate buffer pH 8.0 was be 1 mg/mL. After, the samples were washed with H <sub>2</sub> O and pH 8.0 buffer.
6	After enzyme immobilisation, the surfaces were washed for 2h at r.t. in a 0.5M NaCl solution in buffer. This is to eliminate non-covalently bonded enzyme.

The immobilization of the enzyme was performed incubating the polymer S4 with 5 mL solution of the enzyme (1 mg of enzyme/mL) in 0.1M K phosphate buffer at pH=8.0, with 0.1 mM PLP overnight at 4 °C. Afterwards, the piece was filtered-off and washed with the same phosphate buffer and a 0.5M NaCl solution in the same buffer to eliminate the enzyme immobilised by non-covalent interactions.

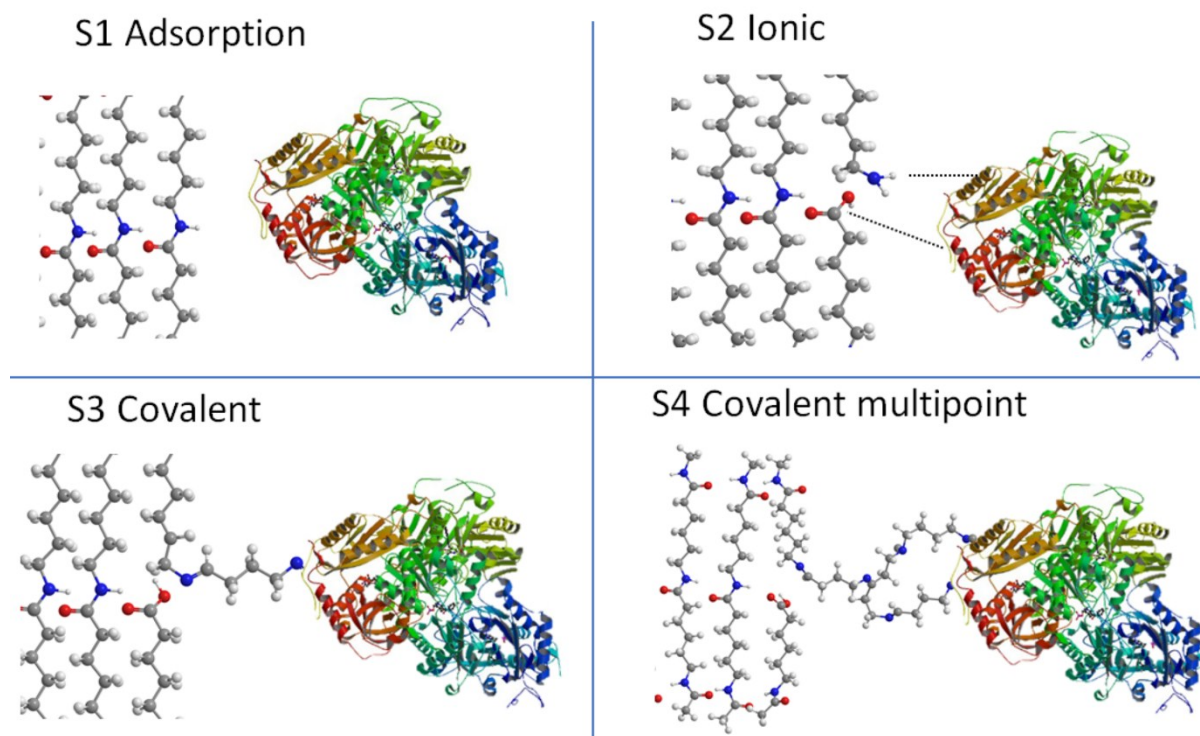
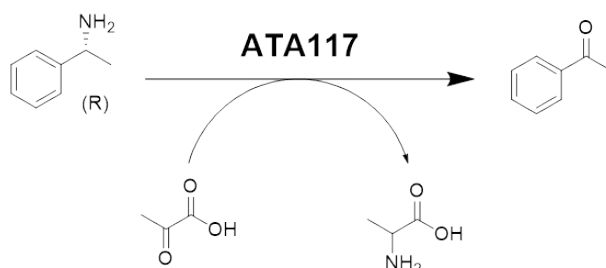


Figure S 2 Scheme of the different types of possible unions of the enzyme in the Nylon surface.

Covalent immobilization (S3) when the chemical modification was stopped after step 2 (Table S2). Step 6 (Table S2) was performed to eliminate S2 type unions.

### 2.3 Catalytic test with modified nylon part

The enzyme ATA117 was supported on a small Nylon piece as described on Table S2. After that, this piece was tested on the transformation of R-MBA in acetophenone to check if the enzyme still has activity once supported in Nylon.



Scheme S 1 Benchmark reaction employed to test the biocatalytic activity of immobilised w-TA on 3D printed parts

Table S 3 Results of the catalytic test with ATA117 immobilised on Nylon

Enzyme state	Conversion (%) <sup>e</sup>			
	Free <sup>a</sup>	Immobilised <sup>b</sup>	Residual <sup>c</sup>	Washing <sup>d</sup>
ATA117	100	22.6	65.5	-

The reactions were performed in batch. Conditions: 5mM R-MBA, 5mM Pyruvic acid, 0.1mM PLP, 30°C, stirring, 17h. a) Free: the reaction was performed in 1ml of a 1mg/ml solution of fresh enzyme (the same concentration used for the immobilisation in step5 Table S.I.X). b) Immobilised: the treated piece of Nylon was submerged in 1ml of 0.1M K phosphate buffer pH 8.0. c) Residual: this was performed in 1 ml of the residual enzyme solution that remains after the immobilisation (step5 in Table S2.). This solution was initially 1mg/ml. d) Washing: this was performed in 1 ml of the NaCl 0.5M washing solution used in step6 Table S2 e) The samples were treated and analysed by GC as described in Analytical methods.

## 2.4 Analytical methods

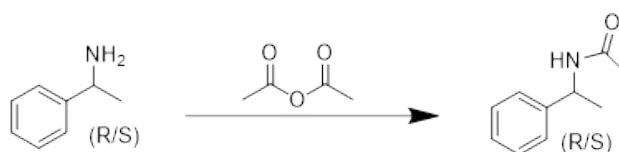
### 2.4.1 Nylon surface modifications

The surface modifications were followed by IR Alpha IR with a resolution of 5 cm<sup>-1</sup>.

### 2.4.2 Catalytic test with pieces. Conditions and enzymes screening in wells.

The reactions were analysed by GC-FID Trace 1310 (Thermo Scientific) with CP Chiralsil Dex CB (25 m x 0.25 mm x 0.25 mm) column from Agilent). The samples were analysed after the following treatment: 100 µL of NaOH (till pH 12) and 750 µL of AcOEt were added to 1 mL of sample. Then it was centrifuged at 15000 g for 2 min. 600 µL of the organic phase were transferred to a MS vial. At this point, 10 µL of acetic anhydride and 10 µL of triethylamine were added to derivatise the MBA.

The samples were analysed by the following method: injector temperature 230°C, split ratio 1:10, continuous flow 1.7 ml/min; 40 °C for 2 min, 20 °C/min to 150 °C, hold 5 min, then 30 °C/min to 225 °C, then hold for 8 min, FID temperature 250°C. Helium was used as carrier gas.



Scheme S 2 Derivatisation of product for GC analysis

## 2.5 Continuous-flow set-up

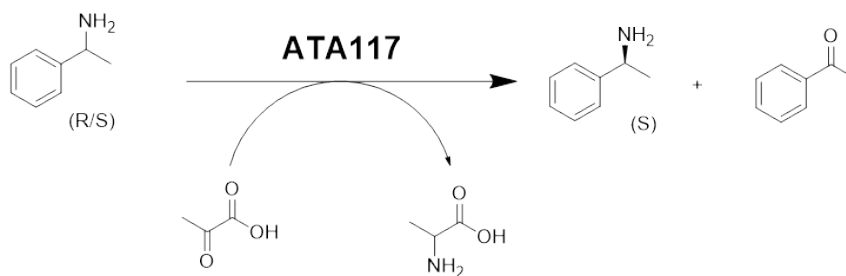
### 2.5.1 Functionalisation of the Nylon Reactor

- i. The reactor was filled manually with HCl 5M using a syringe. The acid solution was left inside for 10 min at r.t.

- ii. The HCl 5M solution was flushed out of the reactor also manually using a syringe full of air. Then the reactor was washed also manually with H<sub>2</sub>O using a syringe. In this moment the pressure inside increased significantly and it was harder to pass more solvent through the reactor.
- iii. The reactor was filled manually with a solution of Glutaraldehyde 25%(w/w) in H<sub>2</sub>O using a syringe. This solution was left inside for 16h at r.t.
- iv. The Glutaraldehyde solution was flushed out of the reactor also manually using a syringe full of air. Then the channel was washed with 0.1 M K phosphate buffer pH 8.0 using a HPLC pump at flow 0.01 ml/min for 5h.
- v. 15 mL of ATA117 enzyme 5mg/ml solution in 0.1 M K phosphate buffer pH 8.0 (with 0.1 mM PLP cofactor) were prepared (75 mg of enzyme were used) and recirculated through the reactor channel at 0.025 ml/min using a HPLC pump at r.t. during 24h.
- vi. 0.1 M K phosphate buffer pH 8.0 was passed finally through the channel also at 0.025 ml/min using a HPLC pump at r.t. for 6h in order to flush out the enzyme solution and leave the reactor full of buffer and ready to perform bioreactions inside.

The 3D printed reactor was connected to a pump and filled with HCl 5M and the flow was stopped for 10 min. After this time, deionized water was pumped through to wash out all the acid until the water at the outlet of the reactor gave a neutral pH. Then, the reactor was further washed with a buffer solution 0.1 M of potassium phosphate buffer at pH=8.0. Then, the reactor with a solution of glutaraldehyde 25%(w/w) in H<sub>2</sub>O to generate a aldehyde-based reactive reactor surface. Once filled it, the flow was stopped and the modification was allowed for 16h at r.t.. After, the reactor was washed with a buffer solution.

## 2.5.2 Enzymatic enantiomeric resolution of MBA under continuous flow conditions



Scheme S 3 Benchmark reaction for the kinetic resolution of rac-methylbenzylamine. Reaction mixture: 65  $\mu$ L of MBA (0.5 mmol), 36  $\mu$ L of pyruvic acid (0.5 mmol) and 2.5 mg of PLP (0.01 mmol) were solved in 100 mL of 0.1 M K phosphate buffer pH 8.0

Table S 4 Results for the enzymatic enantiomeric resolution of MBA under continuous flow conditions.

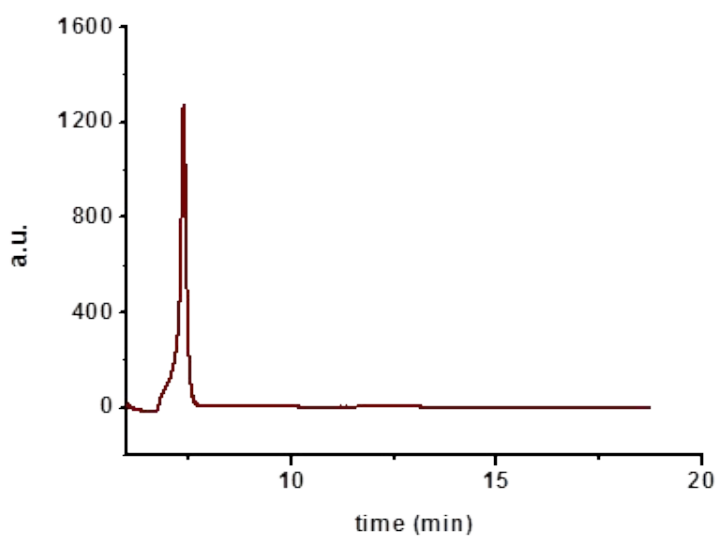
Time (h)	Flow (ml/min)	Conversion (%)	%ee
2	0.025	87/44	77
5	0.025	96/48	93
11	0.01	99.9/49.9	99.9
19	0.01	99.9/49.9	99.9
25	0.01	99.9/49.9	99.9
<b>Stored in buffer at 4 °C for 48 h.</b>			
28	0.01	88/44	78
40	0.01	96/48	92
48	0.01	99.9/49.9	99.9
66	0.01	97/48	95
74	0.01	98/49	96
90	0.01	98/49	95
96	0.01	97/48	94

Conditions: 5mM MBA, 5mM pyruvic acid, 0.1mM PLP, r.t., Reactor volume: 0.5ml.

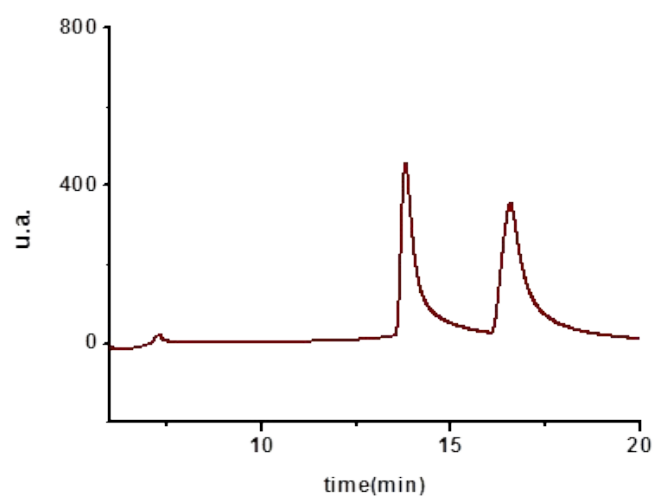
Samples treatment: All the samples were basified with NaOH 2M till pH 12 and then extract with AcOEt (1 ml/ml of sample). The organic phase was dried with MgSO<sub>4</sub> anhydrous.

Samples analysis: The samples were analysed by HPLC (Merck HITACHI LaChrom). Conditions: Daicel Chiralcel OD-H, n-hexane/ethanol (99/1), 1ml/min, 210nm, 25°C, 25 $\mu$ l of sample. Retention times: acetophenone 7.32 min, R-MBA 15.05 min, S-MBA 17.30 min.

### 2.5.3 HPLC spectra



*Figure S 3 HPLC spectra of acetophenone 2.5 mM*



*Figure S 4 HPLC spectra of the initial reaction mixture*

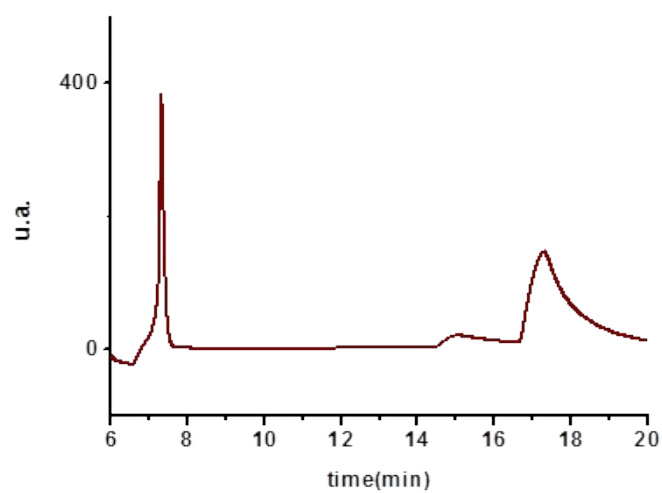


Figure S 5 HPLC spectra of the reaction at flow 0.025 ml/min

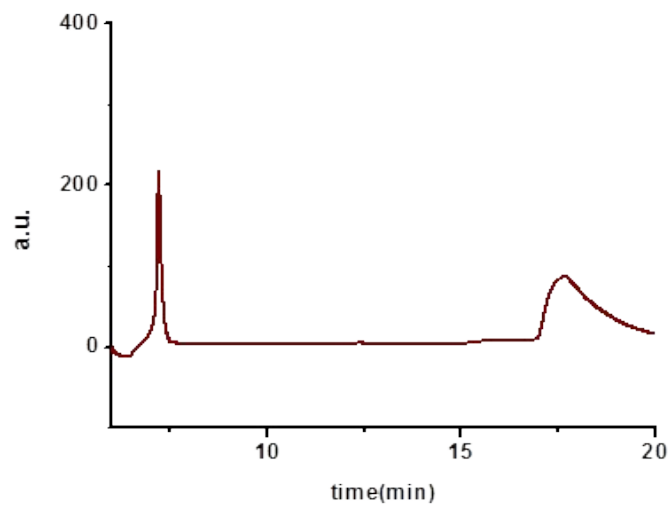


Figure S 6 HPLC spectra of the reaction at flow 0.01 ml/min



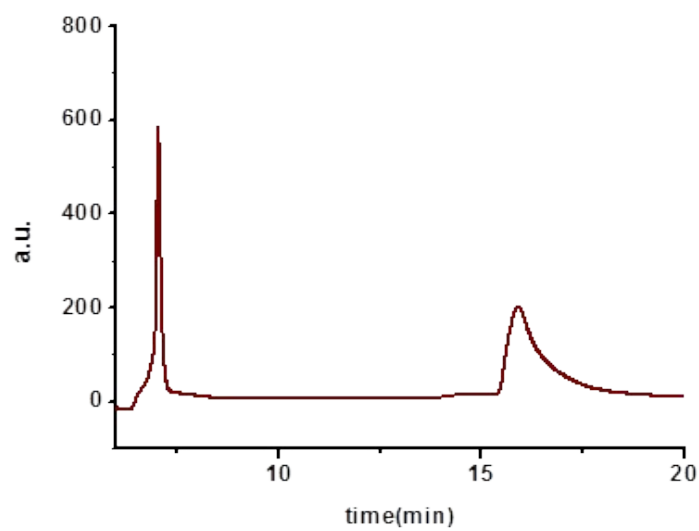


Figure S 7 HPLC spectra of the reaction when reuse the reactor at flow 0.01 ml/min

### 3 References

- [1] F. Steffen-Munsberg, C. Vickers, A. Thontowi, S. Schätzle, T. Tumlrirsch, M. Svedendahl Humble, H. Land, P. Berglund, U. T. Bornscheuer, M. Höhne, *ChemCatChem* **2013**, 5, 150-153.



# **Final Conclusions**

## **CHAPTER 8**



## 8. FINAL CONCLUSIONS

Conclusions for the work presented here have been shown and developed in each chapter. However, it is worth to highlight the most relevant and general ones in the following lines:

- ❖ The advantages and possibilities of **supported ionic liquid-like phases** (SILLPs) for developing green and efficient **catalytic flow processes** have been demonstrated for three important C-C bond forming reactions such as cyanosilylation, Strecker and Negishi cross-coupling. The modular structural features of SILLPs allow fine-tuning their catalytic efficiency and properties by varying parameters such as the SILLPs loading, the substitution pattern of the imidazolium units and the nature of the counteranion, leading to stable catalytic supported systems. Moreover co-catalysts, including organocatalysts or metal nanoparticles, can be supported efficiently in SILLPs to get extra catalytic activity, which opens even more the broad range of catalytic possibilities of these materials. Here we demonstrated that the synthesis of a broad family of SILLPs through simple approaches as compared with other supported catalysts reported in the literature.
- ❖ The potential of the use of **continuous flow** techniques as a **tool** for achieving **sustainable processes** has been demonstrated. Good to excellent productivities, long-term stabilities, catalyst efficient reuse, solvent-less procedures, use of neoteric solvents such as scCO<sub>2</sub> and the absence of complex and laborious product isolations or purification procedures have been described.
- ❖ A valuable **telescoped multi-step**, multi-catalytic and metal-free **continuous flow** protocol for the **synthesis of chiral cyanohydrins** has been developed **combining SILLP-based organocatalysts and supported biocatalysts**. Incompatible catalysts have been used together in a single process using a multi-reactor telescoped continuous flow strategy. With this procedure, a **lowest E factor** compared with previously described cyanohydrin synthesis has been reached.
- ❖ A **divergent synthetic multi-catalytic flow procedure** for the preparation of two valuable building blocks like protected

cyanohydrins and  $\alpha$ -amino nitriles from allylic alcohols has been implemented. Three individual **IL-based catalytic flow platforms** have been successfully combined. Both continuous flow catalytic platforms for cyanosilylation and Strecker reaction of less reactive aliphatic ketones have been developed which allows reaching a **broad scope of carbonyl substrates** suitable for these procedure.

- ❖ A better comprehension of the effects of supported ionic liquid-like phases on the Negishi cross coupling reactions has been achieved. Tunable **SILLPs allow synthesising supported NHC-Pd complexes** by modifying the imidazolium units, which solves the difficulties observed when using homogeneous analogues due to the need of separation of products and recovery the palladium from the solution. Moreover, the modular structure of SILLPs allows **including ligands** that have been shown as favourable for Negishi cross coupling reactions such as phosphines and PEPPSI-like structures. **SILLPs also act** at the same time **as scavengers** recapturing the Pd active species, and thus providing more stable catalytic systems that can be applied under continuous flow conditions.
- ❖ Possibilities of new **additive manufacturing technologies** for the obtaining of **flow devices** have been demonstrated. A tailored 3D printed Nylon flow reactor has been chemically modified to covalently support enzymes in its internal channels providing **active and stable bioreactors**. With the protocol reported, transaminase enzyme supported showed a comparable activity to the free enzyme and was successfully recycled keeping its **activity over extended periods of time** (*circa* 100 hours) **under continuous-flow conditions** for the transamination of *rac*-methyl benzylamine. With economically affordable materials like Nylon and simple chemical modifications, functional bioreactors could be achieved, which highlights 3D printing as a promising tool in the field of continuous flow chemistry.



